I

Geology and Mineral Resources of Northwest Swaziland (Barberton Greenstone Belt)

C.M. BARTON B.SC., PH.D.

Barton, C. M. (1982): Geology and Mineral Resources of Northwest Swaziland. – Geological Survey of Swaziland, Bulletin, 10:1–97, 64 Abb., 46 Tab.

SWAZILAND GEOLOGICAL SURVEY AND MINES DEPARTMENT
1982

PREFACE

Twenty years have passed since "Mineral Resources of Swaziland" was published by the Geological Survey and Mines Department. During this time, considerable changes have taken place in the country. The Kingdom achieved independence in 1968 and has also experienced rapid economic growth. During 1981, the country celebrated this progress with the Diamond Jubilee of the Ngwenyama, Sobhuza II.

Significant developments in the Swaziland mining industry have taken place during the same period. Mineral production from major asbestos and iron ore deposits described in this report have dominated mining activities in recent years. The contribution of mineral sales to Swaziland's economy is now in a period of decline, accelerated by the recent closure of Ngwenya iron ore mine. However, as this report shows, the mining-sector could have a significant impact on the future economy.

This Bulletin represents a systematic account of the most extensively mineralised area in the country. It is encouraging to read of substantial reserves of gold, iron and barite in the Hhohho District. The nation-wide extent of low-grade iron deposits (almost a billion tons) has not previously been recognised. Together, these minerals are regarded as potentially significant resources.

This work also represents an important advance in the understanding of an area of complex geology. With this contribution, the search for new mineral deposits may more easily proceed.

A.S. DLAMINI
Director,
Geological Survey and
Mines Department

Mbabane
June 1982

SUMMARY

The principal conclusions of this report concern the distribution, origin and potential reserves of mineral deposits along the eastern edge of the Barberton greenstone belt in northwest Swaziland:

Chrysotile asbestos — the Havelock asbestos deposit is one of the most important chrysotile occurrences in southern Africa. The asbestos orebody occurs within an allochthonous serpentinised dunite-harzburgite as a stockwork of cross-fibre seams. It is argued that fibrous chrysotile within the Havelock orebody formed by diffusion of fluids into dilating cracks, at temperatures below dehydration of lizardite serpentinite. A model is described in which processes of rock dilatancy, diffusion and fluid circulation operated in that part of the serpentinite where tectonic stress rose to relatively high levels. It is suggested that the asbestos deposit formed near the leading edge of a thrust sheet in a region where the décollement was not a simple planar surface. From a description of the geometry and grade of the orebody, it appears that ground developed in deep mine levels is considerably less payable than on surface.

Gold — all gold deposits in northwest Swaziland are closely associated with ultramafic sequences of the Onverwacht Group. The most productive deposits are located 4 km or less from the granitic edge of the greenstone belt; those farther than ±3 km from granite outcrop are associated with zones of translational deformation. Lodes that occur within or near the thermal aureole are sulphide-poor, while those in the interior of the greenstone belt contain high concentrations of the volatile species Sb, As and Hg, together with other low-temperature base metal sulphides and free silver. The formation of most lodes can be described in terms of directions of fluid flow with respect to impermeable cap-rocks.

The presence of extensive chromiferous sericite wall-rock alteration indicates that fluids with potassic compositions were closely associated with lode gold deposits. It is suggested that the concentration of precious metals in greenstone belts was favoured by a unique combination of high-level ultramafic sequences and the general restriction of potassic batholiths to Precambrian terranes.

Potential ore standing in old mine workings, orebody extensions in the sulphide zone of several deposits and high tonnage, low-grade gold deposits (±1 g/t) are evaluated in turn. A potentially large occurrence (the Wyldsdale deposit) that has not been systematically exploited near suface is described. Extensions to the large Piggs Peak and Avalanche deposits may exist but require additional exploration data to prove. Together, over 2 $.10^6$ tons potential gold ore (1–9 g/t) is indicated in six deposits.

Iron — field relations and mineralogical studies allow the recognition of two important types of iron deposit in the Swaziland Supergroup. Small, lenticular-shaped units of iron-formation occur closely associated with Onverwacht Group mafic (tholeiitic) volcanic sequences that have been subjected to a "spilitic metamorphism". Iron deposits of this type are of economic interest only when upgraded by metamorphism to minnesotaite-ferroactinolite-magnetite assemblages.

Second, laterally extensive deposits of hematite iron-formation occur interlayered with thick clastic sedimentary sequences of the Fig Tree and Moodies Groups. Deposits of this type overlie both silicified units and talcose schists of the Onverwacht Group. Available evidence suggests that processes of replacement operated during their formation. Where sampled below the deep zone of sub-tropical weathering, iron in both types of deposit is stored mainly in carbonates.

Total reserves of ±700 $.10^6$ tons potential ore that contain an average 41,8 per cent iron are available in 12 deposits. The estimate includes 23,4 $.10^6$ tons potential high-grade ore (±60 per cent Fe) below existing pit-levels, and 58,6 $.10^6$ tons low-grade iron-formation both *in situ* and on dumps at the Ngwenya hematite deposit. Though the deposits in northwest Swaziland represent the most important iron resources in the country, more than 80 per cent are located within the Malolotja Nature Reserve.

Barite — the Londosi barite deposit is a ±10 km-long stratiform sulphate horizon that includes massive silica and volcanic detritus. A metamorphosed igneous sequence of mafic to ultramafic composition forms the depositional base to the mineralised horizon. Crystal tuffs and sequences interpreted as silicic ash-flows overlie the sulphate deposit. Analogy with similar barite-opal volcanic rocks described from a present-day marginal basin suggests that barite, silica and base metals were

leached from the underlying Onverwacht Group sequences by hydrothermal solutions, and that inorganic precipitation occurred when these solutions came into contact with cooler seawater.

Indicated reserves in the Londosi deposit are 286 000 tons mineable barite. Probable ore in the vicinity of the dormant mine is estimated to be 145 000 tons of which 15 000 tons is blocked out. Barite reserves are probably sufficient to support a small mine (1 000 tons/month) for 15 years.

Antimony and mercury — field relations indicate that the distribution of minor antimony and mercury mineralisation is controlled by patterns of faulting. Their occurrence is thought to define quite closely the low-temperature edge of a geothermal field associated with emplacement of the Lochiel batholith.

CONTENTS

TEXT FIGURES

TABLES

INTRODUCTION

The Barberton greenstone belt and surrounding granitic terrane is one of the best preserved and closely studied areas of early Precambrian crust. The region has become classic ground largely through the work of M.J. and R.P. Viljoen, Hunter and Anhaeusser whose observations and different interpretations have resulted in widely accepted models of Archean crustal evolution.

It is perhaps surprising then that there is no general account of the geology of a large segment of the Barberton greenstone belt that crops out in Swaziland. Though lithological distribution maps at a scale of 1:25 000 have been made available as a result of work completed by the Geological Survey, relatively little has been written about the geology of the Swaziland highveld Two Survey Officers, Urie and Jones, mapped almost single-handedly and in great detail the rugged terrane that forms much of this area. Without high-quality maps of this type the present study would not have been possible.

New field and analytical data from all important mineral occurrences in northwest Swaziland are described here. These data are based on the writers' own rather limited experience of an area of extremely complex geology. Extensive use has been made of previous unpublished Geological Survey reports: notable contributions to the economic geology of the area have been made by Hunter, Jones, Mehliss, Urie and Clarke, and these are acknowledged in the text. In addition, numerous mine reports together with exploration data provided by mining companies are cited, by author wherever possible.

At the time of writing (1982), border adjustments between Swaziland and South Africa are under discussion. The present study area is delimited by the international boundary drawn in 1880 (see Fig.1). Within this boundary, a total of 63 400 ha or 18,4 per cent of the area occupied by the Barberton greenstone belt is enclosed in Swaziland territory.

ACKNOWLEDGEMENTS

Numerous individuals and organisations have been especially helpful during the course of this work. It is a pleasure to record the generous hospitality and free access to data provided by the management of Havelock Mine. Discussions with mine geologists N. Morris and B.G. Eaton were particularly useful, while B.C. Honey with the assistance of S. Fakudze first introduced the writer to the underground geology at Havelock.

The first-hand knowledge of many of the disused gold mines provided by E. Wiseman was invaluable, as were field discussions with R. Randell on the Piggs Peak gold deposit. R. Attridge drew the writer's attention to relevant data on the Ngwenya hematite deposit, and D. Newman provided other unpublished company reports.

S. Agrell of Cambridge University kindly provided electron microprobe analyses of the Havelock iron-formation, E. Kinloch of J.C.I. determined the ore mineralogy of the She and Ivanhoe gold lodes, D.H. Sims performed the brucite determinations and C. Frick made available analytical facilities at the Geological Survey in Pretoria.

R.M. Barton spent many long hours in painstaking preparation of the diagrams, and these were subsequently drafted by N. Tsela. Field and other logistical support given by D. Masango, Nelson Nkambule, Gasolo Nkambule and G. Junge is greatly appreciated. K. Bloomfield, M.J. de Wit, R. Fripp, D.H. Laubscher and N. Morris commented on portions of the original manuscript.

This work was completed between 1978–1982 while the writer was on secondment from the Institute of Geological Sciences, Natural Environment Research Council, United Kingdom.

GEOLOGICAL DATA

Physical features and climate

The highveld of northwest Swaziland is deeply incised terrane drained by the Lomati, Komati and Umbuluzi Rivers. The Mgudugudu, Mzimnene and Phoponyane Rivers drain north into the Lomati basin, and the Nkomozane and Malolotja Rivers join the Komati near the border with South Africa (see Fig. 2). Approximately 1 km of vertical relief is present in the area near Lufafa Mountain.

The area is subjected to sub-tropical weathering with strongly seasonal rainfall. Bulembu town has an average annual precipitation of 1 750 mm, of which 80 per cent falls during the period October–March. The effects of sub-tropical weathering processes on the supergene enrichment of iron-formation are discussed below.

Recent rates of uplift

Precambrian basement in Swaziland and adjacent parts of South Africa is exposed in an erosional window through younger cover sequences (Fig. 1). Recent vertical rates of deformation of at least 100 mm per 1 000 years are implied from a study of archaeological sites in the Komati River valley (Price-Williams, pers. comm., 1979). Regional uplift of southern Africa is estimated to be ±1 km since the Miocene (A.G. Smith, pers. comm., 1981).

Stratigraphy

A three-fold stratigraphic subdivision of the Barberton greenstone belt is now widely accepted (Viljoen and Viljoen, 1969, a–c; Anhaeusser, 1973). The Onverwacht Group forms the basal sequence of the greenstone belt, and together with the overlying Fig Tree and Moodies Groups constitutes the Swaziland Supergroup (Fig. 1).

According to Viljoen and Viljoen (1969 a), the Onverwacht Group consists in large part of volcanic sequences that attain a thickness of 15 km. Basal formations contain abundant extrusive units of ultramafic composition (komatiites), while units of mafic to felsic composition are more typical of the upper formations. Details of the Onverwacht Group stratigraphy in South Africa are not described here.

The Onverwacht Group is conformably overlain by the Fig Tree Group, a 2,5 km-thick sequence of clastic and chemical sediments (Reimer, 1967; Condie and others, 1970). Coarse greywackes within the Fig Tree Group contain sedimentary structures that indicate deposition from turbidity currents.

The Moodies Group consists of a 3,5–4 km-thick sequence of conglomerates and quartzites that is both conformable and disconformable with the underlying Fig Tree Group. Sedimentological studies indicate that the Moodies Group was deposited in a shallow water, sometimes intertidal environment (Eriksson, 1977).

Recent field studies indicate that the stratigraphic thickness of the Onverwacht Group measured by Viljoen and Viljoen (1969 a) does not allow for the effects of deformation (Williams and Furnell, 1979; de Wit, in press). Evidence for major tectonic duplication described by these authors implies a considerable reduction in the ±20 km stratal thickness normally attributed to the Swaziland Supergroup.

No formal stratigraphy is presented here. Instead, a number of measured lithological sections are given for sequences associated with individual mineral deposits. These sections are thought to form part of an essentially tectonic stratigraphy.

Structure

The Barberton greenstone belt in northwest Swaziland has been telescoped by thrusts. Evidence for a "thin-

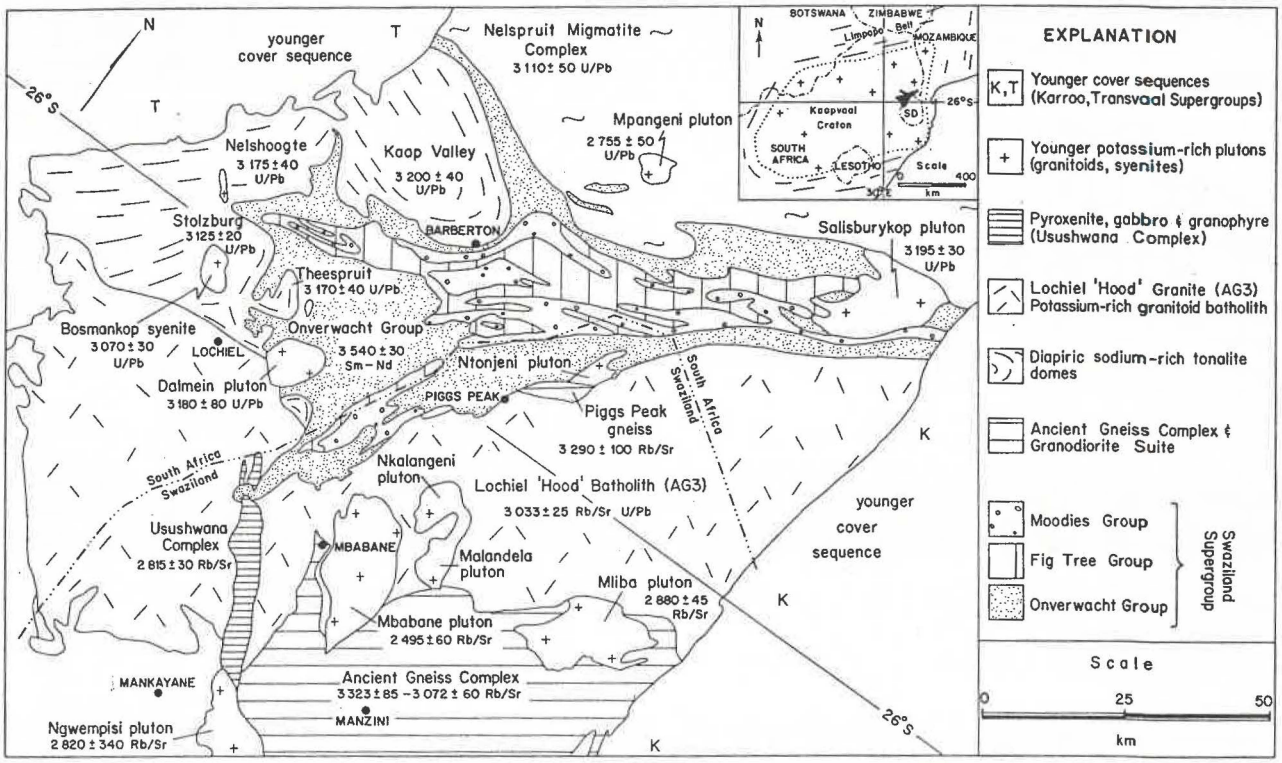

Figure 1

The Barberton greenstone belt and surrounding granitic terrane. Radiometric age data are taken from Snelling (in preparation) and Hamilton and others (1979).

skinned" interpretation comes from mapping by the writer in the area between Bulembu and the Piggs Peak gold deposit, and in the vicinity of gold deposits and prospects farther north (see Fig. 2). Repetition of lithological sequences and large-scale inversion of metamorphic zones are conspicuous in these areas. Major tectonic duplication in the area south of the Komati River is also indicated from recent mapping (S. Lamb, personal communications 1980–1982).

In large part, directions of thrusting are toward the interior of the greenstone belt (toward the northwest), except in the Lufafa zone area west of a line of 'older' granitoid plutons where the tectonic transport direction is toward the southeast. Amounts of thrust displacement could be quantified by the construction of balanced sections across the exposed edge of the greenstone belt. Estimates of stratal shortening must await until the results of careful sedimentological and structural studies are available. Maximum thicknesses of stratigraphic units that have been measured unambiguously within individual thrust sheets are summarised briefly as follows:

Onverwacht Group: (1,5–2 km)

1. 500 m of largely talcose ultramafic sequences. Units with spinifex-like textures (komatiites) are only extensively developed in Swaziland in the area immediately west of the Ntonjeni pluton where the intrusion separates the greenstone belt sequences from the AG3 batholith (Fig. 2).
2. 800–1 000 m pillowed and spilitised tholeiitic volcanics. Mafic extrusives of this type are extensively developed in the central area, and near the southern extension of the greenstone belt.
3. 300 m-thick volcaniclastic sequence, minor shales and volcanics of unknown composition. Extensive silicification is characteristic of this sequence.
4. silicic intrusive and extrusive igneous sequences occur in the vicinity of Kobolondo Mountain (Fig. 2). Stratigraphic thicknesses are not known with certainty but are thought to total less than 500 m.

Lithological units 1–3 are extensively repeated by thrusts in the central area of the greenstone belt.

Fig Tree Group: (360–540 m)

Sections measured below Lufafa Mountain in the lower plate of the Manhaar-Mgudugudu fault include thick greywackes, shales, debris flows with redeposited iron-formation and minor redeposited barite (see Fig. 30).

A massive depositional basin of carbonate iron-formation occurs together with thick clastic sequences in the area between Emlembe and Ngwenya, above the Manhaar fault.

Moodies Group: (1–1,5 km)

Between Lufafa and Makonjwa Mountains, quartzites, conglomerates and a persistent horizon of amygdaloidal lava are present in a single thrust sheet mapped as part of the Moodies Group.

Total stratal thickness of the Swaziland Supergroup in Swaziland is less than 5 km.

Metamorphism

Pillowed tholeiitic sequences of the Onverwacht Group have been subjected to a pervasive hydrothermal metamorphism with the formation of ubiquitous albite-chlorite-ankerite and andesine-chlorite-magnetite assemblages. The effects of this 'spilitic metamorphism' can be resolved in areas outside the thermal aureole of the AG3 batholith (see Havelock iron deposit).

Ultramafic sequences of the Onverwacht Group are altered to talcose and talc-carbonate schists on a regional scale, particularly in areas near the granitic edge of the greenstone belt. The age of metamorphism is unknown.

Horneblende-hornfels facies metamorphic sequences (±garnet) are developed in the contact aureole of the AG3 batholith. The high temperature part of the aureole

is only 400 m in width though greenstone xenoliths occur as far as 5 km from the edge of the belt. Biotite in mafic igneous sequences is developed up to 2–3 km from granite outcrop. Jones (1969) mapped albite-epidote facies sequences (trem/act±talc±chlorite) in a zone 1–1,5 km wide, parallel with the margin of the batholith north of the Lomati River.

Preservation of carbonate iron-formation (Havelock- and Ngwenya-types), as well as finely laminated graphitic shales indicates the effects of any regional metamorphism to have been slight.

Metasomatism

1. **Silicification:** all Onverwacht Group volcaniclastic and felsic volcanic sequences are extensively silicified. Numerous layers and lenses of chert that were mapped by the Geological Survey as stratigraphic horizons are now considered to have formed by replacement of volcaniclastic detritus. Silica replacement of quartz-poor volcaniclastic sequences was first documented from the Onverwacht Group by Lowe and Knauth (1977) and the processes involved are described by these authors.

Field relations and textural evidence for silicification, and the irregular three-dimensional geometry of a single chert body of replacement origin are described here from the Piggs Peak gold deposit. Cherts of the Piggs Peak-type acted as impermeable cap-rocks or 'bars' during later hydrothermal events.

2. **Carbonation:** where sampled in deep excavations (± 100 m below outcrop) or in boreholes cores, unmetamorphosed iron deposits in the Fig Tree and Moodies Groups consist of carbonate iron-formation. For reasons given below, deposits of this type are thought to have formed by exhalative processes during regional metasomatism. Massive amounts of iron, silica and carbonate were transported during this event.

Extensive carbonation of Onverwacht Group pillow lavas has been documented by Viljoen and Viloen (1969 b). Spilitised and carbonated pillow lavas of a similar type are described below from the footwall of the Havelock asbestos deposit.

3. **Sericitisation:** most lode gold, antimony and mercury occurrences in northwest Swaziland exhibit potassic wall-rock alteration. Numerous unmineralised faults and fractures are also extensively altered to sericite.

Much of the sericite is chromiferous in composition. The bright green micaceous mineral characteristic of many lode gold deposits, both here and elsewhere is referred to as chromiferous sericite, following the terminology of Knopf (1929). The distinctive combination of potassic fluids and ultramafic chrome-bearing sequences required to form this mineral point strongly to the processes involved in the concentration of some lode gold deposits.

Lochiel "Hood" batholith

Field relations show that the Lochiel (AG3) batholith has the form of a "hood" or horizontal carapace over older gneissic terrane (Hunter, 1974; Fig.1). Banded tonalitic and granodioritic gneisses that form much of the Swaziland middleveld pass progressively into grey, medium- or coarse-grained granite (quartz-microcline-plagioclase-biotite ±hornblende) on higher ground.

Deep erosional re-entrants (Fig.1) indicate that the batholith has a rather narrow vertical extent. Sections measured across the 30–60 km-wide granite outcrop on published 1:50 000 geological maps give an average maximum vertical thickness of 525 m (range 300–800 m). The basal surface of the batholith is inclined north at a very small angle (<1°).

At present vertical rates of uplift and erosion, the Lochiel batholith may disappear without trace within 10 Myr. Hunter (1974) has suggested that a granitic carapace may already have been removed by erosion from the Nelspruit migmatite complex (Fig.1).

It is noted that both the Lochiel batholith and the Nelspruit migmatite complex have highly potassic compositions (>4 per cent K_2O). Granitoid bodies of this type are correlated below with areas of gold mineralisation.

Ntonjeni pluton

A large granodiorite intrusion (the Ntonjeni pluton), and several smaller satellite bodies including the Wyldsdale and Mzimnene plutons can be distinguished from the AG3 batholith on textural and compositional grounds. The Ntonjeni pluton contains conspicuous ultramafic (pyroxenitic) inclusions, several modal per cent of biotite and a high proportion of sodic feldspar.

A variety of quartz-porphyries, granophyres and other granitoid bodies crop out in ground between Kobolondo mountain and Piggs Peak (Fig. 2). These silicic bodies are thought to include intrusive equivalents of the Kobolondo silicic volcanic centre.

The age of the Ntonjeni pluton is not know. Analogy with plutons emplaced along the margin of the Barberton greenstone belt elsewhere (Fig.1) suggests that it may be older than the AG3 batholith. The structural and stratigraphic position of auriferous iron-formation that may have formed during emplacement of the Wyldsdale pluton suggests (though does not demonstrate) that this intrusion pre-dates deposition of the Moodies Group.

Granodioritic gneiss

Vertical slivers of silicic gneiss with a pronounced compositional layering crop out in deeply incised areas along the edge of the greenstone belt. Tectonic rotation of the gneissic layering horizontal implies a minimum vertical displacement of ±1 km along the faulted margins of the Swaziland Supergroup (see Molybdenum prospect).

Age

A precise crystallisation age for igneous sequences in the Onverwacht Group is given as 3 540 ±30 Myr by Hamilton and others (1979). The age was obtained from Sm–Nd analyses of whole-rock samples and according to these authors is definitive.

A weighted mean of three U/Pb and Rb/Sr determinations ($^{87}Rb\ \lambda = 1{,}42\ .10^{-11}\ yr^{-1}$) of 3 033 ±25 Myr is the age preferred by Snelling (in preparation) for the Lochiel (AG3) granite. Most mineral deposits described in this report formed either at the same time as or in the interval between these two events.

Initial formation of the Ancient Gneiss Complex 3 323 ±85 Myr ago was followed by a ±200 Myr period of repetitive Sr isotope rehomogenisation (Hunter, 1974; Snelling, in preparation). These data imply that the Ancient Gneiss Complex, and probably the gneissic slivers along the edge of the greenstone belt in Swaziland, were undergoing high-grade metamorphism during formation of at least part of the Swaziland Supergroup (see data in Fig.1).

Analytical methods

Major and trace element determinations of lode gold, iron, asbestos and barite deposits are given below. Precious metal abundances were determined by duplicate fire assay fusions on 25 g samples, followed by flameless atomic absorption spectrophotometry (AAS). Detection limits are 0,05 g/t (Au) and 0,1 g/t (Ag & Pt).

B, Ba, Cr, Sn, W, Y, & Zr were determined by X-ray fluorescence spectrometry (detection limits 10 or 20 ppm), Co, Ni, Cu, Pb, Zn by conventional AAS (detection limit 2 ppm), and As, Sb and Hg by flameless

GEOLOGY AND MINERAL RESOURCES OF NORTH–WEST SWAZILAND
(Barberton Greenstone Belt)

Approximate Scale 1:100 000

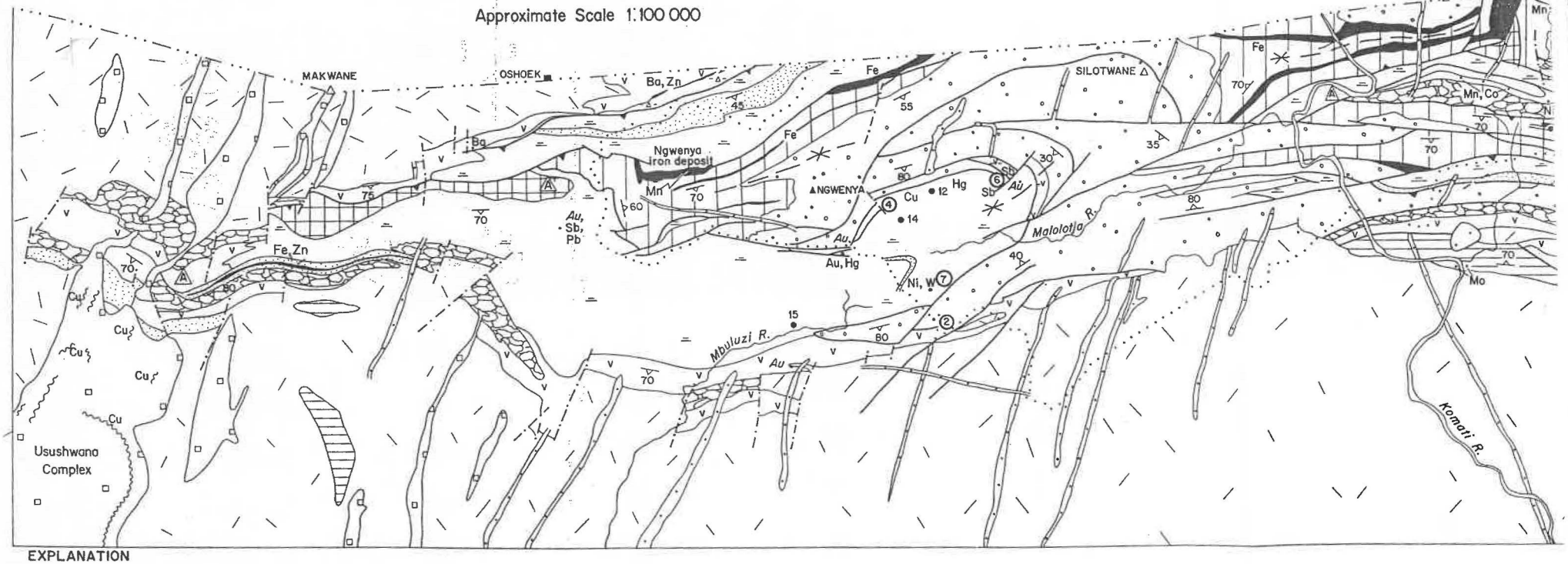

EXPLANATION

- conglomerates, quartzites
- amygdaloidal lava
- shales, greywackes
- volcaniclastics, silicified ± sericitised sequences
- silicic volcanics
- mafic volcanics, mafic schists
- talcose schists
- amphibolites (± spinifex-like textures)
- serpentinite

MOODIES GROUP; FIG TREE GROUP; ONVERWACHT GROUP

- granodioritic gneiss
- granitoid pluton
- Lochiel batholith (AG3)
- diabase dyke
- pyroxenite, gabbro, granophyre (Usushwana complex)
- thrust fault (teeth on upper plate)
- normal fault
- foliation with dip
- area enclosed by Malolotja Nature Reserve

- Chrysotile asbestos occurrences
- Iron deposits

GOLD DEPOSITS (1–15)

- (1) > 1 000 kg
- (9) 100 – 1 000 kg
- • < 100 kg

OTHER MINERAL OCCURRENCES

barite (Ba), antimony (Sb), cinnabar (Hg), manganese (Mn) various base metals (Ni, Co, Pb, Cu, Zn)

Figure 2
Geology and mineral resources of northwest Swaziland (approximate scale 1: Hunter and Jones, 1968; 1969) with modifications and additions in the central : arranged in order of declared output and are listed in Table 10.

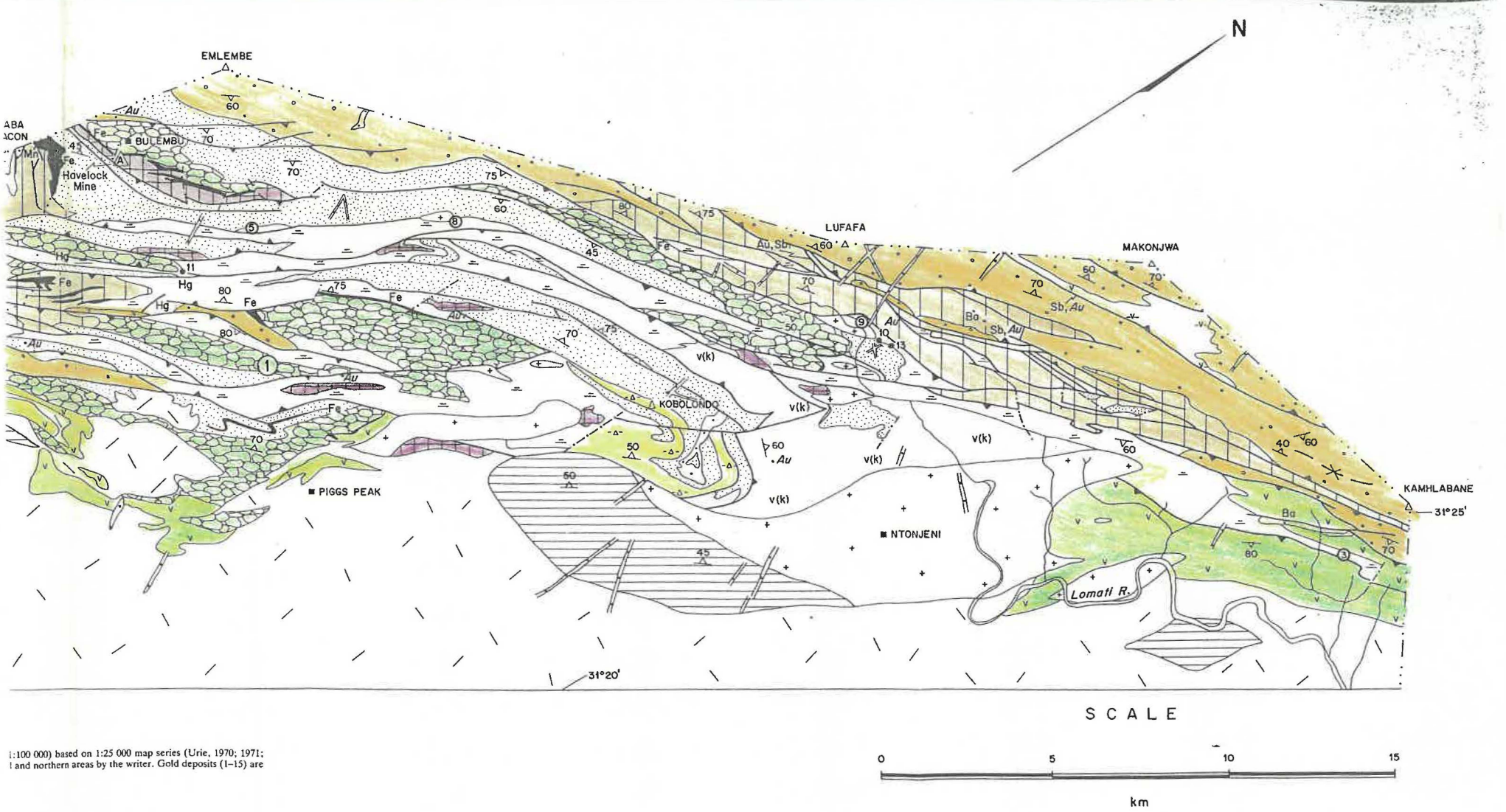

1:100 000) based on 1:25 000 map series (Urie, 1970; 1971;
l and northern areas by the writer. Gold deposits (1–15) are

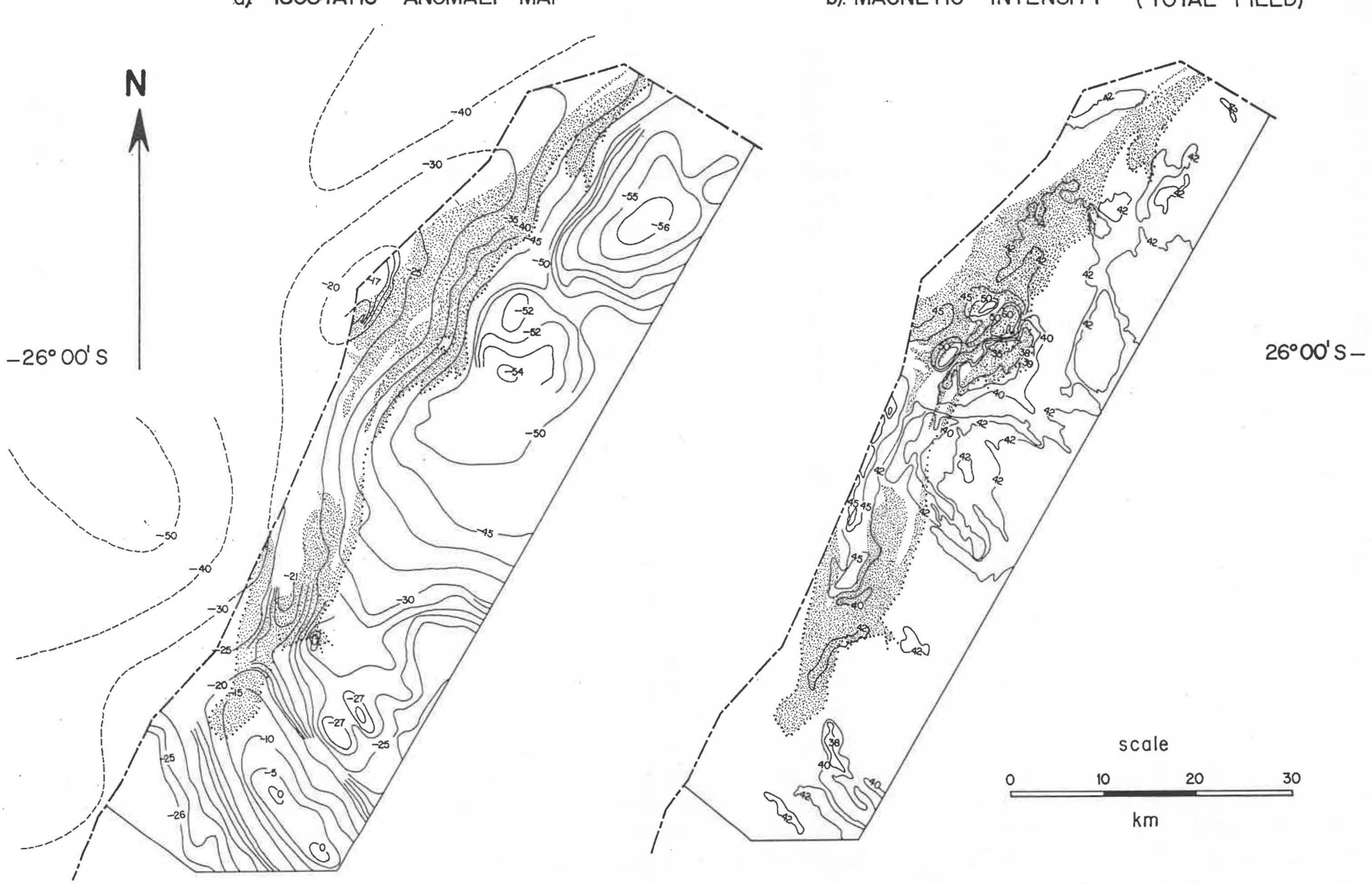

Figure 3
Isostatic anomaly and aeromagnetic intensity maps of northwest Swaziland. The area occupied by the Onverwacht Group is shown stippled (for explanation and description of data see text).

AAS (detection limits 1 ppm and 50 ppb for Hg). Unless stated otherwise, analysts are McLachlan & Lazar, Johannesburg.

GEOPHYSICAL DATA

Gravity

A regional gravity study of Swaziland was conducted by the Institute of Geological Sciences during 1965, and the results given by Masson Smith and Evans (1966), and Burley and others (1970). Free air, Bouguer and isostatic data are available for 2 248 stations (one station per 800 ha), and include 100 stations on ground underlain by the Swaziland Supergroup. The isostatic reduction assumes a 30 km crustal thickness of mean density 2,68 g cm^{-3}, and can be compared directly with equivalent data from South Africa given by Hales and Gough (1962).

The main features of the isostatic anomaly map of northwest Swaziland (drawn with a minimum 5 mGal contour spacing in Fig. 3) are as follows:

1. Well defined positive isostatic anomalies are associated with the Swaziland Supergroup (35 mGal) and the Usushwana igneous complex (30 mGal). Both anomalies are superimposed on a broad region of negative gravity (−40 mGal) over the AG3 batholith (Burley and others, 1970). The region of negative gravity extends well into South Africa.

2. The trends of the isostatic anomaly contours are approximately parallel to exposures in the greenstone belt. The regional gradient trends NE–SW and varies from +2,92 mGal .km^{-1} between Piggs Peak and Emlembe mountain to +1,30 mGal .km^{-1} across the southern extension of the greenstone belt around Forbes Reef.

3. Positive isostatic anomalies progressively increase over synformally folded sequences within the Swaziland Supergroup. A comparison of Figs. 2 & 3 shows that thick Moodies Group quartzites near Emlembe and at Ngwenya are marked by relatively high positive gravity (+35 mGal and +10 mGal respectively). In South Africa, the only positive 35 mGal anomaly within the Swaziland Supergroup is centred on Skokohla, in the Moodies Group of the Saddleback syncline (see Hales and Gough, 1962).

4. The Havelock ultramafic complex is marked by the highest positive gravity anomaly recorded in northwest Swaziland (+38 mGal). Though the uppermost 0,5 km of the Havelock body is completely serpentinised (and field evidence shows that the body is allochthonous), it is possible that unserpentinised peridotite may be present at depth.

Burley and others (1970) constructed a geological model (Fig. 4) in which they showed that the observed isostatic anomaly profile across the Swaziland Supergroup could be accounted for by assuming a 0,2 g cm^{-3} density contrast with adjacent granitic terrane. The 60 km-wide positive anomaly is consistent with a composite model consisting of a northwest block 2,8 km deep and 16,8 km wide, a central block 2 km deep and 16,8 km wide, and a southeast (Swaziland) block 3,2 km deep and 16 km wide (Fig. 4).

In addition, a reasonable fit to the main 160 km-wide 40 mGal negative anomaly was obtained by assuming a density contrast of −0,06 g cm^{-3}, and a granitoid block 91 km wide and 16 km deep, lowered in the centre to allow for the Swaziland Supergroup. Quantitatively similar geological models of the gravity anomaly in the Barberton area are given by Darracott (1975).

Principal conclusions drawn from the gravity data are:

1. There is an extremely good correlation between gravity and near surface geological features within the Swaziland Supergroup. Thick clastic sequences together with the allochthonous Havelock serpentinite body are both associated with high positive isostatic anomalies.
2. Using reasonable estimates of mean density of AG3 granite, and of a variety of lithologies within the Swaziland Supergroup (2,78–2,95 g cm^{-3}, Burley and others, 1970), the observed isostatic anomaly associated with the greenstone belt is consistent with an average crustal thickness of 3 km. The vertical thickness may be considerably less in areas where the batholith has an intrusive rather than a faulted margin.

Magnetism

An aeromagnetic survey of Swaziland was conducted during the initial phase of the UNDP mineral survey of the country (UNDP, 1970). The results were given in a report by the consultants (Isaacs and Hartman, 1966), and a more detailed regional interpretation is given in Bacon (1970).

Total field measurements were recorded along east-west flight paths (perpendicular to the principal strike direction), at 0,8 km intervals and 150 m terrane clearance. The magnetic values obtained were reduced to an arbitrary datum of 4 000 gamma, and plotted with a minimum contour spacing of 10 gamma on 1:50 000 maps. The simplified magnetic intensity map of northwest Swaziland (minimum contour spacing 100 gamma) shows the following features:

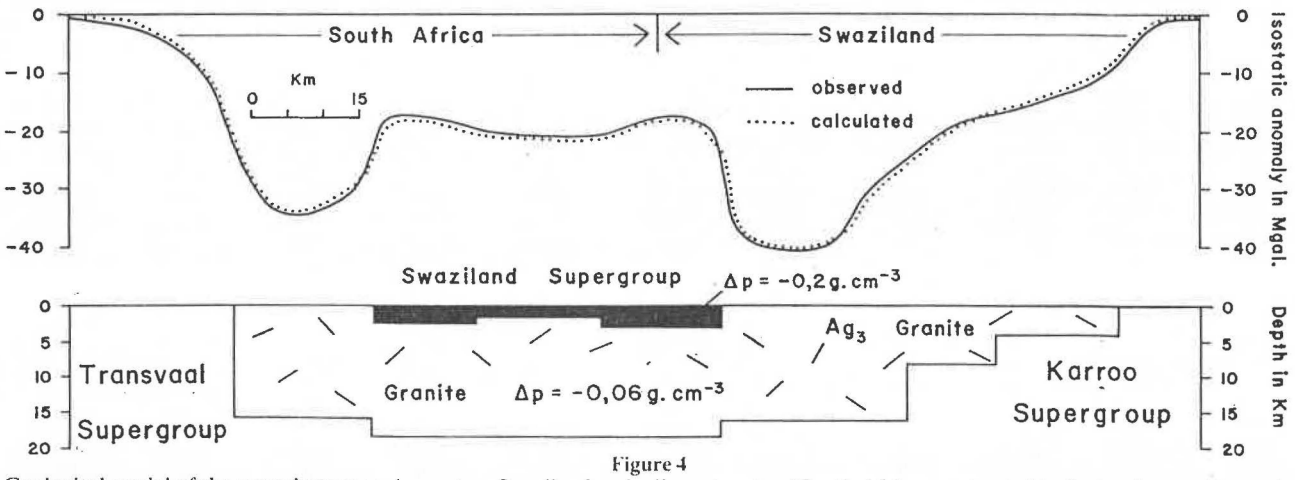

Figure 4

Geological model of the crustal structure in western Swaziland and adjacent parts of South Africa constructed to fit the observed isostatic anomaly profile (after Burley and others, 1970).

1. Several high intensity magnetic anomalies (up to 8 000 gamma above background) occur in the Swaziland Supergroup. Large anomalies can be correlated directly with occurrences of magnetite-bearing iron deposits. Ground measurements recorded after the airborne survey was completed show that the two highest anomalies (Mhlatane and Nottingham Peak) are associated with economic or sub-economic deposits that contain 20–30 per cent magnetite by volume (Evans, 1967). The hematite deposit at Ngwenya which was a producing mine at the time of the survey, records a much lower magnetic intensity of 1 000 gamma above background.

2. In contrast, other areas within the Swaziland Supergroup and the AG3 granite are marked by an average magnetic intensity close to the datum value of 4 000 gamma. The Forbes Reef synform and Malolotja valley are areas of low magnetic intensity, consistent with the low susceptibility of talcose schist (Bacon, 1970) and probable shallow depth to granite. The area around the Wyldsdale and adjacent plutons exhibits low magnetic intensity for similar reasons.

3. Contours of magnetic intensity are parallel or sub-parallel with exposures of Fig Tree and Moodies Group sequences north of Emlembe. Continuity of the Ngwenya and Makonjwa sequences is suggested by the uninterrupted magnetic signature across Silotwane.

Thus, magnetic data show a close correlation with known geology and structure. Evans (1967) pointed out that any departures from intensity contours predicted by the geology may be due in part to the rugged terrane of northwest Swaziland. Variations of up to 60 m in ground clearance were recorded during the airborne survey.

MINERAL RESOURCES

ANTIMONY AND MERCURY

ANTIMONY

The distribution of antimony mineralisation in northwest Swaziland (Fig. 5) is known from regional geochemical surveys (UNDP, 1970). Analyses of 10 000 stream sediment samples (5,8 per 100 ha) show anomalous values of antimony in two main areas:

1. A zone 6 km in length located along the western limb of the Forbes Reef synform. Mineralisation occurs near the sheared contact between Onverwacht and Moodies Groups, and is associated with a number of small lode gold deposits of the Avalanche-type (deposits that contain base metals, free silver and significant amounts of volatile metal species).
2. A 25 km-long zone that extends from the international border south of Lufafa mountain as far north as the Ntintinyane River basin (Lufafa zone, Fig. 5). The Lufafa antimony zone coincides in large part with a tectonic stack of Onverwacht and Fig Tree Group sequences. Anomalous antimony values also occur within the Moodies Group in the extreme northwest of the Lufafa zone near Makonjwa mountain.

In addition, a number of small streams that drain the Mhlangampepa valley north of Ngwenya mountain, the area immediately north of the oxbow on the Komati River, and the southern extension of the Devils Reef gold deposit all contain alluvial sediment with high contents of antimony (Fig. 5).

Visible antimonial mineralisation is only recorded from the southern section of the greenstone belt. Bindheimite (hydrous antimonate of lead) occurs in the She gold lode and at the She antimony-lead prospect 300 m farther north (Fig. 5). The same mineral is associated with the Oban, Buckingham and Motjane gold deposits. Argentiferous tetrahedrite ($CuAg_{12}Sb_4S_{13}$) is abundantly developed in the Avalanche gold deposit, and ullmannite (NiSbS) enclosed in pyrite is documented below from the Ivanhoe Acid Reef (see Forbes Reef gold deposits). Nests of stibnite have been reported from the Primrose lode and in the central section of the greenstone belt from Piggs Peak New Section.

None of these occurrences is considered to be of economic interest for its antimony content alone. The largest deposit is the prospect north of the She gold deposit (Fig. 5) where antimony and lead mineralisation occur within a unit of deeply weathered phyllites within the Moodies Group. Mineralisation is associated with pods and stringers of sugary quartz aligned in the schistosity and inclined at ±70° toward the south.

A strike length of 275 m at the She prospect was examined in trenches dug at 40 m intervals (Hunter, 1962). The main mineralised zone is siliceous in composition, ±90 m long and 0,9–1,4 m wide. A maximum value of 0,56 per cent Pb and 0,60 per cent Sb over 0,3 m, and an average value of 0,30 per cent Pb and 0,21 per cent Sb over the entire width of the zone were returned from 18 assays (Hunter, 1962).

A single borehole (BH 292, Ann.Rept., 1966) intersected the horizon 90 m below surface but cores recovered contained no antimony or gold. Lee (1964) also reported that gold determinations on samples collected from the surface trenches assayed trace.

High antimony-lead values occur in phyllites of a similar type to the She prospect in ground between the She and Oban gold deposits (see Fig. 36). Average contents of 1,42 per cent Pb, 0,91 per cent Sb and 2,75 g/t Au over 0,78 m were given by Hunter (1962) for 3 assays of samples taken over a strike length of ±630 m (see also sample 8, Table 27).

Bright yellow-coloured antimonial pods in talcose schist have been described by Clarke (1971 a) from Motjane Reefs (Fig. 5). Lenses of this type are ±0,1 m in size, and associated with a swarm of southeast-striking quartz veins. Bindheimite together with malachite, crocoite, galena and erratic gold and silver values (as much as 40 g/t Ag) are present in the mineralised zone. Large crystals of tourmaline (>50 mm), considerable amounts of chromiferous sericite and extensive deposits of soapstone also occur at the same prospect. (see sample 10, Table 27). Clarke reports that 4 assays give average values of 0,2 per cent Sb, 0,9 per cent Pb, 0,2 per cent

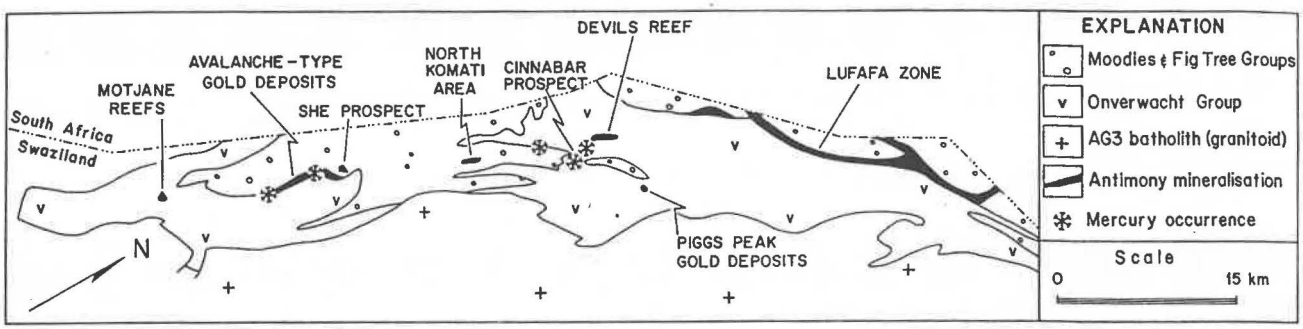

Figure 5
Distribution of antimony and mercury mineralisation in northwest Swaziland.

Cu, 2,5 g/t Au and 5 g/t Ag over a 2,5 m width.

Antimony mineralisation in the Lufafa zone appears to be much lower in grade. Values of ±10 ppm Sb in units of quartz-chromiferous sericite schist and brecciated iron-formation, both of which are associated with moderate gold values, are considered typical (samples 10–12, Table 26).

A horizon of carbonated amygdaloidal mafic lava in the Moodies Group near Makonjwa mountain (see Fig. 2) is associated with gold and arsenic mineralisation (sample 13, Table 26). This unit appears to be the source of anomalous antimony values in streams draining the Ntintinyane basin. The extent of mineralisation in this area has not been defined.

An extrusive horizon of a similar type has been described by Visser (1956) and Anhaeusser (1976 a) from the middle formation of the Moodies Group in the Eureka Syncline. The same horizon may be represented in a more deformed phyllitic state at the She antimony prospect, and within the Moodies Group sequence between She and Art Union gold deposits (Fig. 36).

MERCURY

Cinnabar, the distinctive red-coloured sulphide of mercury, has been documented from 5 localities in northwest Swaziland (Fig. 5) Gold lodes at Art Union and Waverley in the Forbes Reef area both contain visible cinnabar, with values as high as 2,5 per cent Hg reported from the Art Union deposit (Sims, 1981). Other base metal-rich gold occurrences in the same area (Avalanche-type deposits) also contain anomalously high mercury values (samples 8–10, Table 27).

Farther north, a discontinuous zone of mercury mineralisation is present along the tectonic break between Onverwacht and Fig Tree Group sequences immediately west of Nottingham Peak (Fig.2). Cinnabar, together with malachite and tourmaline stars occur in sericitic lithologies adjacent to a tectonic sliver of talcose schist. Bushell (1972) reported that trenches totalling 155 m in length were dug in heavily mineralised areas but that the best assay (Goldfields laboratory) contained only 0,05 per cent mercury.

Jones (Ann. Rept., 1966) reported the presence of cinnabar in the main lode at Nottingham Hill gold deposit. In structural position the Nottingham Hill gold deposit is identical with the prospect described above, and the two cinnabar occurrences are considered to be strike equivalents.

The largest mercury deposit in Swaziland (the "Cinnabar Prospect", Figs. 5 & 6) is located on a ridge 4,5 km southwest of the Piggs Peak gold deposit. The Cinnabar Prospect was mapped and described by Urie (1960), who noted the presence of a small quarry, a shallow shaft, an adit and numerous trenches (Fig. 6). The early history of the deposit is not known.

The geological structure of the Cinnabar Prospect can be described in terms of at least three thrust slices (Fig. 6). Each slice consists of a basal unit of talcose schists ±30 m thick overlain in turn by quartz-chromiferous sericite schists (10–20 m) and silicified shales (30–40 m). Fac-

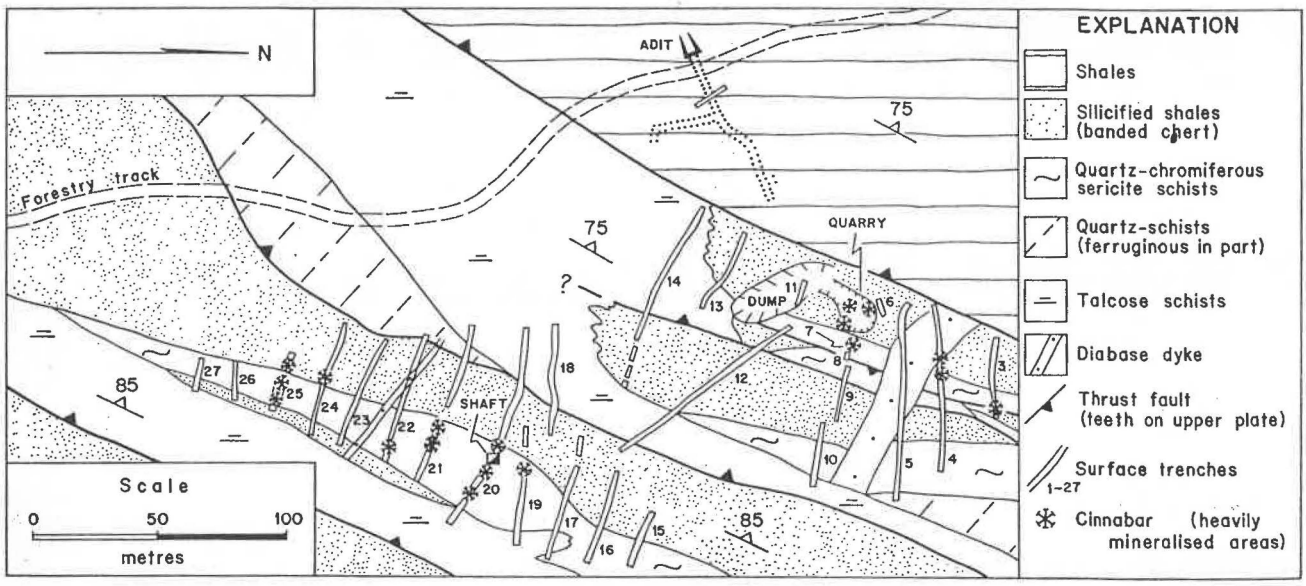

Figure 6
Geological plan of the Cinnabar Prospect (after Urie, 1960).

ing directions inferred from the lithological stacking sequence are toward the west and slightly overturned. Tectonic slivers of intensely deformed quartzites and conglomerates of the Moodies Group occur along both strike extensions of the deposit.

Cinnabar is widely distributed in both quartz-chromiferous sericite schists and sericitic chert units, though because it is so sparsely disseminated it is not always visible. The greatest concentration of mercury occurs in the quarry chert unit (Fig. 6), where cinnabar is associated with mm-sized stringers of black quartz, bright green-coloured chromiferous sericite and iron oxides. Quartz stringers of a similar type occur near the shaft (Fig. 6) and are also associated with visible cinnabar. In both occurrences, cinnabar occurs within quartz veinlets as well as along foliation surfaces.

In addition to cinnabar, Urie (1960) reported that hematite, magnetite, pyrite, limonite, botryoidal manganese oxides, tourmaline needles and occasional specks of gold were observed in panned concentrates. The same author described quartz stringers with iron and manganese oxides but no mercury in the yellow-brown-coloured shale formation west of the quarry (Fig. 6).

A geochemical analysis of chromiferous sericite schist with quartz stringers and visible cinnabar is given as sample 5 (Table 26). The analysis contains above average abundances of Au, B, Ba, Sb, and Cr, and an extremely high W content (244 ppm).

A maximum content of 0,47 per cent Hg and an average value of 0,21 per cent Hg over 0,7 m are given by Urie (1960) for samples taken in the quarry (see also sample 5, Table 26). Elsewhere, Urie reports that 634 samples ±0,9 m long (occasionally 0,6 m) were cut from old trenches. Samples were panned, and those collected from trenches 4, 7, 20, 21 & 25 (Fig. 6) were sent for assay. Maximum values of 0,13 per cent Hg were obtained from trenches 20 & 25, and the average value of all 25 determinations was 0,03 per cent Hg over 0,91 m. An additional 18 samples taken from the adit were panned but revealed no minerals of economic worth.

Urie (1960) concluded that the distribution of more highly mineralised areas is very erratic (see Fig. 6). While values of economic grade occur locally, for example in the quarry, the available tonnage is too small to be considered a mining proposition.

Field relations indicate that the distribution of both antimony and mercury mineralisation in Swaziland is controlled by patterns of faulting. A model in which volatile metal species were distilled along thrusts around the low-temperature margin of a geothermal field associated with emplacement of the AG3 batholith is described elsewhere (see origin of the gold deposits). Bailey and others (1975) reported that all mercury deposits in California occur within ±1 km of the Coast Range thrust.

ASBESTOS

The Havelock asbestos deposit in northwest Swaziland is one of the most important occurrences of cross-fibre chrysotile in southern Africa. Asbestos has been mined continuously from the Havelock deposit since the 1930s, and may continue to be mined until the turn of the twenty-first century. Total recorded production of chrysotile asbestos from Havelock (1939–1980) is 1,25 $.10^6$ tons, an average of 30 000 tons per annum.

The contribution of asbestos sales to the economy and development of Swaziland has been substantial. During the early years of production, asbestos was the most valuable export commodity in the Kingdom, surpassing both sugar and wood pulp. Sales of asbestos are still an important earner of foreign currency, and in 1980 accounted for 85 per cent of the total ex-mine revenue in Swaziland.

HAVELOCK ASBESTOS DEPOSIT

The Havelock mining lease area falls within the now lapsed Mineral Concession 41, originally granted to Thomas Rathbone on behalf of a prospecting syndicate. In 1886, the area ceded to Rathbone was named the Havelock Concession, after the then Governor of Natal, Sir Arthur Havelock.

Though gold and asbestos were discovered on the Concession in 1887, asbestos did not receive serious attention until 1918 when Izaak Holtzhausen of Barberton rediscovered the Havelock deposit. The present owners began underground exploration in 1929, and exercised their option to purchase the property in 1930. Opening of the mine was delayed until 1939 when the first fibre was processed by the mill. An aerial ropeway was completed during the same year, and connects the mine with the nearest railhead at Barberton. The ropeway is 20 km long, and transports the asbestos over the rugged terrain of the Barberton Mountainland.

Early quarrying operations at Havelock gradually declined and by 1948 the operation became almost totally sub-surface. At first, the mine was served by a three-compartment incline shaft comprising two hoisting compartments and one travelling way. Since 1964, access to the mine has been via a single 6,1 m diameter vertical shaft. The principal mining method is a type of caving (sub-level shrinkage), in which sub-levels are established at 12 m intervals and main haulage levels 72 m apart.

Regional geology

The Havelock ultramafic complex is one of a number of steeply inclined serpentinite bodies that crop out along the southeastern edge of the Barberton greenstone belt (Fig.7). Deformation and associated chemical and mineralogical alteration are characteristic of this ancient tectonic regime. In Swaziland, serpentinites are often found close to large thrust faults and are extensively replaced by talc. The Havelock body is one of the better preserved serpentinites, and the only one in Swaziland to contain economic vein chrysotile (Urie, 1961).

According to the stratigraphy of Viljoen and Viljoen (1969b), the Havelock serpentinite occurs as a conformable lens within the uppermost division of the Onverwacht Group (Swartkoppie Formation of the Mafic to Felsic Unit). These authors maintain that serpentinite pods of the type shown in Fig. 7 occupy stratigraphic horizons within the Onverwacht Group. They consider that both the Havelock body and the closely related Msauli serpentinite in South Africa (Fig. 7) originally formed a continuous or near-continuous differentiated sill. Viljoen and Viljoen believe that deformation has disrupted the sill and produced isolated serpentinite boudins.

The geology of the area between Havelock and Msauli Mines is not known in detail. According to Visser (1956),

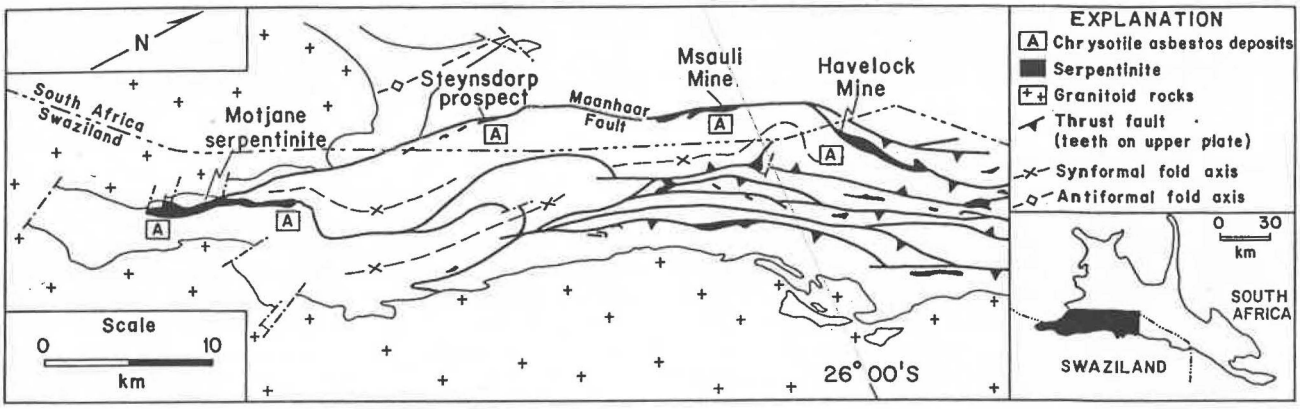

Figure 7

Simplified interpretation of the principal tectonic elements along the southeastern edge of the Barberton greenstone belt (inset), showing locations of the Havelock and Msauli chrysotile asbestos mines, and the Steynsdorp and Motjane prospects. The Motjane serpentinite body contains antigorite in significant amounts, and uneconomic deposits of brittle chrysotile fibre. Structural data are based on the Swaziland Geological Survey 1:25 000 map series (Hunter and Jones, 1969; Urie, 1970, 1971) with modifications, and unpublished mining company reports. The fold structure west of the Steynsdorp prospect (Steynsdorp Anticline) is taken from Viljoen and others, (1969, Fig. 2).

the serpentinite is not a continuous body and is faulted out for at least part of its length. The Msauli serpentinite is itself located on a similar structural trend to an abandoned chrysotile prospect in the Steynsdorp valley (van Biljoen, 1959, and unpublished mining company reports; Fig. 7). There have been suggestions (e.g. Pretorius, 1961) that south of the Steynsdorp prospect the same asbestos-bearing "line" may reappear in Swaziland near Motjane (Fig. 7)

The area which includes the Havelock body has been mapped by the writer (Fig. 8). Field relations show that the Havelock serpentinite is elongate and closely aligned with the regional structural trend. For most of its length the serpentinite body is inclined at 45°–70° toward the south or west.

Regional deformation in the area south of the mine has produced large refolded isoclinal folds. Axial surfaces of first folds are sub-parallel to the margin of the ultramafic body, and to a single steep cleavage. Second-phase folds are open structures with no associated cleavage. Both deformations are recorded in talcose schists and volcaniclastic lithologies of the Onverwacht Group as well as in younger sequences that include banded iron-formation and shales of the Fig Tree Group.

The structural thickness of the Havelock serpentinite varies considerably. West of the mine, the serpentinite has been tectonically thinned by a steep fault along the southern edge of the body, and adjacent lithological units are clearly truncated by this fault. East and southeast of the mine, the serpentinite is repeated by imbricate faults and the apparent structural thickness increased by the tectonic inclusion of rafts of country rock. Serpentinite adjacent to imbricate fault surfaces is extensively altered to talc.

The northern or footwall margin of the serpentinite is also a thrust surface, but it is not marked by a major talc zone of the type found within and along the southern edge of the body. Banded iron-formation in the immediate footwall is offset by transverse faults, but never obliquely truncated by the serpentinite. The history of deformation along the basal thrust appears to differ from other fractures associated with the serpentinite.

A major tectonic break, known as the Maanhaar Fault, is closely associated with asbestos-bearing serpentinites in

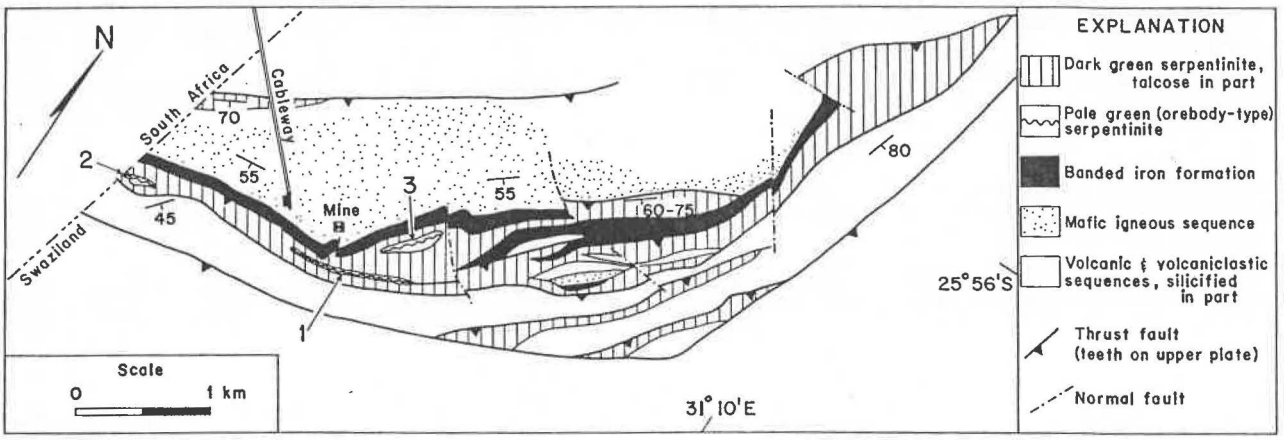

Figure 8

Geological map of the Havelock ultramafic body, based on mapping by the writer, with data from Urie (1961). Pale green, asbestos-bearing serpentinite occurs within the Havelock body in three main areas: 1. Havelock orebody (see Fig. 9); 2. Havelock West prospect; 3. footwall body (slip-fibre only).

The Havelock complex is interpreted as an allochthonous serpentinite body that was emplaced along thrusts toward the northwest; tectonic slivers of serpentinite and talc schist are present south of the main body and are interpreted as thrust imbrications. The mafic volcanic sequence north of the basal serpentinite décollement attains its maximum stratigraphic thickness immediately below the producing orebody.

adjacent parts of South Africa. The Maanhaar Fault truncates the eastern limb of the Steynsdorp anticline (Viljoen *et al.*, 1969; Fig. 7), but the position of the fault elsewhere, and the nature of its displacement have not been documented.

Mine geology

Vein chrysotile occurs within the dark green Havelock serpentinite in three distinct pale green bodies (Urie, 1961; Fig. 8). Apart from the main producing orebody, only the Havelock West prospect adjacent to the border with South Africa contains significant amounts of cross-fibre (fibre that occurs in seams oriented at a large angle to the seam wall).

A geological plan of the mine, and cross-sections representative of the main east and west ore shoots are shown as Figs. 9, 10 & 11. Both orebody and non-fibrous serpentinites are inclined south at 50°–60°; lithology and structure are described below in a traverse from north to south.

Footwall

A full description and interpretation of two very distinctive lithological units that occur in the structural footwall of the Havelock body is given elsewhere (see Fig. 40). A lowermost pillowed mafic igneous unit is exposed in the western mine section (Fig. 10), and is considered to be an extrusive sequence of broadly tholeiitic composition that has been subjected to a "spilitic metamorphism". Carbonate (ankerite/ferrodolomite) iron-formation immediately overlying the mafic igneous sequence is essentially unmetamorphosed. However, mineralogical observations show that close to the serpentinite, the uppermost member of the same 35–40 m thick iron-formation is moderately metamorphosed to mixed oxide-silicate facies (magnetite — minnesotaite — ferroactinolite). Metamorphic isograds within the iron-formation parallel the base of the ultramafic slab and are structurally inverted.

Serpentinites and related rocks

East of zero section in Fig. 9, the footwall iron-formation strikes north away from the main orebody. The thickness of serpentinite increases rapidly, and includes an additional mass of pale green serpentinite of the orebody-type. Though the colour and texture are identical with the main chrysotile deposit, this pale green footwall body is not known to contain economic fibre. Fibre that does occur is usually of the ribbon-type, and where exposed underground (7E) it has a maximum length of 1,5 mm. There, the fibre is in closely spaced parallel fractures, and accounts for less than 1 per cent of the total volume.

In addition, borehole data near 2E show a 10 m wide zone of 1 per cent brittle cross-fibre close to the footwall iron-formation. Unlike most cross-fibre at Havelock, this fibre occurs in dark green serpentinite.

One of the main features of the central and eastern mine geology is a major talc zone (Fig. 9). Where talc is schistose and oxidised by the circulation of meteoric waters, the trace of a fault (the talc shear) has been mapped. Massive talc is typical of the margins of the zone. In thin-section, talcose lithologies contain conspicuous octahedra of magnetite.

The talc shear records an apparent 40 m left-lateral offset of a diabase dyke in the west ore shoot (Fig. 9). However, neither the relative age of dyke intrusion nor the complete displacement history of the talc shear are known with certainty. Near the dyke, chrysotile fibres lose their silky properties and no longer separate readily. This fibre deterioration is interpreted as the result of locally unfavourable conditions for chrysotile formation.

A discontinuous lithology known locally as "pseudochert" occurs within the eastern talc zone (Figs. 9 & 11).

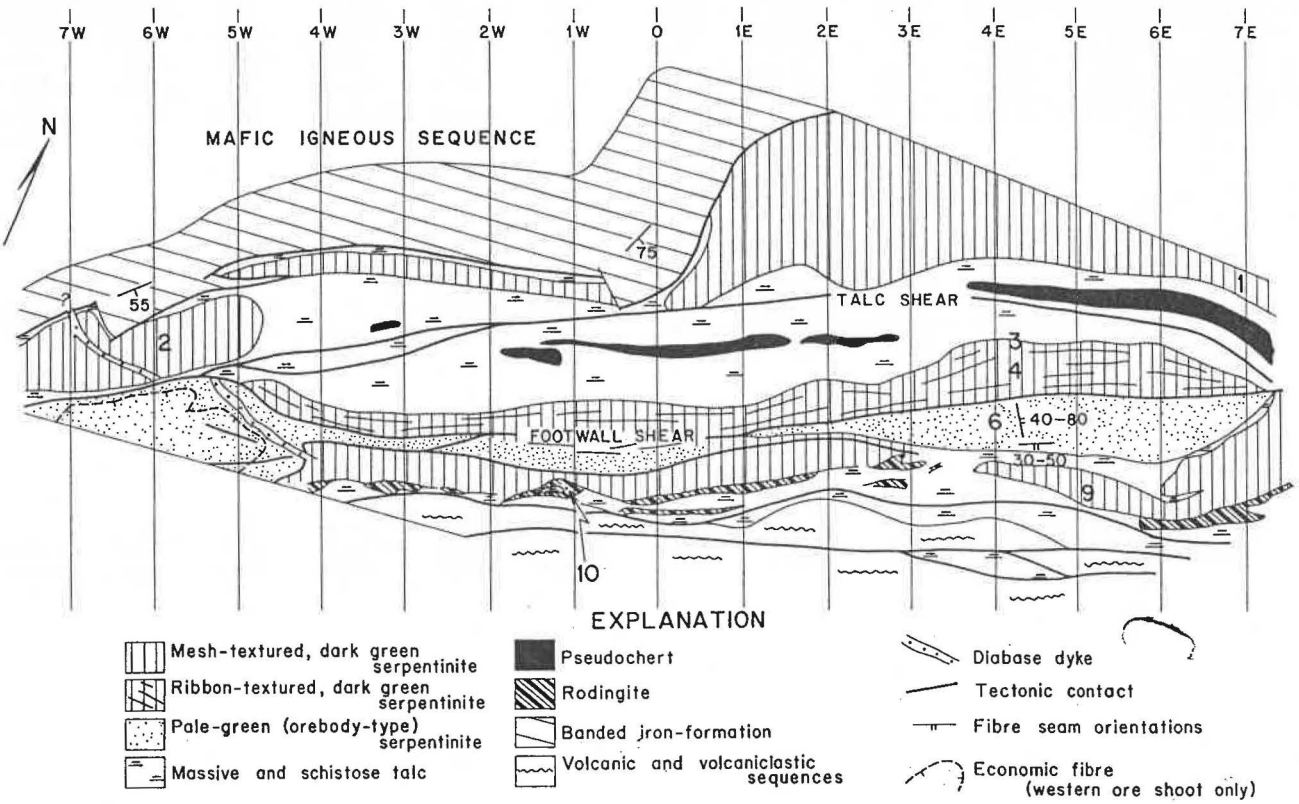

Figure 9

Plan of Havelock Mine geology at 390 level (*c.* 400 m below outcrop); mining blocks are 60 m wide. Dark green serpentinised dunite (with minor lherzolite) exhibiting mesh- and ribbon-textures occurs north of the footwall shear, and gives way to mesh-textured serpentinised harzburgite south of the orebody. Orientations of prominent fibre seam directions shown in the eastern ore shoot were measured on 315 level. Samples collected for chemical analysis on or close to 390 level are indicated by numbers (see Table 3).

Pseudochert is composed of black glassy silica, and contains pyrite and fractures filled with massive white quartz. Talc adjacent to the pseudochert is almost always foliated. Abrupt thickness variations occur both between levels (Fig. 11), and along the strike: at 7E the pseudochert is 17 m thick, but west of 3W on 390 level it is absent.

The orebody serpentinite is described in detail below. Here it is noted that the serpentinite in the east footwall of the orebody is highly deformed and contains a coarse foliation inclined at 50°–60° toward the south. As a result, the ground conditions for mining are particularly poor in the east footwall. In the west footwall, the serpentinite is massive, and the orebody has taken up more of the deformation.

Almost none of the serpentinites exhibits compositional banding. A single 50 cm-wide orthopyroxenite dyke is known in the relatively undeformed west footwall. Between 4¼ E and 5E (see sample locality No. 3, Fig. 9), serpentinite with an irregular streaking of opaque minerals forms the basal 4 m of the orebody footwall immediately above the talc zone. A similar lithology also occurs at 2½E close to the footwall iron-formation. The possibility the serpentinites of this type are more extensively developed toward the base of the footwall serpentinite body (particularly east of about 5E) cannot be excluded since few exploration data are available from this area.

Finally, a lithology known in local mine terminology as the "hangingwall sill" occurs along the upper structural surface of the Havelock serpentinite (Figs. 9 & 11). The calcium-rich mineralogy, and a coarse or pegmatitic texture, make the hangingwall sill a useful marker horizon. It is interpreted here as a rodingite, and in common with rodingites described elsewhere (e.g. Coleman, 1967) it is thought to have formed by metasomatism during serpentinisation.

Underground mapping and borehole data show that the hangingwall sill always occurs as irregular lenses and stringers (Figs. 9–11). Abrupt thickness variations to a maximum of 10 m are typical. Individual lenses are about 3 m wide and up to several tens of metres long. Inclusions of altered (talcose) serpentinite have been mapped in larger pods. Margins are irregular and frequently sheared; zones of cataclasis oriented at high angles to the margin of the serpentinite often terminate rodingite pods.

Rodingite mineralogy is variable: zoisite and tremolite (in the ratio 2:1) occur together with minor feldspars and calcite. Feldspars are replaced by, and enclose large euhedral epidotes. In addition, minor chlorite, small (30 μm) radiating bundles of a mineral presumed to be prehnite, pods of cataclastic quartz, and patchy green amphiboles which poikilitically enclose fresh albite are present. Hydrogrossular has also been observed in Havelock rodingites (C. Frick, personal communication, 1979).

Hangingwall

Underground development in the hangingwall is not extensive, and the description below is based on exposure between 1W and 5E (Fig. 9). There, a complex igneous and volcaniclastic pseudostratigraphy is present, which cannot be correlated along the strike with any certainty.

Massive and schistose talc adjacent to the rodingites extends into the hangingwall and rapidly gives way to a talc-colourless amphibole lithology. Long amphiboles (up to 5 mm) with sub-radiating habit, and a fine-grained talc matrix occur within 10 m of the serpentinite body. Textures of this type resemble metamorphosed dendritic and skeletal crystal forms that reflect rapid cooling from some magnesian liquids (spinifex-like textures).

Above, and in igneous contact with the talc-amphibole rock is a banded lithology with a volcaniclastic texture ("hangingwall chert"). This unit contains irregular iron-oxide coated fragments, mosaics of epidote and deeply embayed quartz crystals (about 5 modal per cent). Elsewhere, the same lithology is almost totally silicified by microcrystalline quartz. The upper surface of this 20 m thick unit is complex, and may represent a sheared igneous contact.

A deformed and metamorphosed mafic or ultramafic unit containing long (up to 30 mm) amphiboles is juxtaposed with the volcaniclastic lithology. Again, it resembles a unit with an original spinifex-like texture. Fragments of "pseudochert" and large tectonic blocks of talc schist occur within the sequence (Fig. 9), and suggest that the entire hangingwall has undergone extensive deformation.

Description of the Orebody

General occurrence

Pale green serpentinite is host to the vein chrysotile deposit. Both the colour and a granular or sugary texture distinguish the orebody from serpentinites that contain no fibre.

The transition from dark to pale green serpentinite is usually gradational. In the east footwall, the dark green serpentinite becomes progressively paler, the texture progressively more granular, and a coarse foliation more pronounced. Broken ground to a maximum of 20 m true thickness is associated with a major structure known as the footwall shear (Fig. 9). Pale green serpentinite in and adjacent to the footwall shear is highly fractured and extremely friable. Slip-fibre is smeared along many of the fractures, and the rock lacks cohesion and disaggregates in the hand.

The footwall shear forms the margin of the orebody in the eastern section of the mine. Farther west, fracture spacing and sometimes fibre length increase away from the footwall shear toward the orebody. As Fig. 9 shows, west of 5½W the footwall shear and main talc shear from a single fracture. There, the transition in colour from dark green footwall serpentinite to pale green orebody-type serpentinite is abrupt.

Gradational contacts occur along the edge of the orebody in the east hangingwall. Pale green serpentinite gradually gives way to dark green and eventually black serpentinised harzburgite. Though the colour changes are gradual, the decrease in economic fibre is rapid. Massive talc has replaced the orebody in the east hangingwall and complete talc pseudomorphs after chrysotile seams are well preserved. A hangingwall shear close to the upper surface of the orebody is only developed in the western section of the mine.

The colour of the orebody is not a uniform pale green and appears to vary with depth below surface. In the up-

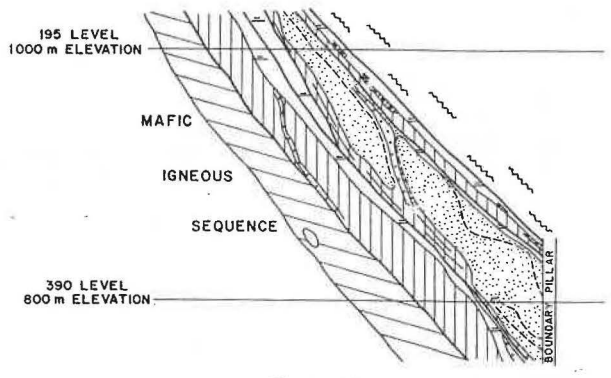

Figure 10
Cross-section at 5½ W, illustrating the main western ore shoot. Uneconomic fibre is encountered within the orebody at depth, and is shown enclosed by a broken line below 390 level. For explanation see Fig. 9.

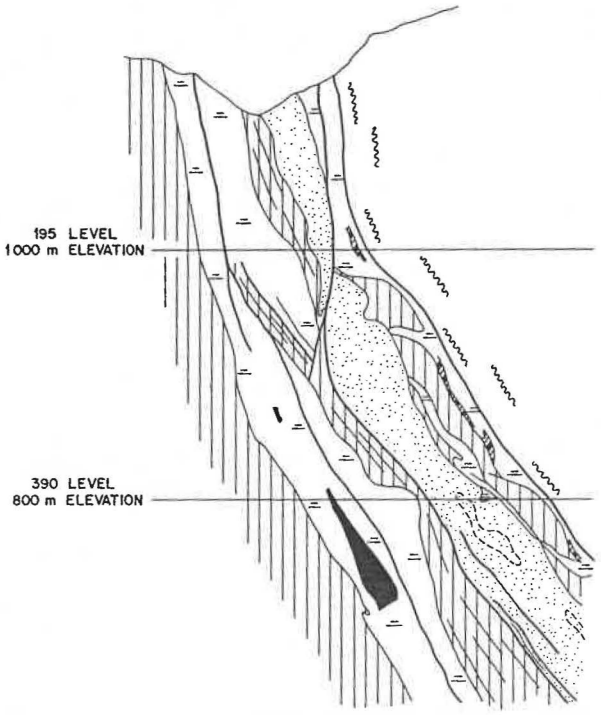

Figure 11
Cross-section of the eastern ore shoot at 4E. The footwall serpentinite exhibits extensive deformation, and above 230 level has been steepened by a near vertical shear. As in Fig. 10, broken lines within the orebody and below 390 level indicate massive, non-fibrous pale green serpentinite. Surface outline at 1975; for explanation see Fig. 9.

per abandoned mine levels, the orebody is a much paler (apple) green than that exposed in the lower levels. This relationship is also apparent when the considerably paler green waste dumps at the Msauli deposit are compared with those at Havelock. Msauli is a much more recent underground operation, and producing levels at the time of writing are still relatively close to the surface. Thus the colour of the orebody seems to be related, at least in part, to the present topography. It is noted that the main talc and footwall shears at Havelock are oxidised to at least 550 level, approximately 500 m below surface.

The average *in situ* fibre content of the orebody is about 5,5 per cent. Mean fibre length is difficult to specify because each grade produced at the mill (Turner & Newall grades 3, 4, 5 & 1877) includes a range of different sizes. A value of 4–5 mm is probably realistic for the most fibre produced between 245 and 340 levels (250–350 m below outcrop).

Though fibre lengths of 60 mm have been recorded in the upper levels of the mine, spinning fibre is not a significant component of the orebody and there is very little short fibre. Both length and amount of fibre decrease with depth in the mine. In addition, the fibre is a better quality (silkier and paler in colour) in the ore shoot west of the dyke (Fig. 9).

Massive non-fibrous serpentinite occurs within the orebody in the lower mine levels (Figs. 10 & 11). Uneconomic chrysotile of this type is a translucent green colour, and lacks the granular texture of the orebody. The sudden appearance of this massive material at depth also suggests that the total fibre content of the orebody decreases down-dip.

Geometry

A true thickness longitudinal projection of the orebody is given in Fig. 12; data from the upper levels (above 245 level) in Fig. 12 are based on old records, and should be regarded as approximate. Thus, while the surface geological map (Fig. 8) shows the orebody schematically as a continuous unit, it may have cropped out as two or more lenses separated by faults. It is probable that faulting reduced the thickness of the orebody to 10 m or less near zero section (Fig. 12).

The total strike length of the deposit is at least 1 200 m, and as Figs. 10 & 11 show, the attitude is rather uniform (inclined at 50°–60°) except east of about 2E and above 230 level where it is near vertical. There, the orebody has been steepened by an oblique shear.

Maximum fibre development occurs at the two extremities of an elongate and broadly elliptical orebody (Fig. 12). At the edges of both ore shoots the thickness decreases rapidly. Talc has eaten away at the orebody in the east, and accounts for the reduced thickness in the vicinity

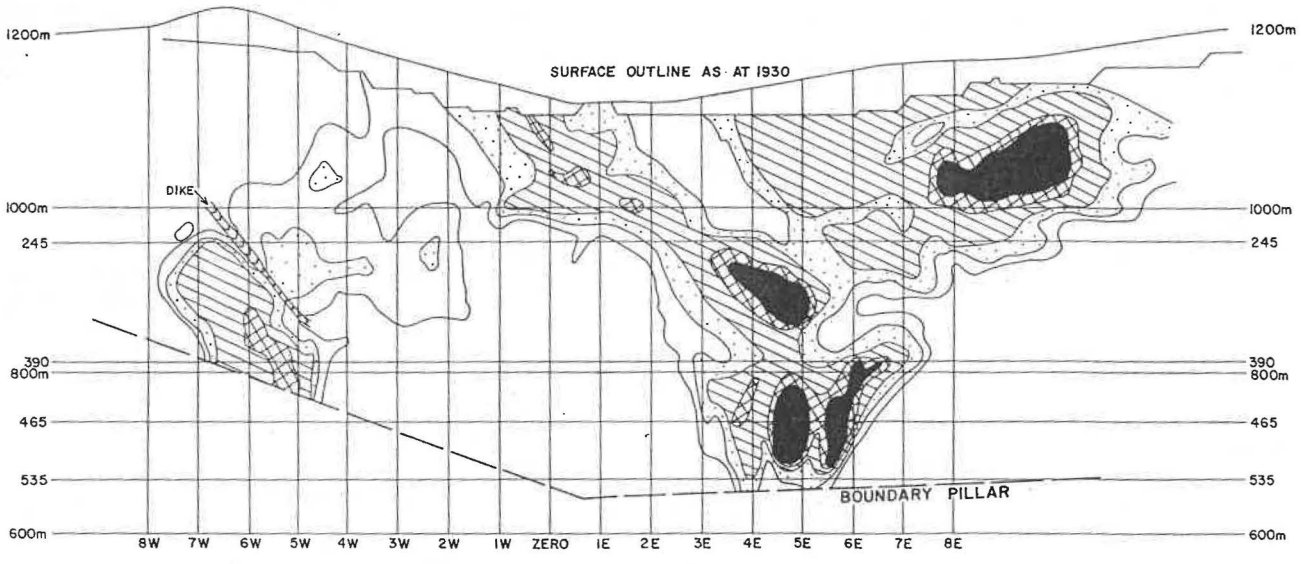

Figure 12
True thickness longitudinal projection of the chrysotile orebody; contours at 10, 20, 30, 40 and 50 m (black) thickness. True thickness is measured normal to the dip of the orebody at each elevation. Pale green serpentinite is present in the centre of the mine, but is mostly sheared and contains slip-fibre. The precision of data above about 245 level is uncertain.

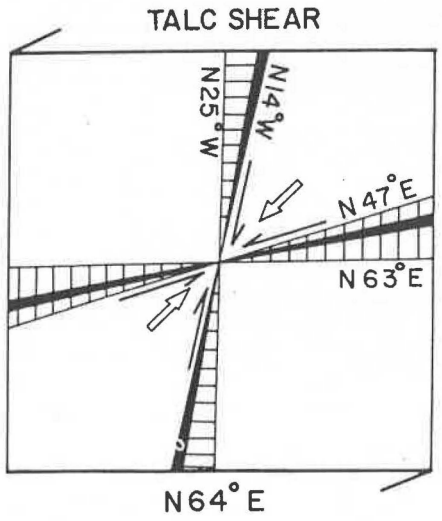

Figure 13
Measured fibre seam orientations (shaded angles) from the eastern ore shoot on 315 level. The simplest interpretation of these data is that the fibre seams represent failure directions resulting from simple shear, as predicted by the Coulomb failure criterion for a material with a peak angle of shearing resistance ϕ, varying between 2° and 34°, and a direction of shear corresponding with the orientation of the talc and footwall shears on 315 level (N 64° E). Black angles are the directions predicted by the Coulomb failure criterion for a material with $20° \leq \phi \leq 25°$, and the same direction of shear (see Tchalenko and Ambraseys, 1970). Other interpretations of the sense of movement on the talc and footwall shears are possible (see discussion in text).

of 315 level. The geometry of the orebody below the boundary pillar is unknown.

It is emphasised that pale green serpentinite is present in the centre of the mine, but that it is thin and highly sheared. A similar sheared lithology that carries less than 2 per cent of fibrous chrysotile is present in development immediately west of the mining lease area, and in the far west body adjacent to the border with South Africa (Fig. 8). Serpentinites of this type contain much of the chrysotile in the form of slip-fibre, that is fibres are oriented parallel or at a very small angle to the seam wall.

Economic chrysotile occurs as a stockwork of cross-fibre seams. There is, however, a pronounced tendency toward sub-vertical seam orientations. Holes drilled through the orebody at 45° to the vertical are most likely to intersect fibre seams at large angles and are therefore the most useful for fibre evaluation.

Structural measurements on 315 and 330 levels show that two seam directions are prominent within the stockwork. They are oriented at 1°–17° and 78°–89° to the strike (N 64° E) of the talc shear on 315 level (Fig. 13). Fibre seam orientations at Havelock are predicted by the Coulomb criterion for simple shear failure associated with a direction and sense of shear close to that inferred for the main talc shear assuming left-lateral strike-slip displacement (Fig. 13).

Fibre morphology

Illustrated descriptions of chrysotile fibre seams from southern African asbestos occurrences have been made available by van Biljoen (1959) and Laubscher (1964, 1968). In addition, fibre seams which closely resemble the chrysotile at Havelock have been described from Canadian asbestos deposits by Riordan (1955) and Laurent (1975). The morphology of crystal fibres in general is given in Durney and Ramsay (1973), and though these authors did not describe chrysotile asbestos specifically, their data are also applicable to this mineral.

Chrysotile seams at Havelock are usually planar, but may be curved or irregular in shape. Individual fibres may be straight, crenulated, kinked or curved, but invariably join points on opposite walls that were once in contact. Slip-fibre is sometimes present within cross-fibre seams, usually along one wall. In these cases, movement parallel to the fibre length has displaced the opposite walls.

Single cross-fibre seams are most common, but more complex types with a single median suture or more than one line of wall rock inclusions often occur. The median suture usually varies in position and is not always located in the centre of the seam. Wall rock material that forms the median suture is either picrolite or magnetite. Picrolite is a splintery, pale green variety of serpentine with a coarsely fibrous texture (see Table 2). A thin layer of picrolite and magnetite frequently separates wall rock and fibre along the length of the seam, it is also common parallel to fractures that contain no fibre.

The formation of crystal fibres by diffusion of fluids into dilating cracks has been described by Durney and Ramsay (1973). A similar mechanism is appropriate here, and is discussed below in more detail.

Serpentinite Textures

Two textural types are widespread within the Havelock body: a mesh-texture, in which the original protolith mineralogy can easily be recognised, and a ribbon-texture which records significant plastic strain.

Mesh- or replacement-textures are best preserved in the hangingwall serpentinised harzburgites, though they are also widespread in the west footwall and in the orebody. Serpentinised olivine grains are 300–2 000 μm in diameter, and in thin-section appear as sub-equant grains often with a central "cross-hatched" core. Orthopyroxenes are totally serpentinised but retain a well preserved cleavage and slightly higher birefringence. They have deeply embayed margins and poikilitically enclose serpentinised olivine grains. Where chrysotile fibre occurs, it is colourless, has lower relief and higher birefringence than the mesh-fabric. Fibre is always accompanied by an incipient ribbon-texture (see below) in serpentinised olivine grains.

Serpentinised lherzolite at the base of the east footwall contains a mesoscopic opaque streaking which in thin-section consists of a series of narrow (50–1 000 μm-wide) seams of fibrous serpentine that cut across a mesh fabric. Aggregates of magnetite are closely associated with these fibrous bands.

In the east footwall serpentinite, and near zones of relatively high strain within the orebody, the original mesh-texture has been destroyed. Instead, a series of parallel ribbons defined by alternating pale and dark grey (first order) interference colours are observed in thin-section. Serpentinised olivine grains are obliterated, and identification of orthopyroxenes is difficult. Every transition occurs between colourless serpentinised olivine grains with broad (100 μm-wide) ribbons, and highly deformed lithologies with ribbons less than 30 μm-wide and considerable carbonate alteration.

Mesh-textures are common in lizardite serpentinites (e.g. Coleman and Keith, 1971), and in serpentinites that have not undergone significant plastic deformation (Raleigh and Paterson, 1965). Thus, regions where mesh-textures are present at Havelock record relatively small strains, and are more likely to preserve the original serpentinite mineralogy.

Serpentinite Mineralogy

Identification of serpentine species

Unambiguous identification of the serpentine minerals is difficult, and requires a combination of techniques:

TABLE 1
Identification of serpentine species at Havelock Mine[1]

	Footwall	Orebody			Hangingwall
	1	2	3	4	5
X-ray Diffraction	lizardite + chrysotile	chrysotile; some lizardite	chrysotile	chrysotile	lizardite; some chrysotile
Electron Microscopy	chrysotile; trace lizardite or antigorite	chrysotile	chrysotile	chrysotile	lizardite or antigorite; some chrysotile
Differential Thermal Analysis	chrysotile or lizardite; trace antigorite	chrysotile or lizardite	chrysotile or lizardite	chrysotile or lizardite; trace antigorite	chrysotile or lizardite; trace antigorite

[1]based on data given in van Biljoen (1959).

Notes: 1, 2 and 5 show persistent X-ray diffraction lines at 2,49 Å (lizardite); lines at 2,45 Å and 2,09 Å (chrysotile) are present in all samples (1–5). 1. deformed east footwall with brittle fibre; 2. orebody whole-rock; 3. chrysotile fibre; 4. picrolite vein; 5. massive serpentinised harzburgite.

TABLE 2
Mineralogical composition of Havelock serpentinites

	Estimated original composition			Present modal composition		
	Olivine	Orthopyroxene	Chromite	Brucite	Magnetite	Carbonate
East Footwall	94,5	5,5 (0,5–10,5)	0,1 (0,0–0,5)	7,4	1,5 (1,0–2,0)	1,5 (0,5–3,0)
West footwall	94,0	6,0	0,1	13,4	0,9	0,3
Orebody	93,0	7,0 (5,0–8,5)	0,0	9,6	2,0 (0,2–5,6)	8,0 (5,0–12,5)
Hangingwall	86,0	14,0 (11,0–24,0)	0,3 (0,0–0,5)	15,5	0,8 (0,5–2,0)	0,5 (0,0–1,0)

Notes: all data except brucite in volume per cent; samples collected at or near 390 level (numbers in parentheses represent range of compositions). Brucite values (weight per cent) are semi-quantitative, and determined on carbonate-free samples by a dilute acetic acid digestion described by Hostetler and others (1966).

Table 1 summarises the available Havelock data. Though van Biljoen (1959) interpreted Havelock as an antigorite body, his data are reinterpreted here on the basis of criteria described in detail by Mumpton and Thompson (1975). It is noted that the samples described by van Biljoen were collected near 155 level (150 m below surface), and may not necessarily be representative of the orebody at depth.

Both massive and deformed serpentinites at Havelock are essentially lizardite-chrysotile mixtures. Trace amounts of antigorite were identified by Differential Thermal Analysis.

Original composition and present assemblage

The estimated variation in protolith composition of the Havelock ultramafic body is given in Table 2. Olivine, orthopyroxene, chromite and minor clinopyroxene are original protolith phases; feldspar was not identified in any of the thin-sections examined. Both footwall and orebody serpentinites are broadly dunitic in composition (less than 10 modal per cent orthopyroxene). The hangingwall consists of serpentinised harzburgite (11–24 modal per cent orthopyroxene), and accounts for the structurally uppermost 20–30 per cent of the ultramafic body.

Minor serpentinised lherzolite has been noted at the base of the east footwall between 4¼ E and 5E (Fig. 9), and in a narrow zone immediately above the footwall iron-formation at 2½E (Fig. 9). This lithology has a mottled appearance and exhibits an impersistent streaking of magnetite in layers 100–2 000 μm-wide and 20–30 mm apart. The original modal composition is estimated as olivine 80 per cent, orthopyroxene 15 per cent and clinopyroxene ±5 per cent. Clinopyroxene grains are fresh or only serpentinised in part.

Most serpentinites at Havelock contain significant amounts of brucite (Table 2), though in some samples brucite is present in amounts considerably less than predicted by Hostetler and others (1966), indicating that addition of silica or loss of magnesia was necessary. Sheared serpentinites of the east footwall contain less brucite than the massive equivalents.

Magnetite is present in all Havelock serpentinites: in the orebody and east footwall, mesoscopic concentrations are present, often parallel with the margins of chrysotile seams. Coarse aggregates composed of individual 1 mm-size octahedra are typical, and are especially prominent in pale green serpentinites. In ribbon-textured serpentinites, magnetite aggregates occur parallel with the ribbon fabric. Though mesh-textured lithologies such as the hangingwall harzburgite appear to contain less magnetite (Table 2), the equivalent amount may be present as a submicroscopic dusting.

The effects of alteration are generally much more extensive in the orebody than either footwall or hangingwall serpentinites. Magnesite accompanied by minor talc increase in amount with increase in deformation, and account for at least 20 per cent of the serpentinites close to the footwall shear. Because the amount of alteration varies considerably, the few carbonate determinations from 390 level given in Table 2 may not be entirely representative of the orebody. Pale green serpentinites from the surface and upper mine levels appear to contain rather more disseminated carbonates than at depth, though the present data are inadequate to state this with certainty. Semi-quantitative thermogravimetric determinations of chrysotile fibre show the following accessory minerals: 0,84 per cent brucite, 0,80 per cent magnetite, 1,71 per cent magnesite, 3,38 per cent talcose minerals (average of 17 determinations, unpublished report, Turner & Newall Ltd.).

TABLE 3
Chemical compositions of Havelock serpentinites, chrysotile fibre and rodingite

	1	2	3	4	5	6	7	8	9	10
SiO_2	36,76	37,23	39,31	37,92	33,82	35,59	39,96	36,91	37,42	28,32
Al_2O_3	3,10	3,42	4,34	2,71	1,57	2,02	0,85	3,52	3,16	20,60
FeO*	8,61	5,36	6,70	4,23	3,59	4,53	3,37	6,32	5,21	5,88
MgO	35,84	38,58	34,79	39,68	44,49	41,50	40,66	39,07	38,64	14,94
CaO	0,89	0,03	3,35	0,12	0,10	0,09	0,24	0,36	0,24	17,27
H_2O^+	12,86	12,86	10,89	13,54	15,05	14,59	12,67	12,66	13,18	12,29
H_2O^-	0,38	0,50	0,21	0,31	0,47	0,52	0,79	0,34	0,29	0,14
Cr_2O_3	0,20	0,27	0,27	0,26	n.d.	0,40	n.d.	n.d.	0,57	0,09
Total	98,64	98,25	99,86	98,77	99,09	99,24	98,54	99,18	98,71	99,53
MgO/SiO_2	0,97	1,04	0,89	1,05	1,32	1,17	1,02	1,06	1,03	

* total iron expressed as FeO; n.d. = not determined.

Notes: 1–2. footwall serpentinised dunites with mesh-textures, 390 level; 3. serpentinised lherzolite, 390 level; 4. serpentinised dunite with ribbon-texture, 390 level; 5. orebody, 155 level; 6. orebody, 390 level; 7. chrysotile fibre, 155 level; 8. hangingwall serpentinised harzburgite, 155 level; 9. hangingwall serpentinised harzburgite, 390 level; 10. rodingite, 390 level.
Samples 5, 7 and 8 taken from van Biljoen (1959); all other analyses performed by the Geological Survey, Pretoria (see Fig. 9 for sample locations).

Serpentinite and Rodingite Chemistry

Several analyses of Havelock serpentinites and a single analysis of a rodingite are given in Table 3. These geochemical data show that the serpentinites have a rather uniform refractory composition: they closely resemble ultramafic nodules, Alphine-type peridotites, and serpentinites dredged from the sea-floor (Hess, 1964).

Havelock serpentinites have high H_2O^+ (10,9–15,0 per cent by weight), and with the exception of sample 3, low CaO contents (0,03–0,89 per cent), values consistent with 100 per cent serpentinisation. The presence of minor unserpentinised clinopyroxene in sample 3 may account for the higher CaO content in that sample. In addition, Al_2O_3 contents are low (1,57–4,34 per cent), and TiO_2 and total alkalies are less than 0,17 per cent and 0,27 per cent respectively.

MgO/SiO_2 ratios of massive serpentinites in Table 3 (samples 2, 4, 6, 8 & 9) are consistent with values of serpentinised peridotites containing brucite, with 5–20 modal per cent orthopyroxene (Coleman and Keith, 1971). The orebody (sample 5) has a high MgO/SiO_2 ratio, which suggests either that the sample contains excess brucite, or that silica has been removed from the system. The value of 0,97 from the dunite of sample 1 is low. However, much of the footwall serpentinite body is deformed and MgO/SiO_2 ratios of sheared dunites decrease to values near unity (Coleman, 1971). Sample 3 has a MgO/SiO_2 ratio (0,89) typical of serpentinised lherzolites and consistent with the pyroxene mineralogy already described.

Representative total iron contents (recalculated as FeO) of totally serpentinised dunite and almost totally serpentinised harzburgite are given as 5,51 per cent and 7,00 per cent respectively by Coleman and Keith (1971). Data in Table 3 show similar values (5,2–8,6 per cent) for the massive serpentinites, but anomalously low values for the sheared east footwall and orebody (samples 4–6). These three samples appear to be depleted in iron, possibly by as much as 1,5 per cent.

Serpentinisation that accompanied deformation of the Havelock body was not isochemical. Deformed serpentinites contain less iron, silica and alumina, and more magnesia and water than their undeformed equivalents.

Chemistry of the "hangingwall sill" (sample 10) is qualitatively similar to that of rocks described elsewhere as rodingites (Coleman, 1967; Honnorez and Kirst, 1975). Enrichment in H_2O^+ and CaO, and depletion in SiO_2 are characteristic of rodingites. Rodingites similar in composition to that described here have been reported from the equatorial mid-Atlantic fracture zones by Honnorez and Kirst (1975).

Interpretation

Origin of the ultramafic body

Were the Barberton greenstone belt not so closely associated with the occurrence of igneous rocks that crystallised from ultramafic magmas, one would have little hesitation in describing the Havelock body as an Alpine-type serpentinite. Structural relations show that the serpentinite is associated with a major tectonic break (Fig. 8). It is an elongate, mesh-textured lizardite body with faulted margins and associated rodingites. Serpentinites of this type are known elsewhere as Alpine-type serpentinites, and have been widely described from many younger orogenic belts. The assemblage lizardite — chrysotile — brucite — magnetite is consistent with the majority of Alpine-type serpentinites (Coleman, 1971).

However, volcanic and sub-volcanic rocks derived from melts that contained over 30 per cent MgO are not considered unusual in the Barberton area. Therefore we cannot reject the hypothesis that the Havelock body represents an ultramafic sill, either because of the bulk composition or from structural evidence alone. Indeed, in an area where deformed stratigraphic sequences of ultramafic composition have been described (Viljoen and Viljoen, 1969a), it may not be easy to distinguish in the field between a mantle- and crustal-derived serpentinite. Here it is noted only that the Havelock body does not exhibit several of the features normally associated with high-level floored intrusions.

Chemical data show that the unaltered Havelock serpentinites contain 35–40 per cent MgO (Table 3). Dunites and harzburgites with these compositions could have formed after relatively small amounts of fractionation of a peridotitic liquid. However, if gabbros or similar differentiates existed once they are now missing, and the reason for this absence is unknown.

Compositional layering is also conspicuously absent. Compositional layering itself is not necessarily indicative of magmatic processes, and in Alpine-type peridotites may be largely deformational in origin (Thayer, 1963; Dick and Sinton, 1979). Features that do characterise magmatic sediments include cryptic variation and progressive changes in composition. It is recognised however, that serpentinisation may have obscured such features at Havelock.

The nature of the original compositional change from dunite (<10 modal per cent orthopyroxene) in the Havelock footwall and orebody, to harzburgite (24 modal per cent orthopyroxene) in the hangingwall is interpreted in terms of fractional crystallisation dominated by the separation of olivine. Progressive changes in mineralogy of this type are often associated with magmatic cumulates, and

are known in ultramafic rocks emplaced by tectonic processes (e.g. Page, 1967). Cumulus sequences form an integral part of many tectonically emplaced ultramafic bodies such as ophiolites. A comparison of the clinopyroxene and chromian spinel compositions at Havelock with those described from metamorphic peridotites and layered intrusions elsewhere may provide less ambiguous evidence.

Harzburgite textures at Havelock resemble those described in ultramafic rocks formed by igneous processes, either in layered intrusions or as part of a cumulus sequence within a tectonically emplaced body. However, qualitatively similar embayed pyroxene textures from an Alpine-type peridotite have been interpreted in terms of deformation processes (Dick and Sinton, 1979). The interpretation of textures in fresh ultramafics is not straightforward, and in serpentinites is equivocal at best.

It could be argued that those lithologies in the structural hangingwall that exhibit spinifex-like texture represent a chilled border facies to the ultramafic body. It is apparent from surface and underground mapping that while talcose schist with elongate tremolite locally occurs in tectonic contact with the serpentinite, elsewhere the same lithology is either absent or contained *within* the hangingwall sequence. Therefore, though possibly related in some way to the occurrence of magnesian liquids, this lithology in no way resembles a continuous chilled border. The absence of such a border facies along both margins of the Havelock body is consistent with tectonic emplacement.

Narrow zones of amphibolite and structurally inverted metamorphic aureoles of the type described briefly from the Havelock footwall are present at the base of several obducted slabs of ophiolite (see Coleman, 1977 for a review). The formation of such metamorphic zones is usually considered to result from the downward conduction of heat from the overlying slab, or shear heating at the fault or some combination of these processes (Graham and England, 1976; Woodcock and Robertson, 1977).

Origin of the asbestos

Internal deformation of the serpentinite, and formation of the chrysotile orebody appear to have been synchronous. A zone of ribbon-textured serpentinites occurs along one margin of the orebody. Foliation surfaces within this zone are parallel or sub-parallel to the length of the orebody, and to the talc and footwall shears. Well preserved mesh-textures only occur toward the edge of the serpentinite, and are thought to record rather smaller strains.

The chrysotile orebody exhibits evidence of deformation by pressure solution — diffusion processes. Analogy with textures described for fibrous growth by Durney and Ramsay (1973) suggests that chrysotile asbestos fibres are syntectonic phenomena, and that growth was synchronous with progressive fissure dilation. At Havelock, fibre length (the amount of dilation) decreases with depth in the mine.

Other observations, particularly the hydrated and carbonated nature of the orebody, and the presence of linear talc zones that contain elongate pods of silica (pseudochert in Figs. 9 & 11) are consistent with massive circulation of fluids. The broadly tabular shape of the orebody, and the fault-like geometry of the talc zones indicate that fluids travelled along structural surfaces parallel with the margins of the serpentinite body. The degree of orebody hydration and the extent of talcose alteration also decrease with depth below surface and suggest a decrease in fluid activity in this direction.

Pressure solution processes and the extent of fluid motion together account for the observed distribution of magnetite within the pale green orebody. Magnetite occurs in concentrations parallel with fibre seams, and forms progressively coarser aggregates as serpentinites become progressively hydrated and paler in colour. Down-dip colour variations from pale to dark green within the Havelock orebody can thus be readily explained in terms of migration of magnetite during deformation and serpentinisation. The effects of any alteration superimposed by late or even present-day meteoric fluids is unknown.

Raleigh and Paterson (1965) noted that the serpentinites visibly damp at the end of their high temperature experiments were also paler in colour. Unlike the experimental material, textural and mineralogical observations show that there is no evidence for dehydration reactions in the Havelock orebody. It appears that in some tectonic environments, significant movement of pore fluid can occur in serpentinites at temperatures less than dehydration.

Though geochemical data are rather sparse, the low Fe, Si and Al-contents of hydrated and deformed pale green serpentinites suggest that formation of the chrysotile orebody was not an isochemical process. Evidence that supports this suggestion is described briefly elsewhere (see Havelock West ironstone pipe).

Two explanations satisfactorily account for the formation of the asbestos orebody in terms of deformation during faulting:

1. Deformation recorded by the orebody is consistent with a regime of *strike-slip faulting* that occurred during or after the tectonic event that turned the regional stratigraphy on edge.

The simplest interpretation of the mine geology is that the diabase dyke in the western ore shoot records the total offset along the talc and footwall shears. The dyke trend is not compatible with a tectonic stress regime of left-lateral strike faulting of the type suggested by the orientation of chrysotile fibre seams (see Fig. 13). Internal deformation of the serpentinite and formation of the asbestos orebody are consistent with relatively small (40 m or less) strike-slip fault displacements.

Dilatancy and fluid diffusion processes are widely believed to occur along several presently active strike-slip faults (for example, the San Andreas Fault), especially in those regimes where tectonic stress has risen to relatively high levels (Nur, 1972; Scholz and others, 1973). A dilatancy-fluid diffusion model is thought to account for anomalous changes in water flow and other physical parameters that occur prior to some present-day shallow earthquakes. The model assumes that the opening of dilation cracks results in an increase in pore volume, which itself induces fluid diffusion. The pressure of pore fluid gradually increases during diffusion and effectively reduces the frictional resistance until an earthquake is triggered.

The orebody at Havelock is close to a fault with an apparent strike-slip offset, and may have formed during the deformation that accompanied fault movement. Dilatancy within the orebody appears to have been largely rate controlled by diffusion. It is possible therefore that the formation of the asbestos deposit was accompanied by ancient seismic faulting.

2. Deformation associated with emplacement of the serpentinite is consistent with a regime of *thrust faulting*. Structural relations and the distribution of asbestos also indicate a pattern of strain that developed within the toe of a thrust sheet.

The autochthonous (or para-autochthonous) mafic volcanic sequence has a pronounced lenticular shape and attains its greatest stratigraphic thickness (±1 km) immediately below the orebody. One consequence of an irregular-shaped unit of this type appears to have been ex-

tensive repetition by faulting in the region where the serpentinite was driven across the southeastern side of the volcanic pile (Fig. 8). For this reason, it is suggested that deforming stresses close to the orebody accumulated in response to movement along an irregular décollement at the base of the Havelock body. Reverse faults and internal deformation of the serpentinite body are thought to be the hangingwall expression of a non-planar thrust surface.

This interpretation assumes that the talc and footwall shears are thrust faults initiated in the mechanically weakest serpentinites (dunites rather than harzburgites). Total displacement along these faults where they form a single fracture at the base of the western ore shoot is about 100 m, assuming thrusting toward 315°. Maximum dilation and the formation of asbestos orebodies occurred above the footwall shear in the upper thrust plate.

Progressive deformation of the serpentinite body during thrusting resulted in the eventual leakage of pore fluid through fractures, including some opened hydraulically. Dilatancy, fluid diffusion and the eventual destruction of the cohesive strength of the serpentinite were followed in turn by the circulation of talc-forming fluids parallel with thrust surfaces.

Field observations are consistent with both of the above models. Structural and stratigraphic evidence for regional telescoping along thrusts suggests that the second explanation may be more appropriate.

Summary and Conclusion

1. The Havelock orebody is a vein chrysotile deposit within the centre of an allochthonous and almost totally serpentinised dunite-harzburgite. Olivine, orthopyroxene, chromite and minor clinopyroxene are original protolith phases; plagioclase was not identified in any of the thin-sections examined. The primary serpentinite assemblage lizardite-chrysotile-brucite-magnetite is present, and it is probable that trace amounts of antigorite also occur. Lizardite is common in Alpine-type serpentinites, and is stable in all serpentinites at low grades of metamorphism (Coleman, 1971).

2. Major element chemistry of the undeformed Havelock serpentinites reveals rather depleted compositions. Ultramafic rocks with a comparable chemistry include tectonically emplaced metamorphic peridotites described from younger orogenic belts, and serpentinites that are forming today in oceanic fracture zones (Miyashiro and others, 1969). Refractory compositions that characterise ultramafic rocks of this type are widely believed to represent residual mantle material. Similar compositions may also characterise ultramafic rocks that occur early in the greenstone belt succession and represent "residual" crustal material.

3. Internal mineralogical variations within the Havelock body are conspicuously lacking. There are no compositional layers or gabbroic lithologies, both of which are ubiquitous in floored intrusions. An increase in orthopyroxene content from serpentinised dunites in the footwall and orebody, to serpentinised harzburgites in the hangingwall is comparable with variations of the type that characterise magmatic cumulates. Other evidence of magmatic sedimentation, such as cryptic layering has not been observed. Almost certainly, evidence of this type would be difficult to recognise in a deformed and almost totally serpentinised ultramafic body like Havelock.

4. Rodingites occur as discontinuous lenses along the faulted southern contact of the serpentinite. The calcium-rich mineralogy is consistent with metasomatism by Ca^{+2}–OH^{-1} type fluids during serpentinisation (Barnes and others, 1967; Barnes and O'Neil, 1969). The association between rodingites and the tectonic margins of serpentinites is well known (Coleman, 1967).

5. Structural relations and the absence of mafic differentiates suggest that the Havelock body was not emplaced into its present position by magmatic processes. Rather, the evidence is consistent with emplacement during tectonic activity. It is not known whether the serpentinite is highly allochthonous or derived locally from the ultramafic succession of the greenstone belt. Thus, the original suggestion by Viljoen and Viljoen (1969b & c) that the Havelock body represents a fragment of a sill may be correct, though their contention that the serpentinite occupies a stratigraphic horizon is disputed. The stratigraphy of the eastern margin of the Barberton greenstone belt proposed by these authors is clearly inappropriate since it does not allow for the effects of deformation.

6. Though both contacts of the serpentinite are tectonic, significant plastic strain is only recorded away from the margins, within the centre of the body. Increasing strain is recorded as the progressive destruction of mesh-textures. Neocrystalline olivine is absent, and this absence suggests that the ribbon-textured serpentinites developed in a low temperature environment of relatively rapid stress accumulation where the pore fluid pressure could not be maintained at the equilibrium value.

7. The morphology of vein chrysotile in the Havelock deposit is closely comparable with the syntectonic fibres described by Durney and Ramsay (1973). It is suggested by analogy that much of the fibrous chrysotile was derived from the surrounding rock by diffusion, and redeposited synchronously with incremental fissure dilation. The diffusion gradient may have been the result of increased pore volume that accompanied dilating cracks. In the orebody, dilatancy and diffusion took place at temperatures below dehydration. According to experimental data, dehydration of mesh-textured lizardite serpentinites occurs in the 300°–350° C temperature range (Raleigh and Paterson, 1965).

8. It is suggested that the orebody formed in the uppermost levels of the crust near the leading edge of a thrust sheet. Field observations in Swaziland indicate a correlation between the distribution of deformed and extensively hydrated pale green serpentinites, and regions of complex thrust faulting where the basal décollement is not a simple planar surface.

OTHER ASBESTOS OCCURRENCES

Havelock West deposit

In addition to the main asbestos deposit, a smaller deposit of cross-fibre chrysotile (the Havelock West prospect) occurs within the Havelock serpentinite body. Havelock West crops out almost entirely in Swaziland, immediately adjacent to the border with South Africa (Fig. 63).

The Havelock West prospect was first described by Urie (1961) who reported a 13,4 m-wide zone of 3,2 per cent fibre (locally 4,5 per cent) in seams inclined south. Significant amounts of 6 mm-long silky fibre are present on surface, and fibre lengths of 9,5 mm were recorded. All cross-fibre chrysotile occurs within a lens of apple-green serpentinite that forms part of the main dark green Havelock body (Fig. 8).

Between 1970–1971, the deposit was assessed by a mining company, and the results of this exploration work summarised in Bushell (1972). From an incline winze in the footwall, drives east and west were developed on three levels with cross-cuts every 15 m: total development from the incline exceeded 800 m in length.

Though widths of 58 m pale green serpentinite with payable fibre occur locally, the average true width of the orebody below outcrop is only 9–10 m. The surface strike length is 365 m, and the vertical depth extent is estimated from data given in Bushell (1972) to be ±60 m. Thus *in situ* reserves of 5.10^5 tons pale green serpentinite are indicated. The deposit contains an average fibre content of 2 per cent; at the time of writing this value is regarded as sub-economic.

During the same period as exploration work conducted at Havelock West, a long adit ("3520′ adit") was driven from the base of the main Havelock Mine dump through the hangingwall of the serpentinite body. Development from 3520′ adit opened up a strike length of ±365 m in the area immediately west of the mine. However, sheared serpentinites with only small amounts of very short slip-or brittle fibre were intersected.

The large body of pale green serpentinite located in the footwall of the main eastern ore shoot has already been described. Though surface outcrops show this chrysotile occurrence to be at least 110 m in width, the deposit is not payable. Asbestos fibres are very short (<1,5 mm) and of the slip-variety.

Finally, small deposits of pale green serpentinite with chrysotile fibre have been observed in the faulted central region of the Havelock serpentinite, and in the far north adjacent to a transverse fault that defines the northern strike extension of the footwall iron-formation (Fig. 8).

Motjane serpentinite

Chrysotile asbestos has been described from two localities within the Motjane area (Hunter, 1951, 1959a; Ann. Rept., 1966). The northernmost occurrence (located close to the paved road between Ngwenya and Mbabane) consists of three small, elongate lenses of pale green serpentinite. Each lens is 18–24 m in length and 9 m-wide, and has its longest axis oriented east-west. This direction is normal to the trend of the main dark green Motjane serpentinite body, though parallel with the strike of the overturned fold limb in Fig Tree Group sequences south of Ngwenya Mine.

Though fibrous chrysotile occurs in 3 mm-wide seams on surface, cores from four shallow boreholes drilled in this northern occurrence contained only small amounts of fibre (Hunter, 1959a), and borehole logs show that thick talcose sequences were intersected. It appears that the fibre-bearing zone does not persist in depth.

Cross-fibre chrysotile seams also occur in serpentinites beyond the southern extension of the Motjane body (Fig. 7). From a prospect that overlooks the Usushwana River, Hunter (1951) described veins that average 7,5 mm in width, some with good quality fibre. Fibre seams occur in zones of pale green serpentinite that alternate with foliated (ribbon-textured) dark green serpentinite.

This prospect was re-investigated during 1966 when four boreholes along 250 m of strike length were sited to intersect the asbestos zone at ±50 m below outcrop. Each hole intersected fibre-bearing serpentinite in a zone which varied from 5–15 m in true width. Fibres 3 mm in width were arranged in a stockwork of near vertical seams. Cores were assayed at Havelock Mine and returned uneconomic values of 1,2 per cent fibre by volume.

Other serpentinites

Chrysotile fibre in small amounts can be observed in all the dark green serpentinites that crop out in the central area of the greenstone belt in Swaziland. Though many are only exposed in part (for example, the large Nkomozane body), none of the serpentinite bodies exhibit surface indications of extensive development of either asbestos or pale green serpentinite on a scale comparable with the Havelock body.

Asbestos is widely distributed in the Mngwaisa serpentinite body, but the total fibre-content is low. Fibres are usually brittle, and dark green or golden brown in colour; picrolite veins with or without fibre are also common.

Bushell (1972) reported fibres of commercial length (±8 mm) in 15 m-wide zones of pale green serpentinite along the faulted and talcose eastern margin of the Mngwaisa body. Shallow excavations showed the fibre to persist in depth but to lens out along the strike.

On a bend in the Komati River, 2 km from the border with South Africa, there is a small body of dark green serpentinite (180 m long and 55 m wide) that contains vein chrysotile in plenty (Fig. 2). Fibres are 3–6 mm long but they are all brittle.

Similarly, chrysotile fibre in veins of up to 12 mm-width are present in the small body of dark green serpentinite 1,5 km south of the disused Nottingham Hill gold mine. There, fibre is short and interlayered with picrolite.

BARITE

The largest occurrence of barite ($BaSO_4$) and the only deposit of economic importance in Swaziland, is located in the valley of the Londosi River near the southern extension of the greenstone belt (Fig. 14). A 5 km-long track north of the Ngwenya — Mbabane road gives easy access to the dormant Londosi mine.

The Londosi deposit is associated with igneous and volcaniclastic sequences within the Onverwacht Group. From the evidence discussed below, it appears that the barite is almost certainly hydrothermal in origin, and may have formed early in the evolution of the greenstone belt. It is thought to be the largest stratiform sulphate body in the Barberton area, and although production has remained small in the past, ore reserve calculations given here indicate the potential for significant future production.

Redeposited barite has been recorded from several localities within the lower clastic sequences of the Fig Tree Group, north of the Lomati River (Fig. 2). None of these occurrences is known to contain barite in economic quantities.

LONDOSI BARITE DEPOSIT

Discovery of barite in the Londosi valley in 1937 and the subsequent pegging of claims were followed by a period of detailed surface exploration. A company was formed in 1945 (Messrs Swaziland Barytes Ltd.) for the purposes of mining the barite, and production began the same year. Production continued until 1976 when the mine closed.

Total production recorded during the period 1945–1976 is 10 746 tons, an average of 336 tons per annum; annual production only exceeded 1 000 tons during one year.

Most barite from the Londosi deposit was mined from a number of small underground workings and shallow quarries. In 1958, a mining company (JCI) completed 60 m of

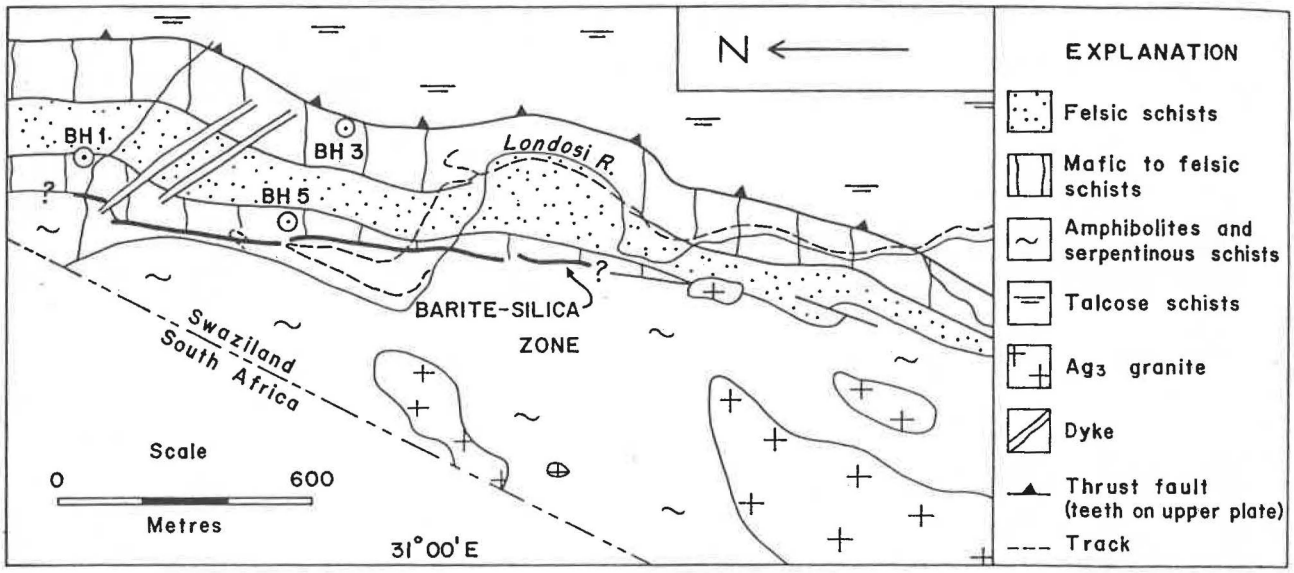

Figure 14
Location and geology of the Londosi barite deposit (modified after Mehliss, 1945; Urie, 1970). The locations of boreholes (BH) are discussed in the text.

underground development from an adit located in the central outcrop area, but with disappointing results. It was not until late 1972 that work began on an adit close to the lower waterfall on the Londosi River in a systematic attempt to develop ore reserves. Estimates of mineable barite proved as a result of this work are described below.

Geological Description

Barite crops out more or less continuously for 1,25 km in a zone that strikes north–south. The orebody is tabular, and inclined east at a uniform dip of 30° ± 5° (Fig. 14).

Strike extensions of barite are known at Droxford Farm (Fig. 2; see below), 4,5 km farther south. In addition, Reimer (1980) reports barite on farms Houtbosch 189 and Witkop 188 in adjoining parts of South Africa. These extensions indicate a discontinuous strike length of 7 km in Swaziland, and ±10 km for the entire deposit.

Continuity down-dip to 125 m is proven by difference in relief on outcrop and boreholes drilled in the Mine block (see Fig. 18). Extensions of less than about 250 m — 275 m down-dip are indicated in the central outcrop area. A vertical borehole (BH3 Fig. 14) intersected granite at 212 m below surface, 9–15 m above the predicted position of the barite (Davies, 1951).

The total composite thickness of barite averages 1,2 m and locally exceeds 2,8 m near the erosional re-entrant formed by the Londosi River (see Table 5). Thickness and strike dimensions are greater than those given for barite deposits elsewhere in the Onverwacht and Fig Tree Groups (see Reimer, 1980 for a review).

A generalised lithological sequence (Fig. 15) and a number of detailed sections measured at intervals along the barite zone (Fig. 16) summarise the regional stratigraphy. As Figs. 15 and 16, and the following description show, barite occurs in a horizon that coincides with a marked lithological break.

Footwall

A metamorphosed igneous sequence of largely mafic to ultramafic composition forms the depositional footwall to the barite. Foliated granitoids intrude this sequence at its base (Fig. 14) and rare microgranitic sills intrude the sequence elsewhere.

Units of massive and layered amphibolite form the uppermost 60 m of the footwall. Talcose and serpentinous schists occur below. Internal igneous contacts occur at ±2 m vertical intervals are oriented parallel with stratigraphic surfaces above. Individual units contain layers of coarse and fine amphiboles that resemble spinifex-like textures.

Major and trace element determinations on whole-rock amphibolites from this sequence are consistent with a basaltic komatiite composition (Table 8).

Barite-silica zone

Massive seams of pure white barite, layers of brown and green coloured silica and fragments of amphibolite occur together in a single horizon. This horizon averages 3–7 m thick, and contains 20–25 per cent barite by volume (see Tables 5 and 6; Fig. 16).

Barite occurs as numerous seams (maximum thickness 1,4 m) which tend to be concentrated toward the top of the barite-silica horizon (Linsell, 1974). Within individual seams strained 60 μm barite grains and coarse (>5 mm) strain-free recrystallised grains occur together.

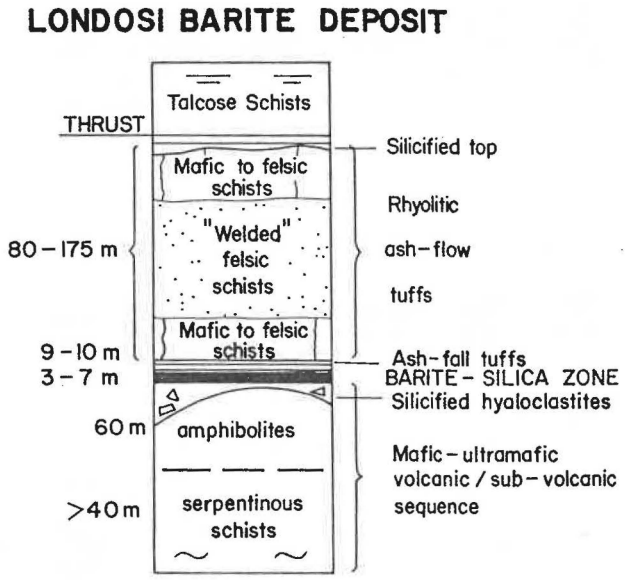

Figure 15
Generalised lithological sequence and interpretation (right-hand column) of the Onverwacht Group stratigraphy in the area of the Londosi barite deposit.

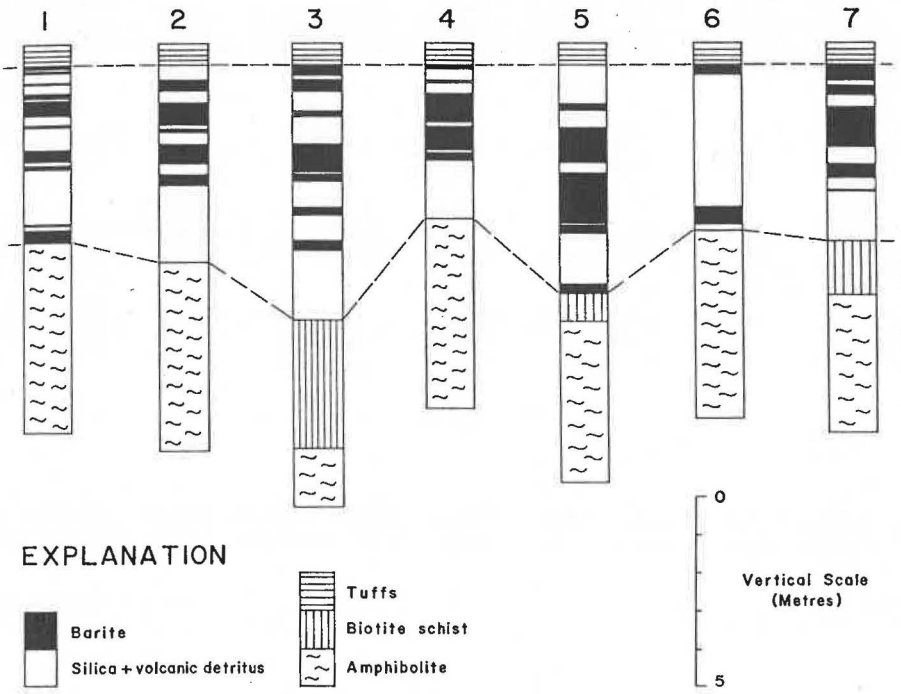

Figure 16
Detailed stratigraphic summary of the barite zone in the Northern (1–2), Mine (3–5) and Southern (6–7) blocks. Sections are located as follows: 1. BH1 (Fig. 14); 2. sections measured on outcrop near BH 5 (this work); 3. BH 107; 4. BH 290; 5. BH 285; 6. BH 103; 7. BH 296; (Hunter, 1960; 1966). Sections 3–7 are at ±100 m strike intervals and located in Fig. 18

Euhedral 30–75 μm blades of barite that may represent unrecrystallised grains occur in tuffs immediately above the barite-silica zone.

Where barite seams are thickest, silica occurs in a brown-coloured phase that contains microscopic biotite in a matrix of recrystallised quartz. Like the barite, silica occurs in discontinuous seams and also as large angular blocks that float in barite. Amphibolitic material is largely absent from thick barite-silica concentrations of this type.

Green-coloured silica that has replaced small fragments of pale green amphibole is more typical in areas where barite is less well developed. Silica is present as a 200 μm quartz aggregate with serrate grain boundaries. Angular fragments of mafic detritus appear to be mostly monomineralic green amphibole of the same type as the footwall sequence.

Footwall amphibolites are brecciated and silicified, sometimes to a depth of 30 m below the barite. Less commonly, thin biotite-barite schists (maximum 3 m) separate the orebody from the footwall (Fig. 16). Amphibolite below such zones is extremely altered, while the barite-silica zone above is often rich in sulphides.

Narrow veins of barite (±10 mm) cut the footwall amphibolite immediately below the main horizon. Minor barite is also present within the felsic sequence 175 m east of the main zone (Mehliss, 1945). Field relations suggest that this occurrence has been faulted into position.

Davies (1951) reported significant concentrations of base metal sulphides in cores from BH 5 (Fig. 14), where an average of 1,78 per cent zinc metal was returned from two intersections totalling 1,08 m. Chemical analyses of a small metalliferous pod sampled on surface (Sample 4, Table 8) contain only small amounts of zinc metal.

Chemical compositions of the silica-barite-amphibolite zone sampled in the approximate ratio 3:2:1 are given in Table 8. In addition, sulphur isotope data for the Londosi deposit are given by Reimer (1980; in press).

Hangingwall

Laminated crystal and vitric tuffs 9–10 m thick overlie the barite-silica zone. Fresh, zoned clinopyroxene euhedra cemented by poikiloblastic barite are a conspicuous feature of the tuffs. Clinopyroxenes exhibit a crude size grading, but average 250 μm in diameter.

Biotite laths, embayed quartz grains and cloudy semi-opaque material presumed to be devitrified glass occur within the pyroxene-bearing layers. They alternate with discontinuous pods and bands of green amphibole and silica. The proportion of devitrified glass appears to increase toward the top of the unit.

Mafic tuffs are overlain in turn by felsic (quartz-muscovite) gneisses that contain a distinctive mm-scale colour banding. Anhedra of K. feldspar, narrow wisps and selvedges of biotite, and 1–10 mm porous fragments of green amphibolite with both embayed and euhedral grains of garnet can be identified in thin-section. The banding resembles a welded texture, and the unit is interpreted below as an ash-flow deposit.

The proportion of mafic material increases toward the base and top of the volcaniclastic unit (Fig. 15). Quartz-amphibole schists are more common, and the colour-banding is replaced by a metamorphic foliation. Angular blocks of a fine-grained mafic volcanic lithology occur along the upper surface of the felsic gneiss. Stratigraphic thickness variations along 7,5 km of strike from ±175 m in the northern area adjacent to South Africa to less than 80 m south of Droxford Farm (Fig. 44) are suggested from regional mapping.

Structure

Intense deformation of the lithological sequence represented in Fig. 15 has produced widespread L–S tectonite fabrics. Nonetheless regional structure appears to be rather simple: the same lithologies can be followed for several strike kilometres without the effects of folding deformation (Fig. 14), and structural contours drawn on the upper surface of the barite zone (Fig. 18) are consistent with an essentially planar surface.

Hunter (1966) and Clarke (1973) suggested that barite ore shoots may parallel the northeast-plunging mineral lineation (Fig. 17). Evidence to demonstrate that this lineation coincides with a direction of maximum extension has not been found. Instead, boudin axes plunge southeast (Fig. 17), and small-scale folds (<1 m amplitude) observed in underground development contain thick barite in the hinge region but are variable in orientation.

Structurally controlled ore shoots with mineable concentrations of barite are not considered likely. The pres-

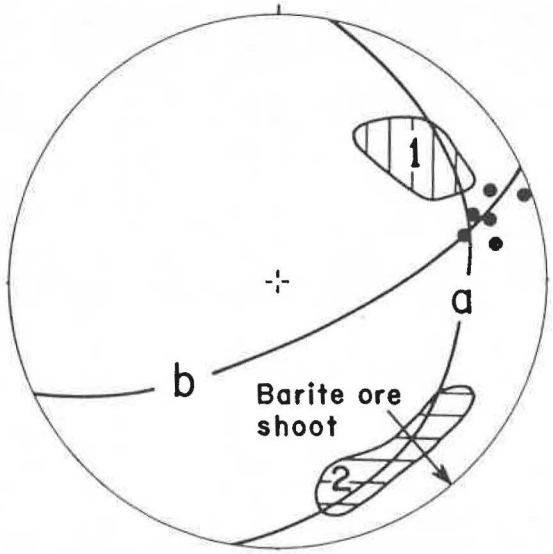

Figure 17
Orientation data measured underground and on outcrop near the Londosi barite deposit. Major lithological units strike N-S (a) and are deformed by reverse faults (b) which together intersect along a crenulation lineation (solid circles). A pronounced mineral elongation direction (Field 1), and extension direction inferred from boudin axes (Field 2) are contained in the regional foliation. The most likely direction for structural elongation of barite is toward the southeast, although ore shoots of this type are probably concealed by original variations in thickness.

ence of ore shoots oriented NW–SE cannot be excluded from the available orientation data (Fig. 17).

Evidence for stratigraphic repetition by large thrusts of the type shown in Fig. 14, is described elsewhere. The recognition of major tectonic duplication requires a reassessment of Onverwacht Group stratigraphy. The Londosi barite is correlated here with an event that discharged hydrothermal fluids onto a sea-floor of mafic-ultramafic composition before the deposition of a felsic volcaniclastic sequence (see below). There is no evidence in Swaziland to suggest that thick mafic or ultramafic volcanic sequences were deposited after this hydrothermal event (*cf.* Viljoen and Viljoen, 1969c; Reimer, 1980).

Interpretation

The Londosi barite orebody overlies an igneous sequence of mafic to ultramafic composition that includes basaltic komatiites (Table 8). Evidence for flows or high-level intrusive contacts, spinifex-like textures and extensive chemical hydration are consistent with emplacement in a submarine volcanic or sub-volcanic environment that was accompanied by extensive fluid interaction.

Sediment cover deposited on this volcanic sequence appears to have been thin or absent. Biotite-schists (Fig. 16) may represent the metamorphosed equivalents of thin sediments, possibly those with a high ferromanganese affinity. Ash-fall tuffs are cemented in part by barite and were probably deposited soon after the main barite-forming event. The tuffs are mafic in composition and may be derived from volcanic sequences of a similar type to those present in the footwall.

An occurrence of barite that closely resembles the Londosi orebody has been described from barite-opal volcanic rocks dredged from a fracture zone in the Lau Basin, a present-day Pacific marginal basin (Bertine and Keene, 1975). Like the Londosi deposit, this occurrence contains variable proportions of barite, silica and material interpreted as silicified hyaloclastite. Both appear to have been deposited on a submarine volcanic basement of mafic composition with sparse sediment cover.

For the same reasons as those given by Bertine and Keene (1975), it seems probable that the silica formed by precipitation from hydrothermal solutions which leached material out of the underlying volcanic sequence. Because the depositional temperature is unknown, devitrification and diagenesis of volcanic debris followed by precipitation of silica at Archean seawater temperatures cannot be excluded. Hydrothermal solutions are also the most probable source for barium (Bertine and Keene, 1975).

Significantly, it is noted that the Londosi barite deposit contanis no sericite. It is unlikely to have precipitated from highly potassic fluids of the type that have been inferred from orebodies elsewhere in the greenstone belt.

Unlike the recent marginal basin analogue, the Londosi barite was buried under thick silicic volcaniclastics. Mafic tuffs are followed in turn by a unit that resembles a single cooling unit of a felsic ash-flow deposit. Field relations are consistent with a non-welded base, a densely welded zone and a non-welded top of the type described by Ross and Smith (1961). Detailed textural studies are required to document the unit more carefully.

Viljoen and Viljoen (1969c) first proposed a hydrothermal origin for the Londosi deposit, and Reimer (1980; in press) suggested that barite deposition occurred during a sedimentary-exhalative event. These suggestions are substantiated by the present work.

Ore reserves

Measurements of barite and silica thicknesses in underground development (Table 4), borehole cores (Tables 5 & 6) and surface exposures (Table 6) provide the basis for ore reserve calculations. These data are used to estimate mineable barite to 150 m down-dip in three blocks of ground with dimensions given below (Table 7).

The $BaSO_4$-content of barite orebody collected from different portions of the mine by Linsell (1974) averages 80,7 per cent and varies from 64,25 – 95,76 per cent. Assays of seams 0,5 m-thick and above given by Mehliss (1945) average 87,6 per cent (69,02 – 96,10 per cent) $BaSO_4$. In the calculations given below it is assumed that the true barite content is 82 per cent, and calculated tonnages are reduced accordingly. Silica intergrowths (65 per cent), amphibole (18 per cent) and calcite (14 per cent) account for the bulk of the gangue.

Mine block

The Mine block includes the most recent underground operation (see Fig. 18), and calculated reserves include proven (developed) ore as well as probable ore based on 10 borehole intersections (Davies, 1951; Hunter, 1960; 1966). Tonnage estimates in the Mine block are regarded with a reasonable degree of confidence.

Linsell (1974) presented measured sections of the barite zone at 2 m intervals along the 160 m of drives and raises shown in Fig. 18. Those sections considered by visual inspection to be representative of the orebody are given in Table 4. Much of the north drive is off reef, and few thickness data are available.

As Table 4 shows, the average barite width south of the adit (1,11 ±0,42 m) is 25 per cent thicker than that exposed by development farther north (0,85 ±0,32 m). These widths resemble those projected down-dip from surface exposures.

Borehole intersections within the Mine block (Table 5) are approximately 50 per cent thicker than barite measured underground. It appears that the development provides an incomplete sample of the total orebody width. However, barite: silica ratios, and proportions of mineable barite are similar in both, and indicate that diamond drill holes give a relatively reliable estimate of ore-

TABLE 4
Barite widths in mine ore reserve block, Londosi barite deposit[1]

	Drive north 1	North Raise 2	North mean 3	Drive south 4	South raise 5	South mean 6	Mean 7
Barite width (m)	0,74	1,04	0,85 (±0,32)	1,09	1,15	1,11 (±0,42)	1,00 (±0,40)
Gangue (m)	0,86	1,01	0,91	1,69	1,03	1,42	1,20
Total width (m)(barite + gangue)	1,60	2,05	1,76	2,78	2,18	2,53	2,20
[2]Specific gravity	3,34	3,40	3,36	3,15	3,45	3,27	3,32
% Barite (by volume)	47	51	48	37	56	45	45
% Barite (by weight)	59	63	61	48	65	55	57

[1]recalculated from data in Linsell (1974); [2]specific gravity $BaSO_4 = 4,3$ and $SiO_2 = 2,5$.

Notes: 1. 0–05 m, 16 values; 2. 4–20 m on incline, 9 values; 4. 10–46 m, 19 values; 5. 31 m on incline, 13 values.
Figures in parentheses are one standard deviation.

TABLE 5
Measured borehole intersections, Londosi barite deposit

Borehole	107	291	290	106	289	284	285	2	288	287	Mean
Silica-barite zone (m)	6,98	5,77	4,11	9,90	>6,94	5,72	6,01	12,31	>7,92	>12,86	7,85
Total barite width (m)	1,99	0,79	1,47	1,89	1,03	1,96	2,83	1,70	0,37	2,64	1,67
% Barite (by volume)	29	14	36	19	15	34	47	14	5	21	21
Mineable barite (m)	1,99	0,79	1,47	1,74	1,03	1,80	2,58	1,35	0,34	2,36	1,55
Gangue (m)	2,90	3,00	0,92	1,98	1,32	3,92	0,76	1,73	1,18	1,01	1,87
Mining width (barite + gangue)	4,89	3,79	2,39	3,72	2,35	5,72	3,34	3,08	1,52	3,37	3,42
Specific gravity	3,24	2,88	3,62	3,35	3,29	3,06	3,89	3,35	2,90	3,76	3,31
% Barite (by volume)	41	21	62	47	44	31	77	44	22	70	45
% Barite (by weight)	54	31	73	60	57	43	85	56	33	80	58

body thickness. Each borehole intersects an average of 5–6 barite seams 0,25 m in thickness; the probability of missing every barite intersection is small.

Estimates given in Table 7 indicate that 15 000 tons proven ore (blocked out by 100 m of development to approximately 50 m down-dip), and a further 130 000 tons probable ore are available in the Mine block. Extensions beyond 150 m down-dip are also likely (see BH 107, Fig. 18).

Southern block

Barite is known to continue for at least 250 m along strike in ground south of the Mine block (Fig. 18), both from surface indications and 6 borehole intersections (Hunter, 1960; 1966). Boreholes drilled in the Southern block show variable and generally narrower barite intersections (Table 6).

Ground immediately adjacent to the Mine block (0–100 m south) may be less than 20 per cent payable (see

TABLE 6
Barite widths in northern and southern ore reserve blocks, Londosi barite deposit.

	NORTHERN BLOCK			SOUTHERN BLOCK						
Borehole No.	1	surface data[1]	mean	286	103	105	296	104	294	Mean
Silica-barite zone (m)	4,74	>3,75	4,25	5,63	4,36	3,87	4,21	1,33	6,59	4,33
Total barite width (m)	1,49	>0,83	1,16	0,20	0,65	0,33	1,91	0,67	1,92	0,95
% Barite (by volume)	31	22	27	4	15	9	45	50	29	22
Mineable barite (m)	1,13	0,83	0,98	0,20	0,65	0,24	1,87	0,67	1,89	0,92
Gangue (m)	1,72	1,78	1,75	0,90	3,58	0,86	0,74	0,66	1,83	1,43
Mining width (barite + gangue)	2,85	2,61	2,73	1,10	4,23	1,10	2,61	1,33	3,72	2,35
Specific gravity	3,22	3,08	3,15	2,82	2,77	2,90	3,80	3,40	3,42	3,20
% Barite (by volume)	40	32	36	18	15	22	72	50	51	39
% Barite (by weight)	53	43	48	27	23	33	81	63	64	52

[1] Average of 9 measured sections.

TABLE 7
Available barite tonnages in the Londosi barite deposit

	Northern block	Mine block		Southern block
	1	2	3	4
in situ (10^3 tons)	970	36,5	350	290
mineable (10^3 tons)	76	15	145	65

Notes: 1. assumes 20 % payability and 48 % barite by weight; 2. proven ore recalculated from Linsell (1974); assumes average width of 2,2 m, 90 % payability and 58 % barite by weight; 3. based on average mineable width in development and borehole intersections (see Tables 5 and 6), 90 % payability and 57,5 % barite by weight; 4. assumes width of 2,35 m, 50 % payability and 52 % barite by weight.

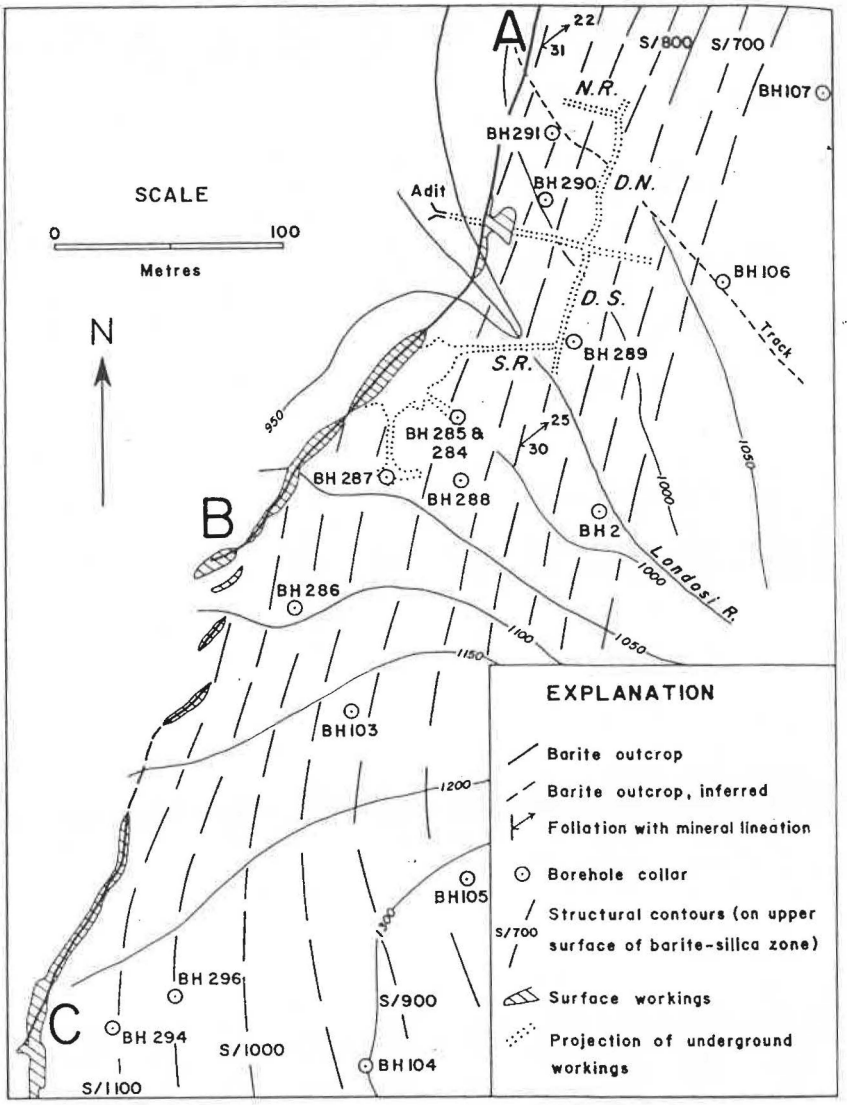

Figure 18
Plan of the Mine (A–B) and Southern (B–C) ore reserve blocks, Londosi barite deposit, showing underground development and borehole locations. N.R. = North Raise, D.N. = Drive North, D.S. = Drive South, S.R. = South Raise (see Table 4).

TABLE 8 (a)
Chemical compositions of the Londosi barite deposit and adjacent units I. Major elements (weight percent)

	1	2	3	4	5
SiO_2	33,30	47,50	50,30	48,40	72,10
TiO_2	0,15	0,34	0,16	0,15	0,32
Al_2O_3	1,20	4,10	2,30	2,80	12,30
Fe_2O_3	1,53	3,02	0,53	6,25	1,03
FeO	4,10	7,27	2,02	4,18	1,94
MnO	0,09	0,14	0,29	0,51	0,16
MgO	37,60	29,00	3,80	12,00	0,30
CaO	0,30	2,42	8,51	13,70	0,51
Na_2O	<0,10	<0,10	0,10	0,10	0,60
K_2O	<0,05	<0,05	<0,05	0,23	6,89
P_2O_5	<0,05	<0,05	<0,05	<0,05	<0,05
SO_3	<0,03	<0,03	8,69	2,22	<0,03
CO_{2+}	18,40	1,11	11,60	1,34	0,35
H_2O	2,80	5,57	3,85	1,90	0,65
Loss	21,50	5,59	2,20	2,62	1,52

Notes: 1. Onverwacht Group talcose schists, 100 m below barite zone; 2. Onverwacht Group periodditic komatiite, 40 m below main barite zone, Londosi River; 3. silica-barite-volcaniclastic zone (in ratio 3:2:1, by visual inspection), Londosi River section, Mine block; 4. black-coloured ferruginous and manganiferous zone with barite and visible sphalerite, on outcrop due west BH 5 (Fig. 14); 5. silicic ash-flow tuff, Londosi River.

TABLE 8 (b)
Chemical compositions of the Londosi barite deposit and adjacent units: II. Trace elements (ppm)

	1	2	3	4	5
Au	<0,05	<0,05	<0,05	<0,05	<0,05
Ag	<0,10	0,10	<0,10	<0,10	<0,10
Pt	<0,10	<0,10	0,10	<0,10	0,10
B	40	155	85	75	250
Ba	57	212	15,3[1]	5,38[1]	495
As	30	30	30	30	30
Sb	<1	<1	<1	<1	2
Cr	1 964	2 261	559	518	58
Co	80	70	50	50	20
Ni	1 450	850	330	370	90
Cu	18	41	47	76	41
Pb	20	70	50	40	60
Zn	25	35	151	456	33
[2]Hg	1 550	1 150	960	150	1 200
Sn	23	<20	27	<20	<20
W	28	20	<20	<20	<20
Y	<10	<10	<10	35	34
Zr	24	29	<10	25	326

[1]reported as %; [2]reported as ppb.

Notes: see Table 8 (a).

BH 286, 103, 105 and surface data in Fig. 18). However, economic intersections were obtained in the deep hole BH 104, and near the southernmost extension (BH 294). The Southern block contains 65 000 tons mineable barite (Table 7); additional exploration data are required for more accurate tonnage estimates.

Northern block

Possible barite reserves have been calculated for the largely unexplored ground that forms the northern 60 per cent of outcrop length (750 m) in Fig. 14. Tonnages are speculative, and based only on surface exposures and a single exploratory borehole intersection (BH 1 Davies, 1951; Table 6). The estimate of 76 000 tons of mineable barite (Table 7) may be significantly increased as more exploration data become available.

Additional borehole data (not tabulated) include BH 5 (Fig. 14), a shallow hole that intersected base metals but only narrow stringers of barite, and BH 3 (Fig. 14), which intersected granite at a projected 296 m down-dip of outcrop (Davies, 1951).

Summary

1. A stratiform horizon that includes barite, silica, base metals and amphibolitic material interpreted as volcanic detritus crops out in the valley of the Londosi River. Analogy with similar barite-opal volcanic rocks described from a present-day marginal basin by Bertine and Keene (1975) suggests that barite, silica and base metals were leached from the underlying Onverwacht Group lithologies by hydrothermal solutions, and that inorganic precipitation occurred when these solutions came into contact with cooler seawater.

2. Hydrothermal deposition resulted in a discontinuous covering of barite along a 10 km segment of volcanic and sub-volcanic basement that was almost devoid of sediment cover. Barite accumulation was thickest in the area shown in Fig. 14, where an *in situ* tonnage of 3 $.10^6$–10^7 tons $.km^{-2}$ is estimated.

3. Reserves of 286 000 tons mineable barite are indicated for the entire Londosi deposit. Tonnages are given for three blocks of ground as follows:

Mine block — 145 000 tons probable ore, including 15 000 tons blocked out.
Southern block — 65 000 tons probable and possible ore.
Northern block — 76 000 tons possible ore.

These estimates are comparable with those given previously by Mehliss (1945) and Clarke (1976), but are lower (by a factor of 3 or 4) than tonnages calculated by Pretorius (1948), Davies (1951) and Hunter (1960).

4. Considerably more underground exploration is required to prove reserves in the Mine block. It is estimated that 15 000–20 000 tons mineable barite could be blocked out by winzing between 10 m vertical levels. The extent to which the deposit is workable would be most easily determined by locating maximum development on reef.

In addition, further borehole data are required from the Northern and Southern blocks before more accurate estimates of mineable barite are possible in these areas. The deposit also has base metal potential and boreholes sited down-dip of sulphides exposed on surface (near BH 5, Fig. 14) may be worthwhile.

5. Barite reserves in the Mine block, and in adjacent ground to the south are sufficient to support a small mine (1 000 tons/month) for at least 15 years. During the previous operation, the proportion of saleable barite obtained after loss in milling was about 85 per cent of the tonnage mined. The high $BaSO_4$-content (±95 per cent) required by most commercial users of barite suggests that a similar loss can be expected in any future operation.

In 1945 Mehliss wrote . . . "the remarkable length of the outcrop of the main barytes zone, the high barium sulphate content of some of the seams, the abundance of cheap water for mining purposes and the development of power, and the relative ease of access are all factors that favour the systematic exploitation of the deposit". At the time of writing the present report (December 1981), this assessment is still valid.

OTHER BARITE OCCURRENCES

Droxford Farm

Barite float was discovered on Droxford Farm (Fig. 44) in 1950, and investigated at depth by three boreholes drilled between 1959 and 1962 (Hunter, 1963). Massive barite occurs close to or within a 3 m thick chert unit that can be traced for more than 150 m on surface. The chert is interlayered with biotite-garnet gneisses and overlain by the same felsic gneiss sequence that forms the hanging-wall of the Londosi barite deposit, 4,5 km farther north.

Diamond drill holes were sited to intersect the chert at 25–30 m down-dip along 80 m strike intervals. Narrow veinlets of barite were recorded in all three boreholes with the largest intersection totalling 0,38 m over 1,5 m, approximately 8 m below the chert unit.

The Droxford occurrence occupies a similar stratigraphic horizon as the Londosi barite deposit and therefore also provides a target for base metal exploration. Anomalous zinc geochemistry is recorded from soils in a number of localities in the Elangeni area of which the closest occurs along the strike extension 1,5 km south of Droxford Farm (see Fig. 44).

Northern Hhohho

Several minor occurrences of barite have been reported from the Fig Tree Group sequences north of the Lomati River (Fig. 2). In at least two localities along the watershed between the Tshelangubo and Ntintinyane Rivers, narrow (<0,1 m) and discontinuous barite veins and barite-cemented siliceous breccias and chert-pebble conglomerates occur within a highly deformed shale-sandstone sequence. This sequence is correlated here with the lower Fig Tree Group.

An occurrence of a similar type is reported by Hunter (1962) 1,6 km northwest of Mashobeni North School (Fig. 2). Here a 0,15 m-thick, conformable barite vein associated with vein quartz occurs within Fig Tree Group shales.

Lenz (Ann. Rept., 1955) described a 1,2 m-thick and 15 m-long vein of barite striking parallel with cherts 400 m north of the Tshelangubo River, and about 1,6 km from the South African border. This locality and various other reported occurrences described from the Tshelangubo — Ntintinyane area (Ann. Rept. 1963; 1972; UNDP Mineral Survey locality 71) have not been located by the present writer.

The association of barite with siliceous breccias and conglomerates is consistent with formation by the sedimentary re-working of a hydrothermal barite deposit, possibly of the Londosi-type. The paleogeographic significance of barite deposits of this type is discussed elsewhere. It is noted here that redeposited barite has not been reported from the upper clastic sequences of the Fig Tree Group in Swaziland.

Sedimentary barite deposits have been described from adjacent parts of South Africa (*c.* 7 km northwest of Emlembe) by Heinrichs and Reimer, (1977) and Reimer (1980). According to these authors, 20–400 m of Fig Tree Group shales and cherts separate the barite from the upper surface of the Onverwacht Group.

COBALT

Several small bodies of manganese oxide with unusually high contents of cobalt occur within Onverwacht Group sequences near the watershed between the Mngwaisa and Entabene Rivers. The mineralised zone crops out over a total strike length of 4,8 km and includes four main oxide bodies (A–D, Fig. 55). Each manganiferous body is lens-shaped, ±150 m in length and occurs within a distinctive sequence of green-coloured siliceous schists with chromiferous sericite (sample 6, Table 26).

In common with sequences described elsewhere that contain large amounts of chromiferous sericite, the mineralised horizon at the Cobalt Prospect may represent a zone of translational deformation. As Fig. 55 shows, the northern strike extension of the unit is isoclinally folded, though the age and significance of the deformation are not known. Detailed structural studies are required in this area.

In area A (Fig. 55), trenches were excavated over a strike length of 384 m to a depth of 2,5 m (Bushell, 1972). The surface gossan is yellow-brown in colour and consists of quartz stringers in chromiferous sericite schist with ±20 per cent black-coloured manganese oxides. The original bulk surface sample returned 1,11 per cent cobalt over an exposed width of 4,6 m (see also Table 9).

Two vertical boreholes drilled in area A during 1972 left the gossan 29 m below surface and intersected talcose schist 20–45,7 m down-hole (Bushell, 1972).

Trenches dug in areas B–D exposed mineralised widths of 2,1–7,6 m with similar base metal contents (±1 per cent Co). The assay results from areas A–D are summarised in Table 9.

TABLE 9
Base metal contents in manganese oxide, Mngwaisa cobalt prospect (weight per cent)[1]

	1	2	3	4	mean
Co	1,00	0,22	1,27	0,84	0,83
Ni	0,26	0,40	0,50	0,20	0,34
Cu	0,35	0,21	0,26	0,58	0,35
Mn	n.d.	n.d.	20,36	23,70	22,03

[1]recalculated from data in Bushell (1972); n.d. = not determined.

Notes: 1. zone A, mean 4 analyses; 2. zone B, 1 analysis; 3. zone C, mean 3 analyses; 4. zone D, mean 2 analyses.
Analysts: Goldfields laboratory.

The final reserves of oxide were estimated at 72 720 tons by Bushell (1972), though the dimensions of potential ore blocks were not given. Mining operations in the area would be staightforward, but the metallurgy of the potential cobalt ore may be rather complex.

GOLD

More than any other commodity, gold has had a profound influence on the economic development and social history of Swaziland. Since the first recorded discovery of precious metals in the country in 1872, numerous mines and prospects have been developed by European entrepreneurs. Surface and underground excavations are widely distributed over the rugged terrane of northwest Swaziland, and attest to the enormous effort required to locate economic deposits. Historical evidence indicates that individual mines operated with varying degrees of commercial success (*see* Sims, 1981).

In terms of present-day world production, gold output from northwest Swaziland was extremely small. Less than half of the thirty-three occurrences which declared output produced more than 10 kg (Table 10). Total recorded production is 6 798,9 kg (218 585 oz) of which 95 per cent comes from nine deposits each with an output of >100 kg. At the time of writing, 6,8 tons gold are consumed world-wide every 3–4 weeks in dentistry alone.

Gold output from Swaziland is also small in terms of production from the Barberton greenstone belt (Anhaeusser, 1976). Though all gold mines in Swaziland are now disused, four mines in the Barberton area are current producers of precious metals. The proportion of total output recorded from deposits in northwest Swaziland was ±3 per cent during 1981. The Piggs Peak gold occurrence is the sixth most productive deposit in the Barberton Mountainland.

Demand for gold, both in fabrication of industrial products and in its traditional role as a store of wealth, is not expected to decrease in the future. With the gradual decline in production widely predicted from the great paleoplacer deposits, attention may turn to small lode gold deposits as a major source of precious metals. Swaziland may again be the focus of gold mining activities.

TABLE 10
Production recorded from major gold deposits in Swaziland, 1881–1977 (kg)[1]

1. Piggs Peak	3 708,72
2. Forbes Main Reef	965,40
3. Daisy	593,20
4. Avalanche	348,00
5. Devils Reef	315,08
6. She	148,30
7. Waterfall	146,44
8. Kobolondo	120,76
9. Wyldsdale	119,28
10. Lomati	93,02
11. Nottingham Hill	38,66
12. Waverley Reefs	28,89
13. Lomati Extension	28,72
14. Windemere	14,48
15. Red Reefs	11,23
16. Alluvial sources	49,55

[1]after Sims (1981).

Geology and exploration data pertinent to all the larger gold occurrences in Swaziland are documented here in some detail. The large deposit at Piggs Peak is described first, while other occurrences are described in a geographic order from north to south.

PIGGS PEAK GOLD DEPOSIT

The Piggs Peak gold deposit is the most important occurrence of precious metals along the southeastern edge of the Barberton greenstone belt. Gold output from the now disused mine was substantial. Total recorded production (1889–1954) is ±3 700 kg, of which ±2 800 kg was produced at the relatively high average grade of 10,2 g/t

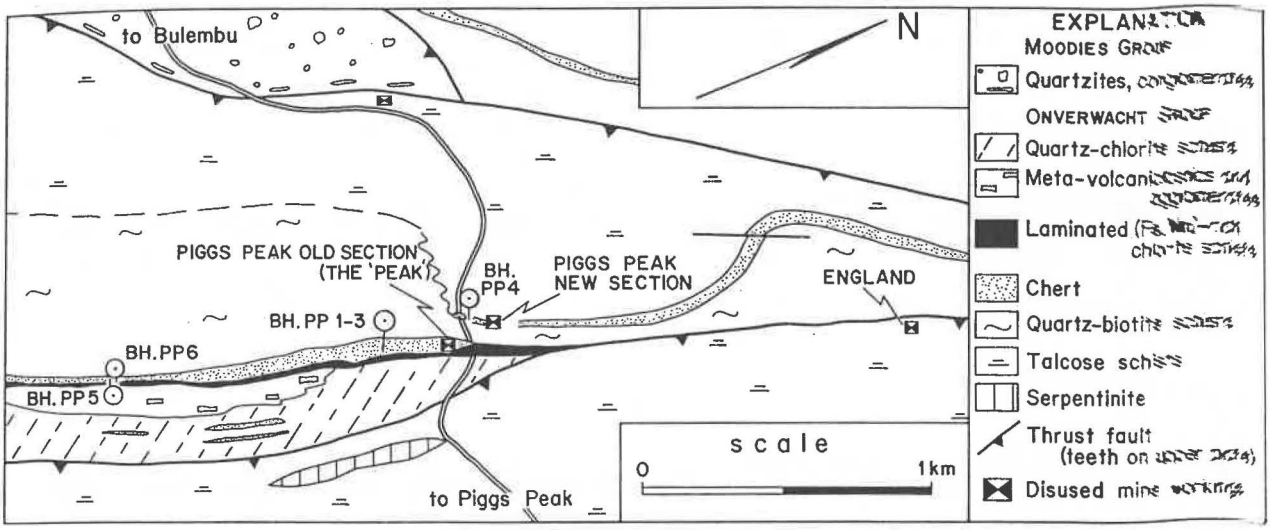

Figure 19
Regional geology and locations of the Old and New Section workings, Piggs Peak gold deposit.

during the period 1889–1917. Piggs Peak gold accounts for 54 per cent of all gold produced in Swaziland, almost four times greater than from any other single deposit in the country.

Furthermore, many of the old surface and sub-surface mine workings at Piggs Peak are still readily accessible. Exposures within these workings provide some of the best material with which to study processes of gold concentration in northwest Swaziland. From the evidence described below, it appears that gold at Piggs Peak was emplaced in solution by the migration of fluids along brittle fractures developed within a chert body (epigenetic-type).

The deposit is located on a conical hill (the 'Peak') 4 km west of the present town of Piggs Peak. Gold was discovered on the Peak in 1884 by William Pigg, and the deposit quickly became famous for its richness and size. Early reports that describe a mountain of auriferous quartzite indicate that the orebody was 12 m wide and ±100 m long on surface (Sims, 1981).

Hall visited the mine in 1916 and provided the first, and only previous published description of the deposit (Hall, 1918). In his account, Hall recorded a number of descriptive terms that were used by the early gold miners at Piggs Peak. Some of these terms ("Cross-Schist", "Little Schist', "Contact Schist" and "Crush-Zones") are still useful and have been retained in the present description.

More recent data have been provided by exploration companies, and these are summarised in Carter (1966) and Randell (1979). The main workings were de-watered by the Geological Survey Department during 1975, and the results of deep sampling (5–8 levels) and estimates of potential ore remaining *in situ* are given in Clarke (1975) and Wiseman (1975). The writer has mapped and resampled surface and underground features to 4 level (Old Section) below which level the mine is flooded.

Regional geology

The Piggs Peak gold deposit occurs within allochthonous Onverwacht Group sequences close to the granitic edge of the greenstone belt (Fig. 19). Granite crops out 2,2 km east of the old workings, and the high-grade zone of the metamorphic aureole (hornblende-hornfels facies) extends to within 1 km of the deposit.

Much of the gold at Piggs Peak is concentrated within a single, sub-vertical horizon of massive chert (Figs. 19 & 20). The chert body can be mapped as a continuous horizon with a strike length of 6 km; it is strongly lenticular in shape in the vicinity of the mine workings.

A moderately metamorphosed mafic and ultramafic schist sequence 1 km-thick crops out west of the chert body. Massive quartz-biotite schists (500 m-thick) and talc-amphibole schists rest with décollement on Moodies Group quartzites and conglomerates farther west (the Midway iron-formation).

In contrast, east of the chert body lithological units are more variable, and at lower metamorphic grade. A 325 m-thick sequence that consists of chlorite schists, ferruginous and manganiferous meta-sediments, coarse tuffs cias with volcaniclastic detritus and units that resemble volcanic agglomerates is present in this area. Irregular pods of silica (ferruginous in part), and a single andalusite-bearing unit occur within the sequence which itself is structurally overridden by a thrust sheet that contains talcose schists and serpentinites.

The lithological succession and its structural interpretation are summarised in Fig. 20. Field relations and min-

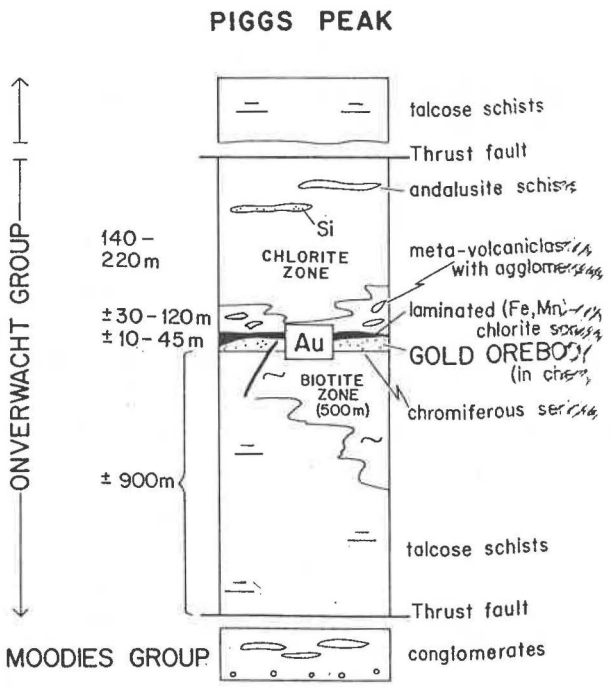

Figure 20
Lithological sequence in the vicinity of the Piggs Peak gold deposit.

eralogical observations indicate that metamorphic grade decreases toward the east, before again increasing within the aureole of the granite. This evidence, together with relationships inferred from fracture geometry and patterns of gold mineralisation described below indicates that the regional stratigraphy faces east, toward the edge of the greenstone belt.

Mine geology

Gold at Piggs Peak was won from two distinct, though related orebodies. Extensive workings known as the Old Section are located in the vicinity of the Peak and are associated with the larger deposit. The Peak is honeycombed with workings to a vertical depth of 240 m below outcrop (8 levels).

Additional workings are located 150–250 m due north of the Peak, and are known as the New Section. Old and New Sections share a common entrance on 4 level, though New Section workings are no longer accessible. Two additional levels are thought to exist below 4 level within the New Section (Hall, 1918). Separate production figures for each section are not available, but it is estimated that the Old Section accounts for at least 75 per cent of the total gold output at Piggs Peak.

Chert body

On surface, the thickness of the main (Old Section) chert horizon is extremely variable (Fig. 21). From a thickness of 75 m in the vicinity of the gold deposit, the chert outcrop increases in width to a maximum of ±160 m in the area 0,5 km south of the mine workings. Rapid thickness attenuation occurs along the strike and 1 km south of the Old Section the chert outcrop is less than 20 m wide.

Similarly, a combination of underground mapping in the Old Section, and borehole data farther south (BH PP1 & 3, Fig. 21), show that the thickness of the chert body changes markedly below surface (Figs. 22 a–c). On 4 level, the chert body is only 35 m wide, and this width decreases further to 15 m on 6 level. The chert body pinches out entirely in the lowermost workings on 7,25 level (Clarke, 1975).

The three-dimensional shape of the chert body resembles a boat with a keel that plunges south: within the mine workings the plunge of the keel is steep, but it flattens to 15°–20° farther south near BH PP1 — 3 (*see* Fig. 23). The western (footwall) chert margin is a planar or sub-planar surface, and all major thickness changes can be accounted for by the irregular shape of the eastern (hangingwall) surface.

The cause of the irregular geometry of the Piggs Peak chert body can be demonstrated from field relations. Stratigraphic sequences within the hangingwall abut against the chert body wherever it exhibits large thickness variations (Fig. 19). Along the northern extremity of the chert subcrop on 2 level, exceptionally well preserved laminated black shales and reddened volcaniclastic units occur within the deformation shadow of the chert body. These sequences pass laterally into massive chert with no discernible fault offset. Compositional layering within the chert body resembles a ghost stratigraphy and can be correlated with bedding in adjacent sequences. Lenses of silica that become drawn out into semi-continuous layers of chert are observed within the clastic shale layering in thin-section, and are interpreted as replacement textures.

Thus, field relations are consistent with chert formation by silicification of layered clastic and volcaniclastic sequences, rather than with deposition of primary silica. It is noted that silicification was not everywhere complete: Clarke (1975) reports mafic layers with carbonate in the chert body below 5 level, and unsilicified volcaniclastic material is present in cores from BH PP5 & 6 (Fig. 21).

From the following description, it appears that the chert body was extensively fractured during gold emplacement. Mineralisation must therefore have followed a period of silicification (and lithification) and cannot have been an early phenomenon.

Chert textures

Within the Old Section workings there are two principal chert types. The basal (western) 30 m of the chert body contains a white and grey colour layering inclined 85° NW on surface and 80° SE on 4 level. Darker-coloured layers consist of 80–120 μm polygonal quartz grains; pale-coloured layers are coarser-grained, and contain 150–1 000 μm (average ±400 μm) irregular quartz grains. Textures of this type are thought to be largely inherited from clastic precursors.

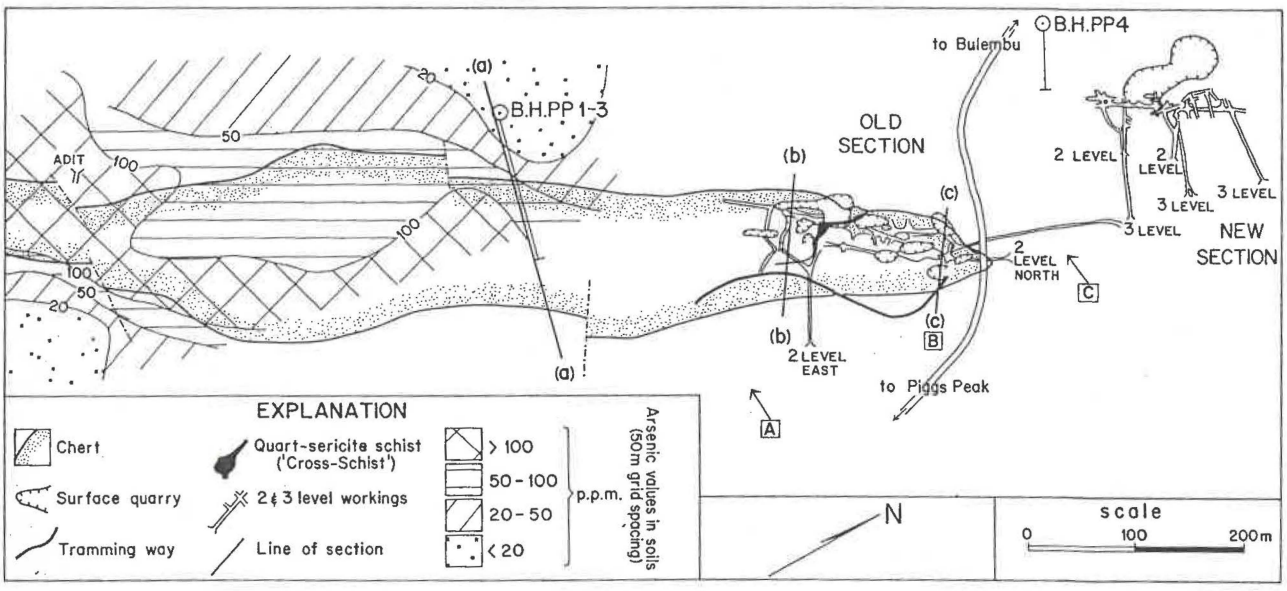

Figure 21

Plan of the Piggs Peak chert body and projection of 2- and 3-level mine workings. Borehole locations and distribution of arsenic values in soils after Randell (1979). Steeply inclined boreholes drilled in positions A–C may intersect orebody extensions (see discussion in the text). Sections along lines (a)–(c) are given in Fig. 22.

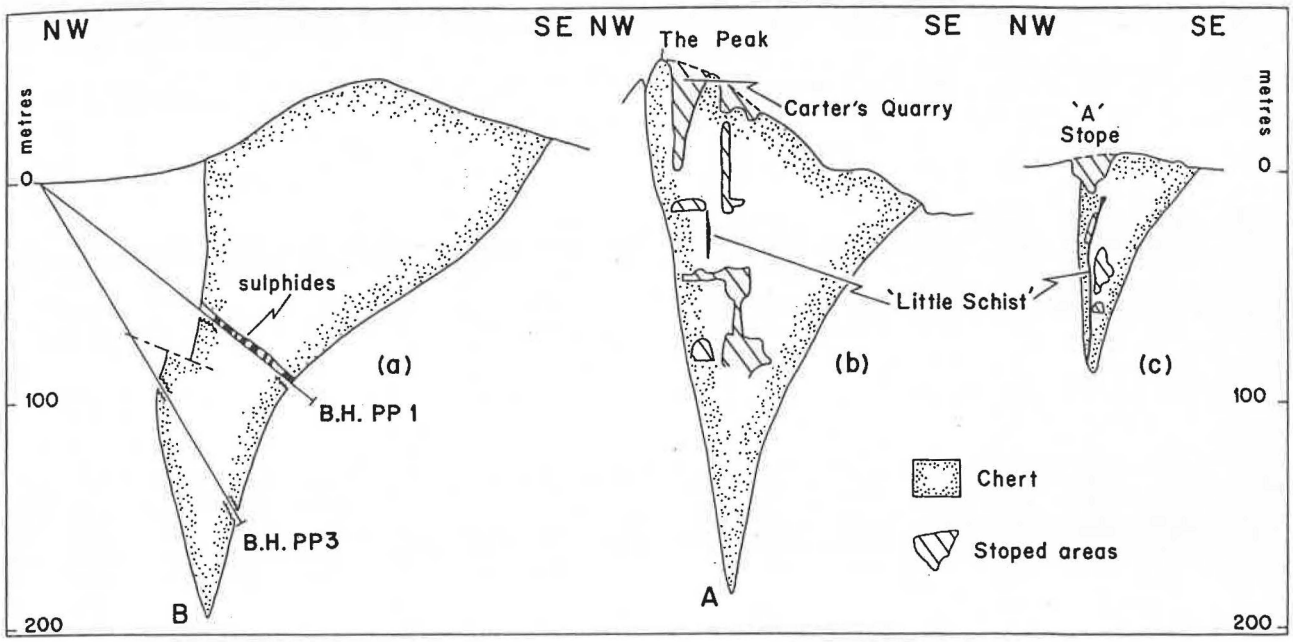

Figure 22
Representative cross-sections of the Piggs Peak chert body along lines shown in Figure 21. The distribution of sulphides (black) in cores obtained from BH PP1 is illustrated schematically. The keel of the chert body between point A and B plunges 17°–18° toward the south.

The upper (easternmost) 60 per cent of the chert body is a massive white lithology with a sugary texture that consists of 200 μm polygonal quartz grains with abundant microscopic fluid inclusions. Similar sugary textures are common in layered chert that has been fractured and mineralised: there, the texture is thought to be associated with processes of hydrothermal alteration.

Dark-coloured chert with a glassy texture was described by Carter (1966), and occurs principally near stopes. Small lenses of dark grey or black quartz with a waxy lustre and small needles of tourmaline occur in all chert types, but also appear to be more common near stoped areas.

Quartz-chromiferous sericite schists ±5 m thick crop out immediately below (to the west of) the chert body. Cherts that directly overlie the schist unit also contain abundant sericite, and the interface reflects a change in sericite content, as well as a change in the proportion of silica. There appears to be a complete gradation between quartz-sericite schist and chert.

Cataclastic textures have been observed locally within the chert body. Though such a study would be valuable, no systematic description of deformation textures is attempted here.

Cross-Schist

The surface plan of the Old Section (Fig. 24) shows a prominent feature known as the "Cross-Schist" that bisects the old workings. In the upper mine levels the Cross-Schist is a closely foliated, and almost pure white quartz-sericite schist. It contains rounded quartz grains of pinhead-size, and 1–3 mm-long needles of tourmaline.

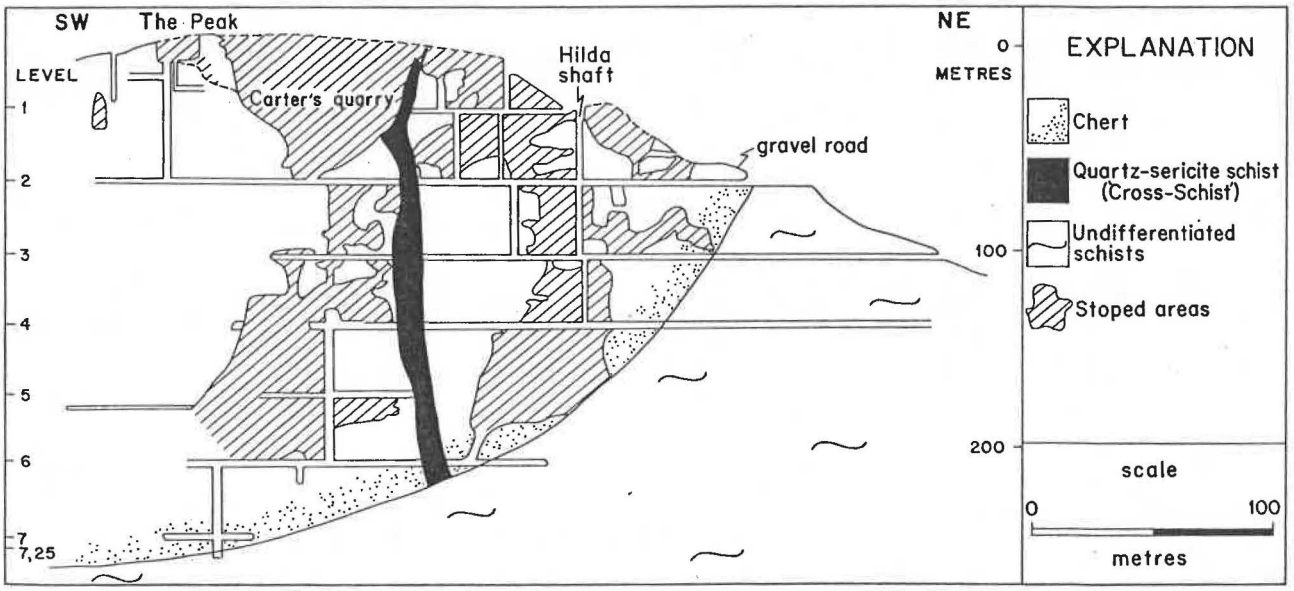

Figure 23
Longitudinal section of the Piggs Peak chert body in the vicinity of the Old Section workings (redrawn from Carter, 1966 and Clarke, 1975).

The Cross-Schist is present on every level down to and including 6 level (Fig. 23), and is often associated with caved ground.

The Cross-Schist intersects the chert layering with an average angle of 30–60°, but as Fig. 24 shows, abrupt changes in its trend are typical. Near surface, the foliation is inclined at 60–85° toward the west or northwest; the same layering is more or less vertical at depth.

Tourmaline needles exhibit a preferred orientation: long axes plunge down the dip of the foliation. Concentrations of tourmaline (>2 per cent B_2O_3, see sample 4, Table 12b) occur along the margins of the Cross-Schist in areas where the trend changes direction (locality 4, Fig. 24). There, quartz-sericite-tourmaline schist that contains significant gold values is associated with pods of black silica.

The average width of the Cross-Schist is 5 m, and this value increases to 12 m in the central outcrop area. The Cross-Schist intersects the hangingwall margin of the chert body on 2 level and below, but pinches out within chert on surface (Fig. 24).

Massive unaltered chert becomes progressively foliated, ferruginous and sugary in texture toward the margins of the Cross-Schist. A coarse hydraulic cleavage oriented parallel with foliation surfaces in the Cross-Schist, and with a 2–10 mm fracture spacing is well displayed near the basal (western) chert contact. A 2–3 m offset and local dip reversal of chert layering occur in the same area (see sample location 6, Fig. 24) and indicate that a small amount of fault movement is associated with the Cross-Schist.

Previous workers have interpreted the Cross-Schist as an altered silicic intrusion that is in some way related to the AG3 granite. Other explanations are possible, and it is suggested below that the Cross-Schist is the expression of a fracture within the chert body along which high temperature hydrothermal fluids were focused.

Little Schist and Contact Schist

Narrow layers of quartz-sericite schist with a similar petrography to the Cross-Schist occur at or near the base of the chert body. One such layer that can be mapped as a recognisable unit on 2 level and below is known as the "Little Schist". The Little Schist extends 90 m between the northern margin of the chert body and the Cross-Schist: it reappears south of the Cross-Schist for a strike length of 10 m before passing laterally into a fracture that contains only a thin film of sericitic alteration. For most of its length, the Little Schist is located near the footwall edge of large stopes (Carter's stope and 'C' stope, Fig. 24).

Unlike the Cross-Schist, the Little Schist is broadly parallel with the chert layering. In structural position it varies between 4 and 9 m above the basal chert margin, and has an average width of 0,6 m. It differs from the Cross-Schist in the general absence of rounded quartz grains, the higher contents of tourmaline and chromiferous sericite, and the presence of small but consistent gold values (1–2 g/t).

An almost identical lithology known as the "Contact Schist" is sometimes, but not always present along the basal edge of the chert body. Though absent on surface, the Contact Schist is known to occur locally on and below 2 level. The Contact Schist is 0,3–1,5 m wide, and like the Little Schist contains large amounts of chromiferous sericite. Chemical analyses of both Contact Schist and Cross-Schist are given in Table 12 a & b.

Crush-Zones and fracture trends

In the vicinity of the Old Section workings the chert body is extensively fractured. Fractures vary in orientation and degree of mineralisation, and the following types are recognised (Types 1 & 2 are equivalent to the "Crush-Zones" of Hall, 1918):

Type-1: 10–50 mm-wide (maximum 0,1 m) ironstone (goethite-limonite) veins. Veins of this type are uncommon, but where observed are inclined at low angles (±30°) toward the northeast. Angular fragments of chert wallrock occur within the ironstone. Type-1 veins are tabular in shape, and invariably have sharp and planar margins.

In polished-section, vein filling consists of massive colloform-textured goethite with a limonitic core zone. Small

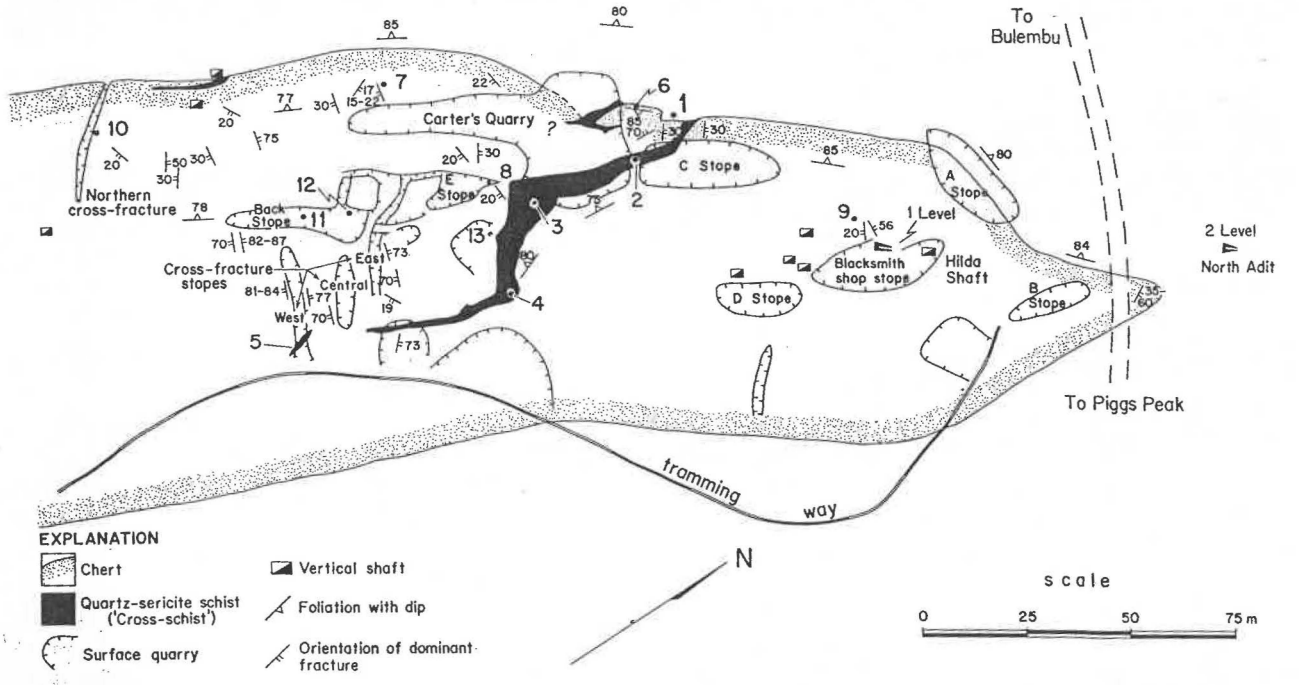

Figure 24

Surface plan of the Piggs Peak gold deposit, Old Section workings, based on mapping by the writer. Major surface excavations are located within the western part of the chert body on either side of the Cross-Schist. Chemical analyses of samples from locations 1–13 are given in Table 12.

veins of goethite cut the limonitic areas; sulphides are absent. Chemical analyses of Type-1 veins (samples 8 & 9, Table 12) show only small gold values, but relatively high base metal contents.

Type-2: low-angle fractures that contain massive white to brown-coloured hydrothermal clay. Along the basal chert margin veins of this type are as wide as 0,3 m, and contain angular chert fragments that average 10 mm in size (150 mm maximum). Vein thickness and degree of fracturing decrease rapidly across the chert outcrop: in the central outcrop area near "E" stope, fractures separated by a vertical distance of 2 m that contain only a thin (1–2 mm) smear of white clay are typical. An average width of 20 mm, and spacing of 0,3–0,4 m is typical of veins near the Cross-Schist along the base of the chert body.

The majority of Type-2 fractures are inclined 10°–30° toward the southeast; others are oriented parallel with Type-1 veins. A number of composite Type-1–Type-2 veins are present and these contain ironstone along the upper surface, and have a layer of clay below. A single 15 mm-wide vein that contains goethite along both margins and clay in the centre was observed near the northern margin of the chert body. This observation, and the small displacements of Type-1 veins by Type-2 fractures suggest a chronology in which ironstone represents the earlier vein material.

The mineralogy of clay material within Type-2 fractures is not known. Chemical analyses (samples 6 & 7, Table 12) indicate highly aluminous compositions, and often include spectacular gold values of 100 g/t or more. It appears that precious metals, together with a number of other major and trace elements are concentrated within Type-2 fractures.

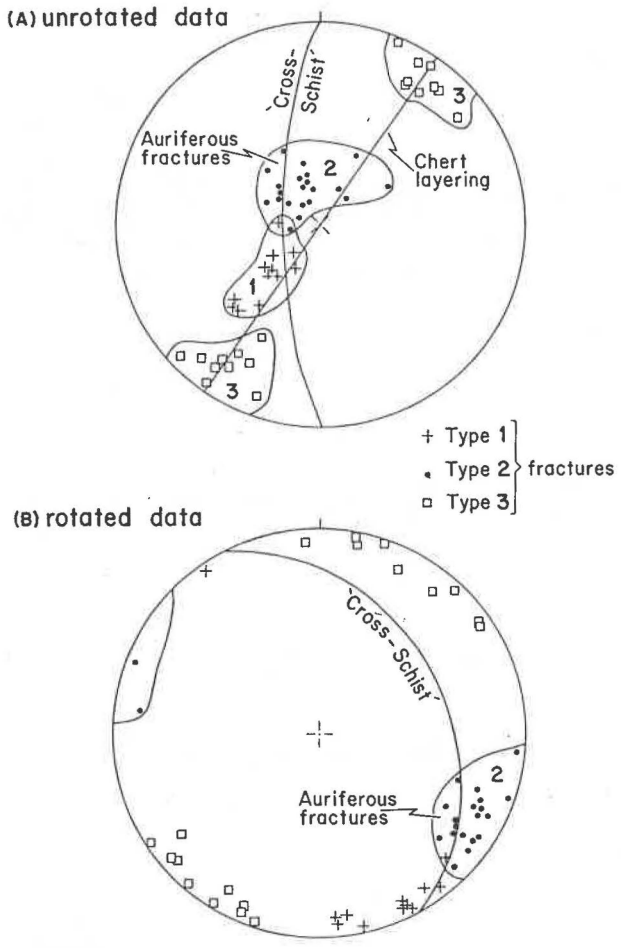

Figure 25
Orientation data and structural elements of the Piggs Peak gold deposit. Because the chert body is turned vertically on edge, all measured data (A) are rotated 80°–95° about a horizontal axis trending 035° (B) to remove the effects of deformation. The primitive in (B) coincides with the inferred initial horizontal layering in the chert body (see text).

Type-3: sub-vertical conjugate fractures occur within the central and eastern chert outcrop, particularly in the vicinity of the Cross-fracture stopes (Fig. 24). Fracture pairs are oriented more or less at right angles to chert layering, major stope trends and to fracture Types 1 and 2. Principal stress directions inferred from conjugate fracture pairs and corrected for the effects of tectonic rotation suggest that during brittle deformation, σ_1 was oriented NW–SE at a very low angle (Fig. 25).

Type-3 fractures are sparsely mineralised. Shallow excavations within 0,6–2,5 m-wide Cross-fracture stopes are only present on surface. At depth, reefs of this type are either absent, or are not payable. It is noted that on surface, the eastern Cross-fracture stope forms the northern extension of the Back stope orebody (Fig. 24).

Gold orebodies

From the distribution of surface workings, it appears that gold was concentrated within the chert body in at least three well-defined horizons. Each gold-bearing horizon is parallel with both the compositional layering and the basal footwall edge of the chert body. Below 3 level, the stoping pattern indicates that only two reefs were mined. Most of the stoped areas on all levels are located within the structurally lower half of the chert body (Figs 24 and 26).

Mining widths were determined by the presence of payable gold values. Stopes average 3–6 m-wide, though Back stope is only 1,3 m-wide near surface, and Blacksmith Shop stope is 8–10 m-wide between 3–5 levels. Stope dimensions are impressive, with vertical faces as much as 85 m high and 50–60 m long.

The average *in situ* gold content of the Piggs Peak orebodies is not known accurately. Samples taken from pillars on 4 level returned gold values of 12–26 g/t over 2–2,5 m, and included individual assays of 2 oz/t (60–70 g/t). While a representative grade is difficult to specify, 12–15 g/t over 2 m is though to be realistic for the central part of the orebody in the vicinity of 4 level. There is no indication that either grade or width is substantially different between 5–8 levels (samples 14–17, Table 12b).

Orebodies within the oxidised zone (4 level and above) consist of irregularly fractured chert, often with a sugary texture, that contains small lenses of black silica. Fracture surfaces are coated with iron oxides, principally goethite and limonite. Within reefs that directly overlie the Little Schist, fracture density and amount of black silica decrease toward the orebody hangingwall.

Gold reefs in the sulphide zone have been described as consisting of dark grey or black silica with pyrite in nests or as disseminations, and minor pyrrhotite (Hall, 1918). Pyrite is the dominant iron phase below 4 level (Clarke, 1975) and is by far the most abundant sulphide present.

De Villiers (1975) reported disseminated and irregular-shaped pyrite grains, broken and skeletal arsenopyrite needles, small amounts of pyrrhotite and chalcopyrite and a few grains of cobaltite in ore from Piggs Peak. A few grains of gold enclosed in silicate (maximum size 10 μm by 30 μm) and a single 2 μm gold inclusion in pyrite were described by the same author. There is no indication of which section of the mine the sample examined by De Villiers was obtained.

In contrast, drill cores of sulphidic chert taken south of the gold workings (BH PP1, Fig. 22a) contain ubiquitous pyrrhotite with little or no pyrite. Pyrrhotite occurs as

both 100–700 μm grains in fractures, and as fine-grained disseminations. Minor chalcopyrite and arsenopyrite are present as inclusions within, and small grains attached to the edges of pyrrhotite anhedra.

New Section

Because of poor exposure and inaccessible workings, few data are available from Piggs Peak New Section. Borehole BH PP4 (Fig. 21) drilled through thick (±110 m) talcose schists before intersecting white, recrystallised chert with conspicuous partings of chromiferous sericite (Randell, 1979). A similar lithology is reported to host the gold mineralisation in the New Section (Hall, 1918).

Stoping patterns suggest that the New Section orebodies were small and irregular. Hall (1918) described ore shoots 0,6–1,8 m-wide, 30–60 m long with a minimum vertical depth extent of 60 m. Richest gold values were associated with pyrite concentrations; arsenopyrite and possible stibnite were also reported by Hall (1918).

Geochemistry

Whole-rock trace element determinations of the Piggs Peak chert body and adjacent units, from cores drilled in the area well south of the gold workings (BH PPl, Fig. 21) are given in Table 11. These data show the chert to contain significantly more As and Ba, and less Cu, Zn, Co and Ni than either footwall or hangingwall units. In addition, the footwall unit contains high Mn values compared with adjacent units. Gold values are everywhere <20 ppb.

A similar element distribution is indicated from soil geochemistry, where high arsenic values in soils quite closely define the outcrop of the chert body (Fig. 21; Randell, 1979). In addition, thin manganiferous chert with wad of the Devils Reef-type (see below) was also identified from the results of soil analyses in the vicinity of BH PP5 and 6 (Fig. 19). The manganiferous unit also contains <20 ppb gold.

The patterns of trace element distribution described above are not spatially related to economic gold — pyrite mineralisation in the Old Section. It is argued below that emplacement of gold occurred during an event that superimposed a later geochemical signature on the chert body which itself had been previously mineralised with Fe, Mn, Ba and As.

Major and trace element analyses representative of oxide and sulphide zone orebodies, Contact- and Cross-Schists, and mineralised fracture Types 1 and 2 are given in Table 12 (a) & (b). These data show that most reefs have highly silicic compositions with ±5 wt per cent Fe, but only trace amounts of Mg, Ca, Na and K. More ferruginous compositions do occur, particularly in the vicinity of Back stope (samples 12–13, Table 12). In addition, manganese values are consistently higher in orebodies below 4 level.

TABLE 11
Geochemical analyses of Piggs Peak chert and adjacent units from cores recovered in BH PP1 (ppm)[1]

	Ba	As	Cr	Co	Ni	Cu	Zn	Mn
Footwall	33	<20	837	59	121	55	78	274
Chert	57	195	135	5	25	16	11	305
Hangingwall	<10	42	191	48	98	62	89	1986

[1]recalculated from Randell (1979).

Notes: footwall data , mean 17 determinations; chert data, mean 55 determinations; hangingwall data , mean 14 determinations. Each determination represents the semi-quantitative AAS analysis of 1 m length of core.

TABLE 12(a)
Chemical compositions of the Piggs Peak gold deposit. I: Major elements (weight per cent)

	Cross-Schist					Crush-Zones				Surface reef				5–6 Level reef			
	1	2	3	4	5	6	7	8	9	10	11	12	13	14	15	16	17
SiO_2	72,10	58,00	67,70	56,10	59,50	35,90	32,20	2,30	4,50	91,50	96,80	66,45	77,00	85,60	92,00	88,60	94,50
TiO_2	0,48	0,05	0,08	0,21	0,92	0,12	0,18	<0,05	<0,05	<0,05	<0,05	0,17	<0,05	<0,05	0,06	<0,05	<0,05
Al_2O_3	18,00	25,60	19,60	25,50	24,60	25,00	11,85	4,00	2,90	0,60	0,10	4,65	3,00	0,20	2,40	0,20	0,50
Fe_2O_3	0,47	3,63	0,68	3,15	1,98	20,20	35,55	77,90	77,20	5,74	0,70	18,65	13,70	6,72	1,83	4,36	1,58
FeO	0,22	0,07	0,12	0,17	0,37	0,07	0,15	0,05	0,07	0,32	1,17	0,37	0,15	0,72	1,90	1,36	1,24
MnO	<0,05	<0,05	<0,05	<0,05	<0,05	0,12	0,18	0,34	0,17	<0,05	0,10	<0,05	<0,05	0,19	0,23	0,15	0,18
MgO	0,60	0,40	0,50	1,80	0,30	<0,10	<0,10	<0,10	<0,10	<0,10	0,10	0,20	<0,10	0,10	<0,10	1,00	<0,10
CaO	<0,05	<0,05	<0,05	0,10	<0,05	<0,05	<0,05	<0,05	<0,05	<0,05	<0,05	<0,05	<0,05	<0,05	<0,05	<0,05	<0,05
Na_2O	0,20	0,20	0,20	0,30	<0,10	<0,10	<0,10	<0,10	<0,10	<0,10	<0,10	<0,10	<0,10	<0,10	<0,10	<0,10	<0,10
K_2O	5,45	3,81	5,17	3,37	6,63	1,25	<0,05	<0,05	<0,05	<0,05	<0,05	1,19	<0,05	<0,05	0,31	<0,5	<0,05
P_2O_5	0,05	0,05	0.05	0,05	0,05	0,25	0,80	0,15	0,63	0,05	0,05	0,05	0,16	0,05	0,05	0,05	0,05
SO_3	<0,02	<0,02	<0,02	<0,02	<0,02	0,02	0,10	0,17	0,05	<0,02	0,20	0,97	0,02	8,11	0,25	4,77	1,07
CO_2	0,10	0,10	0,10	0,10	0,12	0,10	0,10	0,10	0,10	0,10	0,12	0,10	0,10	0,34	0,10	0,63	0,10
Loss	2,56	7,18	3,99	4,89	4,52	15,50	16,75	13,80	14,30	1,57	0,61	7,27	5,25	5,43	0,74	2,90	0,67

Notes: see Fig. 24 for sample localities 1–13.

1. quartz-chromiferous sericite schist ("Contact Schist"), 2 level; 2. pale brown coloured quartz-sericite schist ("Cross-Schist"), 10 m from footwall contact; 3. white quartz-sericite schist (central "Cross-Schist"), 25 m from footwall contact; 4. quartz-sericite-tourmaline schist ("Cross-Schist") interlayered with black silica, 47 m from footwall contact; 5. quartz-sericite schist ("Cross-Schist" extension), 70 m from footwall contact, western cross-fracture stope; 6. soft, pale brown coloured clay in 100 mm-wide Type 2 fracture, footwall margin of chert body; 7. ferruginous, hydrothermal clay in low-angle 60–300 mm-wide Type 2 fracture with angular chert fragments, northwest footwall margin (mean 2 analyses); 8. 20 mm-wide goethite/limonite-filled Type 1 fracture with angular chert fragments, 'E' stope; 9. 20–90 mm-wide brecciated ironstone-filled Type 1 fracture, Blacksmith Shop stope, 2 level; 10. 1,5 m-wide conformable reef with iron oxide alteration, northern cross-fracture stope; 11. Back stope siliceous reef with sulphides, composite 6 m-long channel sample; 12. narrow ferruginous reef, Back stope (mean 2 analyses); 13; ferruginous chert reef, 0,5 m from Cross-Schist (mean 2 analyses); 14. 5 level stope bottom, far north reef, 15 m from footwall, 10 m from hangingwall (M.C.G. Clarke samples 366–368); 15. stope bottom 5/6 level, 1,5 m from footwall (samples 123–126); 16. stope bottom 5/6 level, 11,5 m from footwall (samples 138–139); 17. 6 level reef, 1,5 m from western footwall contact (composite of samples 42–43 and 80–83).

TABLE 12 (b)
Chemical compositions of the Piggs Peak gold deposit II: Trace elements (ppm)

	Cross-Schist					Crush-Zones				Surface reef				5–6 Level reef			
	1	2	3	4	5	6	7	8	9	10	11	12	13	14	15	16	17
Au	0,06	0,34	0,31	8,70	13,80	8,70	61,50	2,80	0,59	3,20	2,30	19,30	8,00	14,30	17,60	20,20	9,20
Ag	<0,10	0,10	0,20	0,30	0,20	0,50	0,45	0,40	0,40	0,30	0,50	15,50	0,30	0,80	0,90	0,70	0,60
Pt	0,30	0,10	<0,10	0,10	0,20	<0,10	0,20	0,10	0,20	<0,10	0,30	0,10	0,20	<0,10	<0,10	<0,10	<0,10
B	214	236	236	6 820	198	136	40	56	37	22	31	174	31	3	59	19	74
Ba	388	376	797	842	1 131	578	1 919	668	<20	<20	<20	1 138	84	<20	85	<20	<20
As	50	1 000	420	910	200	9 900	15 200	24 400	10 030	2 100	1 000	4 000	4 200	1 000	6 300	2 600	1 600
Sb	2	9	3	4	10	11	75	9	13	5	8	12	10	3	8	4	6
Cr	1 095	<340	<340	<340	<340	753	1 779	<340	<340	<340	<340	2 258	479	<340	<340	<340	<340
Co	<10	10	<10	<10	10	40	50	90	80	10	10	45	10	30	50	60	20
Ni	13	144	29	53	46	265	97	231	126	25	23	49	20	82	130	77	97
Cu	3	121	7	9	46	502	304	792	538	36	29	680	52	68	48	36	31
Pb	12	23	18	22	22	76	130	57	59	28	11	71	28	25	13	20	11
Zn	13	21	11	9	10	75	83	241	176	21	6	10	16	14	12	15	13
[1]Hg	268	446	337	46	22	71	26	364	232	196	130	54	431	237	676	356	1 538
Sn	46	<20	23	<20	<20	<20	<20	<20	22	<20	<20	<20	<20	<20	<20	<20	<20
W	<20	<20	<20	<20	<20	<20	25	<20	<20	<20	<20	<20	<20	<20	<20	<20	<20
Y	<10	<10	<10	<10	31	12	11	<10	<10	<10	10	10	<10	n.d.	<10	n.d.	<10
Zr	54	125	159	176	213	66	67	16	22	17	18	51	31	n.d.	23	n.d.	19
[2]Au/Ag				29,0	69,0	17,4	136,7	7,0		10,7	4,6	1,2	26,7	17,9	19,6	28,9	15,3

[1]reported as ppb; [2]where Au >1 g/t; n.d. = not determined; [for notes see Table 12 (a)].

Though data are sparse, there is some indication that Ag values are higher in the structurally upper (hangingwall) member of the chert body. Certainly all concordant reefs contain proportionally more Ag than the Crush-Zones that fed them (see interpretation below). The average *in situ* reef has an Au/Ag ratio of 17,8, compared with 29,5 for the entire deposit. Both As and Sb are concentrated in significant amounts in all gold reefs.

Analyses of Cross-Schist and related quartz-sericite schist units contain 3,4–6,6 per cent K (samples 1–5). These values are consistent with lithologies that contain 30–60 per cent sericite by volume. Relatively high values of B, Ba, Zr, Sn and small gold values are thought to be characteristic of the trace element distribution of the Contact and Cross-Schist.

In contrast, sample 7 (Table 12) is a Type-2 vein filling located 65 m south of the Cross-Schist that contains K (and thus sericite) in only trace amounts. Both ferruginous and aluminous Crush-Zone compositional types contain relatively high Mn, P and Ba contents, and show exceptionally high As and Sb values. In addition, samples from Type-2 fractures contain very high Au contents, high Au/Ag ratios and Cr in significant amounts.

Interpretation

An interpretative sketch of the Piggs Peak gold deposit is given in Fig. 26. Because the chert body is turned vertically on edge, this cartoon can be viewed both as a surface plan and in section but should be read together with the orientation data plotted in Fig. 25. Figures 25 and 26 show the following features:

1. All gold reefs of economic importance are located within the basal, layered member of the chert body. Major orebodies of this type are tabular in shape, concordant with the chert layering, and before tectonic rotation were flat-lying.

2. All mineralised fractures (Types 1 and 2) were inclined at angles of 60°–80° toward the west or northwest before tectonic rotation (in present-day co-ordinates). Most mineralised fractures cut the basal member of the chert body, and both fracture density and vein width (amount of dilation) progressively decrease at higher structural levels. Where composite Type-1 — Type-2 veins occur, it appears that ironstone (Type-1) was deposited on the fracture hangingwall and aluminous hydrothermal clay with

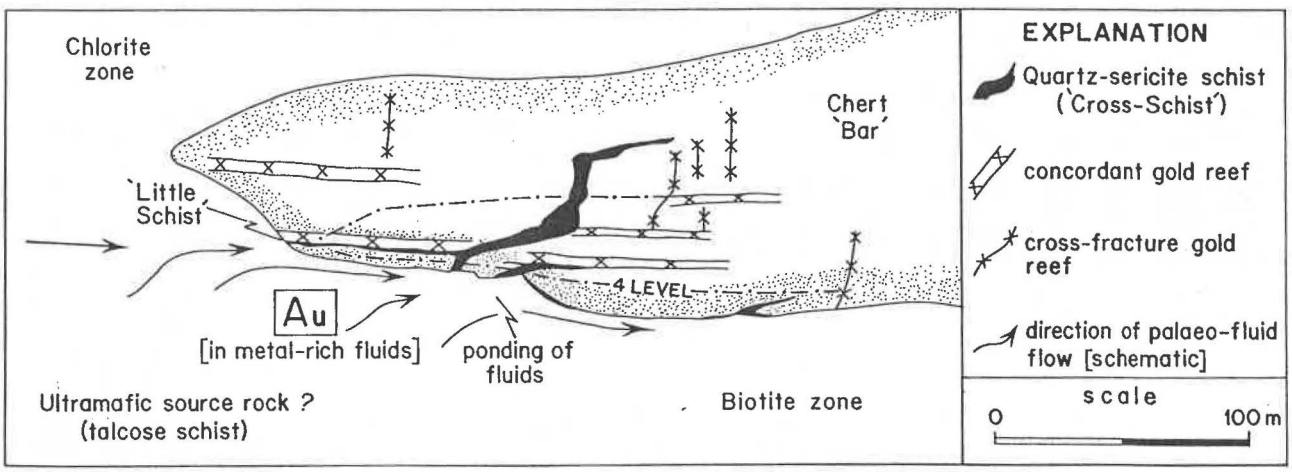

Figure 26
Summary and interpretive sketch of the main features of the Piggs Peak gold deposit. In this cartoon, the chert body is interpreted as a classical "bar" or impermeable cap rock below which gold-bearing fluids were ponded before being emplaced along hydraulic fractures. The cartoon can be viewed in section since the dip of the chert body is near vertical. Mineralised fractures of Types 1 and 2 are oriented in the plane of the page.

rich gold values (Type-2) was deposited on the fracture footwall.

3. The initial orientation of sparsely mineralised conjugate fracture pairs (Type-3) was also steep, but approximately normal to the fracture direction of Types 1 and 2. Type-3 fractures are found in large part within the upper member of the chert body, and within the upper levels of the old workings.

4. Gold orebodies have a symmetrical distribution to either side of the Cross-Schist (within 100–150 m strike). Most of the important reefs are located in areas where the Cross-Schist intersects the chert layering with a relatively small angle. The Cross-Schist occupies a stepped fracture that before tectonic rotation had an average dip of 33°–37° toward the northeast.

The simplest interpretation of these data is that fluids rich in precious metals were emplaced along fractures that propagated upward from the base of the chert body. Most mineralised fractures appear to be tensile in origin; chert layering was not displaced laterally during dilation. The association of tensile cracks with bulk movement of fluids is consistent with a deformation in which fractures were opened hydraulically.

Deposition of gold occurred principally in flat-lying, concordant reefs. For this reason, Carter (1966) believed Piggs Peak to be a palaeo-placer deposit, whereas Clarke (1975) thought that syngenetic processes were more important. However, the same pattern of flat-lying mineralisation could be accounted for if permeable horizons within the chert body acted as horizontal channels along which gold-bearing fluids drained to the surface. Geometry and fracture patterns of all major reefs are consistent with an environment in which fluids travelled laterally, parallel with stratigraphic surfaces. Some Type-3 fractures may have resulted from overpressuring by pore fluids within horizontal channels of this type.

Though numerous small mineralised fractures are present, auriferous fluids appear to have been focused along major fractures now occupied by quartz-sericite schist. Ponding of fluids within the footwall chromiferous sericite schist unit (Fig. 26), followed by the progressive wedging-open of fractures provides the simplest explanation of gold concentration at Piggs Peak. If correct, the model implies a hydraulic gradient in which fluids migrated along the base of the chert body from an area further north (see Fig. 26).

The initial orientation of the Cross-Schist is consistent with a stepped, low-angle fracture that cut up through the lithologic sequence toward the southwest (Fig. 25b). Directions of fluid movement within the Cross-Schist may be indicated by the steep tourmaline lineation which before tectonic rotation plunged northeast.

Though no substantial fault displacement is recorded along the Cross-Schist, its trend is parallel with the trace of the décollement in the overlying tectonic unit (Fig. 19). For this reason, it is suggested that the accumulation of high pressures of pore fluid, fracturing and gold mineralisation may have taken place during tectonic loading and high fluid activity associated with regional thrusting.

Gold reserves and future exploration

The results of a sampling program of stope faces, drives and cross-cuts in the upper mine levels (1–4) indicate that workings in the Old Section have been very thoroughly cleaned and that very little potential ore remains (Carter, 1966). Clarke (1975) and Wiseman (1975) estimate that 10 000 tons of ±5 g/t gold reef remain *in situ* in the walls of development within the oxide zone (4 level and above), and this figure is consistent with the results of assays obtained during the present study.

There has been considerable stoping between 4 and levels, and it appears that most of the rich ore betwee these levels has also been mined out. Nonetheless, on th basis of assays from 430 channel (1 m) samples, Clark (1975) estimated that 90 000 tons of potential ore with ar average grade of 9 g/t remain in the flooded section of the mine.

The assay plan of 6 level given in Clarke (1975) suggests an average grade of 5.3 g/t for the basal (footwall) member of the chert body (mean of 104 samples). This value is considered appropriate for the block of ground 100 m long, 8 m wide and 30 m deep above and below 6 level that represents the bulk of the available tonnage below the standing water-level.

A combined estimate of 75 000 tons potential ore of ±5 g/t is considered realistic for both upper and lower levels in the Old Section. Tonnage could be increased (though not by a large amount) by working lower grade material. These reserves would support a mill production rate of 15 000 tons/year (50 tons/day) for five years.

Possible additional tonnage may be present in undeveloped ground south of the Cross-Schist. A block of ground that represents an *in situ* tonnage of $2{,}5.10^5$ tons is present between 1–3 levels and does not appear to have been explored (see Fig. 23). The model described above suggests that an area of this type is likely to contain economic quantities of gold. A short cross-cut from the long exploration drive on 2 level is required to confirm the presence of payable zones.

Exploration for more substantial ore shoots may also be worthwhile. It is possible that the total production from Piggs Peak, though significant, may have come from only a fraction of the entire orebody. If this were so, and if the mineralisation model described above is correct, then future exploration should be directed toward locating the strike and dip extensions of the Cross-Schist. Clearly, orebody extensions along the strike of the chert body in excess of ±150 m from the Cross-Schist are unlikely. Steeply inclined boreholes sited in positions A and C (Fig. 21) with a vertical borehole (B) in between the two collars are more likely to intersect payable values.

Finally, it is noted that gold in small amounts is present in the sands dump from the 1941–1951 operation. A survey and sampling program was conducted by Clarke who estimated 75 000 tons sands containing 1 g/t (Ann. Rept., 1975).

Conclusions

1. An irregular-shaped body of massive chert hosts the Piggs Peak gold deposit (Old Section). The chert lithology represents a silicified clastic or volcaniclastic sequence and is located close to the surface that separates the biotite and chorite metamorphic zones.

Sulphides (pyrrhotite with minor chalcopyrite and arsenopyrite), and local concentrations of manganese oxides are associated with the chert horizon and may have formed during silicification. The chert body is enriched in Fe, Mn, Ba and As, and depleted in most base metals relative to both footwall and hangingwall units.

2. Gold mineralisation was accompanied by brittle deformation of the chert body. Thus formation of the gold deposit is consistent with processes that operated after silicification was complete. Gold-bearing fluids were emplaced and focused along steep fractures: the larger of these fractures now exhibit extensive potassic (sericitic alteration and high contents of B, Ba, Zr and Sn.

Deposition of gold with ubiquitous pyrite and minor arsenopyrite occurred in flat-lying reefs that average 15 g/t Au over 2 m widths. Geochemical data show that exceptionally high As and Sb contents are associated with economic gold values.

3. A model is described in which the Piggs Peak chert body is interpreted as a classical chert "bar", below which hydrothermal fluids were ponded. The simplest interpretation of the data is that hydraulic fractures of the type inferred at the base of the chert body formed during the accumulation of high pressures of pore fluid sustained during regional thrusting. Fluids that travelled laterally (rather than vertically) within the chert body, cooled and deposited precious metals. Major gold reefs are interpreted as permeable horizons along which gold-bearing fluids drained to the surface during a tectonic (thermal) event.

4. *In situ* gold reserves of 75 000 tons proved potential ore that contains ±5 g/t is present in the Old Section workings. This figure is conservative, and takes no account of potential ore within surface excavations. Additional tonnage may exist in ground south of the Cross-Schist, and small pockets of reef may be identified in other areas in the vicinity of what is inferred to have been the main hydrothermal vent. Prospecting for blind ore shoots along the strike and dip extensions of the Cross-Schist is considered worthwhile, and possible locations of diamond drill holes are suggested.

DAISY GOLD DEPOSIT

In terms of its declared output (593,2 kg), the old Daisy Mine is the third-largest gold deposit in Swaziland. In the past, gold was won from the oxidised zone of the orebody, and ground 40 m below surface was considered unpayable. Recent data from borehole intersections presented here suggest that significant potential ore remains *in situ* below the level of the deepest stope.

From a brief description of the mine geology, it appears that the Daisy deposit provides a rather clear example of a mineralised thrust surface, and as such resembles a number of other deposits in northwest Swaziland. Evidence for this interpretation comes from the inverted metamorphic sequences to either side of the orebody, and the associated tectonic duplication. This evidence is important, and is described in some detail below.

Geological description

The Daisy gold deposit is associated with metamorphic sequences mapped as part of the Onverwacht Group and is located 1,75 km northwest of the AG3 batholith. A regional geological account, and a full description of the gold deposit are available in Hunter and Jones (1963) and Jones (1969); these sources provide the basis of much of the interpretation given here.

Figure 27 is a geological plan of the Daisy gold deposit. Old workings consist of 5 adit levels and 4 main quarries that extend over a strike length of 700 m. Most of the mining took place in the vicinity of No. 1 quarry, and it is in this area that orebody extensions are known to be present. Underground workings are no longer accessible and the following description and geochemical data are based on observations and samples taken in and around the surface excavations.

The lithological sequence at Daisy (Fig. 28) can be accurately compiled from measurements taken on cores recovered from a total of 18 boreholes drilled into the deposit. Borehole data show that lithological units dip more or less uniformly at 70° towards the southwest (range 50°–85°). All boreholes were sited to intersect the orebody from collars in the structural hangingwall of the deposit (Fig. 27).

The gold orebody is located along a line of complex deformation marked by fault repetition, small-scale folding and extensive sericitisation. Upper amphibolite facies metamorphic sequences structurally overlie the deposit. Foliated amphibolites (quartz-actinolitic hornblende schists) with layers of biotite schist comprise a hangingwall unit that is not less than 150 m thick. The basal 20–30 m of the amphibolite unit is garnetiferous (Hunter and Jones, 1963).

Layers of biotite schist within the hangingwall amphibolite sequence range in width from 5 mm to a maximum of 3 m, and are extensively developed immediately above the orebody. In thin-section, biotite has a distinctive reddish-coloured pleochroism that resembles vermiculite. Sulphides that include arsenopyrite, quartz and carbonate veins and tourmaline are invariably present within the biotite-garnet amphibolites.

Exploration boreholes drilled through the Gordon gold deposit 0,8–1,0 km WSW of the Daisy workings intersected abundant layers of grey foliated granite (maximum 6 m thick) up to 40 m above the Daisy thrust. BH 177 (Fig. 27) intersected two 1 m-wide layers of granite oriented parallel with the amphibolite foliation within the same structural horizon (Jones, 1969).

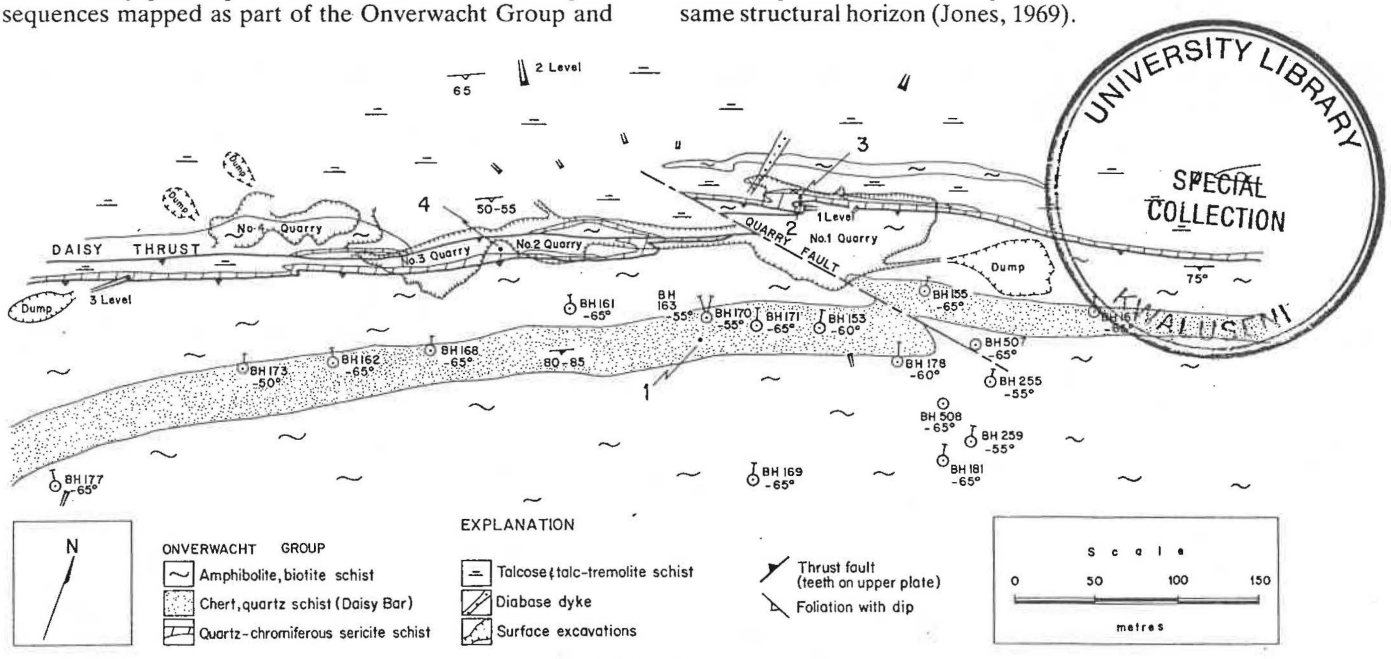

Figure 27

Geological plan of the Daisy gold deposit with the locations of borehole collars (after Hunter and Jones, 1963, Jones, 1969 and Clarke, 1978, with additions). Geochemical analyses of samples from localities 1–4 are given in Table 26.

A marker horizon known as the "Daisy Bar" is present within the amphibolite unit ±50 m above the orebody. The Daisy Bar is a totally recrystallised chert body (sample 1, Table 26) and contains abundant sericite within the basal (northwestern) member. Andalusite occurs with sericite near the Jackal Prospect, 430 m ENE of the Daisy deposit. With the exception of BH 255 (Fig. 27) which intersected gold values along the basal chert-amphibolite surface, the Daisy Bar is not known to be associated with gold mineralisation.

South of the Mhlotshane River, the Daisy Bar decreases in thickness to 7 m and contains abundant inclusions and layers of amphibolite and biotite schist. For this reason, the Daisy chert is considered to represent a silicified horizon of the type described from gold deposits elsewhere (see Piggs Peak deposit).

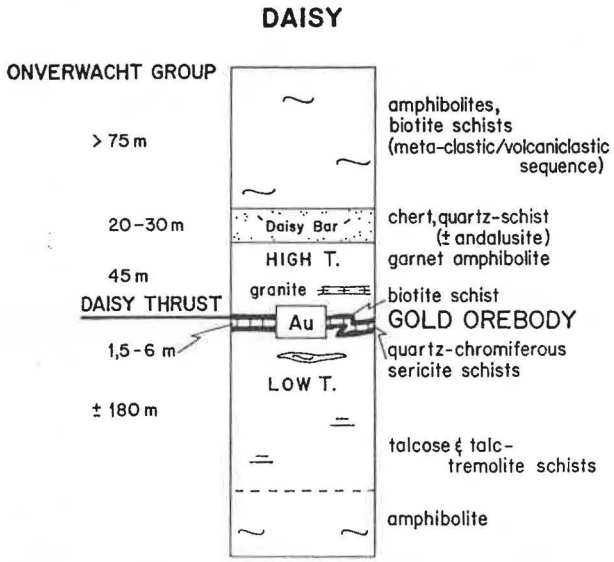

Figure 28
Lithological sequence in the vicinity of the Daisy gold deposit.

Gold is concentrated at the base of the amphibolites within a 1–3 m-wide biotite schist unit (sample 2, Table 26). The orebody contains lenses and stringers of black quartz, abundant ferroan carbonate, and is frequently associated with sulphides (pyrite, pyrrhotite, arsenopyrite and chalcopyrite). The presence of biotite schist rich in sulphides but without economic values of precious metals indicates that much of the gold was introduced with silica alone.

Quartz-chromiferous sericite schists (sample 3, Table 26), occur in the immediate footwall of the orebody in the vicinity of quarries Nos. 1 & 2. There, the unit is 1,5–6 m thick, contains narrow layers and lenses of biotite schist, and is closely associated with zones of faulting. Elsewhere (No. 4 quarry) gold occurs in quartz lenses within talcose schists below the sericitic unit. Thin tectonic slivers of biotite schist are present below the sericitic unit in areas where the lithological sequence has been repeated by faults.

Various talcose schists with carbonate segregations form the footwall sequence of the Daisy deposit (sample 4, Table 26). Tremolitic amphibolite that exhibits a spinifex-like texture is present 50 m below the orebody (near 2 level adit) and appears to increase in proportion downsection until talc-tremolite schists pass into massive amphibolites with increase in metamorphic grade. The entire footwall sequence is allochthonous and thrust over Moodies Group quartzites at the foot of Kamhlabane mountain (Fig. 2).

Structure

The structure of the Daisy deposit can be accounted for in terms of the deformation and displacements associated with two faults, termed the Daisy and Quarry Faults by Jones (1969; see Fig. 27). Tectonic duplication and thickening are associated with the Daisy Fault, and borehole data (BH 173 & 162) indicate reversed fault offsets. Though Jones (1969) inferred that the Daisy Fault had strike-slip displacement, the available data can more easily be interpreted in terms of a thrust regime and the Daisy Fault is correlated here with a décollement surface (Fig. 27).

The Quarry Fault is a left-lateral strike-slip fault (with a 6 m dip-slip component) inclined at ±50° toward the north. Small-scale folding is closely associated with the fault surface: evidence from the BH 171 log indicates that fold axes plunge east at ±45° (Jones, 1969). Gold content can be directly correlated with degree of deformation and high values are often found in areas deformed by small S-shaped folds (see also She and Waterfall fold deposits).

It is noted that the line of intersection of the Quarry and Daisy Faults plunges east at ±25° and is approximately parallel with an ore shoot inferred from borehole data and described below. It seems likely that the Daisy and Quarry Faults and the gold orebody formed during a single tectonic stress regime.

Ore mineralogy

Jones (1969) reported that ores from both the Daisy and Gordon deposits consist primarily of pyrite, with lesser amounts of chalcopyrite and pyrrhotite. Pyrite is present in both quartz veins and in adjacent wall-rocks as undeformed grains <200 μm in size. Pyrite is often rimmed with other sulphides and appears to be early in the paragenetic sequence.

Pyrrhotite anhedra with exsolution lamellae of pentlandite are common and are often moulded around pyrite grains. Irregular veinlets of chalcopyrite cut pyrrhotite grains and represent the paragenetically youngest sulphides present.

Jones (1969) also observed irregular 1–25 μm particles of gold, most of which occur in silicate (quartz). Gold is also present along grain boundaries of various sulphide phases. A single grain of gold within euhedral pyrite, and a second grain within a pyrrhotite vein were recorded by the same author.

Exploration data and gold reserves

An extensive drilling program of 14 boreholes was completed by the Geological Survey Department during 1962–1963 (Hunter and Jones, 1963). Four boreholes have been drilled since then, two (BH 255 & 259) in 1965 (Ann. Rept., 1965), and two (BH 507 & 508) in 1976 (Clarke, 1978). Together, a total of 2 422 m drilling has been completed.

Gold values and widths measured from core intersections are given in Table 13. Cores from nine of the 18 boreholes returned gold values on assay; six of these are payable and were obtained from the down-dip extension of No. 1 quarry area. Boreholes drilled below quarries Nos. 2 and 3 detected no gold, and values intersected below quarry No. 4 were sub-economic (Table 13). Borehole logs and reliable assays for BH 507 and 508 are not available though Clarke (1978) reported preliminary values below economic grade.

The first boreholes drilled below No. 1 quarry (BH 153 & 155) intersected high values in sulphide zone reef 45 m and 21 m below 2 level respectively. These data confirm reports that only the oxidised zone of the deposit was mined. The depth of weathering in borehole cores indicates that oxidation has proceeded to the level of the deepest stope (±40 m below surface).

TABLE 13
Width and grade of lode intersections, Daisy gold deposit[1]

	1	2	3	4	5	6	7	8	9	10	11	12	Average (3–12)
Borehole No.	173	162	163	—	—	—	170	153	178	155	259	255	—
Width (m)	0,91	0,86	0,79	0,91	1,52	1,00	1,96	1,63	1,52	1,30	1,24	0,76	1,40
Grade (g/t)	5,5	5,0	2,6	24,3	7,9	17,8	5,7	28,5	9,9	21,1	7,8	5,3	13,53

[1]recalculated from Hunter and Jones (1963) and Jones (1969)

Notes: 1. biotite schist along fault surface below No. 4 quarry, 82 m down-hole (excludes additional 2,9 g/t over 0,84 m in talc-tremolite schist 100 m-down hole); 2. talc-tremolite schist 15 m below Daisy thrust, No. 4 quarry dip extension; 3. reef 1,5 m above quartz-sericite schist unit, dip extension between quarries Nos 1 & 2; 4–6. biotite schist and amphibolite within 2 m of thrust surface, 1 level adit main lode; 7. reef 1,8 m above quartz-sericite schist unit, 2 level extension, No. 1 quarry; 8. quartz-biotite schist, 5,5 m above quartz-sericite schist unit (excludes additional 8,4 g/t over 0,69 m, and 4,4 g/t over 1,19 m in ground immediately above sericitic unit); 9. quartz veins in amphibolite 2 m above quartz-sericite schist unit, 105 m down-dip of outcrop; 10. reef 1,5 m above sericitic unit (excludes additional 3,03 g/t over 1,91 m and 4,11 g/t over 1,3 m in amphibolites 42,5 m and 61 m down-hole respectively); 11. reef 7,5 m above quartz-sericitic schist unit, 126 m down-dip of outcrop; 12. quartz veins in amphibolite, 10 m above sericitic unit, 97,5 m down-dip (excludes additional 5,59 g/t over 0,46 m immediately below Daisy Bar).

Exploration at the Gordon deposit included two drill holes, the second of which intersected 6,5 g/t over 1,04 m with core loss reported in the first hole (Hunter and Jones, 1963). Adit sampling was also carried out at the Jackal prospect, but with negative results.

Gold reserves have been calculated for a block of ground below No. 1 quarry for which there are data from six borehole intersections (7–12, Table 13). These data suggest, though by no means prove, the presence of an ore shoot that pitches at ±30° toward the east. For the purposes of tonnage calculation, the width of the ore shoot is assumed to be 70 m, measured within the plane of the Daisy Fault and normal to the direction of pitch. In ground between 2 level and the deepest borehole intersection (BH 259) the oreshoot has a cross-sectional area of 12 500 m^{-2} equivalent to an *in situ* tonnage of 46 300 tons (see data in Table 13).

At the grade estimated from borehole intersections (13,5 g/t), the potential tonnage contains 626 kg gold metal. Mined at 40 per cent payability (equivalent to 5,4 g/t) the ground immediately below No. 1 quarry would yield ±250 kg gold from sulphide zone reef.

Gold is present in two tailings dumps located on alluvial flats of the Mhlotshane stream, west of No. 4 quarry. According to Hunter and Jones (1963), the larger dump contains 14 800 tons with an average gold content of 1,3 g/t, while the smaller dump contains 3 175 tons assaying 3,3 g/t. Both dumps were resampled by Clarke (GSD diagram no. 1492) who reported 21 000 tons tailings with an average grade of 1,2 g/t in the larger (sands) dump, and 3 000 tons assaying 2,5 g/t in the smaller (slimes) dump.

WYLDSDALE, LOMATI AND LUFAFA ZONE GOLD DEPOSITS

In many ways, the gold deposits located in the valley of the Lomati River below Lufafa mountain are the most interesting in Swaziland. Though past production is relatively small (250 kg), the potential for a future gold mining industry in this area is thought to be considerable. Three distinct gold deposits, as well as two low-grade, high-tonnage occurrences are described below. All occurrences fall within an area of radius 1,5 km of the now disused Wyldsdale Mine.

Bulk variations in lithological composition that are generally assumed to have largely determined the patterns of distribution and concentration of gold everywhere in the greenstone belt can be clearly documented in the vicinity of the Wyldsdale deposit. It appears that when high-level granitoid intrusions such as the Wyldsdale pluton are emplaced into hydrous ultramafic sequences, economic deposits of gold very often result.

There is almost 1 km of topographic relief between the summit of Lufafa mountain and the valley of the Lomati River below. Largely unsilicified clastic sequences, as well as an imbricate stack of shales repeated with silicified and sericitised lithologies crop out on the steep mountain slopes and provide some of the best exposed stratigraphic and structural sections in northern Hhohho.

Regional geology

Field relations indicate that the Wyldsdale granodiorite pluton crops out close to an important tectonic break (Fig. 29). East and southeast of the pluton, the regional structure can be described in terms of a series of stacked and folded thrust sheets, each containing predominantly igneous sequences and each of which cuts up-section toward the west. The Mgudugudu thrust is the décollement at the base of the tectonic pile.

For much of its length, the Mgudugudu thrust is a well-defined fracture with a more or less constant trend. However, in the vicinity of the Wyldsdale pluton the position of the thrust is less clear. Though outcrops are sparse, evidence that the granodiorite intrudes the fault is lacking.

Allochthonous sequences also crop out west of the Wyldsdale pluton in an area known as the Lufafa zone. In contrast with sequences farther east, the Lufafa zone consists almost exclusively of tectonically stacked sedimentary units. Furthermore, the regional dip within the stack is toward the interior of the greenstone belt. Fine-grained lithologies contain a slatey cleavage also inclined steeply toward the west or northwest. Evidence from overlapping thrusts (Fig. 33) indicates that the tectonic transport direction is *toward* the edge of the greenstone belt.

High in the Lufafa zone stack is a complex tectonic stratigraphy that consists of at least five thin (150–220 m) thrust slices (see Fig. 29). Each thrust plate rests on either talcose schist or a related lithology immediately above a décollement. Grey laminated shales, silicified in part to chert, together with tuffs, iron-formations and gold-antimony deposits are repeated by thrusts. Ubiquitous sericite, usually chromiferous in composition, and a variety of green cherts occur along or close to fault surfaces. The entire sequence is interpreted as an imbricate stack in which talcose schists and shale horizons low in the regional stratigraphy have been caught up in major movement horizons.

A sequence of unmineralised coarse greywackes and volcaniclastic sandstones 200–300 m thick occurs above the basal shale member. The greywackes are poorly sorted and consist principally of angular clasts of chert, vein quartz and silicic volcanic material. Normally-graded units are present and these are consistent with upright stratigraphic facing directions.

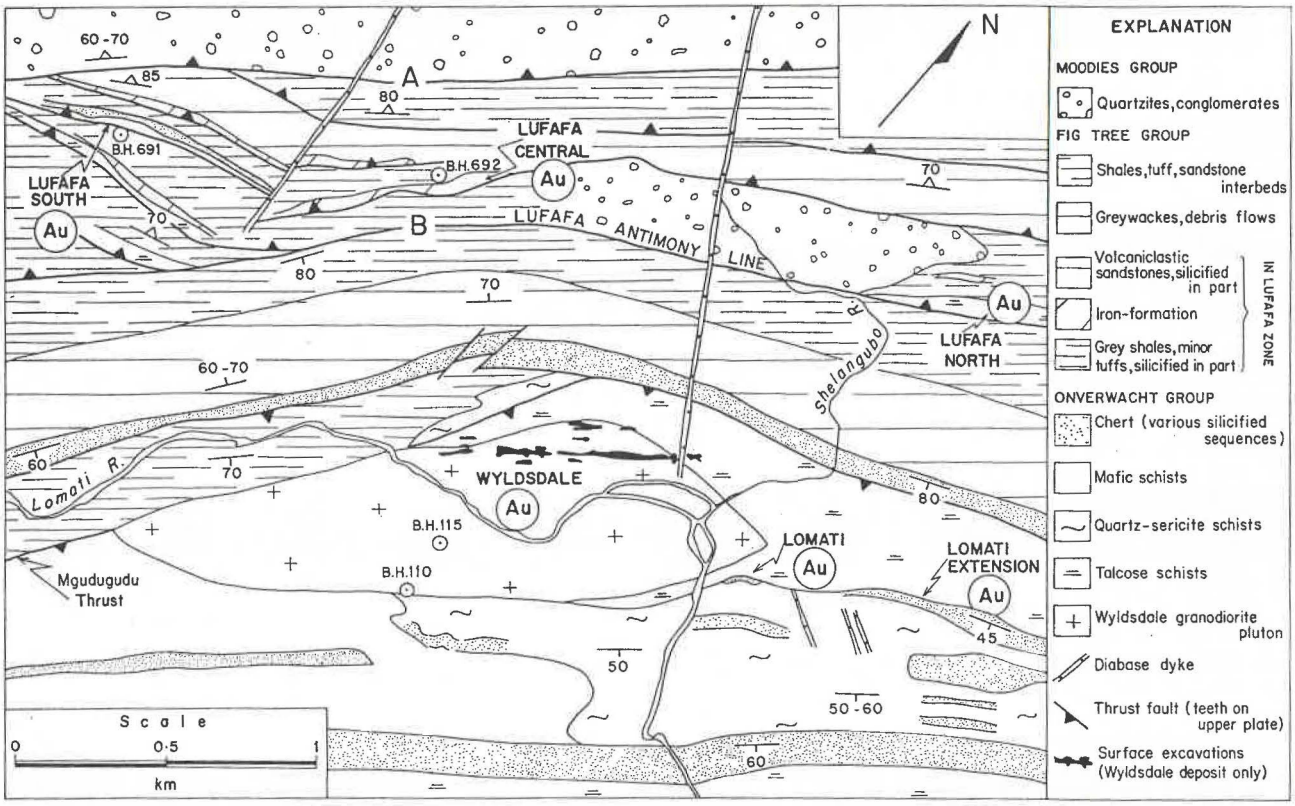

Figure 29

Geological map and locations of the Wyldsdale, Lomati and Lomati Extension gold deposits, and the Lufafa zone prospects (with data from Hunter, 1959b). Thrust faults A and B define the margins of a complex zone of thrust belt tectonics associated with gold and antimony mineralisation (Lufafa zone).

Rounded, boulder-sized clasts (≤1 m) of hematite iron-formation or ferruginous chert occur within the upper part of the clastic sequence. Compositional layering in the iron-formation is often oblique to the coarse bedding of the enclosing greywacke matrix. Individual boulders are as much as 5 m apart and suggest matrix-support during transport. Redeposited iron-formation of this type forms part of a coarsening-upward sequence ±50 m thick that is structurally overridden by a thrust sheet that consists in large part of shale.

A structural interpretation of the lithological sequence is given in Fig. 30. Though the Lufafa zone sequences were correlated with the Onverwacht Group by Hunter and Jones (1968), regional stratigraphic considerations suggest that the sequence forms part of the Fig Tree Group.

Sedimentological studies are required before more precise stratigraphic interpretations are possible.

WYLDSDALE GOLD DEPOSIT

Gold in the Wyldsdale deposit is concentrated within and along the margin of a granodiorite pluton (the Wyldsdale pluton, see sample 8, Table 26). As Fig. 29 shows, the Wyldsdale pluton is 2,1 km long, a maximum of 600 m wide and lensoid in shape. The long axis of the intrusion is parallel with the regional structural trend.

Country-rocks in the aureole of the intrusion vary in lithology along the length of the body. Talcose schists, metamorphosed to amphibolite in the vicinity of the Lomati gold deposit surround the northern end of the intrusion. Quartz-sericite schists up to 380 m-thick that contain massive layers and lenses of silica are developed south and southeast of the Wyldsdale workings, immediately above the ultramafic unit. The sericitised sequence is overlain by thin andalusite-bearing silicic ash-flow deposits (Fig. 30).

Elsewhere, the Wyldsdale granodiorite body is emplaced into a variety of unmineralised mafic schists, shales and volcaniclastic material. It is significant that gold mineralisation is restricted to those areas where sequences of ultramafic composition surround the pluton, and where thick sericite-schists occur in the structural hangingwall of the intrusive body.

Several features of the Wyldsdale pluton distinguish it from granites of the AG3-type:

1. The intrusion is flooded with black quartz veins. These average 10 mm in width, but veins and pods of black silica 0,5 m wide are also present. Individual veins are several metres in length. Drusy quartz textures have been observed within veins in 10 mm-wide vugs. Pyrite, minor pyrrhotite and coarse molybdenum sulphides are associated with the black silica, and Hunter (1959b) reported the presence of scheelite.

Quartz veins show a preferred orientation. Measurements in outcrops along the south bank of the Lomati River where the granodiorite is well exposed indicate veins that trend 010°–055° and dip at large angles (≥65°) toward the southeast are relatively common within the stockwork. The density of veining varies considerably in different parts of the intrusion, and appears to be relatively high in areas mineralised with gold.

2. The intrusion is extensively fractured. Fractures with a 20–50 mm separation, and a sub-horizontal orientation are dominant: along the south river bank they are inclined ≤45° toward the southeast (see also Fig. 32). Unlike the quartz veins, the fractures are not mineralised and everywhere displace the quartz veins, sometimes by several centimetres.

Fracturing and quartz veining of a similar type to the Wyldsdale body have been noted in the nearby Mzimnene

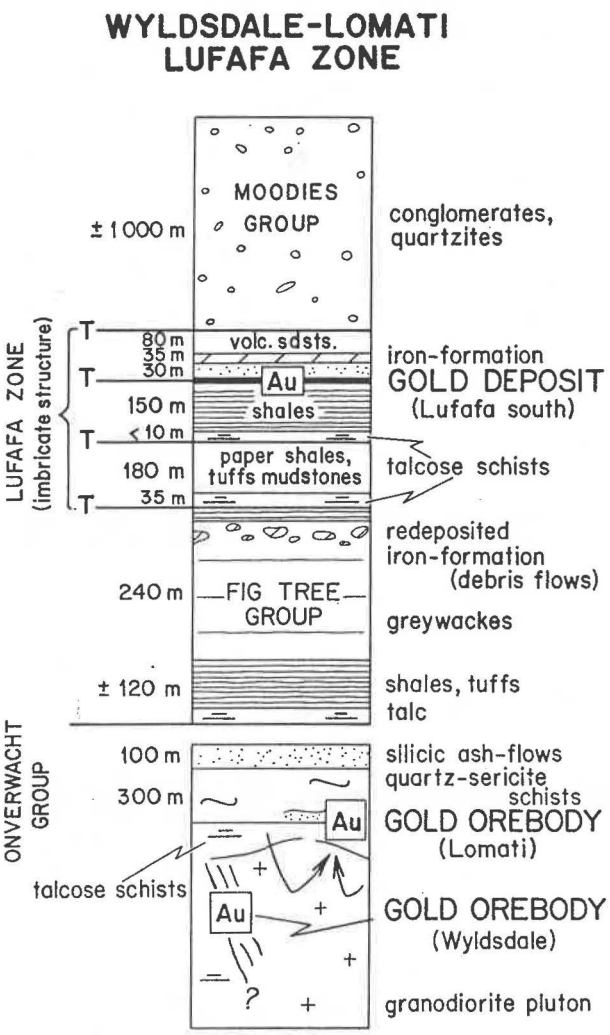

Figure 30
Interpretative lithological sequence showing the present order of tectonic stacking and distribution of gold deposits below Lufafa mountain. The Lufafa zone sequence is interpreted as an imbricate stack that includes the basal shale members of the Fig Tree Group.

pluton. There, fracture density is an order of magnitude lower than in the Wyldsdale body.

3. The intrusion has been subjected to extreme mineralogical alteration consistent with a pervasive hydrothermal metamorphism. The breakdown of feldspar (microperthite and oligoclase) to sericite, and to a lesser extent ferroan carbonate is typical. Sericite is pale green in colour close to the talcose margins of the intrusion.

Large clots of primary biotite are almost completely replaced by chlorite, and steep chlorite and sericite-filled shears rich in sulphides, black silica and gold are common. Shear zones of this type are sub-parallel with the principal direction of quartz veining and with the trend of surface mine excavations north of the river (Fig. 29). Granitoid lithologies metamorphosed in shear zones have ribbon-quartz textures.

4. The intrusion contains numerous inclusions of country-rock. South of the river, small xenoliths of amphibolite that contain a foliation surface that is parallel with the mineralised fracture direction are closely associated with zones of deformation within the pluton. Exposures of granodiorite are scarce elsewhere, though Hunter (1959b) described linear zones of "dolomitic phyllite" close to the northern edge of the intrusion (Fig. 32). According to Hunter one of the xenoliths forms a marker horizon 7,5–9 m wide that extends for a strike length of several hundred metres (see reef 'B', Figs. 31 and 32).

Though the composition of the inclusions in the vicinity of the mine workings is uncertain, it seems probable that they include amphibolites rich in ankerite of the type observed within and around the margin of the intrusion elsewhere. It is not clear whether the elongate xenoliths described by Hunter (1959b) were emplaced by magmatic stoping processes, or were tectonically interleaved during translational deformation.

Exploration data

The Wyldsdale gold mine operated more or less continuously between 1938–1951, and during this period produced almost 120 kg gold. A small output was also declared for three additional years (Sims, 1981). The average grade at which the deposit was worked is not known.

Intensive prospection of the deposit was undertaken by the Geological Survey Department between 1958–1960. The results of this work were described in Hunter (1959b) and later summarised in Davies and Hunter (1964). The geology of the deposit has been re-examined by the writer though data obtained during the earlier exploration phase form the basis of gold reserve estimates given below (Tables 14 and 15).

Hunter (1959b) reported that existing workings extend for a strike length of 640 m, and consist of 23 adits and a number of small quarries. Underground workings can be

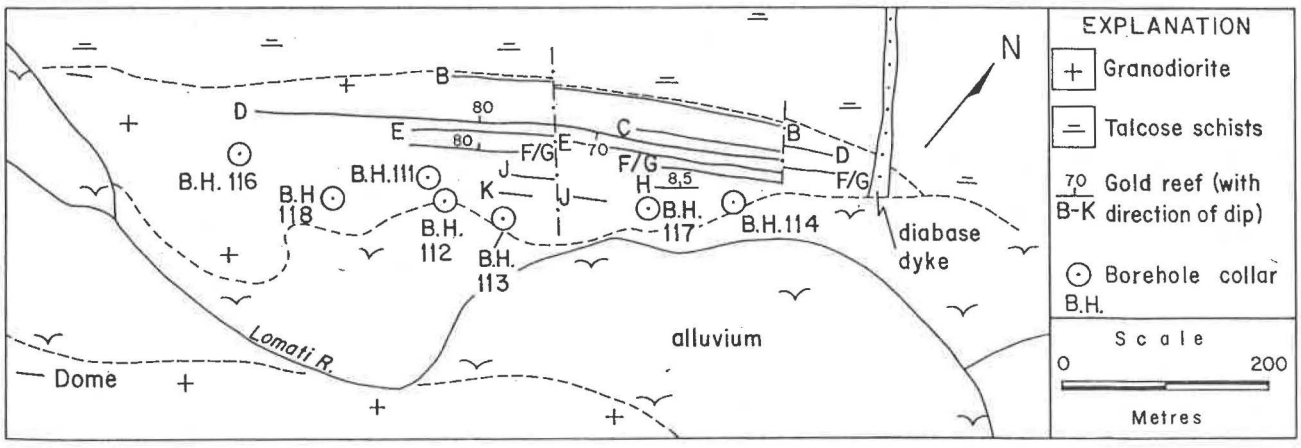

Figure 31
Surface plan of payable auriferous reefs with borehole collars, Wyldsdale gold deposit (after Hunter, 1959b; Davies and Hunter, 1964). Reefs F and G are separated by a 1,5–3 m thickness of granodiorite and are drawn together; there is no reef I. All drill holes were inclined at −30°, except BH 111 (−50°), BH 113 (−25°) and BH 116 (−40°). Pay limit is 435,4 cm-g.

TABLE 14
Gold values from borehole intersections, Wyldsdale deposit[1]

Borehole No.	111	112	113	114	115	117	118	mean
Reef width (m)	1,12	1,47	2,57	3,07	2,21	3,51	1,70	2,24
No. intersections	3	4	3	7	4	4	4	4,2
Width country-rock (m)	24,8	69,3	51,0	59,3	32,1	57,8	32,7	49,2
Average grade (g/t)	34,4	8,1	13,5	9,3	2,6	3,3	16,2	14,1

[1]recalculated from Hunter (1959b).

Notes: intersections <0,1 m in width and <2 g/t are not included; mean excludes BH 115 in Dome Rock.

described in terms of 5 levels, each ±10 m apart, though according to Hunter these are not developed in a systematic manner. Unoxidised granodiorite occurs below 3 level. Hunter estimates that of a total of 792 m underground development, only 177 m is on reef.

During 1959, seven boreholes were drilled in the vicinity of the Wyldsdale workings on the north bank of the Lomati River (Fig. 31). A further two boreholes were drilled south of the river (BH 115 and 110, Fig. 29); BH 110 in the Far West Section was eventually abandoned in weathered granodiorite after the third attempt to collar the hole. From a total metreage of 883,7 m approximately 713,8 m was drilled north of the river. All seven boreholes in the northern area intersected the granite-talcose schist contact: the deepest intersection was 137 m below outcrop in BH 112.

Visible gold was present in cores from four of the seven holes (BH 113, 114, 117 and 118), and additional very high gold values (74 g/t and 63 g/t) were obtained in cores from BH 111 and BH 118. Only BH 116 failed to intersect economic values.

Measurements of mineralised intersections (Table 14) show that on average, a gold lode 0,56 m in true width that assays ±14 g/t is present within each 10 m width of granodiorite. A range of 3–7 lode intersections was obtained from each borehole.

As Hunter (1959b) pointed out, because the boreholes were not sited to intersect down-dip extensions of specific reefs identified on surface, the consistently high gold values returned are significant. It is noted that numerous unpayable values (<2 g/t) and/or widths (<0,1 m) were intersected but are not included in the data in Table 14.

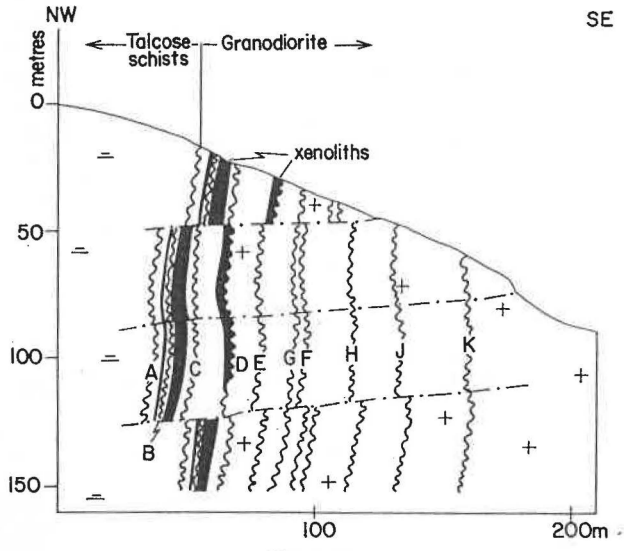

Figure 32
Schematic distribution of gold reefs (A–K) and sub-vertical xenoliths (black) within the Wyldsdale pluton north of the Lomati River (redrawn from Davies and Hunter 1964). Sub-horizontal fractures displace both reefs and xenoliths.

Adits, drives and stope faces were sampled during the same program, and assay values obtained indicate a general decrease in gold content in areas without quartz vein or xenolithic material. A marginally lower average grade of ±13 g/t (mean 164 assays) is indicated from this work, though isolated values of 300–350 g/t were recorded. Because most of the rich ore within existing development has in large part been mined out (e.g. in D reef), the average grade probably represents a minimum estimate. Assays of several grab samples collected on reef by the writer returned uniform values in the range 15–25 g/t. Estimates of *in situ* gold reserves given in Table 15 are derived from a combination of surface, underground and borehole data.

Polished-sections of fractured sulphide zone granodiorite contain coarse (100–500 μm) pyrite euhedra with minor goethitic alteration, as well as thin smears of pyrite along recrystallised quartz subgrain boundaries. Relatively unmetamorphosed granodiorite contains biotite with exsolved rutile along cleavage traces, major pyrrhotite as 100–700 μm rhombohedral grains and minor pyrite and chalcopyrite (<100 μm grains). No gold was observed in polished-section. Gay (1968) reported that a sample of Wyldsdale reef assayed 886 fine (Au/Ag = 7,7) and contained trace amounts of Cu, Sb, Co, Pb, Ni, Pt and Sn in spectrographic determinations.

Borehole and development intersections were correlated by Hunter (1959b) who distinguished 10 major reefs (A–K, Fig. 32), and a number of miscellaneous smaller reefs. Most reefs correspond with shear zones in granodiorite or surfaces that separate granodiorite and xenoliths of country rock. Reef A is located along the granodiorite — talcose schist contact. All reefs strike ±060° and are sub-vertical; most are inclined 75°–85° toward the northwest, others are inclined at similar angles toward the southeast.

Gold reserves

The percentage payability of each reef was calculated by Hunter (1959b), based on a mining width of 0,76 m and a pay limit of 435,4 cm-g (100 inch-dwt). His data indicate an average payability of 19,7 per cent for the entire deposit (including miscellaneous reefs) and 24,1 per cent for major reefs alone.

With the strike and dip extensions for individual reefs given in Table 15, Hunter calculated that 331 900 tons of potential ore grading 5,4 g/t (±1,8 tons gold) is present *in situ* in 8 reefs. The 4 richest reefs (B, D, F and G) contain 204 100 tons with 7,4 g/t (±1,5 tons gold) to 60–107 m below outcrop (Table 15).

The *in situ* tonnages given by Hunter for the block of ground around the Wyldsdale workings (Table 15) are felt to be entirely reasonable. What is less certain is the most suitable mining operation by which the gold can be won. Because further boreholes are unlikely to yield much additional information, the next stage of prospection should include driving to the margin of the intrusion from 4 or 5 level, followed by development and bulk sampling on reef (see also Hunter, 1959b).

TABLE 15
Grade and tonnage estimates, Wyldsdale gold deposit[1]

	1	2	3	4	5	6	7	8	9	10	11	12
Grade of pay sections (g/t)	29,5	11,7	14,6	7,9	42,5	15,0	7,7	10,5	30,0	17,7	17,7	17,7
Overall grade (g/t)	10,7	4,1	5,1	2,5	5,8	5,3	1,8	3,9	10,2	5,4	7,4	17,7
In situ tonnage (10^3 tons)	79,4	105,8	49,8	15,0	34,5	40,5	4,5	2,4	1,2	331,9	204,1	65,6

[1]recalculated from Hunter (1959b) and based on 49 borehole intersections and 164 reef intersections in underground development. All grades based on a mining width of 0,76 m; pay limit taken at 435,4 cm-g (100 inch-dwt); S.G. = 2,15. Data exclude Miscellaneous and "A" reefs.

Notes: 1. "B" reef, 1,5 m from granodiorite contact, strike length 457 m, dip extension 107 m (mean 6 assays, 2 payable); 2. "C" reef, strike length 610 m, dip extension 107 m (mean 8 assays, 2 payable); 3. "D" reef, strike length 366 m, dip extension 84 m (mean 33 assays, 8 payable); 4. "E" reef, strike length 152 m, dip extension 61 m (mean 9 assays, 2 payable); 5. "F" reef, strike length 347 m, dip extension 61 m (mean 15 assays, 2 payable); 6. "G" reef, strike length 408 m, dip extension 61 m (mean 53 assays, 16 payable); 7. "H" reef, strike length 73 m, dip extension 38m (mean 14 assays, 2 payable); 8. "K" reef, 95,0–105,8 m from granodiorite contact, strike length 107 m, dip extension 15 m (mean 7 assays, 2 payable); 9. Far West reef, south bank Lomati River, strike length 61 m, dip extension 12 m (mean 16 assays, 5 payable); 10. grade and tonnage in 8 reefs (1–8), excluding "A", Far West and Miscellaneous reefs; 11. grade and tonnage in 4 reefs, B, D, F and G (1, 3, 5 and 6); 12. selective mining on 9 reefs (B to K and Far West reefs) at 19,7 per cent payability (>435,4 cm-g).

LOMATI AND LOMATI EXTENSION GOLD DEPOSITS

The Lomati gold deposit is located within the aureole of the Wyldsdale pluton and 0,5 km from the disused Wyldsdale Mine (Fig. 29). Old workings consist of a quarry excavated on the summit of a small conical hill 36 m above the Lomati River, and two adit levels. The distribution of workings indicates that past production (93 kg) represents ore mined within 25–35 m of the surface.

Two distinctive gold bearing lithologies crop out within the quarry. Massive, translucent green chert, rich in chromiferous sericite (sample 7, Table 26) and with veins of black quartz is interlayered with extremely friable and ferruginous quartz-sericite schist (samples 5 & 6, Table 26). Only the soft quartz-sericite schist has been mined: the main sericitic lode is a tabular body 1,7–2,5 m wide and inclined at ±45° toward the southeast. Small veins of sericite schist are present and cut the massive chert.

Below the basal chert member is a 20 m thickness of actinolitic hornblende amphibolite that contains carbonate rich in ankerite and fractures smeared with iron oxides. The metamorphosed ultramafic unit rests on the veined and fractured Wyldsdale granodiorite.

Detailed sampling of the Lomati orebody and adjacent chert units was conducted along three traverse lines within a 20 m strike length. Assays of 0,1 m-wide channel samples (40 determinations) show that the main lode has an average grade of 11,9 g/t over a width of 1,7 m. Individual assays are extremely variable and range between 2–100 g/t. Small gold values (±4 g/t) are associated with the chert body, which is auriferous several metres from the sericitic reef.

Lomati Extension is located 250 m northeast of the Lomati deposit, and is a true strike extension of the main occurrence (Fig. 29). Surface workings extend along a strike length of 180 m, and three adits have been driven in talcose schist to intersect the reef. Hunter (1959b) records a 0,5 m-wide vein of granodiorite within the lower adit level.

Chromiferous and sericitic cherts are also associated with the Lomati Extension orebody. Massive silica of this type is absent in ground between the two deposits (see Fig. 29) and it appears that silicification, the introduction of chromiferous sericite and gold mineralisation were synchronous.

It would be a simple matter to re-open both Lomati and Lomati Extension underground workings for the purposes of winzing and sampling on reef. Diamond drilling from surface in order to intersect the sulphide zone of both deposits may also be worthwhile.

LUFAFA ZONE GOLD DEPOSITS

The Lufafa zone is a linear belt of highly deformed, mostly clastic sedimentary sequences that are closely associated with low-grade antimony mineralisation. The zone extends for at least 20 km in Swaziland and is interpreted here in terms of thrust belt tectonics. A 4 km-long section of the Lufafa zone has been examined in the vicinity of the Wyldsdale deposit (see Fig. 29).

Lufafa south (Figs. 29 & 33), was identified as an area of anomalous antimony mineralisation during the UN mineral survey of Swaziland (UNDP, 1970, location 69). An airborne EM anomaly was recorded in the area, and follow-up ground geophysical measurements revealed two linear zones of high electrical conductivity in the vicinity of the geochemical anomalies (Burley and Andrew, 1969).

A total length of 500 m shallow trenches were excavated across a strike width of 410 m during the present investigation. A measured structural section through the lithological sequence, and its interpretation are given in Fig. 30. Significant gold-antimony mineralisation was intersected in a single horizon 130–150 m south of the thrust surface at the base of the Moodies Group (Fig. 33).

The gold-bearing horizon is a ferruginous wad rich in chromiferous sericite (samples 10 & 11, Table 26). The sericitic unit is 20–30 m thick and structurally overlies a deformed shale-tuff sequence. Silicified shales, ferruginous cherts and banded iron-formation form the structural hangingwall of the auriferous unit.

Grab samples of reef material contain ±10 g/t Au and 10 ppm Sb. From surface indications alone, the main mineralised zone has a strike length of 140 m, a width of 23 m and an average grade of ±1 g/t (Table 16). Shallow boreholes (BH 691, Fig. 33) drilled with a portable machine proved the potential orebody to a depth of 20 m, though core recovery was low. A block of ground 50 m long and 6 m wide intersected in trenches 2 and 12 (Fig. 33) contains ±110 kg gold that could be easily won by shallow quarrying operations (see Table 16).

Lufafa central (Fig. 33) was described briefly by Hunter (1959b) who reported average grades of 5,6 g/t Au over 1,3 m in trenches excavated in ferruginous sequences along a 70 m strike length. During the present study, 415 m of trenches were reopened or dug within two horizons of banded iron-formation (Fig. 33; sample 12, Table 26). Both units of iron-formation are extensively deformed by minor folds with steep plunging axes.

Of the 515 m total strike length examined, gold mineralisation was confirmed within a zone 165 m long (between trenches 10–21, Fig. 33). It is noted that trenches 3–9 (Fig. 33) were excavated on steep, scree-covered

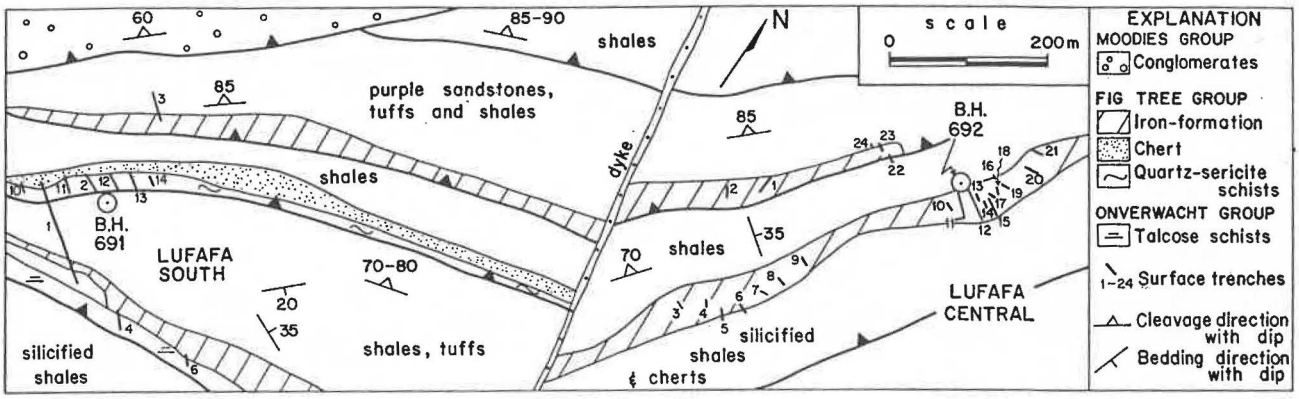

Figure 33

Location and geology of low-grade, high-tonnage gold deposits below Lufafa mountain. West of the dyke (Lufafa south) gold-antimony mineralisation is associated with quartz-chromiferous sericite schists; east of the dyke (Lufafa central) gold is contained in brecciated hematite iron-formation. The attitude of overlapping thrusts requires that directions of tectonic transport were toward the southeast.

slopes and much of the material assayed may not have been representative of hematite iron-formation *in situ:* deeper sampling methods are required in this section. Borehole BH 692 (Fig. 33) was abandoned after intersecting 25 m of fractured ground.

Relatively high gold values (5–7 g/t) are associated with zones of brecciation and quartz veining within the iron-formation. An average grade of 1,65 g/t and a payable width of 16,3 m (Table 16) indicate that ±1,4 tons gold are present *in situ* to 100 m down-dip. Bulk sampling and metallurgical tests are required on the potential ore. The terrane in both Lufafa central and southern areas is such that adits could readily be driven to intersect pay zones at considerable depths below surface.

In the Lufafa north area (Fig. 29), small quantities of gold are found in association with quartz veins in talcose schists. Urie (in Hunter, 1959b) reported a maximum value of 2,9 g/t over 0,64 m in surface trenches, and his data are consistent with assays obtained during the present investigation. Twenty one trenches totalling 206 m in length were dug over a strike length of 350 m parallel with a major thrust trace (Fig. 29). A small mineralised section 12,5 m long returned an average grade of 3,1 g/t but with very erratic gold values (Table 16).

The results of prospecting in two additional sections of the Lufafa zone are briefly reported here. Both prospects were identified by the UN mineral survey as areas of anomalous antimony and arsenic mineralisation (locations 71 & 73, UNDP, 1970). Subsequent regional geochemical data (Forgeron, 1979) confirmed the presence of highly anomalous arsenic values in stream sediments in one of the areas (location 71).

Near the Ntintinyane River (location 73), talcose schist and shale are present in the upper plate of the same thrust fault that brings up Onverwacht Group sequences at the Lufafa north prospect (Lufafa antimony line, Fig. 29). Trenches excavated in the talcose schist revealed only sparse gold mineralisation (1–2 g/t) of a similar type to Lufafa north. The area is not considered to be of economic interest.

Mineralisation in the Kuthayela area (location 71) is more interesting. Four trenches dug over peak antimony anomalies in soils during the UN survey were reopened and the samples collected and assayed for gold. Small values (≤4 g/t) were obtained from the extreme south-eastern section (trench 2), and similar values were obtained by extending the excavations along the strike for a further 80 m. Gold appears to be associated with black quartz veins and sulphides within a coarse clastic and volcaniclastic sequence, 10–20 m from the basal thrust of the Moodies Group. Unexpected gold and antimony mineralisation was also recorded from an amygdaloidal lava flow within the Moodies Group near Makonjwa mountain (sample 13, Table 26). More systematic exploration is required in this area.

KOBOLONDO AND BLACK DIAMOND CREEK GOLD DEPOSITS

Both Kobolondo and Black Diamond Creek are located in the rugged and heavily afforested central section of the greenstone belt. The regional geology, and a full description of both deposits is given in Jones (1963).

The Kobolondo deposit, including the Hilltop gold mine (the southwestern section of Jones, 1963) and various alluvial sources has a recorded output of ±140 kg, of which the bulk was produced at an average grade of 6,7 g/t (Sims, 1981). Much of the Kobolondo orebody has been mined by surface excavation alone, though seven irregularly-spaced levels can be recognised (Jones, 1963).

Gold at Kobolondo is associated with a small, elliptical-

TABLE 16
Tonnage estimates of low-grade gold deposits, Lufafa zone

	Lufafa south		Lufafa central		Lufafa north	Total	
	1	2	3	4	5	6	7
Average width (m)	23,4	6,3	16,3	6,5	6,3	19,9	6,4
Average grade (g/t)	0,89	2,95	1,65	3,05	3,10	1,27	2,97
in situ tonnage (10^3 tons)	819,0	39,4	833,7	12,6	—	1 652,7	52,0

Notes: 1. strike length 140 m, down-dip extension 100 m, S.G. = 2,5 (mean 117 assays of quartz-chromiferous sericite schist from 5 trenches); 2. highest grade area of above, 50 m strike and dip extensions (mean 18 assays from 2 trenches); 3. strike length 165 m, down-dip extension 100 m, S.G. = 3,1 (mean 165 assays iron-formation from 11 trenches); 4. highest grade area of above, 25 m strike and dip extensions (mean 13 assays from 2 trenches); 5. strike length 12,5 m (mean 19 assays talcose schist with quartz veins from 3 trenches); 6. total *in situ* tonnage (mean 1 and 3); 7. total highest grade material (mean 2 and 4).

shaped intrusive body of granodiorite. The intrusion is 520 m-long, and has a maximum width of 150 m; the long axis of the body is oriented NE-SW parallel with the regional structural trend.

The granodiorite is emplaced into a series of talcose schist, quartz-sericite schist and quartz-cabonate schist country-rocks. A small lens of granodiorite is present within the sequence north of the main body and indicates that the roof of the intrusion is irregular in shape. A large xenolith of quartz-carbonate and talcose schists 20–40 m wide occurs as a pendant within the roof of the intrusion: it is along one margin of this xenolith that gold is concentrated.

The petrography of the granodiorite closely resembles the Wyldsdale pluton. Highly sericitised andesine phenocrysts, minor K.feldspar, biotite almost totally replaced by chlorite and accessory hornblende are observed in thin-section.

A single milky-white coloured quartz vein that carries pyrite and visible gold was worked in the past and is now entirely stoped out in the upper mine levels. According to Hall (1918), the reef was 1,2–3,7 m wide, and steeply inclined (60°–80°) toward the southeast. The quartz vein trends parallel with the long axis of the intrusion and has a proven strike length of 102 m (Jones, 1963).

On 5-level and above, the vein overlies a 10–15 m-wide footwall unit of ankeritic schists while granodiorite forms the structural hangingwall. Below this level the reef is entirely enclosed by deformed and brecciated granodiorite. Ferroan carbonate and pyrite are present in wall-rocks on all levels, and the reef itself contains green-coloured lenses and partings of material presumed to be chromiferous sericite. Jones (1963) reports that the milky-coloured quartz vein contains veinlets of black quartz that carry arsenopyrite and chalcopyrite. The same author described coarse molybdenite flakes on fresh surfaces of granodiorite.

During 1962, two boreholes were drilled at Kobolondo that intersected the main lode 55–65 m below surface. From a total vein width of 1,3 m, one borehole (BH 156, Ann.Rept.,1962) intersected quartz reef that assayed 2,62 g/t over 0,46 m. The other (BH 159) intersected a 1,57 m-wide quartz vein that was entirely barren, though small gold values were obtained from veins located deeper in the footwall. Adit levels were also sampled by Jones (1963) and his assay plan shows an average value of 1,2 g/t from 18 gold determinations.

While these data are not encouraging, it does seem possible that additional reefs of the Wyldsdale-type are present in the Kobolondo pluton. Such reefs could be detected during a systematic diamond drilling program.

Black Diamond Creek is a much smaller gold deposit (5,1 kg production). Gold occurs in narrow, tourmaline-bearing quartz veins within talcose schists and chert. In the vicinity of the old Black Diamond Creek workings, the talc schist unit is 45 m thick and inclined northwest: it is interpreted here as a major movement horizon. Jones (1963) sampled quartz veins on surface and underground and reported a maximum value of 11,8 g/t over 0,46 m.

DEVILS REEF GOLD DEPOSIT

Devils Reef is quite unlike any other gold deposit in Swaziland. First, though small in size the orebody was exceptionally rich. During 1890–1891, 87,63 kg gold were produced from only 69 tons of ore, an average grade of 1,27 kg/t (>0,1 per cent Au). This return exeeds that of any comparable initial gold crushing in southern Africa (Sims, 1981). Thus, in part the orebody contained 6.10^5 times the average crustal abundance of gold.

Second, Devils Reef is the only deposit documented here in which gold occurs in pockets rich in manganese oxides and hydroxides together with large drusy quartz crystals. Evidence described below is consistent with very rapid deposition of gold from hydrothermal fluids focused along zones of faulting. Like the Piggs Peak deposit, emplacement of gold appears to have post-dated earlier processes of sedimentation. Unlike other gold occurrences, Devils Reef is closely associated with an iron deposit of the Ngwenya-type, and may have formed at the same time (see Devils Reef iron deposit).

Geological description

The lithological sequence in the vicinity of the Devils Reef gold deposit is correlated with part of the Onverwacht Group (Fig. 34). The correlation is suggested by lithology and regional structure which indicate that the Devils Reef sequence forms part of the Havelock tectonic unit. Structural facing-directions derived from the geometry of funnel-shaped bodies of ferruginous wad (see below), and grading in lapilli-tuffs show that the Devils Reef sequence faces west, toward the Havelock serpentinite.

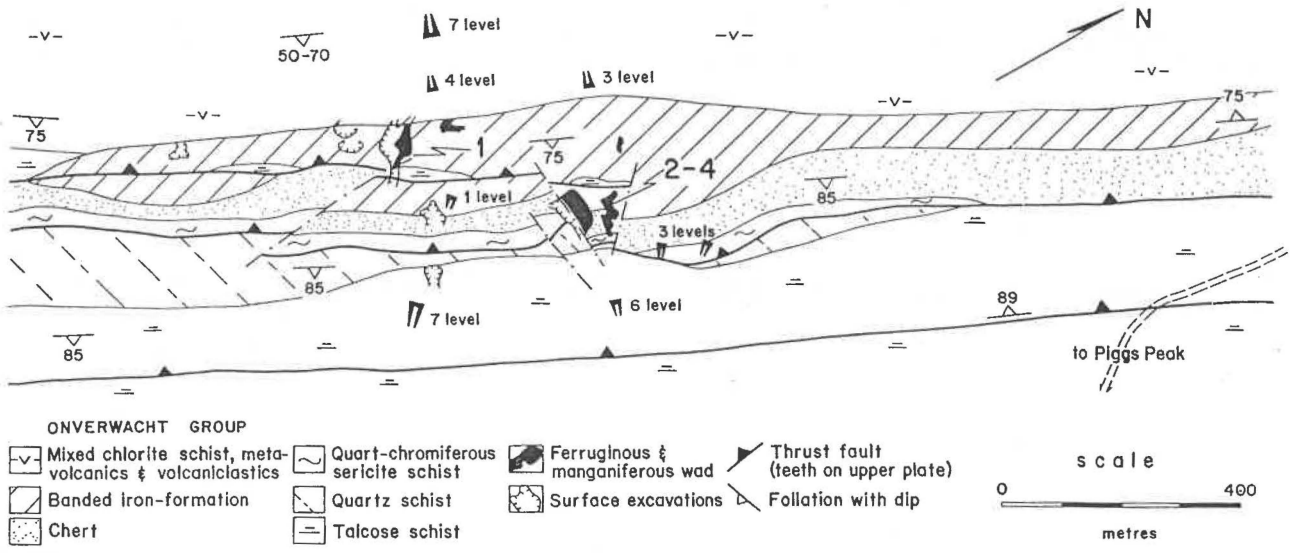

Figure 34

Geological plan of the Devils Reef gold deposit and iron-formation (modified from Jones, 1962). Gold is associated with pockets of ferruginous and manganiferous wad located within the central section of the lenticular-shaped hematitic chert body. Geochemical analyses of samples 1–4 are given in Table 27.

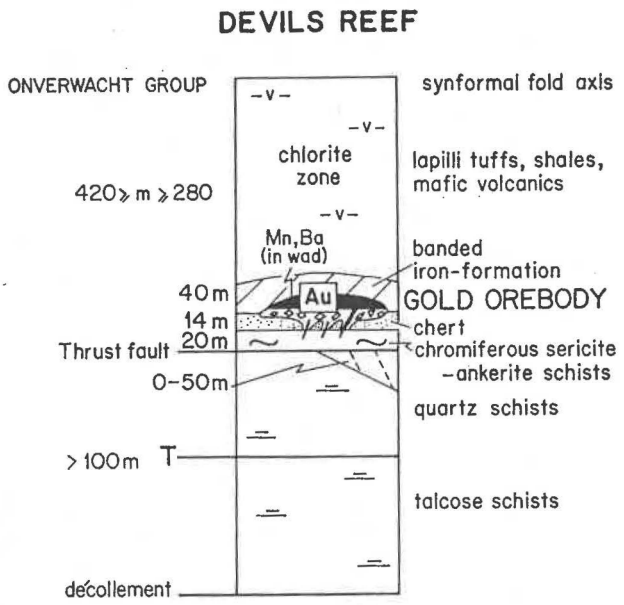

Figure 35
Lithological sequence in the vicinity of the Devils Reef gold deposit and iron-formation.

The décollement at the base of the Havelock thrust sheet reappears as a vertical zone of talcose schists 200 m east of the old workings at Devils Reef. A flat-lying zone in which foliation surfaces in chlorite schists are <20° is present 0,5 km west of Devils Reef, and occupies the core of a synformal fold.

A summary of the lithological sequence (Fig. 35) shows that the stratigraphic hangingwall of the near vertical Devils Reef iron-formation consists of thick quartz-chlorite schists together with more massive chloritic units. Mafic volcanics with pillow-like structures, various volcaniclastic horizons and slates can be recognised, all at low grades of metamorphism. Jones (1962) described an amygdaloidal lava flow from the same sequence which is almost certainly a coarse lapilli-tuff horizon.

The Devils Reef iron-formation rests above banded cherts and passes laterally into ferruginous and non-ferruginous cherts north of the gold workings. In this respect it resembles iron-formations in the Fig Tree and Moodies Groups of the type that formed by processes of replacement.

Underlying the Devils Reef iron-formation and ferruginous chert body is a unit of quartz-chromiferous sericite-ankerite schists. The schists are vivid emerald green in colour, and contain unusually large amounts of ankerite/ferroan dolomite. The unit is invariably separated from talcose schists in the footwall of the deposit by siliceous schists with occasional podiform jasper layers that contain very little sericite.

Ferruginous and manganiferous wad

Irregular masses of soft, black-coloured wad are present within the iron-formation and chert bodies at Devils Reef (Fig. 34). Wad is composed of specular hematite, limonite, manganese oxides and hydroxides, and frequently contains superb idiomorphic smoky-quartz crystals several centimetres long. It also contains rich pockets of gold, and as Fig. 34 shows, many of the surface excavations are located in areas where wad is extensively developed.

Wad occurs in lenticular-shaped bodies oriented parallel with the layering in the iron-formation. Larger bodies have a width of ±40 m on surface; wad thickness decreases to zero 65–70 m below surface, on or near 6 level (Jones, 1962).

Chemical analyses (Table 27) show the wad to have a ferruginous composition with ±13 per cent Mn in samples collected from surface quarries (samples 2–3, Fig. 34). Jones (1962) reports manganese contents of ±8 per cent in Devils Reef wad, and an average Fe/Mn ratio of 6,8 (mean of 83 analyses). Trace element determinations reveal anomalously high barium contents (0,2–1,0 per cent Ba) in manganiferous lithologies (see also analysis No. 309, Bulletin No. 6, Swaziland Geological Survey).

Cross-cutting pipe- or funnel-shaped bodies of ferruginous breccia underlie the irregular masses of wad. Breccia pipes decrease in diameter toward the base of the iron-formation (toward the east) and pass into well-defined normal fault zones ±5 m wide. Zones of this type appear to terminate against the quartz-chromiferous sericite schist unit.

Breccia zones consist of angular fragments of iron-formation or chert up to 1 m in size, within a wad matrix. Jones (1962) reported broken fragments of talc schist within the breccia. Because of the close association with zones of normal faulting and brecciation, mineralisation and the formation of wad are thought to be coeval.

Exploration data

Surface workings at Devils Reef consist of five main quarries, four of which are developed in manganiferous iron-formation. Underground workings are distributed in six levels set at unequal vertical intervals. A tunnel driven through the hill was constructed on 7-level for haulage purposes (Fig. 34). Some of the workings are still accessible though areas of ferruginous and manganiferous wad are frequently associated with caved ground.

Jones (1962) mapped the underground development and noted that the main workings are on 6-level elevation southeast of the iron-formation ridge, and 2–3 levels in the hangingwall. Jones pointed out that there is a high proportion of cross-cutting development relative to driving and stoping: mining of this type could not have exploited the ground to its maximum.

Underground workings on all accessible levels were sampled by Jones (1962). Assays of 179 channel and grab samples indicate an almost complete absence of potential ore. Most samples returned values of <1 g/t and the maximum gold value obtained was 4,5 g/t over 0,69 m.

While the intersection of small pockets of rich potential ore by more systematic underground development cannot be excluded, it seems likely that much of the Devils Reef orebody above 6-level has been worked out. Exploration for extensions down-dip with drill holes sited northwest of the old workings may be worthwhile.

EMLEMBE AND NOTTINGHAM HILL GOLD DEPOSITS

Emlembe and Nottingham Hill are two deposits located in the central area of the greenstone belt for which only a small gold output is recorded (10,0 and 38,7 kg respectively). In both deposits, gold is associated with quartz veins in ultramafic and related schists that occur along zones of translational deformation.

The Emlembe gold deposit is located 0,5 km northwest of Havelock Mine, about 8 km from the granitic edge of the greenstone belt. The deposit occurs within a 75 m-wide tectonic sliver of talcose schists that crop out below the mafic volcanic sequence in the Havelock Mine footwall (Fig. 8). The talcose unit represents an important tectonic break that is in some way related to the thrust at the base of the Havelock serpentinite.

Hunter (1960) mapped and sampled the workings which include a shallow 180 m-long quarry, a vertical

shaft 25–30 m deep, and two adits located below the level of the road to Barberton. The trend of surface workings indicates that the ground exploited follows an auriferous zone that parallels the regional structural trend (±065°). Within the ore shoot, gold occurs in a stockwork of quartz veins in talc-carbonate schists. Of the 50 samples submitted for assay, only 3 returned values >3 g/t (average 7 g/t Au over 0,43 m; Hunter, 1960).

Gold within the Nottingham Hill deposit is associated with two milky-white coloured pyritic quartz veins. Both veins occur within a silicified and sericitised unit 24–40 m in thickness that is inclined south or southeast. Talcose schists with quartz veins and nests of tourmaline structurally overlie the deposit, and a sequence of dolomitic schists and phyllites crops out in the structural footwall.

The siliceous gold lode contains chromiferous sericite, ankeritic carbonate and visible cinnabar. The mineralised unit can be mapped as a more or less continuous marker horizon that is closely associated with the faulted surface between Fig Tree and Onverwacht Groups west of Nottingham Peak. Though folded and displaced by faults in the vicinity of the Nottingham Hill gold deposit, the same horizon may reappear within sequences exposed on Cinnabar Ridge (see Cinnabar Prospect).

Surface and underground workings at Nottingham Hill were mapped and sampled by Hunter (1961). These consist of a surface quarry and an adit driven on a level 43 m below the hill summit. Ore above the 43 m-level has been completely stoped out over strike lengths of 82 m and 30 m along two quartz veins. A lower (82 m-level) adit was abandoned after 60 m of development and does not intersect the reef. A number of short adits and surface excavations also occur within talcose schists and phyllites south of the main workings.

A quartz vein exposed in the sides of the last-worked 3 m-wide stope below the 43 m-level was sampled by Hunter (1961) who reported an average value of 30,6 g/t over 0,18 m (mean 5 assays). The results of the sampling program generally indicate that the reef was rich though too narrow to obtain large tonnages.

Two boreholes were drilled in 1960, both sited to intersect quartz lodes 30 m down-dip of the 43 m-level. A north-trending vein gave 3,8 g/t over 0,23 m with considerable core loss; the east-trending vein observed in underground workings was not intersected, and no gold values were returned. Hunter (1961) reported that pyrite is oxidised to at least 73 m below surface: gold will be free-milling to at least this depth.

Though no further work was recommended at the Emlembe deposit by Hunter (1960), Nottingham Hill may be suited to a small-worker operation. Narrow pay-shoots with rich values can often be worked profitably by this type of operation.

GOLD DEPOSITS IN THE FORBES REEF AREA

There are over thirty named occurrences of gold in the Forbes Reef area, many of which have little economic significance. Only the most productive deposits are described here: Forbes Main Reef, Waterfall, She and Avalanche together account for 95 per cent of total recorded gold production in the area south of the Komati River. The reader is referred to Sims (1981) for additional, mostly historical data relevant to the smaller mines and prospects.

Both Waterfall and She Mines first recorded production in relatively recent times (1960–1966). New geochemical and mineralogical studies from these and other deposits in the area are described briefly. Field relations suggest that large "hidden" deposits of gold are likely to exist in the Forbes Reef area.

Geological description

The structure of the Forbes Reef area is dominated by both a major synform and a regional stratigraphic inversion (Urie, 1967; Fig. 36). Talcose schists of the Onverwacht Group occupy the core of the synform, and are surrounded by younger quartzites and conglomerates of the Moodies Group.

Though emphasised by Urie (1967), the importance of the Forbes Reef synform was recognised by a number of

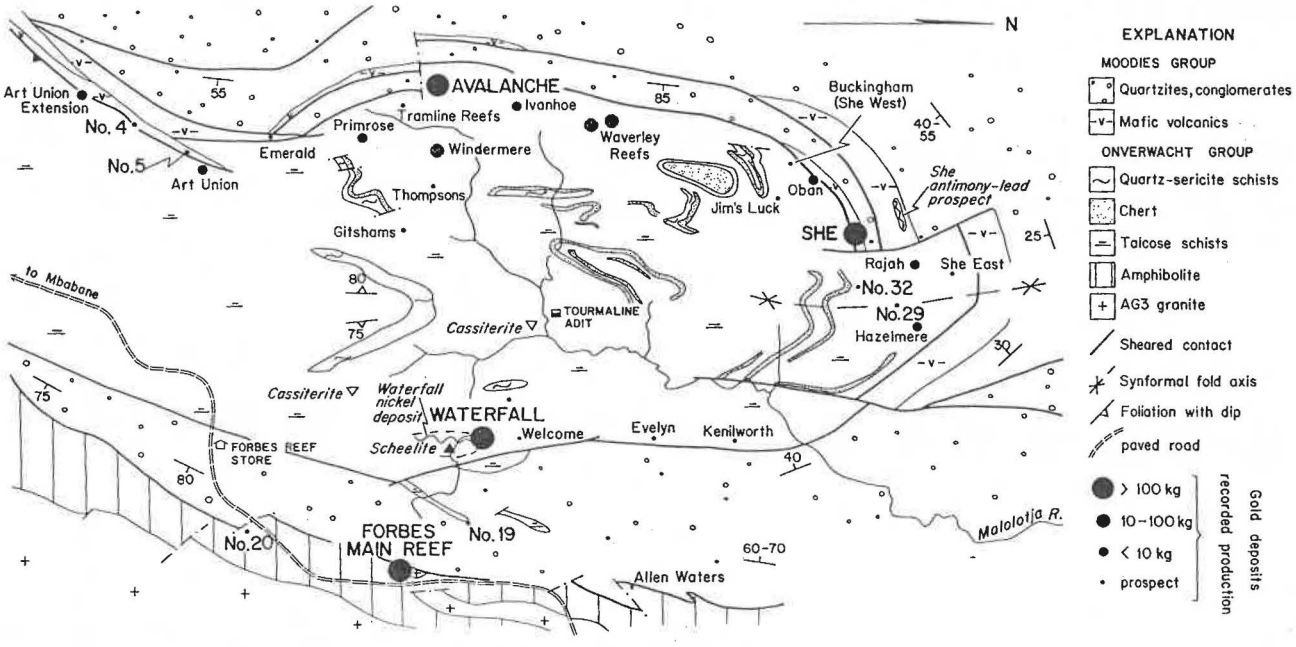

Figure 36

Geological plan of gold and base metal deposits in the Forbes Reef area (after Urie, 1970, with additions). Gold deposits west of the synformal fold axis (Avalanche-type) are associated with base metal sulphides and free silver; those east of the fold axis (Waterfall-type) are massive sulphide-poor quartz lodes. A regional ore shoot between Avalanche–Windermere–Waterfall–Forbes Main Reef deposits is postulated and discussed in the text.

Officers of the Geological Survey (Pretorius, 1961; Jones, 1963). These and other workers have generally interpreted the fold as a large downward-facing structure closing to the east (see Pretorius, 1961, Fig. 1b; Hunter *in* Pretorius, 1961). Other interpretations are possible, and the application of modern mapping techniques is required to document the structure of the area in more detail.

For the purposes of the present discussion it is noted that the folded surface separating the Onverwacht and Moodies Groups is everywhere sheared. Most gold deposits within the synform are located 200 m or less from the sheared surface (Fig. 36). Recent field observations in the area suggest that the fault may be an important structural break (S. Lamb, pers.comm., 1981).

Forbes Main Reef gold deposit

With a declared production of 965 kg, Forbes Main Reef is the second largest gold deposit in Swaziland. Mining operations (conducted in large part at the end of the nineteenth century) were centred on a massive body of quartz contained within hornblende-hornfels facies sequences of the Onverwacht Group. Though underground workings are no longer accessible, Forbes Main Reef is thought to provide a good example of a sulphide-poor lode within the high-temperature aureole of the AG3 batholith (Fig. 36).

Old reports indicate that the gold reef was a quartz vein that cropped out over a strike length of 73 m and was inclined at ±65° toward the south. On surface, the vein was 6 m-wide and composed of blue-black coloured quartz with tourmaline. The reef was rich, and carried at least 60 g/t free-milling gold; values as high as 900 g/t have been reported (Sims, 1981).

When early quarrying operations declined, an adit level was driven 29 m below surface and ore stoped out to the quarry floor. Below the adit on the 46 m-level, the quartz vein opened up to ±30 m in width. An incline shaft followed at 61 m by a prospect winze were then sunk. The winze showed the quartz vein to flatten and 79 m below surface the orebody was cut off by the granite.

Between 61 m–79 m levels, ore was recovered from two lenses: one contained 17,1 g/t Au over 0,69 m, the other 31,7 g/t over 0,66 m. Accessory chalcopyrite was recorded within the quartz reef at depth, though elsewhere sulphides are absent or present in only trace amounts.

The granitic body that intersects the orebody 79 m below surface is a 20 m-wide offshoot of the main batholith. In the upper mine levels the same intrusive body is concordant with, and forms the immediate footwall of, the quartz lode. Borehole intersections reported by Hunter (1969) indicate that the intrusion is a lenticular-shaped body of pegmatite.

Though pegmatite is not exposed in the surface workings, a 1,2 km-long tongue of granite crops out 120 m east of the disused mine (Fig. 36). There, granite and pegmatite intrude a variety of tremolitic, hornblendic and serpentinous schists, the foliation of which is inclined at high angles toward the east. The southern extension of the granitoid tongue is terminated by a major north-trending fault. The fault can be traced for 7,5 km and resembles a number of similar major fractures in the Malolotja area.

Recent systematic exploration work at Forbes Main Reef has been conducted by the Geological Survey Department and described in Hunter (1969). Cores from a series of eight boreholes demonstrated that ground in the vicinity of the mine workings is extensively faulted and intruded by steep, east-dipping diabase dykes. Though only trace amounts of gold were intersected, Hunter suggested that the main lode pitches west at 70° and terminates in highly fractured ground ±90 m below surface.

Evidence for both intense deformation of the down-dip extension of the orebody, and the complete removal of ore above the 60 m-level together indicate that payable quantities of gold at Forbes Main Reef may now be difficult to locate.

Waterfall gold deposit

Gold at the Waterfall deposit was rediscovered during the 1950s by panning streams near the headwaters of the Malolotja River (E. Wiseman, pers.comm., 1979). Apparently, the deposit had been noted in 1889 but because the surface width of the reef was only 0,38 m, no development took place at that time (Sims, 1981).

Orebodies at the Waterfall deposit are of two types. In the upper levels, gold and scheelite occur in a translucent quartz vein enclosed in talcose schist. The vein contained an average gold value of 12 g/t over a mining width of 0,91 m and was mined both from a quarry and underground to 60 m below outcrop.

Below the 60 m-level, ore was taken from two reefs composed almost entirely of talcose schist with very little free quartz. The reefs are 6 m apart, and the larger is 2,4–3,6 m wide. Like the quartz vein in the upper mine levels, both reefs are inclined at 60°–70° toward the south.

Talcose schist that carries gold is reported to be darker in colour than the adjacent talcose wall-rock (Lee, 1964). Lodes contain scheelite, gersdorffite and minor pyrite and pyrrhotite, usually in small quartz lenses lying along the talcose foliation. Visible gold is common, and assay values vary from trace to >150 g/t. Talcose schists with carbonate stringers rarely contain gold values (Lee, 1964).

Structural control of the Waterfall deposit is evident at both strike extensions of the orebody. The western extension of the main lode is abruptly terminated along a N–S trending fracture inclined at a high angle toward the west (Lee, 1964). Near the fracture, the ore shoot pitches 70° west. Lee suggested that the fracture acted as a channel for ore fluids though orebody extensions parallel with the trend of the fracture are not known.

A series of steep-plunging folds within quartzites of the Moodies Group occur at the eastern orebody extension. The trace of an asymmetric synform with an axial surface inclined 65° toward the south (parallel with the main lode) lies along the orebody extension at the contact between Onverwacht and Moodies Groups. The plunge of the fold is 70° W, parallel with the pitch of the ore shoot.

These data indicate that the transport of gold was accompanied by deformation along the Moodies-Onverwacht Group surface. Similar relationships between deformation and gold mineralisation are inferred from field relations at the She deposit.

She gold deposit

She Mine was discovered by Baragwanath in 1954, though as pointed out by Sims (1981) the deposit had almost certainly been noted by the Forbes Reef Company in 1895 but was too low in grade to be of interest.

Though only 1 km from the nose of the Forbes Reef synform, the lithological sequence at the She deposit has been turned almost vertically on edge. The orebody and adjacent units are inclined south at 60°–70° (Fig. 37).

Old workings consist of a series of surface quarries distributed along a strike length of 150 m, together with four adit levels. There is approximately 75 m of relief on outcrop. Levels 1–3 are driven into the oxide zone of the orebody which is estimated to be 35–45 m below surface. Four-level intersects sulphidic reef (see sample 8, Table 27).

A preliminary drilling program consisting of three boreholes was completed by the Geological Survey Department in 1956 (Ann. Rept., 1956). Two of the holes intersected payable values over mineable widths. The original assay data are no longer available though Clarke (1971b)

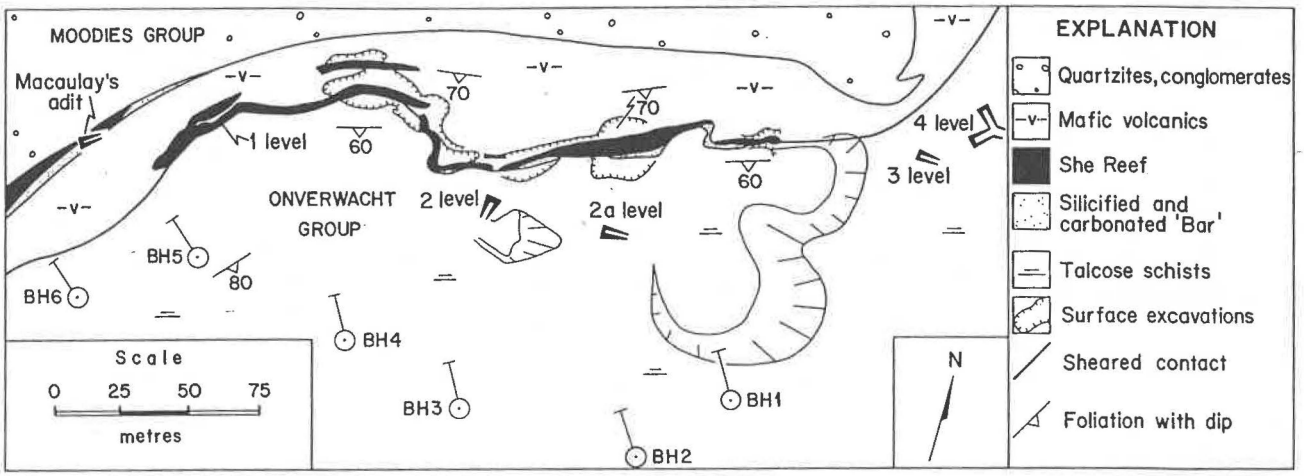

Figure 37

Geological plan of the She gold deposit (after Lee, 1964). Highly deformed and schistose mafic volcanics in the immediate footwall of the She reef are correlated with an amygdaloidal lava flow horizon in the Moodies Group below Makonjwa mountain in the northern section of the greenstone belt (see Fig. 2).

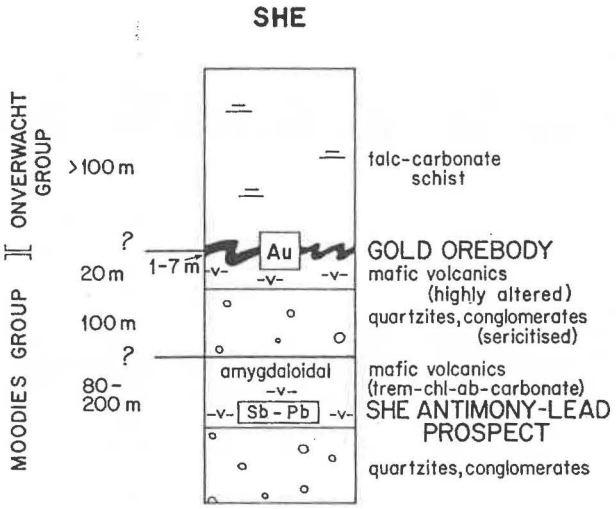

Figure 38

Lithological sequence in the vicinity of the She gold deposit and antimony-lead prospect.

suggests that values of 8–9 g/t over 1–2 m widths were obtained in both intersections, and that values are representative of the oxide zone of the deposit.

Each of the three boreholes drilled through ±100 m talcose schists before intersecting a 15–20 m-thick silicified and carbonated phyllite sequence. All boreholes ended in hard, sericitised quartzites of the Moodies Group (Figs. 37 & 38). The horizon mineralised with gold is invariably 1–3 m thick and is located immediately below the basal surface of the talcose schist unit.

Phyllites in the footwall of the orebody resemble the highly altered and carbonated mafic sequence that crops out at the She antimony-lead prospect (*see* Antimony and Mercury). In the vicinity of the She gold deposit, the sequence has been the locus of intense structural deformation. Clarke 1971b) reported steep-plunging folds with axes inclined down-dip at ±60° and axial surfaces aligned close to the regional foliation. Zones with tight fold closures often contain the best gold values.

The results of exploration undertaken in 1963 that included 6 boreholes drilled into the deposit 36–55 m apart (Fig. 37) are given in Lee (1964) and summarised in Table 17. Five of the six boreholes intersected the sulphide zone 27–58 m below surface; BH 6 (Fig. 37) was drilled into an unmineralised section of the oxide zone of the deposit.

The average orebody width measured from borehole cores is 1,92 m and contains 5,4 g/t gold. Compared with the assay results from 3 and 4-levels (Hunter, 1962; Lee, 1964; sample 8, Table 27, this work), the borehole intersections are 50 per cent wider though significantly lower in grade (by a factor of two). It is not known if the decrease in grade below surface can be explained in terms of supergene enrichment processes or whether it represents a real variation in gold content.

Borehole data do indicate that the surface strike length of ±165 m remains constant to at least 50 m below outcrop. Gold values appear to be higher in the east though the data are rather sparse. Deep drilling is required to prove the potential orebody to at least 100 m below surface.

Lee (1964) suggested that pyrrhotite is the dominant

TABLE 17
Borehole intersections drilled at the She gold deposit

	1	2	3	4	5	6	7	mean
width (m)	0,66	3,00	1,52	1,88	2,54	nil	1,24	1,81
grade (g/t)	9,6	7,7	2,7	2,6	5,2	nil	15,8	6,56

Notes: 1. Rand Mines borehole, 2–6 Falconbridge boreholes, recalculated from data in Lee (1964). See Fig. 37 for collar locations (BH 1–6); 2. intersection includes 0,76 m at 18,0 g/t along talc schist contact (8 % sulphides), 0,97 m at 1,7 g/t (1 % sulphides) and 1,27 m at 6,0 g/t along base of reef (2 % sulphides). Excludes footwall reef 7,3 m below main lode 1,83 m wide containing 4,5 g/t; 3. 58 m below surface, 3–7 % sulphides, excludes several small values in hangingwall talc schists (0,3–1,4 g/t) and footwall volcanics (<1,7 g/t); 4. intersection between 2–3 levels, 7 % sulphides; 5. includes 1,75 m at 1,2 g/t (She reef) and 18,2 g/t over 0,61 m in uncorrelated reef. Excludes several values of <4,1 g/t in footwall mafic unit; 6. oxide zone 22 m below surface, excludes 1,4 g/t over 0,61 m with ±10 % sulphides near footwall of mafic unit; 7. 3 level, average values from sampling 46 m strike length (Hunter, 1962).

sulphide in the eastern section of the deposit, while pyrite is more common in the western ore shoot. Recent mineralogical studies of sulphidic reef from 4-level east (see below) did not reveal even trace amounts of pyrrhotite.

Work conducted by the United Nations during 1967 confirmed that streams in the She deposit area contain sediment with high arsenic contents (UNDP, 1970 location 53). High arsenic and particularly antimony values in soils also correlate with the talcose schist —quartzite interface (Onverwacht — Moodies Group contact). This work did not define any new areas where gold might be expected, and as pointed out by Clarke (1971) and Dlamini (1972), the striking oxidation colours of minerals such as bindheimite (hydrous antimonate of lead) and crocoite (lead chromate) were known to the old prospectors and correspond well with the distribution of gold deposits in the She area (see Mineralogical studies of Forbes Reef gold deposits).

Avalanche gold deposit

Avalanche was one of the richest of the Forbes Reef gold deposits and one of the few in which mining extended well into the sulphide zone. Old workings consist of a quarry and three adit levels, 20 m, 40 m and 56 m below surface. A winze was sunk to an 85 m-level where all traces of ore are said to have disappeared (see Sims, 1981).

Orebodies mined from the Avalanche deposit are very distinctive. They consist of very narrow but very rich gold-bearing quartz stringers that contain free silver and copper sulphides. Veins of this type were known as "erubescite-leaders" though erubescite (bornite) was misidentified by early prospectors and was later confirmed to be tetrahedrite (see Hunter, 1962).

A bornite-leader with a strike length of 30 m was located on surface, and another with a similar length and a width of 0,1 m was discovered 61 m below outcrop. One assay of the latter vein returned values of 125 g/t gold, 12 500 g/t silver and 6 per cent copper.

Narrow quartz stringers, some with silver and copper sulphides, are still present in the upper levels of the mine workings. Most appear to be milky-white in colour, and are inclined east at high angles, concordant with the foliation in the talcose schists. In these respects, Avalanche resembles most of the gold deposits along the western limb of the Forbes Reef synform.

Immediately south of the main Avalanche gold occurrence is the so-called "Acid Reef". The Acid Reef is a siliceous body 1,5–2,75 m wide that invariably carries high values of precious metals. The unit extends between the Ivanhoe and Emerald deposits (Fig. 36) with a discontinuous strike length of 1,5 km. Production recorded from the Avalanche deposit includes material mined from the Acid Reef. The mineralogy of the Ivanhoe section of the Acid Reef given below is thought to be similar to that of the same body at Avalanche.

Gold reserves in the Forbes Reef area

Most of the gold deposits in the Forbes Reef area visited by the writer contain potential ore, either standing in existing workings or in down-dip extensions of the oxide zone of the orebody. However, large tonnages would be required to work most deposits profitably and large tonnages are almost impossible to prove without systematic sub-surface exploration.

At least 6 000 tons potential ore containing ±8,5 g/t and 0,25 per cent arsenic are present in old workings at the Ivanhoe deposit. A sample of arsenical reef on the lower level (under cone from the surface) returned 29 g/t over 3,96 m, and similar values are reported elsewhere (see sample 9, Table 37).

Underground exploration at the Ivanhoe deposit, and a systematic mapping and diamond drilling program in the area between Ivanhoe and Emerald are required before gold reserves can be estimated. In particular, the strike and dip extensions of the Acid Reef need to be defined more carefully, and the distribution of copper-silver veins at the Avalanche deposit evaluated in the vicinity of existing workings.

More speculative reserves of precious metals can be inferred from structure and field relations in the Forbes Reef area. Because gold mineralisation is concentrated at or near the surface between the Onverwacht and Moodies Groups, it seems likely that precious metals of a similar type are present in the sub-surface along the same interface. The entire synformal fold closure below the Forbes Reef flats must therefore be considered a potential exploration target.

The 1 km-wide block of ground between the Ivanhoe and Avalanche deposits in the west and Waterfall–Forbes Main Reef in the east appears to represent the richest ore shoot within the synform. If it can be assumed that production declared from each deposit within the ore shoot represents complete extraction to 100 m down-dip, then at least 3,5 tons Au km^{-2} may be concentrated along the sheared surface between the Moodies and Onverwacht Groups.

When the effects of deformation are allowed for, the length of the Avalanche–Forbes Main Reef ore shoot is ±5 km. It can easily be calculated that at least 15 tons of gold may be concealed to a depth not exceeding 1,5 km. The estimate assumes that the ore shoot is contained within a continuously folded surface and trends approximately normal to the margin of the AG3 batholith. Regional structural analysis is required to define the exact geometry of the Forbes Reef synform.

Finally, exploration for massive copper-nickel sulphides in the Forbes Reef area was conducted during 1973–1974 (Lane, 1974), but gave no positive results. A total of 10 500 soil samples were analysed for Cu, Ni and Zn content, and 22 line-kilometres of Turam were completed. No significant geochemical anomalies or electrical conductors were recognised.

Mineralogical studies of the Forbes Reef gold deposits

The ore mineralogy of the major Forbes Reef group gold deposits is given in Table 18. The mineral list is complete only for the She and Ivanhoe deposits where numer-

TABLE 18
Ore mineralogy of the Forbes Reef Group gold deposits

Forbes Main Reef	free gold, trace pyrite, chalcopyrite
Waterfall	free gold, gersdorffite, scheelite, minor pyrite & pyrrhotite
She East	arsenopyrite, pyrite, pyrrhotite, gersdorffite, chalcopyrite
Rajah	arsenopyrite, crocoite
She	arsenopyrite, pyrite, minor chalcopyrite, trace chalcocite, covellite, sphalerite, stibnite, bindheimite
Oban-Buckingham	bindheimite
Waverley	crocoite, galena, cinnabar
Ivanhoe	pyrite, minor arsenopyrite, chalcopyrite, trace chalcocite, covellite, pyrrhotite, ullmannite, sphalerite
Avalanche	tetrahedrite, free silver, chalcopyrite, malachite, pyrite, galena
Primrose	free silver, crocoite, galena, stibnite, malachite, chalcopyrite
Art Union	cinnabar
Motjane	crocoite, bindheimite, azurite, malachite, chalcopyrite, galena.

TABLE 19
Major crystalline constituents of Ivanhoe and She reefs from X-ray diffraction data

	quartz	arsenopyrite	pyrite	chlorite	dolomite	sodic plagioclase	sericite
Ivanhoe	predominant	detected	fairly abundant	-	abundant	minor	minor
She	predominant	abundant	very minor	very minor	detected	fairly abundant	-

ous polished sections have been examined. Elsewhere, additional metallic phases may be present but these have not been identified from drill cores or hand-specimens.

Representative samples of Acid Reef on the lower (30 m-level) at the Ivanhoe deposit, and sulphidic ore from 4 level east at the She deposit have been analysed at JCI laboratories by X-ray diffraction, polished- and thin-sections and electron microprobe. The results are given in Tables 19–23; whole rock geochemical analyses of both reefs are given as samples 8 and 9 (Table 27).

Gangue mineral constituents were determined by X-ray diffraction scans (Table 19) and indicate that both reefs are siliceous in composition. Dolomite is an important constituent of the Ivanhoe reef and sodic plagioclase (? oligoclase) was identified in both reefs and is fairly abundant in the She lode.

Ore minerals consist in large part of pyrite and arsenopyrite (Table 20). Pyrite is of two types: Type I has very serrate grain boundaries and contains numerous inclusions of metallic phases that include gold. Type II pyrite grains occur as inclusion-free euhedra that could be interpreted as recrystallised Type I grains.

Arsenopyrite is present as well crystallised disseminated laths, needles and rhombic cross-sections, and is ubiquitous in She reef (±15 per cent As by weight). Because of its crystalline nature and the absence of any clear spatial correlation with gold, most arsenopyrite resembles Type II pyrite in morphology. Small inclusions and intergrowths of arsenopyrite also occur in pyrite Type I grains and suggest that like the pyrite, there may be two generations of this mineral.

Chalcopyrite, chalcocite and covellite occur together in siliceous layers that alternate with layers of pyrite and arsenopyrite. Pyrrhotite, ullmannite (SbNiS), galena and sphalerite are present as minute inclusions in pyrite Type I.

The mode of occurrence of gold is summarised in Table 21. Twenty-seven gold grains were found in four polished-sections of the Ivanhoe sample. Only six gold grains were found in 10 polished-sections of the She reef, and it appears that the sample is not entirely representative of the assayed material (sample 8, Table 27).

Gold in the Ivanhoe reef occurs in large part as inclusions within, or attachments to pyrite Type I grains. A small proportion of the total gold content (±15 per cent) occurs as inclusions within the quartzose gangue. Though only six grains were found in the She reef sample, at least 50 per cent of the gold there is associated with silicate while the remainder is occluded in pyrite Type I. Size distribution data of gold in both reefs are summarised in Table 22.

Energy dispersive microprobe analyses (Table 23) indicate that the silver content of gold from the She reef (±18 per cent) is more or less twice that of the Ivanhoe deposit (±9 per cent silver). These compositions show very different Au/Ag ratios of those determined by whole-rock analysis (see samples 8 and 9, Table 27). Because only small amounts of silver are alloyed with gold in the Ivanhoe reef, it can be assumed that either free silver or argentite are present elsewhere. It is noted that the iron content of gold in pyrite is higher than that of sulphide-free inclusions in quartz grains (Table 23).

TABLE 20
Ore mineralogy of Ivanhoe and She reefs

	pyrite I	pyrite II	arsenopyrite	chalco-pyrite	chalco-cite	covellite	pyrr-hotite	ullman-nite	galena	hematite/ goethite	sphale-rite
Ivanhoe	abundant	predominant	minor	very minor	trace	trace	trace	trace	detected	trace	trace
(size range μm)	5–400	5–450	1–50	1–45	±10	5–50	±20	±10	±5	30–70	10–30
She	fairly abundant	abundant	predominant	very minor	trace	trace	-	-	detected	trace	trace
(size range μm)	5–400	5–450	(2×1)–(100×40)	1–(200×70)	5–30	5–30			±5	20–50	±10

trace = 1–3 %; detected <1 %.

TABLE 21
Mode of occurrence of gold particles in the Ivanhoe and She reefs

		pyrite I	pyrite I/ silicate	silicate	total number gold grains
Ivanhoe	% by number	74,1	18,5	7,4	27
	% by volume	41,4	43,5	15,1	
She	% by number	50,0	—	50,0	6
	% by volume	45,6	—	54,4	

TABLE 22
Size distribution of gold particles in the Ivanhoe and She reefs

class limits (μm)		31,2–22,1	22,1–15,6	15,6–11,0	11,0–7,8	7,8–5,5	5,5–3,9	3,9–2,8	2,8–2,0	2,0–1,4	1,4–1,0
mid-point (μm)		26,2	18,6	13,1	9,3	6,5	4,6	3,3	2,4	1,7	1,2
Ivanhoe	number frequency	14,8	14,8	33,3	59,2	66,6	81,4	85,1	88,8	88,8	100,0
	volume frequency	54,6	54,6	78,6	93,6	95,0	99,5	99,9	99,95	99,95	100,0
She	number frequency	—	—	33,3	66,6	83,3	100,0	100,0	100,0	100,0	100,0
	volume frequency	—	—	42,3	89,2	98,0	100,0	100,0	100,0	100,0	100,0

TABLE 23
Electron microprobe analyses of gold particles in the Ivanhoe and She reefs (weight per cent)

	Ivanhoe				She	
	1	2	3	4	5	6
Au	92,12	92,43	91,00	87,79	80,17	83,56
Ag	8,92	6,74	10,92	9,86	18,86	16,11
Fe	-	-	0,35	1,18	1,11	1,27

Notes: 1–2. gold in silicate; 3. gold on pyrite/silica interface; 4. gold in pyrite; 5. gold in silicate with small euhedral pyrite attachment; 6. gold in fractured pyrite.

Interpretation

Mineralogical observations allow the division of the Forbes Reef area gold deposits into two contrasting types. West of the synformal fold axis, most deposits are rich in sulphides, contain significant amounts of the volatile metal species Sb, As and Hg, relatively high base metal contents and high values of silver. The largest occurrence of this type is the Avalanche deposit. Allowing for the effects of folding deformation, Avalanche-type deposits are located 3–6 km from the granitic edge of the greenstone belt.

East of the synformal axis and within or close to the high-temperature aureole of the granite (<2 km from the intrusion margin), gold deposits contain only sparse sulphides, and are associated with scheelite, cassiterite, gersdorffite and tourmaline. Waterfall and Forbes Main Reef are deposits of this type. The western limit of Waterfall-type deposits coincides with the maximum development of black schorl tourmaline 2–3 km from the granite contact.

Pretorius (1961) recognised that a group of low-temperature gold deposits are located several kilometres from the granite margin and that these differ in mineralogy from the high-temperature metamorphic assemblages observed at Forbes Main Reef. Further mineralogical evidence as well as the discovery of new deposits that are consistent with the same pattern of mineralisation appear to confirm the temperature distribution suggested by Pretorius. Some differences between Avalanche- and Waterfall-type deposits are summarised in Table 24.

Gold transport was accompanied by deformation along the Moodies–Onverwacht Group surface. Axial regions of small-scale folds in the She and Waterfall deposits are enriched in precious metals. There is no evidence, either from field relations or mineral parageneses to suggest that gold is re-concentrated from an earlier depositional event.

The simplest interpretation of these data is that a fracture surface or surfaces acted as a discharge zone along which high temperature mineralising fluids travelled laterally toward the interior of the greenstone belt. Pro-

TABLE 24
Some characteristics of gold deposits in the Forbes Reef area

	Avalanche-type	**Waterfall-type**
Mineralogy	sulphide-rich volatile metals Sb, Hg & As typical base metal (Cu, Pb & Zn) sulphides and carbonates present chromiferous sericite at She, Waverley and Emerald scheelite and gerdorffite absent	sulphide-poor volatile metals absent no base metals; carbonate-poor chromiferous sericite not recorded scheelite and gersdorffite present
Refractory nature	>50 % gold locked in pyrite (require roasting)	gold-free milling
Silver content	free silver recorded; fineness 800 (Avalanche) — 912 (She) Au/Ag <10	no free silver fineness 957 (Waterfall) Au/Ag ±20
Deposit spacing	0,54 ±0,14 km (1σ)	—
Grade	5–15 g/t	±20 g/t
Past production	±560 kg (10 deposits)	±1 110 kg (2 deposits)
Origin	low-temperature vapour-dominated deposits located >2 km from granitoid heat source	high-temperature fluid dominated deposits located within metamorphic aureole or along thermally detached zones immediately above granitoid intrusion

gressive enrichment in S, CO_2 and volatile metals is inferred from the ore and gangue mineralogy and suggests that a vapour-dominated geothermal system operated ±5 km from the margin of the batholith. Zones of recharge have not been identified but may have been located within the fractured volcanic roof of the granitoid batholith.

GOLD RESERVES OF NORTHWEST SWAZILAND

Known potential ore from gold deposits in northwest Swaziland (Table 25) is of three main types:

1. material standing in old mine workings that was considered unpayable during a previous operation (e.g. Piggs Peak, Ivanhoe);
2. orebody extensions in the sulphide zone of the deposit (e.g. Daisy, She), and
3. high tonnage, low-grade deposits (e.g. Lufafa).

The only potentially large occurrence that has not been systematically exploited near surface is the Wyldsdale deposit. Small amounts of gold are also present in tailings from previous operations at Piggs Peak and Daisy Mines.

Exploratory adits are required to evaluate the Wyldsdale — Lufafa deposits and determine to what extent the ground is payable. Additional borehole data are required in this area in the vicinity of the Lomati deposit.

Detailed mapping and borehole data are required to define and sample the Acid Reef between the Ivanhoe and Emerald deposits. Geophysical techniques and deep diamond drill holes may be necessary to test for the presence of a potential ore shoot between the Avalanche and Waterfall deposits.

Extensions of the Piggs Peak lode may exist and exploration across (rather than along) the strike of the chert body is considered worthwhile. Ground between the Old and New Section workings is a potential exploration target.

Because of their small size, concealed lode gold deposits are extremely difficult to locate. Nonetheless, the Lufafa zone north of the Wyldsdale deposit contains areas of anomalous arsenic and antimony geochemistry for which there is no available explanation. This area has not received sufficient attention in the past because of the rugged nature of the terrane.

For reasons given below, it is argued that most important lode gold deposits of the Barberton-type are either associated with sequences of ultramafic composition particularly where these occur within the thermal aureole of a granitoid intrusion, or are located along major tectonic breaks (or more often both). Exploration for concealed deposits of this type will require sophisticated techniques that begin with a detailed knowledge of field relations.

TABLE 25
Summary of known gold reserves in north-west Swaziland

	In situ							On dumps		
	Piggs Peak 1	Daisy 2	Wyldsdale 3	Lufafa 4	She 5	Ivanhoe 6	sub-total	Piggs Peak 7	Daisy 8	sub-total
tonnage (10^3 tons)	75,0	46,3	331,9	1 652,7	25,0	6,0	2 136,9	75,0	24,0	99,0
grade (g/t)	5,0	5,4	5,4	1,3	6,6	8,5	2,24	1,0	1,4	1,1

Notes: 1. 1–8 level, Old Section, Piggs Peak; 2. proven ore shoot in sulphide zone, Daisy deposit (assumes 40 % payability); 3. 8 reefs, Wyldsdale deposit (excludes 'A' reef, Far West reef and miscellaneous reefs). Average dip extension 67 m (range 15–107 m); 4. quartz-chromiferous sericite schist, Lufafa south and banded hematite iron-formation, Lufafa central, both to 100 m down-dip; 5. speculative reserves in sulphide zone, She deposit (100 m strike- and 50 m dip-extensions); 6. potential ore in existing workings, Ivanhoe deposit; 7. sands dump, Piggs Peak; 8. includes 21 000 tons containing 1,2 g/t (sands) and 3 000 tons containing 2.5 g/t (slimes), Daisy deposit.

TABLE 26 (a)
Chemical compositions of lode gold deposits and associated lithologies, northern area: I. Major elements (weight per cent)

	Daisy				Lomati			Wyldsdale		Lufafa Zone				
	1	2	3	4	5	6	7	8	9	10	11	12	13	14
SiO_2	96,20	44,40	62,40	45,40	46,65	74,10	74,15	66,40	3,40	43,50	63,80	49,40	40,90	75,20
TiO_2	0,40	0,59	1,43	0,52	0,79	0,44	0,84	0,53	0,30	0,51	0,19	0,05	0,82	0,19
Al_2O_3	0,20	8,90	13,95	8,50	6,80	10,80	11,90	19,10	2,90	21,30	8,70	1,45	7,50	14,00
Fe_2O_3	0,21	10,25	4,35	10,12	35,35	7,88	6,31	3,62	85,92	20,30	19,40	43,50	5,82	0,77
FeO	0,22	4,90	1,89	4,75	0,15	0,32	0,25	0,43	1,51	0,28	0,07	0,05	7,99	0,25
MnO	<0,05	0,42	0,07	0,12	0,11	<0,05	<0,05	0,14	0,08	0,14	0,22	0,22	0,35	0,06
MgO	0,10	14,00	3,40	20,50	<0,10	0,10	0,15	0,20	<0,10	0,90	0,20	<0,10	7,00	<0,10
CaO	<0,05	7,20	2,94	<0,05	<0,05	<0,05	<0,05	<0,05	<0,05	<0,05	<0,05	<0,05	6,77	<0,05
Na_2O	<0,10	0,30	1,25	<0,10	<0,10	0,30	0,10	0,25	<0,10	<0,10	<0,10	<0,10	2,00	3,90
K_2O	0,05	0,54	1,94	<0,05	1,28	2,72	3,34	2,26	<0,05	6,22	1,95	<0,05	<0,05	4,56
P_2O_5	<0,05	<0,05	<0,05	<0,05	<0,05	0,06	<0,05	<0,05	<0,05	<0,05	<0,05	0,10	<0,05	<0,05
SO_3	<0,03	0,15	0,41	0,05	0,05	<0,03	<0,03	0,03	<0,03	<0,03	<0,03	0,10	1,22	<0,03
CO_2	0,14	0,10	0,42	0,46	<0,10	<0,10	<0,10	0,10	0,51	<0,10	0,10	<0,10	8,87	0,10
H_2O^+	0,64	3,45	2,91	7,45	n.d.	n.d.	n.d.	5,30	3,24	n.d.	n.d.	n.d.	3,51	1,03
Loss	0,16	6,17	4,43	8,45	7,54	3,25	2,76	6,12	4,77	6,46	5,37	5,06	9,31	0,95

n.d. = not determined.

Notes: 1. Daisy Bar, south of No. 1 Quarry, Daisy Mine; 2. basal 1 m amphibolite, portal 1 level adit, No. 1 Quarry, Daisy Mine; 3. uppermost 2 m quartz-sericite schists, portal 1 level adit, No. 1 Quarry, Daisy Mine (mean 2 analyses); 4. talcose schists 1 m below quartz-sericite schist unit, No. 2 Quarry, Daisy Mine; 5–6. weathered ferruginous reef, surface quarry, Lomati gold deposit; 7. chert with chromiferous sericite, immediately above weathered reef, Lomati gold deposit; 8. pale-coloured granodiorite, oxidised zone, Wyldsdale gold deposit (mean 2 analyses); 9. deep red-coloured granodiorite, oxidised zone, Wyldsdale gold deposit; 10. quartz-chromiferous sericite schist, trench 1, Lufafa south prospect (see Fig. 33); 11. as above, trench 2; 12. auriferous iron-formation, trench 11, Lufafa Central prospect (mean 2 analyses); 13. mineralised amygdaloidal lava flow, Moodies Group, Ntintinyane River, 3,8 km SSW Makonjwa Mountain (Bearded Man); 14. Quartz-porphyry, Onverwacht Group, 5,5 km SSW Lufafa Mountain.

TABLE 26(b):
Chemical compositions of lode gold deposits and associated lithologies, northern area: II. Trace elements (ppm)

	Daisy				Lomati			Wyldsdale		Lufafa Zone				
	1	2	3	4	5	6	7	8	9	10	11	12	13	14
Au	<0,05	17,80	0,78	0,09	9,45	4,30	19,85	0,41	<0,05	4,00	9,00	2,90	1,70	<0,05
Ag	<0,10	1,40	0,65	<0,10	1,00	0,30	1,75	<0,10	0,10	0,30	0,40	0,40	<0,10	<0,10
Pt	<0,10	<0,10	<0,10	0,20	0,10	0,20	0,20	<0,10	<0,10	<0,10	<0,10	0,10	<0,10	<0,10
B	150	2 300	790	195	146	102	226	210	35	186	50	53	497	70
Ba	608	362	575	44	173	296	255	375	183	512	288	153	192	676
As	63	604	127	490	13300	1800	1600	77	399	980	2000	2400	11300	30
Sb	10	3	2	<1	11	10	9	4	1	9	11	9	5	<1
Cr	502	2649	824	5940	3626	411	616	128	345	6432	3353	411	1055	37
Co	10	100	70	120	100	20	10	10	90	80	50	100	90	20
Ni	100	940	210	1380	1155	328	204	45	330	463	646	110	510	80
Cu	24	148	120	232	189	90	108	22	34	56	58	40	161	12
Pb	40	70	70	60	57	27	28	55	130	53	43	62	60	30
Zn	10	123	88	120	148	16	24	55	52	129	120	51	120	71
[1]Hg	510	170	765	1160	189	160	78	2860	860	239	111	231	1090	540
Sn	30	<20	<20	<20	<20	21	<20	40	<20	<20	<20	<20	<20	<20
W	24	34	30	<20	38	<20	<20	35	<20	<20	<20	<20	<20	<20
Y	<10	<10	33	<10	11	15	32	23	<10	<10	<10	<10	14	<10
Zr	35	50	216	41	55	107	84	202	30	85	50	19	104	118
[2]Au/Ag		12,7			9,5	14,3	11,3			13,3	22,5	7,3	17,0	

[1]reported as ppb; [2]where Au ≥1,0 g/t.

Notes: see Table 26(a).

The majority of gold deposits in northwest Swaziland contain $\pm 10^5$ tons potential ore or less in bodies that are difficult to prove. While a few deposits may be of interest to large mining houses (Wyldsdale, Piggs Peak, Avalanche), many others could be worked profitably by small operators. Small, labour intensive operations are especially attractive, and could make a significant contribution to the economy.

GEOCHEMISTRY OF THE GOLD DEPOSITS

Major and trace element determinations for most of the important gold deposits in northwest Swaziland are given in Tables 26 & 27; geochemical data for the Piggs Peak deposit are given elsewhere (see Table 12).

Element concentrations in gold lodes compared with average abundances in primary basalt determined by Turekian and Wedepohl (1961) are given in Table 28. Concentration factors ($\bar{X}$) of precious metals in the lodes are $\pm 10^4$ for Au (locally as high as $6 .10^5$ at Devils Reef), and ± 10 for Ag, relative to background abundances.

A number of other elements, particularly As, Sb and B exhibit high degrees of concentration in the lodes. Arsenic locally attains 14 per cent in the She deposit, a value which implies a concentration of $7 .10^4$ times the background abundance of 2 ppm in basalts. Similarly, B exceeds 2 per cent along the edge of the Cross-Schist at the Piggs Peak deposit. Mesoscopic concentrations of tourmaline both at Piggs Peak and in other lodes imply concentrations of at least $4 .10^3$ times the background abundance of 5 ppm B in basalts.

TABLE 27a
Chemical compositions of lode gold deposits, cinnabar and cobalt prospects, central and southern areas: I. Major elements (weight per cent)

	Devils Reef				Cinnabar Prospect	Cobalt Prospect	Green Schist	She	Ivanhoe	Motjane Reefs
	1	2	3	4	5	6	7	8	9	10
SiO_2	67,30	2,10	4,15	95,13	80,90	96,80	70,80	50,50	50,80	52,70
TiO_2	0,07	0,08	0,08	0,05	0,39	0,07	0,12	0,37	0,42	0,09
Al_2O_3	2,30	1,10	0,30	<0,10	8,90	0,40	3,30	3,00	7,60	3,90
Fe_2O_3	25,80	66,20	66,00	2,86	1,52	0,65	0,78	19,25	5,86	0,88
FeO	<0,05	<0,10	<0,10	<0,10	0,14	0,36	1,66	4,72	2,63	4,97
MnO	2,25	13,00	13,50	0,72	0,08	0,12	0,25	0,12	0,14	0,14
MgO	<0,10	0,50	0,10	<0,10	0,30	<0,10	3,90	0,10	4,30	28,70
CaO	<0,05	<0,05	<0,05	<0,05	<0,05	<0,05	7,13	0,41	6,34	<0,05
Na_2O	<0,10	<0,10	<0,10	<0,10	0,20	<0,10	0,10	2,00	0,90	<0,10
K_2O	<0,05	<0,05	<0,05	<0,05	1,91	<0,05	0,64	<0,05	1,77	<0,05
P_2O_5	<0,05	<0,05	<0,05	<0,05	<0,05	<0,05	<0,05	<0,05	<0,05	<0,05
SO_3	<0,02	0,23	0,18	<0,02	0,17	<0,02	0,05	18,80	9,84	0,01
CO_2	1,76	0,24	1,22	0,06	0,09	0,12	10,10	5,63	3,75	0,08
H_2O^+	n.d.	10,50	8,77	0,57	1,90	4,62	0,56	1,04	1,35	5,80
Loss	2,31	15,80	13,20	0,72	1,69	0,26	11,30	17,40	13,10	5,94

n.d. = not determined.

Notes: 1. ferruginous wad, south end No. 2 Quarry, Devils Reef; 2. typical black-coloured manganiferous wad, No. 1 Quarry, Devils Reef; 3. manganiferous wad with patchy development of orange-weathered limonite, No. 1 Quarry, Devils Reef (mean 2 analyses); 4. drusy quartz with manganiferous wad, No. 1 Quarry, Devils Reef (Mercey); 5. quartz-chromiferous sericite schist with visible cinnabar, main quarry, Cinnabar Prospect; 6. massive green-coloured silica with minor manganese oxides, Area A, Cobalt Prospect; 7. quartz-chromiferous sericite-ankerite schist, décollement zone at base of the Fig Tree Group, Komati River; 8. sulphidic ore, 4 level, She gold deposit ("sulphide facies iron-formation"); 9. "Acid Reef", Ivanhoe gold deposit; 10. massive talcose schist (soapstone), Motjane Reefs.

TABLE 27 (b)
Chemical compositions of lode gold deposits, cinnabar and cobalt prospects, central and southern areas: II. Trace elements (ppm)

	Devils Reef				Cinnabar Prospect	Cobalt Prospect	Green Schist	She	Ivanhoe	Motjane Reefs
	1	2	3	4	5	6	7	8	9	10
Au	n.d.	<0,05	<0,05	<0,05	0,06	<0,05	<0,05	31,00	26,00	0,43
Ag	n.d.	0,20	0,40	<0,10	<0,10	<0,10	<0,10	1,00	2,10	0,40
Pt	n.d.	0,20	<0,10	<0,10	<0,10	<0,10	<0,10	<0,10	0,10	0,10
B	34	150	113	70	1 438	147	165	477	407	210
Ba	236	2 833	2 467	49	4 343	<20	826	37	311	20
As	90	215	210	50	62	<30	<30	14,21[1]	6 910	345
Sb	1	2	5	<1	6	1	1	215	80	50
Cr	479	224	927	41	641	591	1 726	1 585	414	2 386
Co	200	240	310	30	20	30	40	80	40	20
Ni	372	1 660	1 990	150	120	140	350	720	190	540
Cu	102	702	603	91	84	39	11	122	102	16
Pb	39	40	85	80	40	40	20	120	330	330
Zn	54	154	175	10	15	10	14	29	119	336
[2]Hg	583	220	710	870	0,18[1]	5 610	190	1 410	1 750	1 330
Sn	<20	<20	<20	41	21	35	30	<20	<20	27
W	<20	<20	<20	<20	244	<20	<20	39	<20	<20
Y	n.d.	38	28	<10	<10	<10	<10	<10	<10	<10
Zr	n.d.	20	14	21	36	20	17	28	42	15
[3]Au/Ag								31,0	12,4	

[1]reported as per cent; [2]reported as ppb; [3]where Au >1 g/t; n.d. = not determined.

Notes: See Table 27 (a).

TABLE 28
Element concentrations in lode gold deposits, northwest Swaziland

	1	2	3	4	5	6	mean	$\bar{X}$	
Au	17,80	11,20	5,30	14,58	31,00	26,00	17,65	8 823	(2 650–15 500)
As	604	5 567	1 793	5 578	142 100	6 910	4 962	2 481	(302–71 050)
Sb	3	10	10	13	215	80	55	275	(15–1 075)
B	2 300	510	310	1 902	477	407	984	197	(62–460)
W	34	38	x	x	39	x	37	93	(< 97,5)
Pb	70	37	53	40	120	330	108	18	(6–55)
Ag	1,40	1,02	0,37	1,65	1,00	2,10	1,26	11	(3–19)
[1]Hg	170	142	194	319	1 410	1 750	664	7	(1,5–19,4)
Cu	148	129	51	203	122	102	126	1,4	(0,6–2,3)
Zn	123	63	100	40	29	119	79	0,8	(0,3–1,2)

[1]reported as ppb; x = below limit of detection.

Notes: 1. Daisy gold deposit; 2. Lomati gold deposit (mean 3 analyses); 3. Lufafa zone (mean 3 analyses); 4. Piggs Peak gold deposit, Old Section (mean 13 analyses); 5. She gold deposit, sulphide ore; 6. Ivanhoe gold deposit, Acid Reef.
$\bar{X}$ = concentration factor (range of values in parentheses). Element abundances compared with average background metal contents in primary basalt given by Turekian and Wedepohl (1961). Highest and lowest arsenic values not included in estimate of $\bar{X}$.

In contrast, the base metals Cu and Zn are very rarely concentrated to any degree in gold deposits described here. Only the Avalanche-type deposits, and Type-1 ironstone veins within the Piggs Peak deposit contain Cu and Zn in significant amounts. Lead values imply high degrees of concentration, particularly when the great age of the greenstone belt sequences is taken into account.

Data of a similar type have been presented from Canadian greenstone belts by Kerrich (1980) and Kerrich and Fryer (1981). These authors suggest that the characteristic patterns of enrichments in lode gold deposits are consistent with mineralising fluids that had very low water/rock ratios. Other explanations are also possible (see below).

ORIGIN OF THE GOLD DEPOSITS

The following observations constrain models of gold concentration in the Barberton greenstone belt:

1. Field relations show that, without exception, all gold lodes in northwest Swaziland are closely associated with ultramafic sequences of the Onverwacht Group. Most deposits occur near the tectonic margins of talcose units; others are located within metamorphosed ultramafic sequences in the thermal aureole of granitic intrusions. Piggs Peak Old Section is ±150 m from a thick talcose schist unit, though inferred directions of fluid flow are consistent with the ultramafic sequence as reservoir rock.

Lithological control of gold mineralisation is most clearly demonstrated by field relations in the Wyldsdale deposit. Gold lodes only occur within and adjacent to that part of the Wyldsdale granodiorite pluton that is emplaced into sequences of ultramafic composition. Elsewhere, the pluton and its aureole are barren.

2. Most of the productive deposits are located 4 km or less from the granitic edge of the greenstone belt. Those deposits that occur further than ±3 km granite outcrop are associated with horizons of translational deformation.

Thus, the geometry of most gold lodes can be described in terms of one of two types: either a variety of fracture-fillings within or close to granitoid intrusions, or as impregnations and veins associated with impermeable cap-rocks in the upper plate of a thrust sheet. Allochthonous bodies of serpentinite and silicified horizons of massive chert appear to have acted as cap-rocks.

3. The mineralogy of some gold lodes includes high concentrations of the volatile species Sb, As and Hg, low-

temperature base metal sulphides and a high proportion of carbonate gangue. Deposits of this type occur in a zone 3–5 km from, and parallel with, the edge of the greenstone belt.

Gold lodes consist for the most part of quartz-pyrite mixtures. Most pyrite-rich lodes occur at some distance from the edge of the greenstone belt while most massive quartz blows occur in the thermal aureole of a granitoid intrusion.

4. Sericitic wall-rock alteration, often chromiferous in composition, is extensively developed in most gold deposits. Hydrothermal fluids of potassic composition are therefore implicated in the mineralisation.

It can be readily inferred from these data that gold concentration in economic amounts was controlled by late deformation and fluid movement. There is no evidence of the type described from the Steynsdorp goldfield by Viljoen and others (1969) for early, syngenetic gold orebodies (volcanogenic processes may however account for the small values of precious metals in the Havelock and Mhlatane iron-formations). Production from the Steynsdorp valley is in any case miniscule: data in Groeneveld (1975) indicate that <70 kg was produced from 32 mines and prospects.

The Model

A rather simple classification of gold deposits in northwest Swaziland can account for the features of most lodes in terms of directions of fluid flow:

1. *gold deposits formed by vigorously convecting fluids travelling across structural surfaces.* Deposits of this type occur within the aureole of the AG3 batholith and Ntonjeni-type plutons. Lodes are highly silicic in composition (black quartz), and tend to be poor in sulphur, volatile metal species and low-temperature base metal sulphides. Gold is very often in a visible form, and is free-milling. Relatively high fluid/rock ratios are inferred from the effects of pervasive hydrothermal metamorphism on large volumes of country-rock.
Examples: Wyldsdale, Kobolondo, Forbes Main Reef.

2. *gold deposits formed by fluids travelling parallel with structural surfaces.* These are the sulphide lodes associated with major zones of faulting. Deposits of this type either formed below impermeable cap-rocks or were emplaced along hydraulic fractures that cut impermeable cap-rocks. Both serpentinite and chert bodies formed barriers to hydrothermal circulation and imply that ore deposition occurred at high values of fluid pressure. Though gold mineralisation was accompanied by deformation, it appears from the presence of serpentinite cap-rocks that much of the structural stacking was already complete.

Where impermeable layers form regionally extensive units gold lodes occur as small, closely-spaced deposits, 0,5–1,0 km apart. Ore shoots associated with deposits of this type are likely to form in regions of extension, parallel with direction of maximum regional compression (toward the west or northwest).

Relatively low fluid/rock ratios, that may have included vapour-dominated systems are inferred from the concentrations of volatile metal species As, Sb and Hg, and the large amounts of carbonate gangue. A steep edge of the AG3 magma chamber may have been located within ±4 km of the present southeastern margin of the greenstone belt somewhere below the inferred vapour-dominated geothermal field.
Examples: Piggs Peak, Daisy, Avalanche-type.

The only deposit that is not easily reconciled with this model is Devils Reef. The close association of manganese oxides, high barium values and drusy quartz, with extreme concentration of precious metals indicates very rapid, high-level emplacement of fluids. Because mineralisation is associated with iron-formation that itself formed by replacement, the Devils Reef gold orebody is thought to have formed at the same time as the large Ngwenya-type iron deposits.

Elsewhere in the Barberton area, closely-spaced sulphidic gold deposits are present along the Barbrooke Fault, ±10 km from the edge of the Nelspruit migmatite terrane (see Groeneveld, 1975; Anhaeusser, 1976). It can be speculated that in the same way as thrusts in northwest Swaziland, the Barbrooke Fault tapped the edge of a silicic magma chamber and acted as a fluid or gas conduit.

Discussion

It is well known that water in natural systems will migrate to a heat source and that convective circulation patterns are rather easily established. Large volumes of high-level intrusive and extrusive magma have been inferred elsewhere from field relations of the Onverwacht Group (Viljoen and Viljoen, 1969a). It is thus reasonable to assume that large amounts of heat were lost to seawater by convection in fluids.

That fluids interacted with igneous sequences of the Onverwacht Group is known from mineralogical observations on a sequence of pillowed tholeiitic lavas in Havelock Mine. However, though many explanations are possible, the absence of large syngenetic gold deposits, as well as the paucity of base metal occurrences in the Barberton area (Viljoen and Viljoen, 1969c) both of which might be expected to form during emplacement of Onverwacht Group sequences, is not understood.

Vigorous convective fluid circulation is inferred from the pervasive hydrothermal metamorphism and fractured nature of the Wyldsdale pluton. High fluid/rock ratios alone do not therefore preclude the formation of gold deposits with low base metal contents (compare with Kerrich and Fryer, 1981).

Some other explanation must account for the ability of silicic magmas to concentrate gold from ultramafic sequences. From the observed nature of wall-rock alteration, and the association with thick talc-carbonate sequences, it is suggested that fluids rich in potassium and carbon dioxide are required for the concentration of lode gold in economic quantities. Fluids with these compositions are known to separate early from some silicic magmas (see Burnham, 1967). Thus the degree of gold concentration may in some way be related to the amounts of potassium and other volatiles emplaced through the roofs of granitoid intrusions. Experimental data that quantify the extent to which precious metals can be stripped from ultramafic sequences during the reaction that forms talc and silica are not yet available.

Numerous occurrences of lode gold (see Boyle, 1979, for a review) appear to be consistent with a model in which precious metals are extracted from ultramafic or mafic sequences by potassic fluids. Any tectonic regime in which large volumes of silicic — potassic magma are emplaced into sequences of ultramafic composition, such as an island arc, is a potential site of gold concentration. The unique combination of extensive ultramafic sequences and the general restriction of potassic batholiths to terranes older than 10^9 years (Hamilton and Myers, 1967) suggests that the Precambrian was an exceptionally favourable time for the formation of lode gold deposits.

IRON

Mining of iron ore for cosmetic and symbolic ritual purposes has been important in Swaziland for at least 40 000 years. Before twentieth-century mining operations in the Ngwenya area began, numerous small workings were observed in a soft, bright-red variety of hematite known as specularite. Excavations carried out between 1965–1967 recovered almost half a million artefacts from these workings. Careful analysis of this material provided remarkable evidence that the history of northwest Swaziland has included a period of extremely ancient mining activities (Dart and Beaumont, 1967).

The most celebrated archaeological discoveries have come from a 10 m-wide cavern cut into a cliff face in the orebody on Lion Peak. Dart and Beaumont (1967) report a Middle Stone Age assemblage (20–30 000 BC) immediately overlying mined bedrock, and charcoal from a trench sunk on the outer, hillside edge gave a ^{14}C age of 41 250 ± 1 600 BC. This is currently the earliest date obtained for a mine anywhere in the world, older by several factors than the earliest dated flint mines of Western Europe. Lion Cavern is now a National Monument, and a million tons of ore was left behind in the open-pit at Ngwenya Mine to support the workings.

In more recent times, iron ore has made a significant contribution to the economy of Swaziland. The value of high-grade hematite ore mined at Ngwenya between 1964–1979 was on average 10 per cent of the gross domestic product. However, the principal benefit to the industrial development of the country was the construction of a 210 km-long railway which in part crosses mountainous and inaccessible terrain. The effects of the railway on the economy of Swaziland, and a financial analysis of Ngwenya Mine are given in Ainsworth (in press).

Although extensive reserves of low-grade iron-formation have long been known to exist in different parts of the country, the long-term future of iron ore mining in

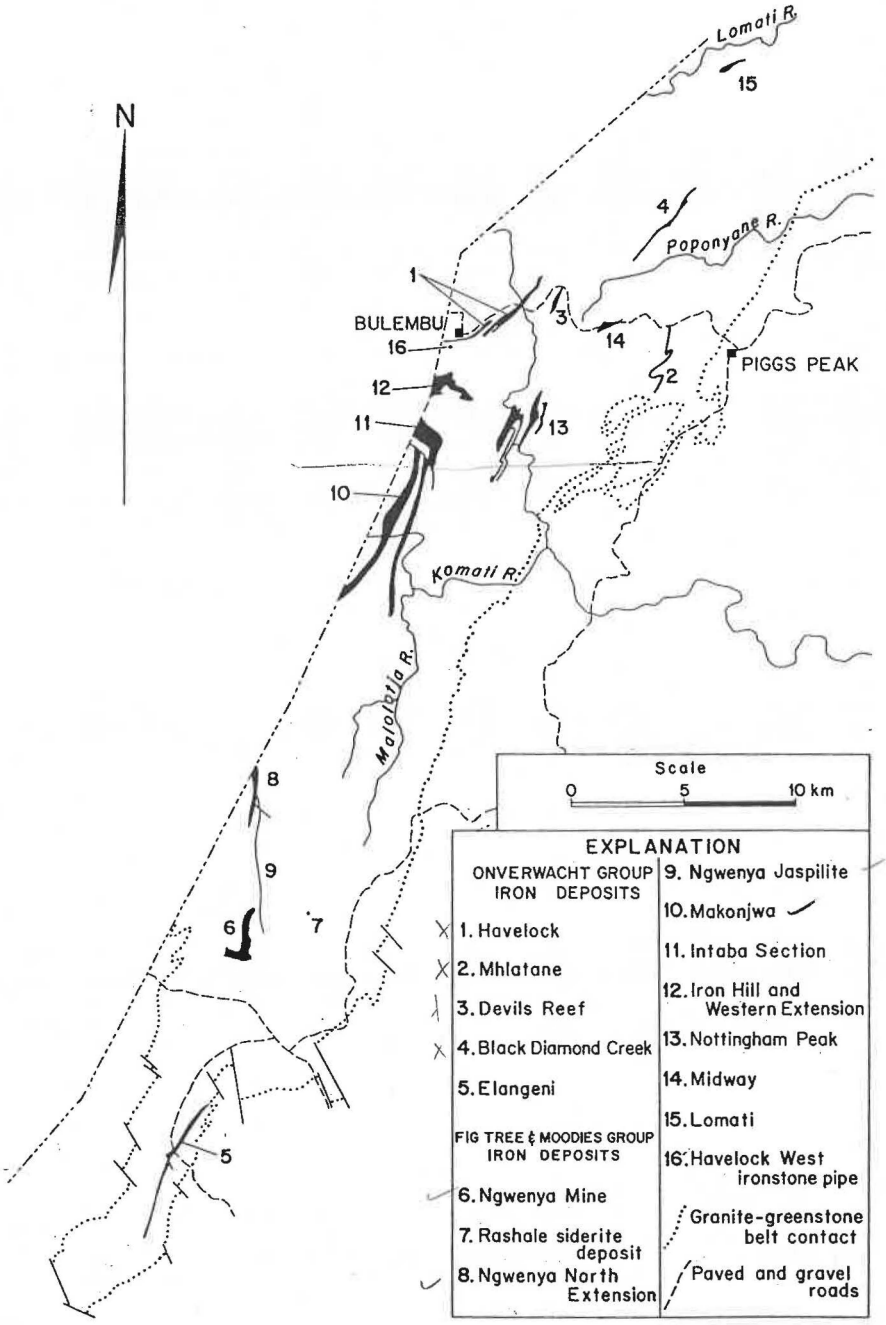

Figure 39
Iron deposits in northwest Swaziland.

Swaziland is difficult to predict. At the time of writing, low-grade iron ore is not economic to export, principally due to high transport costs and competition from massive deposits elsewhere. Nevertheless, the expansion of the domestic market will eventually lead to a re-examination of local resources, and for this reason individual iron deposits are documented here in some detail. Available data suggest that almost a billion (10^9) tons of low-grade (30–45 per cent Fe) iron-formation are available *in situ* in the country, of which 70 per cent or more is located along the eastern edge of the Barberton greenstone belt in northwest Swaziland.

Iron deposits are described below according to their stratigraphic status. With the exception of the Mhlatane iron-formation (Fig. 39), those deposits that occur in the Onverwacht Group form uneconomic or sub-economic horizons of carbonate iron-formation, or its metamorphosed equivalent. In contrast, iron deposits that occur in the Fig Tree and Moodies Groups include massive hematite ores of the Ngwenya-type that have been enriched by processes of supergene leaching. Following the description of individual deposits, geochemical data are presented, and the origin of both types of occurrence discussed briefly.

IRON DEPOSITS IN THE ONVERWACHT GROUP

A number of small, lenticular bodies of iron-formation are associated with volcanic and volcaniclastic sequences in the Onverwacht Group. Two deposits are described in detail: the first (Havelock iron-formation) crops out 8–10 km from the granitic edge of the greenstone belt and includes unmetamorphosed iron-formation. Complete sections through this horizon are exposed underground at Havelock asbestos mine. The second deposit (Mhlatane iron-formation) is a massive, potentially mineable occurrence of magnetite iron-formation within the aureole of the AG3 granite. Other Onverwacht Group iron deposits are known in Swaziland (Devils Reef and Black Diamond Creek deposits, Figs. 39), but these are low-grade and not of economic interest.

HAVELOCK IRON DEPOSIT

A thin but laterally persistent horizon of iron-formation occurs in the immediate footwall of the Havelock serpentinite (Fig. 8). The iron-rich unit has a discontinuous strike length of ±7 km in Swaziland and adjacent parts of South Africa. The unit is repeated in part by thrust faults and is everywhere structurally overridden by the allochthonous Havelock ultramafic body. The Havelock body is an elongate and totally serpentinised dunite-harzburgite, that contains economic deposits of vein chrysotile (*see* Asbestos).

Geological description

A section through the western footwall of Havelock Mine (Fig. 40) shows a 35–40 m thick unit of iron-formation below the Havelock serpentinite and above a mafic igneous sequence that includes pillow structures. The basal member of the iron-formation is essentially unmetamorphosed, and iron is stored in carbonates, and to a much lesser extent in sulphides. Metamorphic grade increases toward the hangingwall, and iron oxide — iron silicate assemblages are present in iron-formation close to the serpentinite (Fig. 40).

Footwall

The pillowed igneous sequence exposed below the iron-formation has the following distinctive features:

1. individual pillows are very pale green, contain abundant variolites and extensive vein carbonate. Variolites occur in both pillow centres, and at margins, and tend to form clusters.
2. a very variable size distribution appears to be characteristic of the pillows. Spherical shapes do occur, but elongate pillows are more typical.
3. pillow edges are very irregular, and in places lobate, and often pass almost imperceptibly into massive, non-pillowed material. Most pillows have gradational margins while some pillows are separated by a small amount of interstitial silica. Thus both pillow margins, and the contacts between pillows and more massive material appear black or dark green.
4. pillows become progressively elongate and irregular and eventually pass into massive pale grey or green non-pillowed material that comprises the uppermost 20–30 m of the igneous sequence (Fig. 40). All pillow structures are steeply inclined, and oriented east-west parallel with compositional layering in the iron-formation.

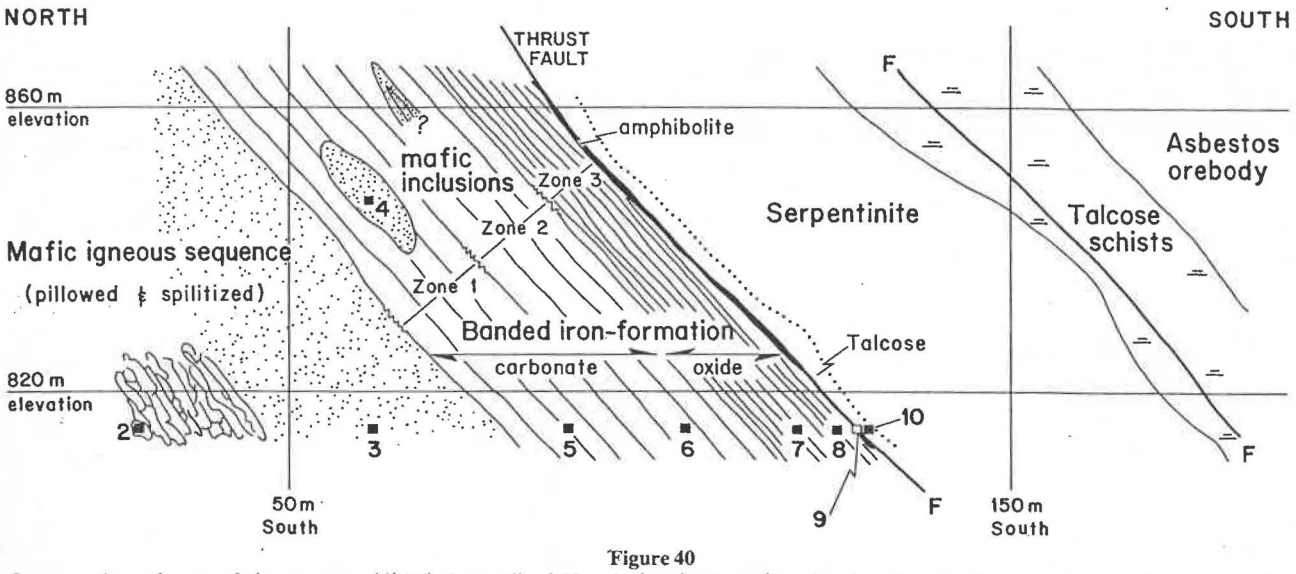

Figure 40

Cross-section of part of the western (5½ W) footwall of Havelock asbestos mine showing the distribution of prograde metamorphic mineral zones in iron-formation: zone 3 — ferroactinolite zone, zone 2 — minnesotaite zone, together with unmetamorphosed carbonate iron-formation in zone 1. Thin amphibolite (black) occurs above the iron-formation at the base of the allochthonous Havelock serpentinite. Chemical analyses of samples located in positions 2–11 are reported in Table 42 (sample 1 is located deep in the mine footwall). Mine co-ordinates can be fixed with respect to the geological plan of 390 level (see Fig. 9).

TABLE 29
Summary of mineralogical observations from the Havelock banded iron-formation and adjacent units.

HAVELOCK SERPENTINITE				lizardite-chrysotile-brucite-magnetite; talcose at base.
			THRUST FAULT	
AMPHIBOLITE			*0–1 m:*	actin/trem — antig — (chlorite) — talc — magnetite
BANDED IRON-FORMATION	3.	*Ferroactinolite zone* (moderately metamorphosed)	*1–6 m:*	40 % monomineralic layers, 1–5 mm-wide ferroact + magnetite; 10 mm-wide layers ferroact-minn intergrowth; <1 % carbonate.
			6–9 m:	25 % monomineralic layers 0,5–1 mm-wide minn. & <15 mm-wide magnetite; 10 mm-wide minn.-ank.-minor ferroact; <20 % carbonate.
	2.	*Minnesotaite zone* (slightly metamorphosed)	*9–15 m:*	magnetite (20–50 μm) + fibrous minn. replacing iron carbonates.
			15–22 m:	platy & spherulitic ("bow-tie") minn. between silica-carbonate layers.
	1.	*Carbonate zone* (unmetamorphosed)	*22–35/40 m:*	layers 6–30 mm-wide (20 μm qtz); ankerite layers 5–15 mm-wide (200 μm rhombs with overgrowths); siderite matrix; pyrite (<5 %); graphite in partings + matrix.
MAFIC IGNEOUS SEQUENCE			*>30 m:* (below iron-formation)	spilites: Ab-ank/ferrodol -minor chlorite; 10 μm diffuse opaque spotting; 15 % carbonate.
			170 m: (below iron-formation)	oligoclase *(200–500* μm laths)-chlorite-skeletal magnetite; no ophitic texture.

5. extensive alteration to carbonate (often >20 modal per cent) is characteristic of the mafic igneous sequence. Chlorite and albite are replaced by ankerite/ferrodolomite and minor calcite. Resulting lithologies are pale in colour and in the upper 30–50 m of the sequence, green (mafic) minerals are often completely absent. Petrographic evidence suggests that carbonation increases up-section to a maximum in the pillowed and massive material close to the iron-formation.
6. the contact with the iron-formation is sharp but irregular. Fragments of glassy, black silica that resembles obsidian occur close (within ±5 m) to the basal member of the iron-formation. There are no scoriaceous flow tops, sediment interbeds and tuffs have not been observed, and there is no indication of major deformation along the contact.
7. inclusions of mafic non-pillowed igneous material occur within the basal iron-formation (Fig. 40). Inclusion margins are either parallel or oblique to the layering in the iron-formation but always extremely sharp; the layering is not deflected around the inclusions. Furthermore, the inclusions are not physically connected in three-dimensions with the main part of the igneous sequence.

Mineralogical observations (summarised in Table 29), pillow morphology and geochemistry (described below) are consistent with an extrusive sequence of broadly tholeiitic composition that has been subjected to a "spilitic metamorphism". The Havelock iron-formation rests on spilites of the same type that are widespread in ophiolite complexes and present-day ocean crust.

Iron-formation

Mineralogical changes observed within the Havelock iron-formation (Table 29; Fig. 41) allow the recognition of two metamorphic zones within the "aureole" of the serpentinised ultramafic body. Each zone may be recognised by the dominant iron silicate present: zone 3 — ferroactinolite zone (moderately metamorphosed) and zone 2 — minnesotaite zone (slightly metamorphosed), where zones 3 and 2 are defined by the first appearance of ferroactinolite and minnesotaite respectively (see Table 30 for electron probe analyses). In addition, a third zone corresponds to essentially unmetamorphosed iron-formation: zone 1 — carbonate zone.

The principal metamorphic changes observed are as follows:

1. a progressive reduction in the amount of carbonate and free quartz between zone 1 and zone 3. Zone 1 consists almost exclusively of layered silica and iron carbonate (oxide-free) iron-formation. Within zone 2 carbonate layers are replaced in part by magnetite and minnesotaite, and oxide — silicate iron-formation accounts for the whole of zone 3. Monomineralic layers of quartz and iron carbonates are entirely absent near the serpentinite.

TABLE 30
Microprobe analyses (weight per cent) of minnesotaite and ferroactinolite from metamorphic zone 3 of the Havelock iron-formation.

	1	2	3	4	5	6	7	8
SiO_2	50,49	53,12	53,28	52,10	53,51	53,65	53,17	53,94
Al_2O_3	1,28	0,89	0,61	0,27	n.d.	n.d.	n.d.	n.d.
[1]FeO	33,73	32,87	33,22	34,01	23,94	23,63	29,54	27,53
MnO	1,84	1,74	1,68	1,65	0,87	0,86	1,35	2,73
MgO	6,09	6,41	5,93	5,86	9,06	8,72	6,99	9,08
CaO	n.d.	n.d.	n.d.	n.d.	10,91	11,86	6,02	3,63
K_2O	1,04	0,71	0,42	0,44	n.d.	n.d.	0,12	n.d.
Total	94,47	95,74	95,14	94,33	98,29	98,72	97,19	96,91

[1]All Fe reported as FeO.

Notes: 1. fibrous minnesotaite within magnetite layer; 2–3. colourless, fine-grained minnesotaite adjacent to magnetite layer; 4. fine-grained fibrous minnesotaite? with brownish alteration haloe, mean 2 analyses; 5. colourless ferroactinolite porphyroblast growing in minnesotaite layer (analyses 2–3); 6. pale green porphyroblastic ferroactinolite with magnetite rim; 7–8. colourless intergrowth of fibrous amphibole and minnesotaite containing porphyroblastic ferroactinolite, analysis 6 (sample 8 contains 1,26 % Na_2O).

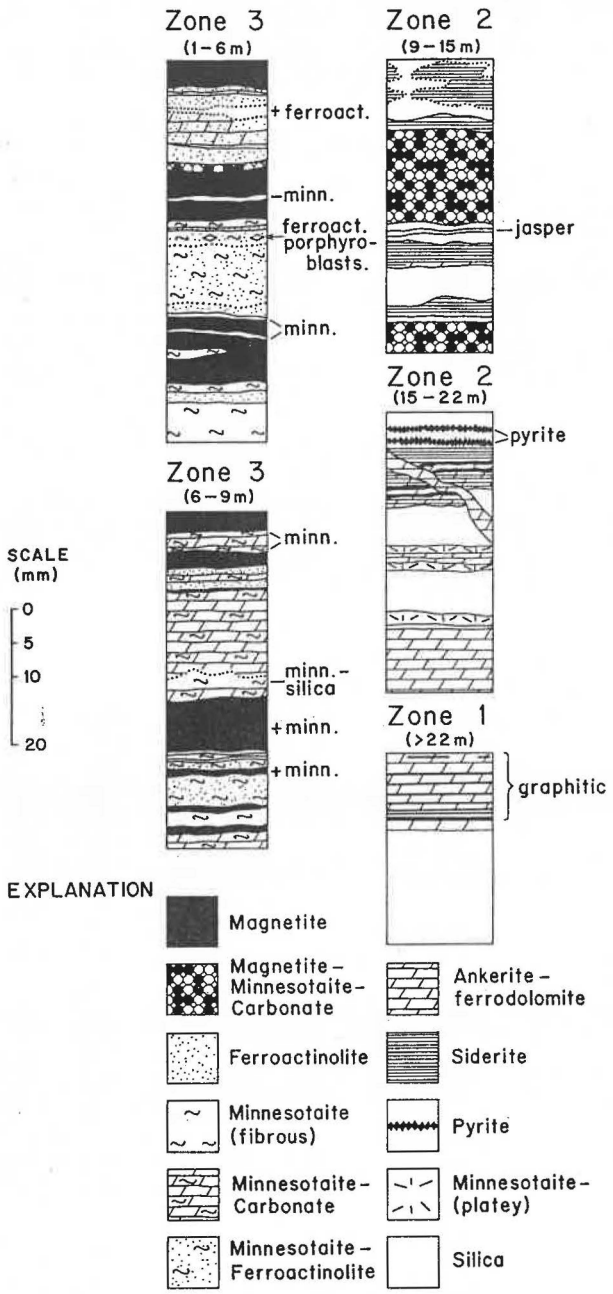

Figure 41
Mineralogical observations in the Havelock iron-formation. Zones 1–3 are shown in Figure 40; measurements in metres refer to true thicknesses below the basal thrust of the Havelock serpentinite.

2. modal iron oxide content increases from ±10 per cent within zone 2 to ±20 per cent at the zone 2/zone 3 contact and ±35 per cent near the serpentinite. Iron silicates vary in amount in the same way: total minnesotaite + ferroactinolite increases from 15 per cent near the centre of zone 2 to 60 per cent in the upper part of zone 3.
3. a progressive reduction in the width of layering from ±15 mm in zone 1 to 1–5 mm in the upper part of zone 3 (Fig. 41). Iron-formation adjacent to the serpentinite is characterised by an exceptionally regular, narrow monomineralic layering with a striking appearance: monomineralic magnetite and ferroactinolite layers are black and green coloured respectively. The grain size of magnetite increases from 50 μm in zone 2 to between 100 and 400 μm near the serpentinite (zone 3).

Metamorphic zones in the Havelock iron-formation resemble closely those described from the Gunflint iron-formation by Floran and Papike (1978), who observed mineralogical changes of the same type within the *outer* contact aureole of the Duluth Gabbro. Hedenbergite, fayalite and ferrohypersthene occur close to (within ±3 km) the Duluth Gabbro, but are absent from the Havelock iron-formation.

Hangingwall

The footwall edge of the Havelock serpentinite is faulted against zone 3 iron-formation. The fault is locally oblique but generally parallel to the layering in the iron-formation. A narrow zone of amphibolite (meta-serpentinite) occurs below the fault and is 0,15–0,6 m thick (see Table 29); where missing, the ultramafic body rests directly on the layered iron-rich sequence. Minor structures and occasional brecciated zones occur in iron-formation close to the fault.

Thin zones of amphibolite and structurally inverted metamorphic isograds of the type described within the Havelock iron-formation are present at the base of several obducted slabs of ophiolite (see Coleman, 1977 for a review). Such inverted metamorphic zones are usually considered to result from the downward conduction of heat from the overlying slab or from frictional heating along a basal fault, or to some combination of these processes (see Graham and England, 1976 and Woodcock and Robertson, 1977).

At Havelock, both the mineralogy (Table 29) and geochemistry (Table 42) of the basal amphibolite are consistent with a serpentinite-bearing lithology metamorphosed at a thrust during a shear heating event of the type described by Graham and England (1976). The origin of the inverted metamorphic aureole with its regular metamorphic layering is more readily explained in terms of the downward conduction of heat from the overlying Havelock ultramafic slab. Contact metamorphism at an intrusive igneous contact *sensu stricto* appears to be precluded because although the contact temperature can be substantially lowered by devolatilisation and the vaporisation of pore fluids (Turner, 1968), original cumulus phases (serpentinised olivine and orthopyroxene grains) can still be recognised in the ultramafic slab adjacent to the fault.

Grade and tonnage estimates

Iron-formation adjacent to the serpentinite has been upgraded by at least 15 weight per cent iron as the result of metamorphism. The highest ore grade occurs within 10 m of the serpentinite, and consists in large part of magnetite iron-formation (20–35 per cent magnetite by volume). Only this upper magnetite-rich member of the unit is included in available tonnage estimates.

Strike length of the Havelock iron-formation in Swaziland (including structural duplication) is 6,6 km (Fig. 8). The total *in situ* tonnage to 100 m down-dip is 21,8 $.10^6$ tons of which 14,9 $.10^6$ tons is present in accessible ground southwest of the Nkomozane River (4,5 km strike length). In addition, it is estimated that 9,2 $.10^6$ tons magnetite iron-formation has been proven by development at Havelock Mine (to 465 level) between 2E and 8W (see Fig.9).

Although the unit is very thin, the coarse grain size of the magnetite (up to 400 μm) and the paucity of silica suggest that the lithology may be suited to inexpensive beneficiation techniques. It is noted that easy direct access to the Havelock iron deposit is possible on existing roads.

MHLATANE IRON DEPOSIT

The Mhlatane iron-formation was perhaps the single most important discovery of the 1966 aeromagnetic survey (UNDP, 1970). A magnetic anomaly located 3 km west of Piggs Peak town was measured along four east —west flight lines (0,8 km-spacing), and has the highest total magnetic fluctuation (9 000 gamma) recorded anywhere in Swaziland.

In 1967, the deposit was mapped at a scale of 1:5 000 by Urie (Fig. 42), and a diamond drilling program (four boreholes) was completed by the Geological Survey Department (Ann. Rept., 1967). Two further boreholes (BH 349 and 352, Fig. 42) were drilled in 1969 in order to obtain a bulk sample for beneficiation tests (Ann. Rept., 1969). These tests were carried out as part of the UNDP mineral survey: the Mhlatane sample, together with borehole cores from the Nottingham Peak, Iron Hill and Ngwenya Jaspilite deposits were sent to a laboratory selected by the UN (Polytechna in Prague) during 1970. Grade and tonnage assessments of the Mhlatane deposit are given by Clarke (1971) and Brech and Lumb (1974).

Geophysical data

Evans (1967) conducted a ground geophysical survey of the area that includes the Mhlatane body as part of a follow-up study of all major aeromagnetic anomalies in Swaziland. Magnetic data were obtained from stations 30 m apart along 140 m-spaced ground traverse lines, and are interpreted as follows (see Fig. 42):

1. the main Mhlatane anomaly has an amplitude of over 30 000 gamma (locally over 60 000 gamma) and can be closely correlated with surface outcrops of magnetite iron-formation. A weaker (5–15 000 gamma) anomaly with the same overall trend was identified in ground 1 km farther east, but is not associated with economic quantities of magnetite.

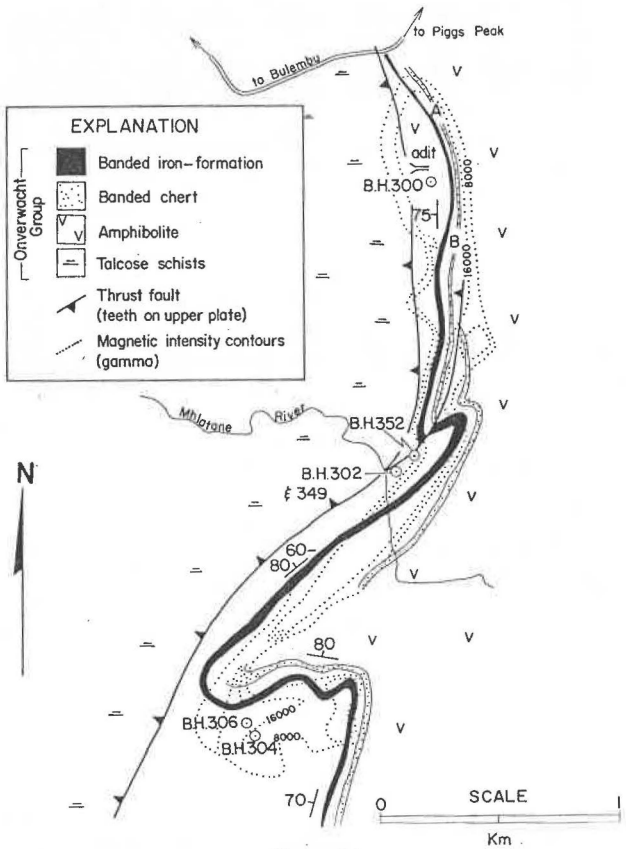

Figure 42
Geological plan of the Mhlatane iron deposit (modified from Urie, GSD 805) with ground magnetic data taken from Evans (1967).

2. the anomaly north of the Mhlatane River was interpreted by Evans in terms of a north–south striking tabular body, 165 m-thick and inclined at a high angle to the west. According to this interpretation, the thickness of the tabular body decreases to 90 m (locally 45 m), and the magnetic intensity increases (by a factor of two) south of the River. An alternative interpretation that is consistent with known surface geology is that the thickness of the causative body decreases, and the associated magnetic susceptibility increases in the area north of the Mhlatane River.

In addition to the magnetic survey, an EM gun was traversed on seven lines in the extreme north of the magnetic anomaly. The resulting data (Fig. 6 in Evans, 1967) suggest that the eastern part of the magnetic anomaly consists of a series of continuous electronic conductors inclined to the west. The coincidence of magnetic and EM anomalies indicate the most likely conductor to be thin, continuous sheets of magnetite (Evans, 1967).

A single gravity traverse was made across the magnetic anomaly immediately north of the Mhlatane River. A 2 mGal gravity anomaly coincides with the main magnetic anomaly and is itself superimposed on a pronounced regional gradient of 0,25 mGal per 30 m (± 8 mGal $.km^{-1}$). According to Evans, the gravity anomaly indicates that the magnetic body must be a dense slab with considerable depth extent and a large mass excess over the surrounding country rock.

Geological description

The Mhlatane iron-formation is a folded and metamorphosed horizon within the aureole of the AG3 granite. Granite crops out south and east of the iron-formation within a radius of 1 200 m (locally 200 m), and is present at shallow depths (± 1 km below surface; see Geophysical data).

The ferruginous horizon is 4,85 km long and lenticular in shape. It is inclined at high angles toward the west except in the structurally overturned area south of the Mhlatane River (see Fig. 43c). The unit has been shortened 20 per cent by folding deformation across steeply plunging fold axes. A mineral lineation, and the axes of small-scale folds both plunge toward the southwest.

Along the northernmost 1,7 km of strike, the iron-formation averages only 18 m in thickness (13 m in BH 300, Figs. 42 and 43). The horizon attains its maximum average thickness of 45 m in the central outcrop area (either side of the Mhlatane River; see Fig. 43b), and this thickness decreases progressively toward the south. BH 352 (Fig. 42) intersected 85 m of iron-formation and this greater thickness is probably due to the effects of deformation near the axial region of a fold (Ann. Rept., 1969). Measured sections give a weighted average thickness of 30 m for the entire length of the unit.

Massive hornblende-oligoclase amphibolites with intercalated horizons of banded chert and banded ferruginous chert form the structural footwall of the Mhlatane deposit. In contrast, layered ferruginous amphibolites that closely resemble the iron-formation form the structural hangingwall. Boudinaged siliceous and iron-rich layers contain garnets in the zone of necking, and the occurrence of both hornblende and grunerite has been reported from this latter sequence (Ann. Rept., 1967). North of the Mhlatane River, the hangingwall amphibolite unit is 50–80 m thick, and structurally overridden by a thrust sheet that includes ultramafic sequences (Fig. 42).

Where least metamorphosed, particularly near fold cores in the central outcrop area, the Mhlatane iron-formation exhibits a distinctive compositional layering:

1. 30 mm-wide layers (range 10–50 mm) that contain alternating 1–2 mm-wide laminae of iron oxides (mostly

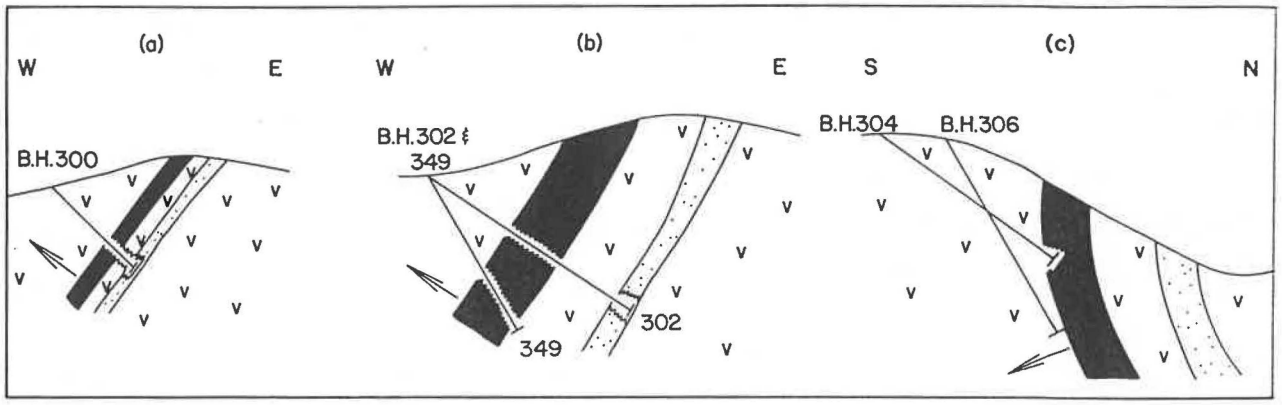

Figure 43
True dip sections through the Mhlatane iron-formation at borehole collars located in Figure 42. Structural facing directions are shown by arrows. For explanation see Figure 42.

magnetite) and silica. Pale green amphiboles (ferroactinolite?) also occur both as narrow and inconspicuous monomineralic layers, and within quartzose layers.

2. Narrow 5 mm-wide (*max.* 10 mm-wide) partings of material with a characteristic orange weathered surface. This material has a texture that resembles soap, and optical properties that are consistent with oxidised minnesotaite.

Chemical compositions of the iron silicates at Mhlatane have not been determined and the presence of ferroactinolite and minnesotaite require confirmation. Grunerite has been noted previously (Ann. Rept., 1967) but has not been observed by the present writer.

Semi-quantitative modal analyses of surface samples indicate that magnetite forms over 90 per cent of total iron oxides. The average grain size of magnetite is 40 μm (range 10–180 μm). Hematite is present as 25 μm subhedral grains that pseudomorph magnetite. Inclusions of pyrrhotite, and more rarely chalcopyrite occur as drop shapes within large (180 μm) magnetite grains. Sulphides (mostly pyrite) and ferroan carbonates also occur in small quantitites as fracture fillings. Beneficiation tests on cores from BH 349 and 352 (Fig. 42) indicate that magnetite is the only iron oxide present at depth (UNDP, 1970).

Precious metal values have been determined in chemical analyses of cores from both BH 300 (0,7 g/t Au, reported in Evans, 1967) and BH 349/352 (0,03 g/t Au, UNDP, 1970). In addition, a 90 m-long caved adit, together with numerous old trenches dug along 500 m strike length of iron-formation between points A and B in Fig. 42, are thought to be associated with a gold-bearing reef known as "Pirate Reef".

Grade and tonnage estimates

Iron at Mhlatane is stored in both oxides and silicates. and the proportions in both can be estimated from mineralogical and geochemical data. Representative cores from BH 302 examined at the Institute of Geological Sciences were reported to contain 24 per cent magnetite by volume (30–45 per cent by weight, Ann. Rept., 1969). Cores from BH 349 and 352 examined at Prague contained 30–80 per cent magnetite by volume (UNDP. 1970). Clarke (1971) estimated that 85–94 per cent of total iron is available in magnetite, based on calculations in which all Fe^{3+} in unweathered iron-formation was assigned to the oxide phase.

Available data are summarised in Table 31 and suggest an average grade of 39,1 per cent Fe, of which ±90 per cent is available as magnetite.

Beneficiation tests have been conducted by Geoindustria and the Ore Research Institute, Prague, under the auspices of Polytechna, the official Czechoslovak Technical Cooperation Agency (UNDP, 1970), and by the Swaziland Iron Ore Development Company (Brech and Lumb, 1974). The results of these metallurgical tests suggest that to upgrade the Mhlatane deposit is a rather straightforward process. Beneficiation would involve the least costly techniques required for any iron deposit in northwest Swaziland.

Using magnetic separation techniques, Brech and Lumb (1974) report a good iron oxide recovery (especially in the coarser fractions) at a high field intensity of 4 000 gauss, although separation was generally poor. It is noted that this work was conducted with unrepresentative surface (trench) samples which may have contained weathered material. The ore also responded well to flotation techniques and upgrading to 64 per cent Fe was readily

TABLE 31
Assays of the Mhlatane iron-formation and adjacent units

	1	2	3	4	5	6	7	8
SiO_2	42,60	44,59	40,91	37,79	44,20	40,90	29,70	38,38
Al_2O_3	3,88	6,14	2,52	2,18	3,71	1,84	1,95	2,47
Fe_2O_3	27,58	32,62	33,43	36,51	31,13	n.d.	62,38	39,98
FeO	19,10	11,63	17,97	18,29	13,86	n.d.	1,91	14,32
Fe	34,15	31,87	37,36	39,77	32,56	35,25	45,15	39,11

n.d. = not determined.

Notes: 1–5 reported in Clarke (1971); 1. BH 300, mean 5 assays over 13 m width iron-formation; 2. BH 300, oxidised hangingwall amphibolites, mean 11 assays over 41,3 m core length (40 % core recovery); 3. BH 302, mean 15 assays over 44,5 m width iron-formation; 4. BH 302, best 21,4 m width iron-formation, mean 7 assays; 5. BH 302, footwall amphibolites, mean 15 assays over 45,7 m core length; 6. BH 349 & 352, bulk assay Polytechna — geoindustria (UNDP, 1970); 7. average surface (oxidised) samples from central orebody, mean 2 assays; 8. average grade, Mhlatane iron-formation.

achieved with recovery in excess of 80 per per cent (Brech and Lumb, 1974).

The *in situ* tonnage of low-grade iron-formation available at Mhlatane, based on an average 30 m unit width, and a specific gravity of 3,6 measured from core samples (Clarke, 1971) is estimated at 52,1 $.10^6$ tons to 100 m down-dip. Because this relatively high tonnage is entirely in the form of magnetite rather than hematite iron-formation, and is therefore suited to inexpensive beneficiation techniques, it appears that the Mhlatane deposit has not received the attention it deserves. Further bulk sampling by adit development is required before a more careful assessment of economic potential is possible.

DEVILS REEF IRON DEPOSIT*

The Devils Reef iron-formation crops out near the disused Devils Reef gold mine 4 km northeast of Bulembu (Fig. 39). The ferruginous horizon is lenticular in shape and 2,75 km long; it reaches its maximum stratigraphic thickness (41 m) in the immediate vicinity of the old gold workings. The unit exhibits a lateral transition with banded and ferruginous cherts, and rests stratigraphically above thin cherts, quartz-sericite-ankerite schists and a talc-carbonate unit (see Devils Reef gold deposit for a more detailed description of the stratigraphic sequence).

Unlike other units of iron-formation described here, the Devils Reef horizon is cut by pipe-shaped breccia zones that are overlain with irregular masses of ferruginous wad that are rich in manganese (Jones, 1961). Breccia zones consist of angular fragments of iron-formation, chert and talcose schist with a matrix of black wad, and are clearly associated with fault surfaces. Ferruginous wad is a soft, black and earthy material that locally attains a thickness of 40 m above breccia pipes. The mineralogy of ferruginous wad consists in large part of hematite (including specularite) with limonite and manganese oxides and hydroxides. Lenses and strings of wad lace the ferruginous horizon at some distance from breccia zones where the iron-formation is typically a layered (5–30 mm-wide) hematite — silica lithology.

Assays of iron-formation and ferruginous wad from surface and underground gold workings (20–25 m below outcrop, Table 32) show consistently high manganese contents (5–13 per cent) and exceptionally high gold values (locally >0,15 per cent Au). Trace element data presented elsewhere (Table 27) show ferruginous wad to have an anomalously high barium content.

The average grades of iron-formation and ferruginous wad are 45,8 per cent and 50,8 per cent Fe respectively; grade of the iron-formation decreases rapidly along the strike. *In situ* tonnage to 100 m down-dip is estimated at 6,6 $.10^6$ tons iron-formation in the vicinity of existing mine workings (±500 m strike length) and 13,6–18,2 $.10^6$ tons for the entire deposit. Jones (1961) estimated that 1,5 $.10^6$ tons ferruginous wad is present *in situ* in the mine area (±60 m below surface).

BLACK DIAMOND CREEK IRON DEPOSIT

Many features of the Black Diamond Creek iron-formation resemble those of Onverwacht Group iron deposits described above. The unit has a strike length of 4,5 km and is inclined at high angles (45°–65°) toward the northwest; it rests with stratigraphic continuity on a thick volcanic sequence of mafic composition and is structurally overridden by a thrust sheet that includes talcose schists above a basal movement horizon.

* Footnote: Though the petrography of the Devils Reef iron-formation closely resembles iron deposits of the Fig Tree and Moodies Groups, on stratigraphic grounds the lithological sequence at Devils Reef forms part of the Onverwacht Group.

TABLE 32
Assays of Devils Reef iron-formation and ferruginous wad

	1	2	3	4	5
Fe	45,17	47,42	55,42	44,73	46,27
Mn	5,67	5,22	8,05	6,41	13,25
SiO_2	20,91	19,63	2,30	19,16	3,13
Al_2O_3	3,31	2,74	3,06	4,24	0,70
[1]Au	0,39	0,18	0,36	0,19	0,05

[1]reported as ppm.

Notes: 1–4 recalculated from Jones (1961); each analysis cited below (in parentheses) represents 1,5 m long channel sample; 1. basal 16,8 m iron-formation, 3 level east, C adit and crosscut (mean 18 analyses); 2. middle 13,7 m iron-formation, 3C level east (mean 9 analyses); 3. 12,2 m ferruginous wad, 3 level west, D adit (mean 8 analyses); 4. uppermost 24,8 m iron-formation, 3 level west, D adit (mean 16 analyses); 5. surface ferruginous wad, mean 3 grab samples.

On surface, the Black Diamond Creek iron-formation contains hematite — goethite — limonite — silica; nothing is known of the mineralogy at depth. The lithology is manganiferous in part, and exhibits a centimetre-scale layering. The basal member of the unit is predominantly goethitic, and may represent oxidised carbonate iron-formation of the Havelock-type. Maximum stratigraphic thickness is 40–50 m, and the horizon is lenticular in shape. Small-scale fold structures are common.

Although the indicated *in situ* tonnage is considerable (>20 $.10^6$ tons to 100 m down-dip), the Black Diamond Creek iron-formation is not considered to be an economic source of iron. Visual inspection of surface material suggest the overall grade to be relatively low. During his reassessment of the Black Diamond Creek gold mine Jones (1963) assayed the iron-formation for gold but no values were returned.

ELANGENI MAGNETITE-PYRRHOTITE DEPOSIT

A massive deposit of magnetite-pyrrhotite crops out near the southernmost extension of the greenstone belt (Fig. 39). Though not a banded iron-formation of the type found elsewhere in northwest Swaziland, and not of economic interest as a source of iron but rather for its base metal potential, it is nonetheless convenient to describe the Elangeni deposit here.

Geophysical data

Electrical conductors were discovered in the Elangeni area during the 1967 UN airborne EM survey (UNDP, 1970). Measurements recorded from a helicopter revealed a number of moderate or high-grade EM anomalies along the eastern edge of the greenstone belt within a broad 8 km-long zone. Magnetic intensity contours (also airborne data) parallel the anomalous zone, and those EM conductors with the highest amplitudes coincide with the maximum total magnetic field fluctuation (4 500 gamma, Fig. 44).

Subsequent geophysical work conducted by a mining company (summarised in Randell, 1978) located the airborne EM anomalies on the ground. Reconnaissance mapping, and the results of 68 line kilometres of Turam survey together with a pulse EM program confirmed the presence of both steeply inclined multiple linear conductors and a limonitic gossan. These data showed that the Turam conductors can be correlated with, but also extend beyond, the gossan outcrop (Fig. 44).

Geological description

Cores from two diamond drill holes (BH EL1 and 2, Fig. 44) show the Elangeni gossans to be the surface expression of thin units of a laminated oxide-sulphide facies

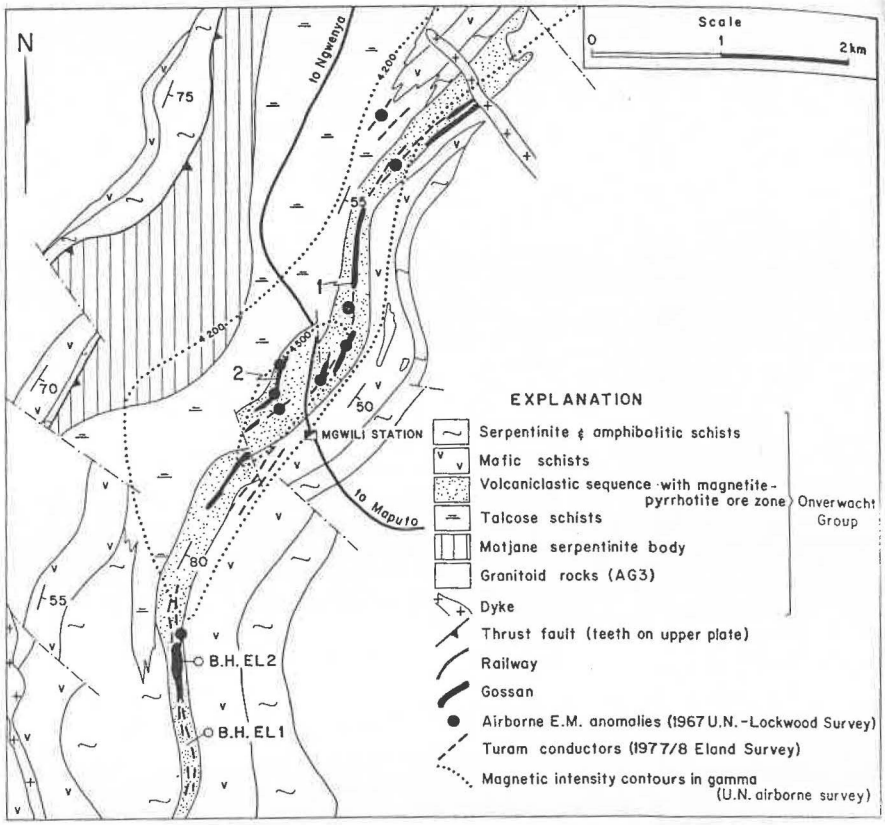

Figure 44
Geological plan of the Elangeni magnetite-pyrrhotite deposit (after Urie, 1971, and Randell, 1978, with additions). Aeromagnetic data taken from the 1:50 000 map series.

iron-formation. Individual ferruginous horizons contain as much as 30 per cent magnetite by volume together with significant amounts of pyrrhotite. Estimates of pyrrhotite content suggest that on average this mineral forms 5–12 per cent of all opaque phases in the Elangeni deposit; concentrations of 30–40 per cent pyrrhotite by volume have been recorded (Randell, 1978).

Iron mineralisation is almost entirely confined to a single stratigraphic unit (Fig. 44). This unit consists of a metamorphic sequence of quartz-biotite schists, various laminated silicic and mafic schists, and more massive amphibolites. Lenticular in shape, the unit has a strike length of 7 km; the northern strike extension is truncated by AG3 granite. Maximum structural thickness is ±300 m in the central outcrop area near Mgwili station (Fig. 44).

Talcose schists (or more highly metamorphosed equivalents) and an allochthonous serpentinite body known as the Motjane serpentinite form a structural footwall to the Elangeni deposit. The Motjane serpentinite is highly deformed along its basal edge and rests with décollement on thin metamorphic sequences near the western margin of the greenstone belt.

A thick (200–500 m) mafic schist unit with a greenschist — amphibolite transition facies mineralogy (tremolite/actinolite — chlorite — clinozoisite ± oligoclase) overlies the deposit. A combination of relic basaltic textures that include 100–200 μm euhedral laths of andesine extensively altered to sericite, and major and trace element geochemistry (Table 42a and b) suggest that the hangingwall mafic schists represent a metamorphosed volcanic sequence of tholeiitic composition.

The mineralised stratigraphic unit is characterised by abrupt variations in composition and a well-defined layering or lamination. Magnetite-pyrrhotite horizons are associated with laminated amphibolites that contain ±75 modal per cent actinolite/tremolite and chlorite but little or no free silica and carbonate. Amphibolites with up to 85 modal per cent quartz and ferroan carbonate but no magnetite are interbedded within the sequence, as are thin recrystallised quartzites and quartz-biotite schists. For the most part, the sequence is thought to be volcaniclastic in origin though thin extrusive units, including some of ultramafic composition may also occur. Further work is required to document the stratigraphy in more detail.

Structures that may be sedimentary in origin are present within the volcaniclastic unit. Facing directions inferred from possible cut-and-fill scours indicate that the stratigraphy is younging toward the east. Because compositional layering is well developed and because the unit is highly deformed, minor tectonic fold structures are also common.

The internal distribution of magnetite iron-formation within the volcaniclastic unit is known from limited borehole data only for the southern part of the deposit. There, magnetite is concentrated in the middle of the unit, within horizons up to 15 m thickness. Cores from BH EL2 show that the main part of the iron deposit is 45 m thick, but that magnetite layers are distributed across a total stratigraphic thickness of 110 m (Fig. 45).

Magnetite occurs as narrow, monomineralic layers 0,5–3 mm-wide), and as minor disseminations within amphibole-rich layers. Much of the magnetite consists of 80–100 μm grains with very irregular margins. Pyrrhotite is present as ubiquitous subhedral inclusions within magnetite, and as isolated anhedra in amphibole-rich laminae. Small grains of chalcopyrite attached to magnetite have been observed in polished section.

Base metal potential

The Elangeni deposit represents a substantial *in situ* tonnage of magnetite. Approximately 6,5 $.10^6$ tons of ±45 per cent Fe iron-formation are indicated in ground between BH EL1 and EL2 (to 100 m down-dip). With an assumed continuous strike length of 6,5 km, this figure can be extrapolated to 72,8 $.10^6$ tons iron-formation for the entire deposit. Elangeni cannot however, be considered an economic source of iron: individual horizons of

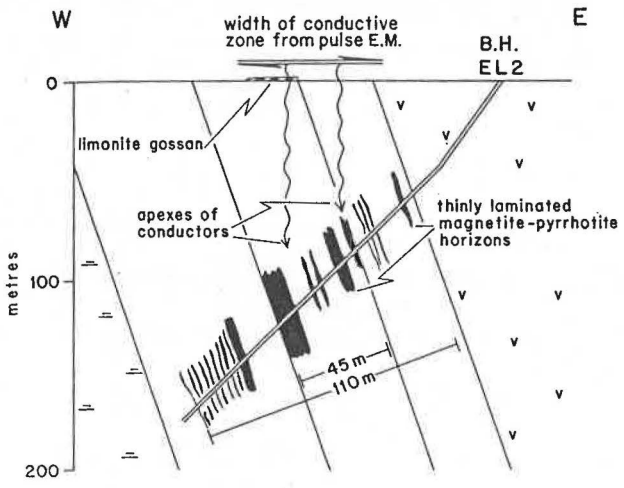

Figure 45
Cross-section of the Elangeni magnetite-pyrrhotite deposit at borehole collar BH EL2 (see Figure 44 for location; redrawn from Randell, 1978).

iron-formation are too narrow, too far apart and not sufficiently high-grade.

Instead, the deposit is considered to be an exploration target for base metal mineralisation associated with massive stratiform sulphides. Randell (1978) reported that the results of core assays from BH EL1 and EL2 for Cu, Pb, Zn, Co, Ni, Sn, Ba, Au and Ag, and a general spectrographic scan indicated the absence of economic mineralisation. It is noted that these data are only applicable to a 600 m strike length in the southern extension of the deposit. Geochemical data farther north have defined areas with anomalous concentrations of zinc in soils (>120 ppm, areas 1 and 2, Fig. 44) which have not been tested at depth.

IRON DEPOSITS IN THE FIG TREE AND MOODIES GROUPS

Almost all the economically important iron deposits in northwest Swaziland occur at or close to the stratigraphic base of the Fig Tree or Moodies Groups. Most are located in the southern half of the greenstone belt where the underlying Onverwacht Group sequences consist in large part of talcose schists. Clastic sequences of Fig Tree and Moodies Group age occur in the area north of the Lomati River but do not contain iron-formations.

Field evidence, that includes the recognition of marked angular unconformities, suggests that many of the major iron deposits formed before deposition of part of the Moodies Group sequence. However, observations described below indicate that some Fig Tree Group iron-formations occur either within or stratigraphically above thin sequences that include lithologies closely resembling those of the Moodies Group. Detailed sedimentological studies of such sequences are required before stratigraphic interpretations are possible.

All Fig Tree and Moodies Group iron-formations are highly susceptible to processes of surface alteration by meteoric water. It is extremely difficult to find fresh, unleached material because such processes often extend to great depths below surface (>150 m). Emphasis is placed here on sub-surface data, obtained either from deep excavations in the open-pit at Ngwenya Mine, or from exploration adits and borehole intersections elsewhere.

NGWENYA HEMATITE DEPOSIT

Rediscovery of the Ngwenya orebody (formely known as Bomvu Ridge) in 1946 is attributed to A.T.M. Mehliss of the Swaziland Geological Survey Department (Ann. rept., 1947). Extensive reserves of high-grade hematite were confirmed by the Geological Survey between 1947–1957 as a result of field investigation in the mountainous terrain 3 km east of the South African border (Fig. 46). Initial exploration (Pretorius in Ann. Rept., 1948) was followed by more detailed work which culminated in important contributions describing the surface geology, structure and petrography of the orebody (Davies and Urie, 1957; Urie, 1958).

Swaziland Iron Ore Development Corporation (SIODC) was formed early in 1958 to continue prospecting activities and study the economics of exploiting the deposit. Between 1958–1960, an underground adit was driven into the orebody, trenches totalling 4 600 m were dug and boreholes that represented 4 900 m diamond drilling were completed. From geological data obtained during this phase of exploration Bursill and others (1964) estimated that 43 million tons hematite (>61 per cent Fe) were present *in situ* at Ngwenya.

Production began in late 1964 when the first ore was taken by rail to Maputo (then Lourenço Marques) for shipment to a Japanese client. Mining stopped in 1977,

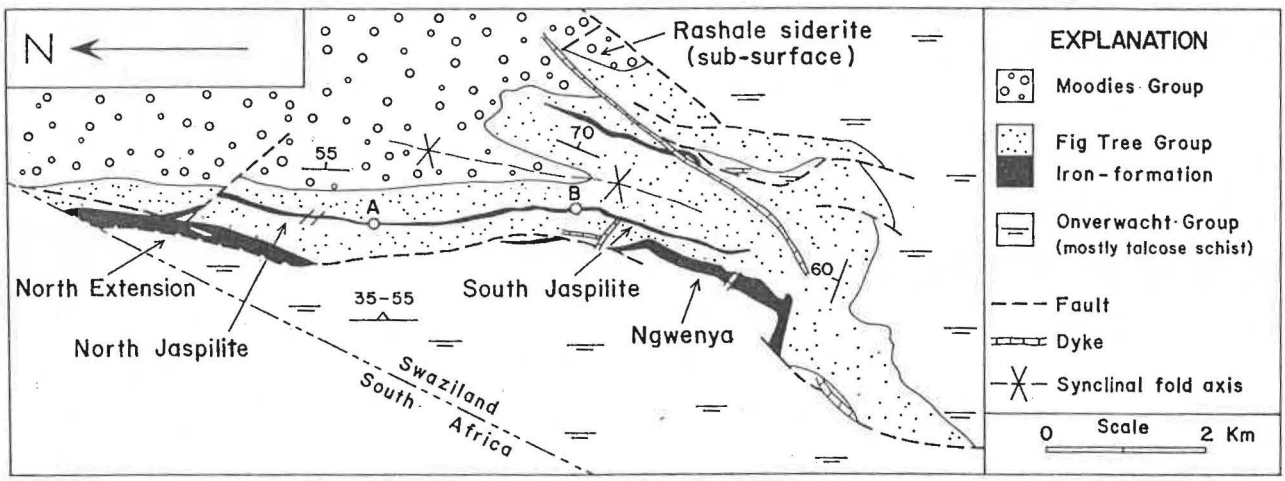

Figure 46
Distribution of major iron deposits in the Ngwenya area (simplified from Urie, 1969; 1970). Ngwenya and North Extension iron-formations occur at or close to the surface between the Onverwacht and Fig Tree Groups, and the Jaspilite horizon is located 200–300 m above this surface. Jaspilite between points A and B is inaccessible, and is not included in tonnage estimates given in the text.

though production was maintained by the treatment of ore from stockpiles until mid-1979 when the treatment plant was closed. Sales were continued by the railage of ore from treated stockpiles and the mine closed after the final shipment was made in mid-1980. Total recorded production (1964–1979) is 28,37 $.10^6$ tons ore (>59,5 per cent Fe); annual production averaged 2,19 $.10^6$ tons between 1966–1976, and 1,77 $.10^6$ tons during the whole of the relatively short life of the mine.

Mining at Ngwenya was by open-pit methods. Bench interval was set at 10 m, with 8 m bench widths, 15 m road widths and an overall slope of ±55°. The footwall perimeter was located at the contact between ore and iron-formation or shale (see Fig. 49 below).

The following account of the geology at Ngwenya, and the estimates of hematite remaining both *in situ* and on dumps draws extensively on two previous SIODC reports. The beneficiation study of low-grade iron-formation (Attridge and others, 1972), and the re-evaluation of the northern part of the orebody described in Brech (1972) together form the basis of much of the following discussion.

Geological description

The Ngwenya hematite deposit forms part of a 70 m-thick unit of banded iron-formation that occurs within the lowermost shale sequences of the Fig Tree Group (Figs. 46 and 47). At its base, the iron-formation passes into thin (<20 m) ferruginous cherts and silicified shales which rest in turn above talcose schists of the Onverwacht Group. The contact between the Onverwacht and Fig Tree Groups resembles a sheared stratigraphic surface. Talcose and other Onverwacht Group schists rest on a basal décollement 1–1,3 km structurally below the orebody (Fig. 47).

The iron-formation is deformed by a large east-plunging fold structure, the two limbs of which crop out for a total strike length of 2 500 m (Fig. 48). The northern, upright limb strikes north–south for 1 900 m and is inclined east at ±55°; the southern limb is structurally overturned and highly deformed. Here, the strike of the iron-formation changes abruptly to 120° for 600 m and the unit dips at high angles (70°) toward the northeast. The southern fold limb is truncated by a fault which itself is oriented parallel with lithological and structural surfaces within the Onverwacht Group.

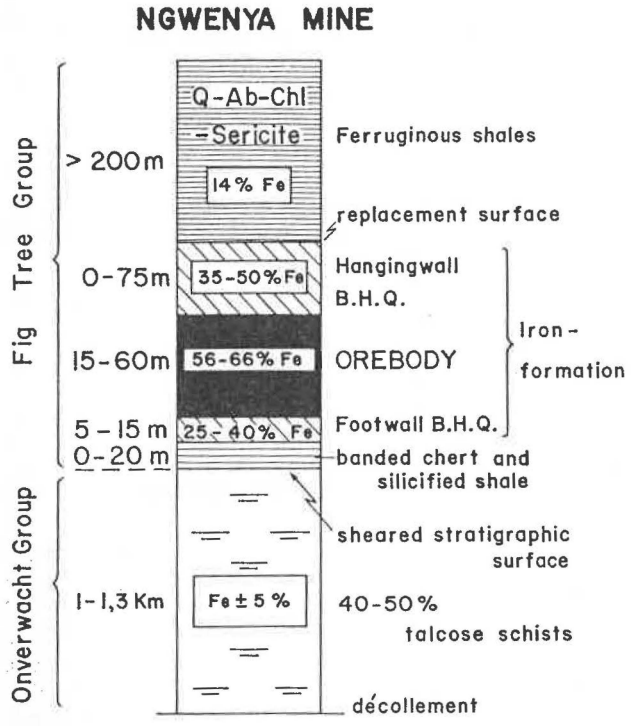

Figure 47
Simplified lithological sequence of the Ngwenya iron deposit.

The orebody is divided into seven ore reserve blocks, each separated by a dyke, a fault or by the major axis of folding deformation (Fig. 48). Although the surface plan indicates continuity along strike, there are important variations in grade and chemical composition between blocks and these differences are described below. Lion North and Stag blocks contain only limited amounts of ore and have not been mined. Ore in South Castle block decreases with depth and mining was discontinued below bench 15 (150 m vertically below outcrop). The orebody in Lion block has been duplicated by a fault and is considerably thicker than adjacent ground in Saddle block.

Footwall and hangingwall

Low-grade hematite iron-formation forms both the footwall and hangingwall of the Ngwenya orebody (Fig. 47), and is known locally as Banded Hematite Quartzite (BHQ). Contacts with the orebody are invariably sharp, but may be transitional over 1–3 m in the hangingwall. BHQ in the hangingwall is higher grade (35–50 per cent Fe) and thicker by a factor of three than BHQ in the footwall (25–40 per cent Fe).

The greatest development of BHQ is in Saddle block where it forms a unit as much as 75 m-thick in the hangingwall of the orebody. Considerable stratigraphic thinning occurs both along strike and down-dip: in North Castle block 20 m of BHQ in the hangingwall on surface is absent at depth (bench 23), and shale rests directly on massive hematite. Similarly, BHQ is replaced by shale north of Saddle block and is thin or absent in parts of Lion block.

Irregular lenses and layers of shale, some of which can be traced for several tens of metres occur within the BHQ. Shale appears everywhere to have been replaced by the BHQ and the BHQ appears to have formed by iron enrichment of shale (see Figs. 48 and 50). The BHQ is itself enriched to pure hematite in lenticular zones parallel with the banding. Replacement of shale by silica to form silicified shales and banded cherts is characteristic of the footwall sequence (Fig. 47).

Typical BHQ contains 1–5 mm-wide bands of alternating silica and iron oxides with a sharp separation of layers. Iron mineralogy is dominated by magnetite that has been completely or almost completely oxidised to martite and hematite. Martite grains average 50–60 μm (range 3–200 μm) in size. Small (3–10 μm) magnetite and quartz inclusions are common and larger (30–50 μm) inclusions of quartz are present within ore layers. Silica layers consist of 10–150 μm equidimensional quartz grains. A thin (1–2 mm) laminated BHQ facies containing goethite occurs in Lion block.

Orebody

Where mined, the hematite orebody is rarely less than 15 m-thick and attains a maximum thickness of 60 m in parts of Saddle and Lion blocks (Figs 49a and 50). Both massive and laminated varieties of ore occur together, and both varieties contain unreplaced layers and lenses of BHQ (Fig. 50). Replacement of BHQ by ore diminishes at depth until 150 m below surface in South Castle block and 25 m below surface in Lion North block, only unenriched BHQ is present.

Removal of silica by secondary weathering processes has enriched the upper part of the Ngwenya orebody in iron. Although the extent of this process has not been documented at Ngwenya, a 15–25 per cent iron enrichment to 25 m below surface is known in Fig Tree Group

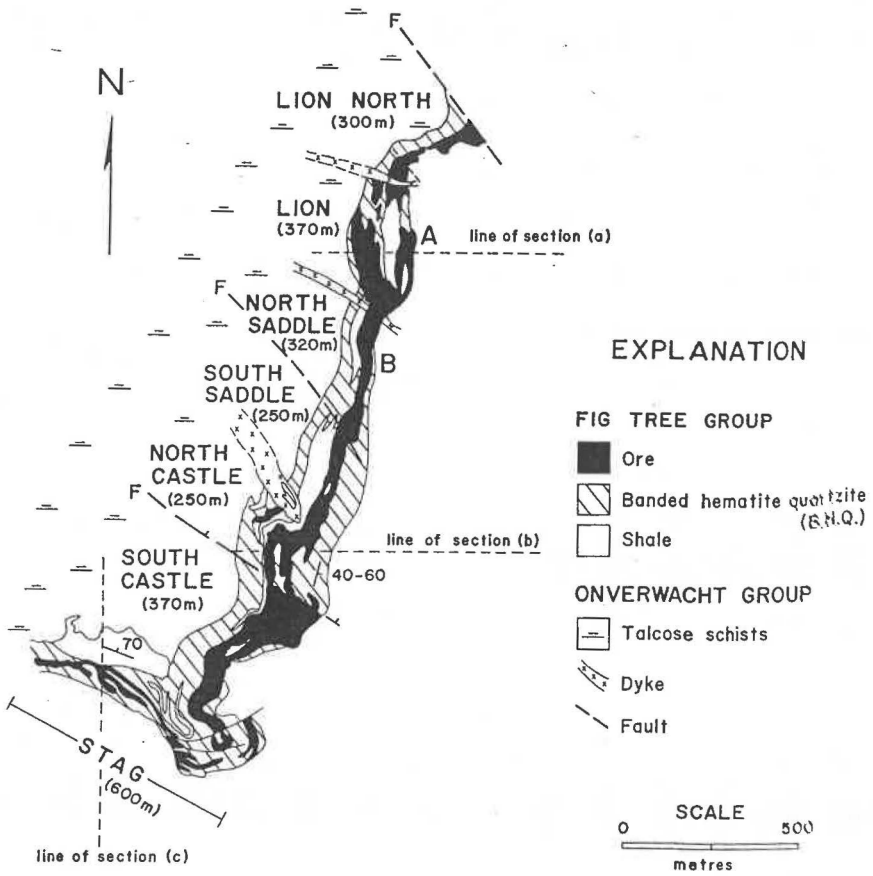

Figure 48
Surface geology prior to mining operations (simplified from Bursill and others, 1964), and the distribution of mining blocks (strike dimensions in parentheses) in the Ngwenya hematite deposit. Limited ore is present in Lion North and Stag blocks, and the amount of ore decreases with depth in South Castle block. Ore in Saddle block contains a high content of manganese, and Banded Magnetite Carbonate (BMC) is known to occur between points A and B in Lion and North Saddle blocks. Representative cross-sections are given in Fig. 49.

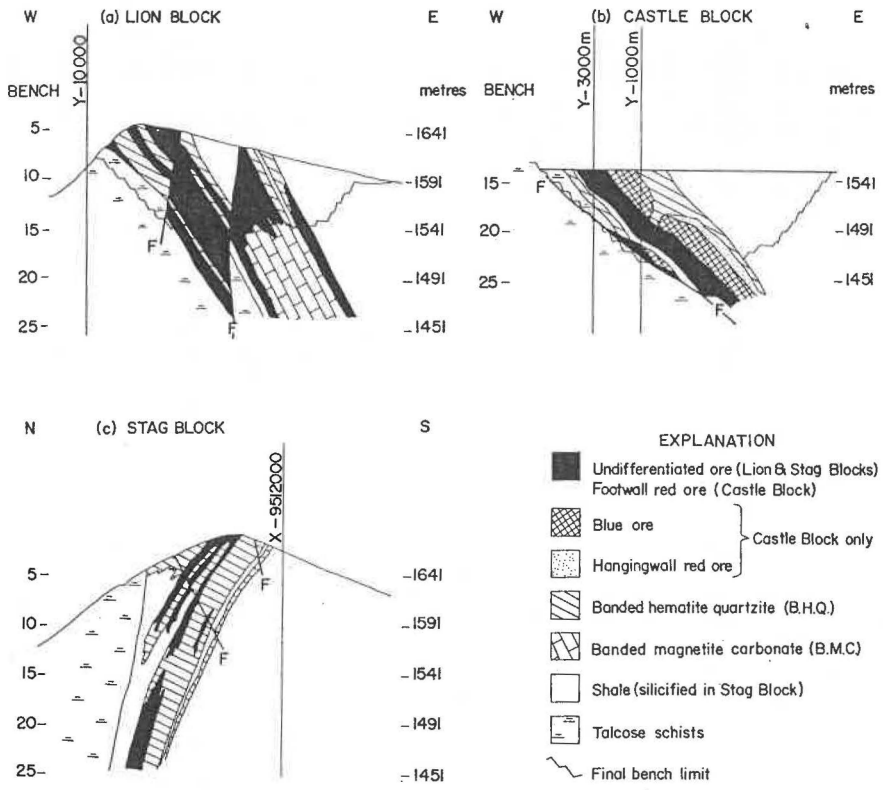

Figure 49
Sections across the Ngwenya orebody along lines shown in Fig. 48. (a) Lion block; (b) Castle block; (c) Stag block.

hematite deposits elswhere (see below). Extreme hydration and the formation of massive goethitic and limonitic ores is common only in Lion block. Ores of this type are interpreted below as the product of fluid movement during orebody deformation.

A compositional sub-division of ore types was suggested by Brech (1974; Fig. 50) on the basis of the following observations:

high-grade ore (60–66 per cent Fe)

High-grade hematite accounts for ±80 per cent of the orebody, and occurs either as a laminated or blocky blue ore, or as a massive red ore. Blue ores contain hematite (>90 per cent), specularite, martite and magnetite in order of abundance. Red ores are similar, but have less magnetite and are more porous with local goethite, cavities containing bladed specularite and fractures filled with psilomelane. Red ore frequently forms the footwall section of the orebody. Distinct blue and red ore zones are a prominent feature of Castle block (Fig. 49b) where 20 m of footwall red ore (62,5 per cent Fe) is overlain by 20 m of blue ore (65,5 per cent Fe) followed by 12 m of hangingwall red ore (62 per cent Fe).

medium-grade ore (58–60 per cent Fe)

Massive, hydrated blue ore containing vugs and cavities filled with secondary hydrated iron and manganese oxides occurs in Lion block (Fig. 50). Bladed specularite, botryoidal goethite and veinlets of psilomelane are common. Ore of this type is thought to have formed during movement of the Lion orebody along a fault. In addition, laminated to blocky medium-grade ore that contains bands of incompletely replaced ferruginous shale is present in limited amount throughout the orebody.

low-grade ore (56–58 per cent Fe)

Ore with a high shale fraction occurs in 1–2 m-wide bands in all ore reserve blocks. In South Saddle block, a 5 m-wide inclusion of low-grade ore is present in the centre of the orebody, and ore of similar type forms a 2–6 m-thick hangingwall to the Lion block orebody.

Other Data

1. In Lion block, and the extreme north of Saddle block hematite ore passes into carbonate iron-formation at depth. The carbonate lithology contains the assemblage quartz — siderite — magnetite, and is known locally as Banded Magnetite Carbonate (BMC).

Within only ±360 m of strike, BMC is present both 130–150 m below outcrop in Lion pit, and as intersections in exploration boreholes 250 m below surface in North Saddle block (Figs. 49 & 50). Farther south the carbonate lithology appears to be absent although few deep exploration data are available.

The contact of BMC with ore is extremely irregular (Fig. 49a); isolated blocks and lenses of BMC occur in ore near the transition. The contact is both sharp and cross-cutting, and is clearly controlled by oxidation.

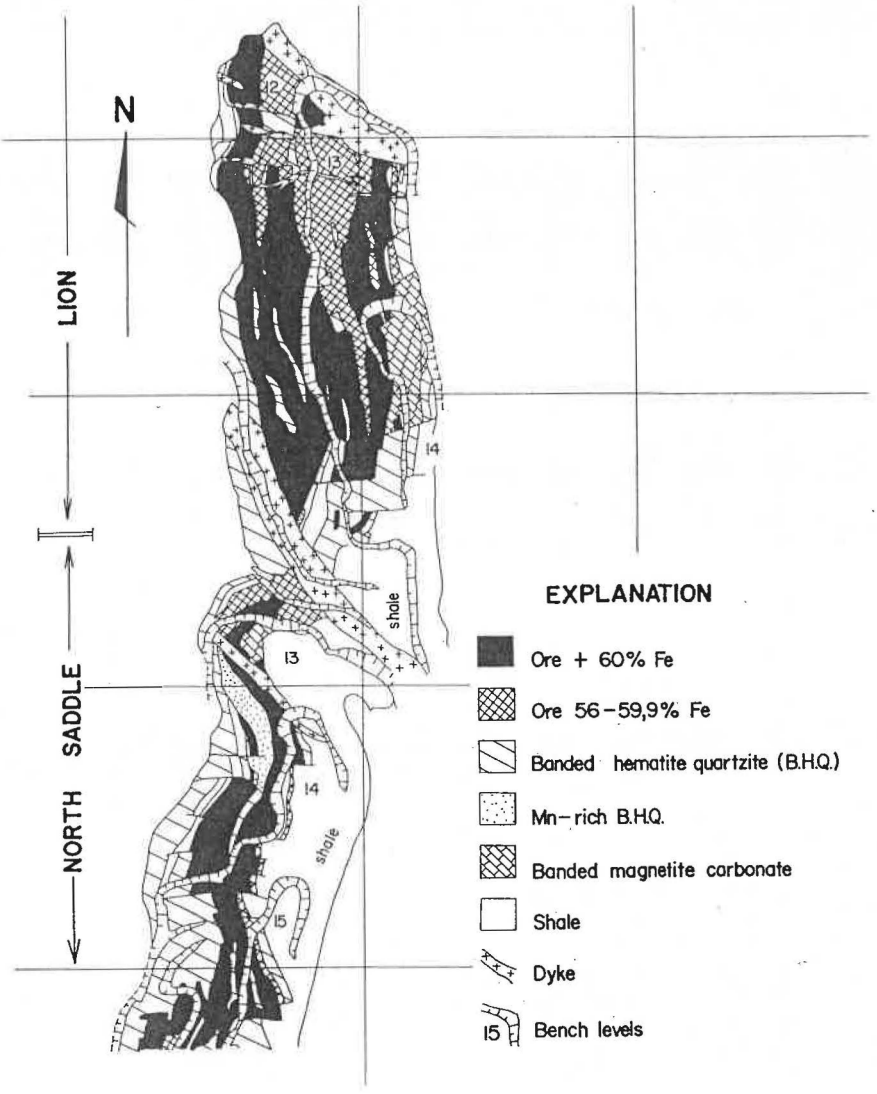

Figure 50
Plan of Lion and Saddle pits (at 1976) showing the distribution of combined low and medium-grade ore (56–60 per cent Fe), high-grade ore (60–66 per cent Fe) and Banded Magnetite Carbonate (37–50 per cent Fe). The 200 m square grid is drawn from mine co-ordinates.

BMC contains fine-grained (10 μm) siderite and magnetite in equal volumes, and on average contains 45–50 per cent Fe by weight. Magnetite occurs as subhedra or anhedra oxidised in part to martite, and concentrated with siderite either in fine laminations or layers up to 20 mm thick. Magnetite appears to be intergrown with siderite and unambiguous textural evidence for primary magnetite was not observed. Siderite occurs without magnetite in silica layers, and is altered in part to goethite where exposed by mining operations. Accessory pyrite, chalcopyrite and marcasite (8–80 μm) occur within siderite grains, attached to iron oxide grains or sometimes as inclusions in magnetite.

The appearance of BMC at depth appears to be related to the presence of a fault which duplicates the orebody in Lion and North Saddle blocks (Fig. 49a). Displacement along this movement horizon is estimated to be at least 90 m, and suggests that before deformation, the ore-BMC oxidation surface must have been at least 220 m below surface. A broad, linear zone of hydrated ores marks the trace of the fault (Fig. 50), and both upper and lower surfaces of the BMC fault block are oxidised to low- or medium-grade hematite ores (Fig. 49a).

The discovery of sideritic iron-formation at depth, both here and at Rashale (Fig. 46) has important implications for the origin of all hematite deposits that occur in the Fig Tree and Moodies Groups. A model in which sedimentary sequences are replaced by iron-rich carbonate-bearing solutions is discussed below.

2. Ores in Saddle block are characterised by their high manganese contents. While the average manganese value of the entire orebody is less than 1 per cent, ores in Saddle block contain as much as 8 per cent, with isolated values of 20 per cent Mn. High manganese contents are accompanied by a corresponding impoverishment in iron. Manganese tends to be concentrated in goethitic red ores as psilomelane, and appears to result from weathering of manganiferous carbonates.

Available chemical data are plotted in Fig. 51, and suggest that on average, Mn-values in parts of the Saddle block orebody are at least 3 per cent higher than those in adjacent ground to the north. Ore with more typical values of ±0,56 per cent Mn occurs in the southern ore reserve blocks Castle and Stag. Together, the data show that pronounced manganese enrichment occurs near the centre of the orebody (South Saddle block). A linear best-fit to the data in Fig. 51 suggests that about 250 m of strike separate each one percentage point increase in managanese.

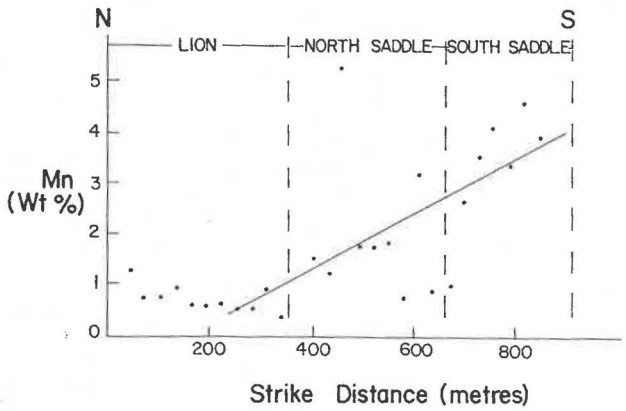

Figure 51
Manganese values in ore from Lion and Saddle blocks. Data points are plotted at 30 m strike intervals and based on weighted values of 198 individual assays from 2 285 m drill core. Solid line assumes a linear fit to the data.

3. The structure of the orebody is characterised by extensive block faulting. Steeply inclined (65–90°) transverse, normal faults with small displacements (few metres to a maximum of 30 m) occur in all ore reserve blocks. Intense faulting and fracturing is developed particularly in the northern area (North Saddle, Lion and Lion North), where fault spacing is often less than 20 m (Fig. 50). Dolerite dykes 2–15 m wide are intruded along several transverse faults of this type, especially in Lion block. A hydraulic fracturing mechanism may account for this deformation, and is discussed elsewhere.

Ore reserves and tonnage estimates

An enormous amount of prospect work was carried out by SIODC during the life of Ngwenya mine. Up to and including 1972, this work involved 13 355 m diamond drilling, 13 287 m percussion drilling and 880 m of adit development (Attridge and others, 1972).

Subsequently, a program of 70 m deep vertical percussion holes were drilled on a 30 m grid spacing in order to re-evaluate the orebody in Saddle and Lion blocks (Brech, 1974). This later program involved sampling at least an additional 5 500 m of orebody. Together, these data form the basis of ore reserve calculations, tonnage estimates and assays given in Tables 33–36.

Assays computed from borehole intersections of BHQ are given in Table 33; these assays are used to estimate the available tonnage of BHQ given in Table 34. Estimates of *in situ* ore (56–66 per cent Fe) below economic pit levels are given in Table 35. Available reserves of *potential mineable ore,* consisting principally of low-grade BHQ, both *in situ* and on dumps, are given in Table 36.

In situ tonnages are estimated by planimetering areas of ore, calculating volume and computing tonnage using weighted specific gravities for different ore grades. From tonnage estimates of this type, open-pits are designed and more accurate estimates of costs and what constitutes "ore" can be obtained. Economic pit bottoms are calculated as the point where total profit is absorbed by the cost of waste removal. Calculations of this type involve mining (ore and waste) and treatment costs, details of which are given in Attridge and others, 1972.

Metallurgical beneficiation

Since 1966, several investigations have been conducted into the economics of up-grading BHQ (*see* Attridge and others, 1972 and Clarke and de Vletter, 1975 for reviews). None of these investigations has shown that beneficiating low-grade hematite ores can be considered economic using existing techniques and at present-day costs.

Most methods of concentration examined were rejected because of low iron recoveries and concentration grades. Ngwenya hematite contains small inclusions and intergrowths of silica (<50 μm) and as a consequence gravity separation is not practicable. Crushing to minus 10 mesh is required before appreciable upgrading is achieved, and minus 300 mesh before silica is liberated.

Similarly, magnetic separation of roasted ore does not yield acceptable grades and recovery is uneconomic. Only by using modern flotation techniques (selective flocculation followed by cationic reverse flotation) can acceptable grades of concentrate for pellet-forming purposes be obtained with a realistic recovery of ±85 per cent iron.

Thus although it is technically feasible to upgrade fine-grained hematite ores, processes of this type are costly. For this reason, together with high mining costs at Ngwenya, it appears that Swaziland pellets cannot compete on present markets. New beneficiation techniques, a change in the world market for iron ore pellets, or the future development of a domestic iron and steel industry may change this position.

TABLE 33
Assays of low-grade iron-formation from borehole intersections, Ngwenya area

				NGWENYA					
%	1 North Extension	2 North Jaspilite	3 South Jaspilite	4 Lion North	5 Lion	6 North Saddle	7 South Saddle	8 Stag	Mean (4–8)
Fe	29,90	28,50	26,47	47,75	42,60	38,07	38,78	44,31	42,30
Mn	0,74	0,29	n.a.	1,03	1,40	2,73	1,93	0,86	1,59
SiO_2	34,80	48,41	n.a.	n.a.	29,81	30,07	34,92	27,63	30,61
Al_2O_3	2,55	2,24	n.a.	2,30	1,97	2,02	2,01	1,53	1,97

n.a. = not available.

Notes: weighted means calculated from assays of the following metreage — 1. 116,9 m; 2. 64 m; 3. 75,3 m; 4. 108 m (Fe), 50,4 m (Mn & Al), BHQ with ore; 5. 109,9 m (Fe), 64,3 m (Mn, Si, Al); 6. 272,2 m (Fe), 169 m (Mn, Si & Al); 7. 488,3 m (Fe), 240,3 m (Mn, Si & Al); 8. 816,1 m (Fe), 751,5 m (Mn, Si & Al), BHQ with ore.

TABLE: 34
Tonnage estimates of Banded Hematite Quartzite (BHQ), Ngwenya hematite deposit

	1 Lion North	2 Lion	3 Saddle	4 Lion + Saddle	5 Castle	6 Stag	7 BMC	8 Slimes	Total
Tonnage (10^6 tons)	5,8	7,1	23,0	15,9	17,0	39,9	3,1	4,0	115,8
Grade (% Fe)	45,3	45,3	43,3	n.d.	43,7	40,6	45,1	50,3	42,89

Notes: 1, 4, 6 and 7 represent *in situ* tonnages; 2. 1,6 m tons *in situ*, 5,5 m tons on dumps; 3. 12,2 m tons *in situ*, 10,8 m tons on dumps; 4. 2,9 m tons above level 15 (Saddle) and level 19 (Lion) and 13,0 m tons below these levels, outside existing pits; 5. 5,3 m tons *in situ* 11,7 m tons on dumps; 7. 0,34 m tons in Lion and Saddle pits and 2,7 m tons outside existing pits to level 25 (Saddle) and 18 (Lion).

TABLE 35
Tonnage estimates of potential ore (56–66 % Fe), Ngwenya hematite deposit

	1 Lion North	2 Lion	3 N & S Saddle	4 Castle	5 Stag	6 On Dumps	Total
Tonnage (10^6 tons)	0,5	1,6	12,2	5,3	3,7	0,1	23,4

Notes: 1. *In situ* to 19 level, 62,5 % Fe; 2. 17–23 levels; 3. 20–35 levels; 4. 25–36 levels; 5. includes 2,8 m tons 60,69 % Fe to 16 level and 0,9 m tons 16–23 levels; 6. near loading station, 63,8 % Fe, fine ore.

TABLE 36
Available potential ore reserves, Ngwenya hematite deposit

	In situ			On dumps					
	Lion North	Stag	Sub-total	Lion	Saddle	Castle	Other[1]	Sub-total	Grand total
Tonnage (10^6 tons)	2,8	23,7	26,5	5,5	10,8	11,7	4,1	32,1	58,6
Grade (% Fe)	46,2	41,0	41,5	45,3	43,3	43,2	50,6	44,5	43,2

[1]Includes 4 023 839 tons 50,3 % Fe in slimes dams, and 97 472 tons fine ore (63,8 % Fe) in high-grade dumps near main loading station.

Summary

1. 28,37 .10^6 tons of high-grade hematite ore (>59,5 per cent Fe) was produced at Ngwenya between 1964–1979.

2. The hematite orebody occurs together with low-grade iron-formation (BHQ) in a shale sequence close to the base of the Fig Tree Group. Irregular layers, lenses and blocks of incompletely enriched shale in BHQ, and BHQ in ore are consistent with massive replacement of shale by iron and silica. Mehliss (1946) recognised that replacement processes account for some features of Fig Tree Group iron-formations, and his ideas were supported at Ngwenya by Pretorius (1961).

3. Textural evidence shows that all hematite at Ngwenya is secondary in origin, and in large part formed by the oxidation of magnetite. Iron-formation that contains no hematite occurs in only one small section of the orebody from 130 m to at least 250 m below outcrop. This lithology contains siderite and magnetite (BMC), and appears to represent the unoxidised and unleached equivalent of the orebody on surface. There is no unambiguous evidence that magnetite in BMC represents a primary oxide phase.

4. Ore with the highest manganese content (>3 per cent), and the maximum thickness of BHQ (75 m) occur close to the mid-point of the orebody. Manganese values and

BHQ thickness decrease linearly toward the northern and southern orebody extensions. These data are consistent with a model in which fluids containing silica, iron and manganese were focused at the Onverwacht — Fig Tree Group surface below the present position of Saddle block.

5. Mineable reserves of 58,6 $.10^6$ tons of low-grade iron-formation (43,2 per cent Fe) are available at Ngwenya at the time of writing. Most of this tonnage consists of BHQ in Lion North and Stag blocks, and on existing dumps. An additional 19,1 $.10^6$ tons *in situ* "ore" (56–66 per cent Fe) in Lion, Saddle and Castle blocks, and 57,3 $.10^6$ tons *in situ* BHQ (42–43 per cent Fe) in all ore reserve blocks is present below existing pit levels (for details see Tables 34–36).

RASHALE SIDERITE DEPOSIT

A sub-surface occurrence of siderite was discovered in 1955 during routine exploration of a radioactive anomaly (the Rashale prospect) within the Moodies Group south of Ngwenya (Fig. 46). The initial intersection (BH 72, Figs. 52 and 53) revealed siderite over a width of 34,6 m with a single 2,4 m thick intercalated chert conglomerate horizon. In the Annual Report for 1955, the ferruginous lithology was described as white to grey crystalline siderite with narrow lenses of chloritic material and some graphite on shear planes.

Extensive surface prospecting during the following year failed to locate a limonitic gossan (Ann. Rept., 1956). However, as Fig. 53 shows, a ferruginous conglomerate crops out along the up-dip extension of siderite, and this conglomerate is presumed to pass laterally into ferrous carbonates at depth (see also Hunter, 1962). The conglomerate contains banded chert and vein quartz pebbles replaced in part by a mixed hematite — goethite matrix.

Additional boreholes drilled in 1965 proved a 25 m thickness of siderite 60 m down-dip from BH 72 (BH 275, Fig. 53), but only 3,5 m of siderite 150 m along the strike to the south (BH 274, Fig. 52). According to Clarke (1971), these cores showed the siderite to have formed by replacement of chloritic shales and conglomerates.

Because the sideritic formation is located close to the contact with the Onverwacht Group, and because similar ferrous carbonates often occur in talcose schists in the Forbes Reef area, Urie (Ann. Rept., 1956) believed the siderite to be genetically related to the Onverwacht Group. It is noted here that the sequence structurally above ferruginous conglomerates on surface is highly altered to sericite, and that metallic sulphides were recorded in all the initial borehole intersections (BH 72–74, Fig. 52; Ann. Rept., 1965). Much of the Rashale sequence has been subjected to extreme mineralogical alteration.

It is argued below that the siderite formation occupies a horizon in the Moodies Group along which iron-rich fluids drained to the surface. The Rashale occurrence may be analogous to carbonate iron-formation (BMC) found at depth at Ngwenya.

Grade and tonnage estimates

An accurate estimate of reserves from only three borehole intersections is not possible. Assuming that the strike extension corresponds approximately with surface exposures of ferruginous conglomerate in Fig. 52, and assuming an average thickness of 15 m, with extension at depth to 100 m (Fig. 53) an *in situ* tonnage of 10^6–1,5 $.10^6$ tons is indicated at Rashale. Assays of cores from all three boreholes suggest an average grade of 37 per cent Fe for the deposit (Clarke, 1971).

NGWENYA NORTH EXTENSION AND JASPILITE

The Ngwenya North Extension and Jaspilite deposits are distinct but closely related orebodies. North Extension is a low-grade iron-formation of the Ngwenya (BHQ)-type. Like Ngwenya, it occurs at the base of the Fig Tree Group and rests on a sequence of schists that include thick talcose units. The Jaspilite body crops out in the ground between North Extension and Ngwenya Mine, 200–300 m above the surface between the Fig Tree and Onverwacht Groups.

Geophysical data

A 2,5 km-long magnetic anomaly with an 1 800 gamma fluctuation was measured over the North Extension and northern part of the Jaspilite horizon during the 1966 UNDP airborne geophysical survey (Fig. 3). Subsequent work with handheld magnetometers resolved this anom-

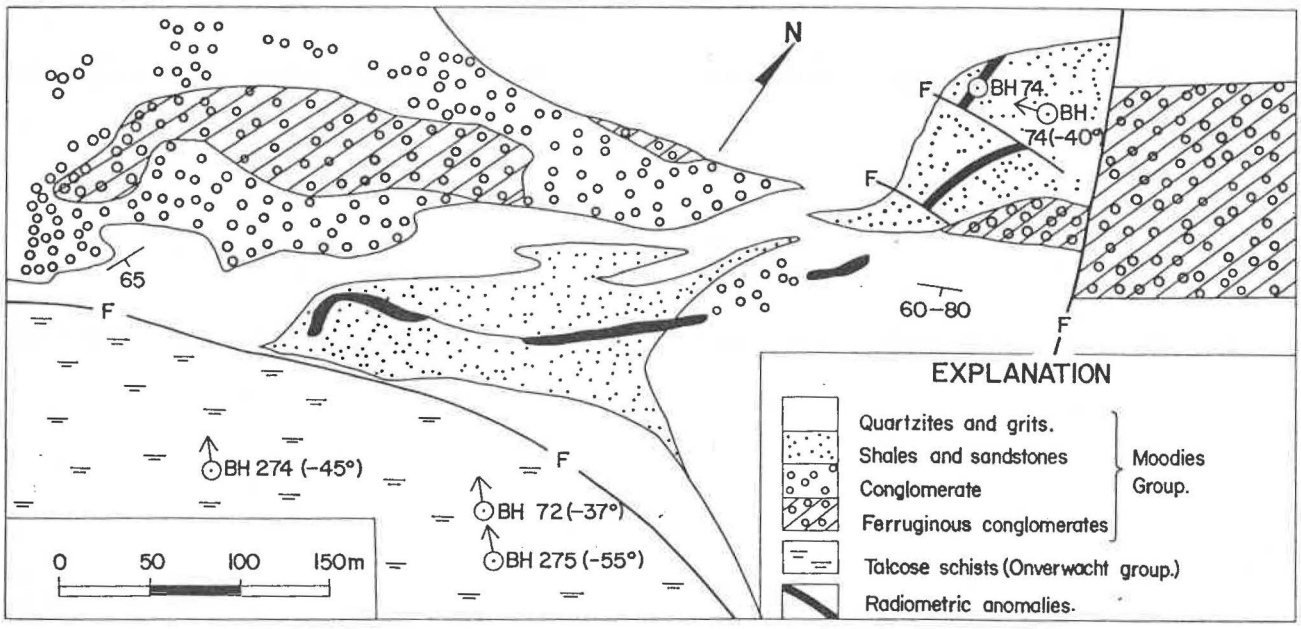

Figure 52
Geological plan of the Rashale iron and uranium prospect (after Michie, 1979). Ferruginous conglomerates on surface pass laterally into massive siderite ±150 m below outcrop (see Fig. 53). Locations of borehole collars taken from Davies (1956).

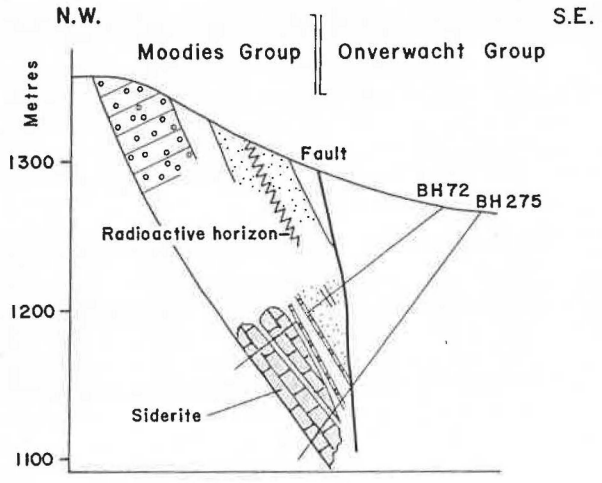

Figure 53
Cross-section of the Rashale iron and uranium prospect (drawn from data given in Davies, 1956). Hematitic conglomerates and quartzites are the surface expression of ferrous carbonates below the zone of sub-tropical weathering. The radioactive horizon was not recorded in either BH 72 or 275 and may be faulted out at the level of intersection (see Fig. 52).

aly into two major zones of high magnetic intensity. The eastern (Jaspilite) anomaly is very narrow, but exhibits extreme peak amplitudes of as much as 100 000 gamma. The original interpreters suggested that the data are consistent with intensity produced by a 30 m-wide unit containing 50–55 per cent magnetite (UNDP, 1970). The western (North Extension) anomaly is 100–200 m wide, but was not documented in detail.

Geological description

Ngwenya North Extension has a strike length of 1 500 m in Swaziland (Fig. 46); the northern 1 000 m crops out along steep slopes and access to the area is extremely difficult. This section of the deposit is not considered to be a mining proposition, and only the southernmost 500 m is included in tonnage estimates given below.

The unit of iron-formation at North Extension has an average structural thickness of 100 m, and is inclined east at 55°–60°. Decrease in outcrop width toward the south appears to be the result of stratigraphic thinning, though the thickness of the unit in the centre of the outcrop has been reduced by faulting.

A hangingwall sequence that includes a large proportion of coarse clastic material overlies the iron-formation and at the same time forms the footwall of the Jaspilite horizon (Fig 54). The contact between iron-formation and hangingwall sequence is gradational and resembles a replacement surface. Sandstone and tuff interbeds cemented with hematite occur within the hangingwall shale sequence. Thin silicified shales are present in the footwall, except where the iron-formation is faulted against talcose schists of the Onverwacht Group.

Both hematite and magnetite iron-formation occur together in the North Extension deposit (Brech, 1972). The former consists of 5–10 mm layers of fine-grained iron oxides and white silica (BHQ), with layers and inclusions of laminated grey shale. Magnetite iron-formation is more regularly banded, contains no shale partings and contains intercalated jaspilites. Iron mineralogy of both types is principally a 5–250 μm hematite — magnetite intergrowth, together with minor chlorite, carbonate and sulphides. Hematite always pseudomorphs magnetite, and is paragenetically the later oxide phase.

The Ngwenya Jaspilite crops out for 7,5 km (Fig. 46), of which the northernmost 2,5 km (Northern Jaspilite) and a section 1,1 km in strike length immediately north of Ngwenya Mine (Southern Jaspilite) have been examined in detail. The remainder of the unit is either inaccessible like the 2,4 km long section between points A and B in Fig. 46, or as in the southernmost 1,5 km, of only marginal economic interest.

On average, the Jaspilite horizon is 70 m-thick (maximum 120 m) and inclined east at 65°. To the north, the unit thins and is displaced westward and faulted against the Northern Extension iron-formation. To the south, the Jaspilite becomes progressively shaley and eventually pinches out within the thick shale sequence in the hangingwall of the Ngwenya deposit. The basal contact with thin (10 m) silicified shales is sharp, while the hangingwall surface is transitional with laminated shales over a 10 m-width.

According to Brech (1972), three types of jaspilite can be recognised, the proportions of which vary from north to south. Much of the Northern Jaspilite consists of hard jaspilite (79 per cent by weight), together with a basal ±8 m rubbly jaspilite (7 per cent) and intercalated shaley jaspilite (12 per cent). The Southern Jaspilite consists almost of shaley jaspilite (30 per cent by weight) and ferruginous shales (64 per cent) with only minor rubbly jaspilite (6 per cent).

Ngwenya jaspilites are characterised by very irregular layering (both in thickness and continuity) that resembles the texture frequently associated with nodular cherts. Lenses and bands of jasper within magnetite layers, and shale within jasper layers are typical. Magnetite in surface exposures is pseudomorphed and intergrown with fine-grained hematite (4–90 μm). Modal hematite decreases with depth and gives way to unoxidised 10–25 μm magnetite grains. Jasper layers consist of 5–300 μm quartz grains and 3 per cent iron oxides by volume (magnetite and hematite). Chlorite, carbonate and sulphides occur in veinlets, and local segregations.

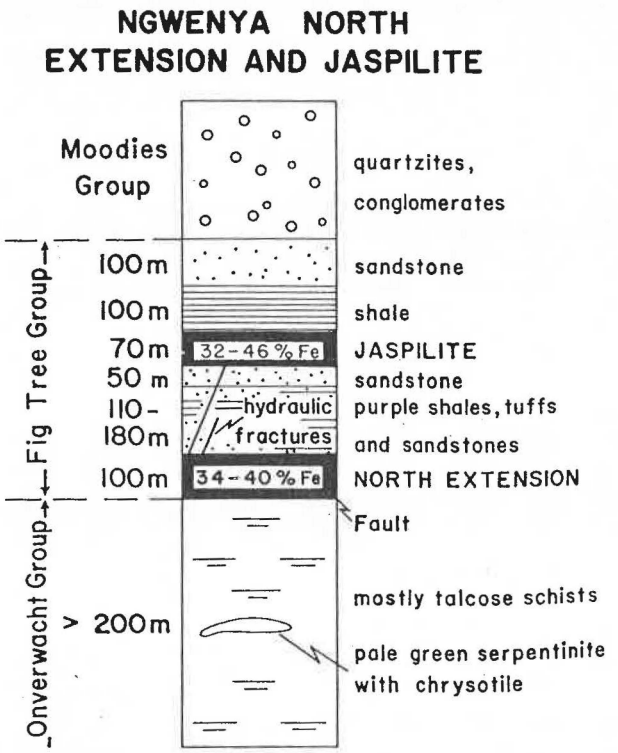

Figure 54
Lithological sequence in the vicinity of the Ngwenya North Extension and Jaspilite deposits.

Grade and tonnage estimates

Both Northern Extension and the Ngwenya Jaspilite contain ±20 per cent more iron in surface exposures than at depth. In the estimates of Table 37, surface grades are accepted to 20 m down-dip, and this tonnage is regarded as proven. Remaining dip extensions (to 100 m) are based on assays of borehole cores (Table 33), and this tonnage assumed to be unproven.

Samples from five trenches totalling 567 m in length dug in Northern Extension give an overall grade of 40,2 per cent Fe, with no significant variation along strike (Brech, 1972). *In situ* reserves to 100 m down-dip are estimated from surface data and a single borehole intersection to be 17,5 $.10^6$ tons low-grade iron-formation (Table 37).

For the purpose of tonnage estimates, Brech (1972) divided the Northern Jaspilite into a northern, central and southern block with strike lengths of 900 m, 500 m and 1 100 m respectively. The average surface grade of each block is 38,1 per cent, 36,0 per cent and 33,3 per cent Fe respectively, and a weighted average grade of the entire Northern Jaspilite (based on assays of jaspilite exposed in 20 surface trenches) is 35,6 per cent Fe. Basal rubbly jaspilite contains 45,7 per cent Fe. A single (SIODC) borehole intersection in the central block returned 28,5 per cent Fe over 63,1 m (Table 33), and GSD borehole BH 326 (reported in Clarke, 1971) 700 m farther south gave 27,7 per cent Fe over 80,7 m.

The equivalent surface grade of the Southern Jaspilite is 29,1 per cent Fe, and is based on samples from three trenches dug along a strike length of 800 m immediately north of Ngwenya Mine. Although in the final summary of iron reserves given below all material containing less than 30 per cent Fe is ignored, the Southern Jaspilite is included here to illustrate the change in grade along strike. It is estimated that grade decreases toward the south by ±2 per cent Fe km^{-1} for the first 2,5 km of Jaspilite outcrop and 1,2 per cent Fe km^{-1} thereafter.

Because there is at least 120 m difference in relief on Jaspilite outcrop, estimates in Table 37 are calculated between surface and 1 540 m height above sea-level (Northern Jaspilite) or between surface and 1 480 m height above sea-level (Southern Jaspilite) in order to give an average down-dip extension of 100 m. *In situ* tonnages (rather than mineable ore) of 73,4 $.10^6$ and 10,4 $.10^6$ tons respectively are indicated for the Northern and Southern Jaspilite deposits.

MAKONJWA AND IRON HILL DEPOSITS

Some of the most laterally extensive horizons of hematite iron-formation crop out in the remote southern Makonjwa and northern Silotwane hills (Fig. 55). Strike continuity of these sequences, both with Ngwenya North Extension (Pretorius, 1961) and Iron Hill (Mehliss, 1946) means that the same iron-rich units within the Fig Tree and Moodies Groups can be traced on surface for at least 30 km in Swaziland and adjacent parts of South Africa. Makonjwa is one of the least accessible portions of this massive iron deposit, and the description given here is based on observations taken along the Komati River valley, and below Diepgezet mountain.

Geological description

The Makonjwa iron-formation is repeated in outcrop by a large-scale synclinal fold (Fig. 55). North of the Komati River, both fold limbs are vertical or sub-vertical and stratal shortening is accommodated by slip along a décollement surface at the base of the Fig Tree Group. Talcose schists of the Onverwacht Group are present below the décollement.

Wrench faults oriented close to the inferred transport direction (toward 300°) displace the trace of the synclinal axis near Intaba beacon (Fig. 55). In this area, the entire northern section of the syncline is refolded in a complex zone of transverse tectonics. Both limbs of the second fold end in décollement and suggest that refolding may

TABLE 37
In situ tonnage estimates (10^6 tons) of Ngwenya North Extension and Jaspilite deposits[1]

	North Extension	Northern Jaspilite				Southern Jaspilite	Grand Total
		northern block	central block	southern block	sub-total		
proved	3,50	4,26	2,37	5,08	11,71	4,77	[illegible]
unproved	14,00	15,90	8,70	37,12	61,72	5,67	[illegible]
grade (% Fe)	34,1	38,2	32,0	33,2	34,39	28,5	[illegible]

[1]Recalculated from Brech (1972).

Notes: Specific gravity (SG) of North Extension taken as 3,5; Jaspilite tonnages based on SG = 3,32 (hard jaspilite), 3,94 (rubbley jaspilite), 3,09 (shaley jaspilite), 3,03 (ferruginous shales).

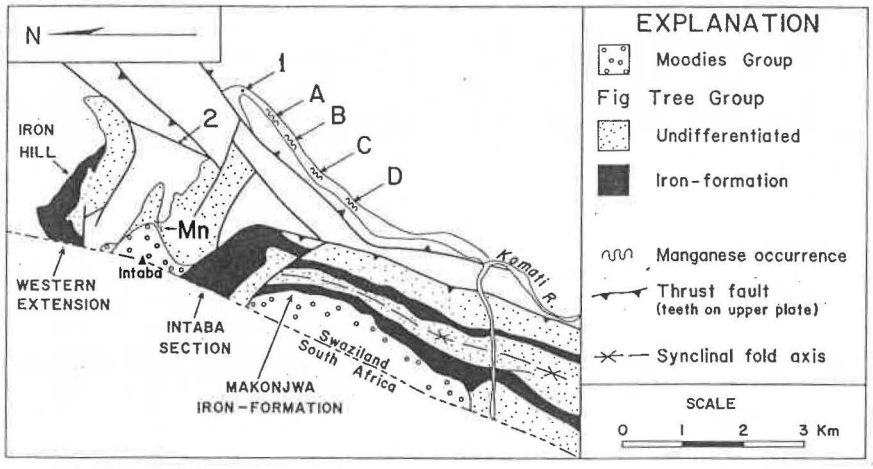

Figure 55
Location and geology of the Makonjwa and Iron Hill deposits (from 1:25 000 geological map series with additions). A–D are manganese-cobalt occurrences (the Cobalt Prospect) and 1–2 are the Intaba nickel prospects described elsewhere.

also result from displacements along a movement horizon.

Iron-formation in the nose of the first fold crops out in the Intaba section and Western Extension of Iron Hill (Fig. 55). There, relatively shallow regional dips (<45°) result in a correspondingly wider outcrop than on the fold limbs. Intense small-scale folding deformation is conspicuous in this axial region of the fold. Mehliss (1946) believed Iron Hill to be an anticlinal structure, but the absence of a mapable fold closure, and the difficulty of establishing structural facing directions in iron-formation units alone do not support his interpretation.

Field observations (Fig. 56) and geophysical data (Fig. 3) show that high-grade iron-formation is best developed in the western limb of the Makonjwa syncline. Within this unit, a 2 km long aeromagnetic anomaly with a fluctuation of at least 1 000 gamma is located 0,75 km south of the Komati River (Fig. 55). The significance of this anomaly is not known.

Iron-formation in the western fold limb consists of 30–40 m of closely laminated (<2 mm) blue hematite. Contorted horizons 10–20 mm-wide, and centimetre-scale structures that disrupt the lamination are typical of this zone. Thick (45 m) jaspilites exhibiting nodular and replacement textures, and ubiquitous medium-scale folds overlie the more massive unit of iron-formation.

In contrast, iron-formation in the eastern fold limb consists of ferruginous conglomerates and thin shaley jaspilites (Fig. 56). A thick (0,5 km) silicified sequence that includes basal lapilli tuffs, followed by banded cherts, shales and eventually coarse clastic material underlies the iron-bearing unit. Clast size increases stratigraphically upwards to an average of ±20 mm in the ferruginous horizon. Individual clasts are cut by vein hematite which suggests that at least some of the iron was introduced or remobilised by fluids.

Thick conglomerates that contain angular clasts as much as 1 m in size form the immediate hangingwall of the iron-formation (Fig. 56). Clasts are composed principally of banded chert with some jasper, and the unit resembles a reworked silicified sequence. Shales replaced in part with iron oxides rest above the conglomerates in the axial region of the syncline.

Iron-formation in the Intaba Section and Western Extension consists in large part of Banded Hematite Jaspilite that contains a 2–5 mm-wide layering. Ores are typically limonitic and incompletely exposed.

Iron Hill is an extensive deposit of Banded Hematite Quartzite of the Ngwenya-type. Reddish shale layers 3–10 mm-wide contain varying amounts of hematite and limonite and alternate with layers of silica. Magnetite is rare (but more common in lower-grade material) and is always pseudomorphed, at least in part, by hematite.

Ore mineralogy of the Iron Hill sequence is dominated by 5–30 μm grains of hematite and martite with 1–3 μm quartz and magnetite inclusions. Larger (10–25 μm) quartz grains comprise less than 10 per cent of individual ore layers. Low-grade Banded Hematite Jaspilite on Iron Hill and in the Intaba Section contains oxidised, euhedral 70 μm-size magnetite grains.

An 18 m-wide dyke trends parallel with the axis of Iron Hill ridge and bisects the outcrop of enriched iron-formation (Fig. 57). Mehliss (1946) notes that this intrusion has alternating dyke and sill phases, and is itself veined by specularite. The influence of this dyke on the circulation of meteoric waters is demonstrated by the occurrence of a 150 m-long 2–3 m wide ore band (>62 per cent Fe) at the northeastern edge of the dyke. Mehliss (1946) suggests that this massive red hematite was deposited directly from solutions in cavities left by the partial leaching of silica.

Finally, a number of manganese occurrences were reported by Mehliss and are noted here. The manganiferous lithology that crops out to the north of Iron Hill (27,6 per cent Mn, Fig. 57) has an erratic distribution and passes laterally into iron-formation by gradual increase in iron content. A discontinuous zone of manganiferous ores occurs close to the southern margin of Western Extension (Fig. 57). The largest body is 60 m-long in outcrop (36,9 per cent Mn, Fig. 57) and consists of banded manganiferous cherts enriched with manganite and psilomelane. Botryoidal manganite and psilomelane also occur 600 m southeast of Intaba beacon (Fig. 55), and Mehliss suggests that 7 .10^3 tons of visible ore (*c.*44 per cent Mn) is exposed in outcrop.

Grade and tonnage estimates

Several compositional grades of iron-formation on Iron Hill were recognised by Mehliss (1946) as a result of surface investigations that included the excavation of trenches totalling 1 326 m, and the results of 63 partial assays. A simplified version of his assay plan appears as part of Fig. 57; contacts drawn between iron-formation and ferruginous chert, and the assay-walls drawn between ore-types in Fig. 57 are gradational.

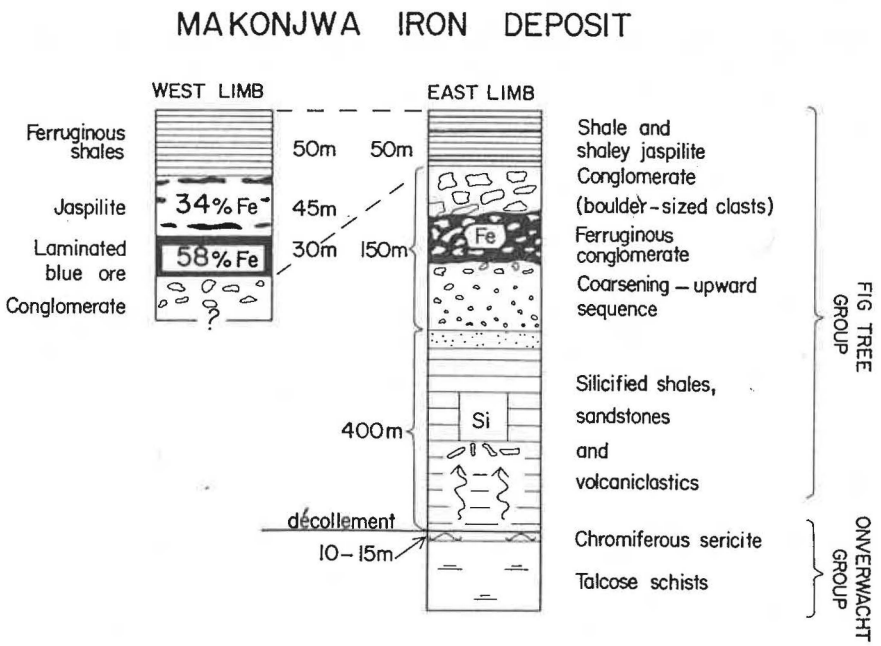

Figure 56
Lithological sequence in the Makonjwa syncline, based on measured sections along the Komati River and below Diepgezet mountain.

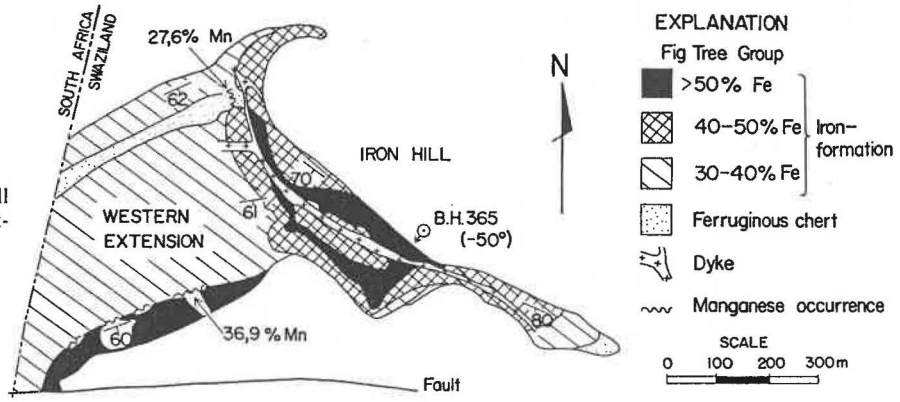

Figure 57
Distribution of surface grades on Iron Hill (modified from Mehliss, 1946), and Western Extension.

A single borehole (BH 365, Fig. 57) drilled by the Geological Survey Department in 1970–1971 proved iron-formation 168 m downhole and included a 27,5 m-wide dyke intersection. The resulting cores were sent to Prague for beneficiation tests (UNDP, 1970), and a single analysis containing 29 per cent Fe was subsequently reported. It is not known which section of core was assayed and the value is not considered representative of the Iron Hill grade at depth. Mehliss's surface ore grades are given in Table 38.

Just over half the total area of 10,5 hectares iron-formation exposed on Iron Hill contains 40–50 per cent Fe; an additional third of this area consists of higher grade (+50 per cent Fe) material. Reserves of low-grade (<40 per cent Fe) iron-formation were not estimated by Mehliss, but represent a significant *in situ* tonnage (Table 39). Western Extension (Fig. 57) is an area of 15,8 hectares that consists almost entirely of low-grade BHQ (35 per cent Fe).

Surface iron enrichment is a conspicuous feature of Iron Hill geology. Silica layers have been leached and often totally removed leaving a "biscuit-ore" to a depth of at least 7 m. For the purposes of tonnage estimates (Table 39), surface grades are accepted to 20 m and this tonnage is taken as proven; a 20 per cent decrease in iron content is assumed below this depth, and the estimated tonnage between 20–100 m regarded as unproven.

Thus the tonnage of 40–50 per cent Fe material given in Table 39 consist first of 40–50 per cent grade iron-formation proved near surface (Fig. 57), and second, unproven iron-formation 20–100 m below +50 per cent Fe outcrop. In this way it can be calculated that 32,7 .10^6 tons of 42,5 per cent Fe iron-formation are present to a depth of 100 m on Iron Hill.

Similar calculations give 10,4, 33,1, and 13,8 million tons of low-grade iron-formation for the Western Extension, Intaba Section and North Makonjwa bodies respectively. Only the northernmost 1 km of strike, where as-

TABLE 38
Surface compositions of Makonjwa and Iron Hill deposits

	IRON HILL				WESTERN EXTENSION	INTABA SECTION	NORTH MAKONJWA	
	1	2	3	4	5	6	7	8
Fe	54,93	48,66	34,87	48,66	35,48	39,13	57,84	34,43
SiO_2	12,54	22,28	43,05	22,28	40,20	40,60	5,60	47,80
TiO_2	0,15	0,14	0,15	0,14	n.d.	<0,05	0,44	0,13
Al_2O_3	3,71	4,11	5,40	4,11	5,49	0,20	4,77	0,40
MnO	0,40	0,46	0,93	0,46	n.d.	0,18	0,12	0,49
MgO	0,04	0,10	0,11	0,10	n.d.	0,10	0,43	<0,10
CaO	0,10	0,19	0,14	0,19	n.d.	<0,05	<0,05	<0,05

n.d. = not determined.

Notes: 1. weighted average of Mehliss (1946) grades I and II (17 assays); 2. average Mehliss grade III (24 assays); 3. average Mehliss grade IV (10 assays); 4. average composition of Iron Hill (Mehliss, 1946); 5. weighted average of 5 BHQ assays (after Mehliss); 6. Banded Hematite Jaspilite (1 assay); 7. average laminated ore (3 assays); 8. upper jaspilite horizon (1 assay).

TABLE 39
Tonnage estimates *(in situ)* of the Makonjwa and Iron Hill deposits

	IRON HILL				WESTERN EXTENSION	INTABA SECTION	MAKONJWA NORTH	MAKONJWA SOUTH
	1	2	3	4	5	6	7	8
proved (10^6 tons)	2,23	4,41	1,39	8,03	10,43	33,10	5,37	—
unproved (10^6 tons)	—	8,24	15,39	23,63	—	—	8,40	92,95
average grade (% Fe)	>50	40–50	30–40	42,54	35,48	39,13	36,78	36,78

Notes: 1. proved ore 2,75 ha, SG = 4,05; 2. proved ore 5,57 ha, SG = 3,96, unproved ore 2,75 ha, SG = 3,74; 3. proved ore 2,12 ha, SG = 3,28, unproved ore 5,57 ha, SG = 3,45; 4. total reserves at Iron Hill (excludes 5,16 .10^6 tons 27,9 % Fe); 5. 15,8 ha, SG = 3,31, excludes 38,6 .10^6 tons unproved 28,4 % Fe; 6. 50,0 ha, SG = 3,31, excludes 132,4 .10^6 tons unproved 31,3 % Fe; 7. proved ore includes 30 m-width enriched BHQ (SG = 3,96) and 45 m-width jaspilite (SG = 3,32), unproved ore is BHQ (SG = 3,5), both along strike length of 1 km; 8. possible tonnage over 6,75 km strike length calculated from (7).

says from a number of surface samples are available is included in estimates for North Makonjwa (see Table 39). A speculative *in situ* tonnage of 93 $.10^6$ tons low-grade material is estimated for the remainder of the unit to 100 m below outcrop.

NOTTINGHAM PEAK

A massive occurrence of low-grade iron-formation straddles the Nkomozane gorge, 3 km from the eastern edge of the greenstone belt (Fig. 39). Nottingham Peak, from which the deposit takes its name, is the summit of a prominent hill north of the Nkomozane River.

The Nottingham Peak deposit consists of three separate units of iron-formation (1–3, Fig. 58), each 70–100 m thick and which together exceed 6 km along strike. In addition, thick ferruginous cherts with narrow bands of iron-formation occur in adjacent ground to the east. This ferruginous chert sequence occupies a similar stratigraphic position to the Nottingham Peak deposit but does not contain sufficient iron to be of economic interest.

Geophysical data

A magnetic anomaly with a total fluctuation of 8 000 gamma was recorded along four flight lines that crossed the Nottingham Peak deposit during the 1966 aeromagnetic survey (UNDP, 1970; Fig. 3). Large fluctuations (4 500–9 000 gamma) were also measured over the nearby Mhlatane iron-formation, and these two deposits exhibit the highest values of magnetic intensity recorded anywhere in Swaziland.

Magnetic data measured during a follow-up ground survey are given by Evans (1967), and shown in Fig. 58. From this work, a rather broad magnetic zone of at least 4 000 gamma fluctuation was defined in the topographically high area centred on Nottingham Peak. The anomaly is closely associated with the eastern and central units of iron-formation (Fig. 58). Evans observed that the same anomaly farther south is narrower (90 m), has a much higher intensity (20–30 000 gamma above background), and closely parallels the regional structural trend (030°). This well defined southern anomaly extends for 900 m both north and south of the Nkomozane River, and locally increases in size to 100 000 gamma on headlands overlooking the reservoir. Large fluctuations of this type were considered by Evans to result from distortion of the local magnetic field by topographic irregularities. The western unit of iron-formation was not included in the ground magnetic survey.

In addition, a reversed magnetic anomaly of 10 000 gamma amplitude (locally 20 000 gamma) was recorded during a waterborne survey of the Nkomozane reservoir (Evans, 1967). A 180 m-long anomaly is located south of the point where the Entabene River joins the reservoir and indicates the approximate position where a steeply inclined magnetic body crosses the gorge. According to Evans, the field reversal is almost certainly caused by the

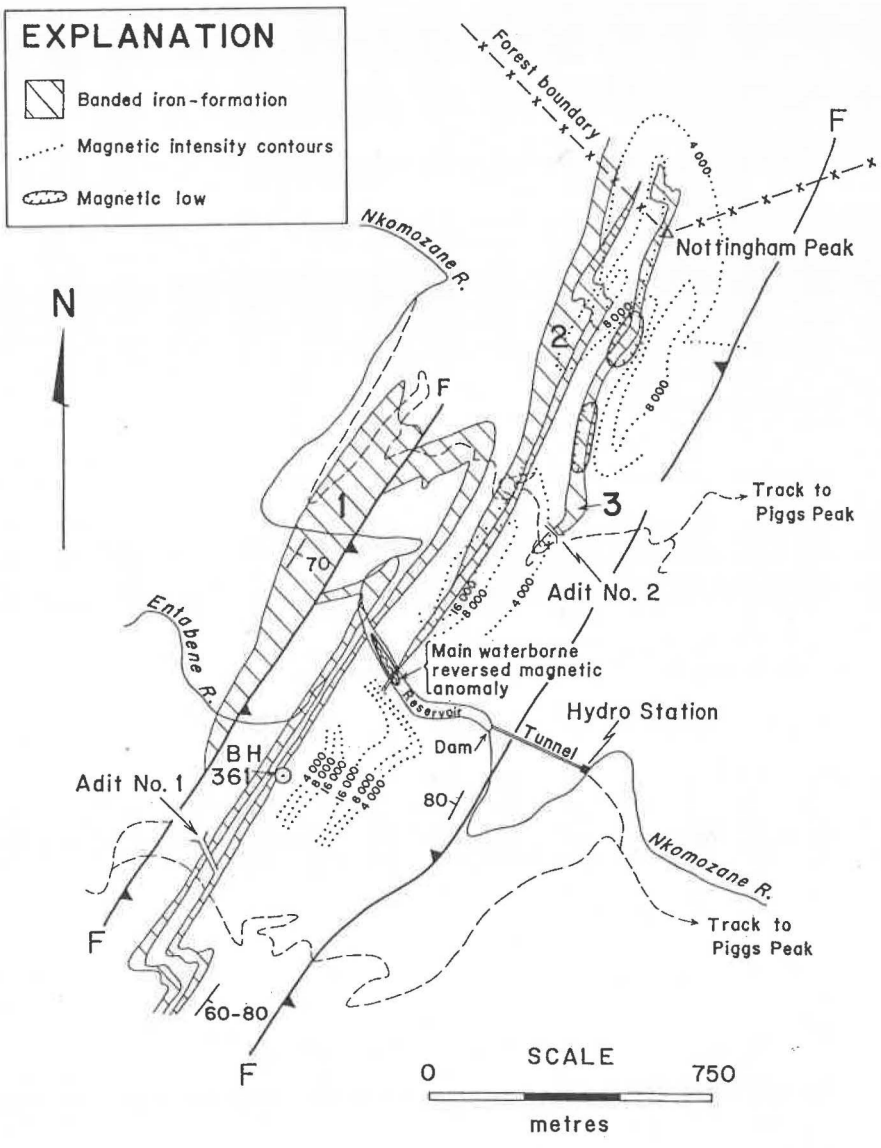

Figure 58
Plan of the Nottingham Peak iron deposit showing the outcrop of the western, central and eastern units of iron-formation (1–3) described in the text (after Hunter and Jones, 1969), ground magnetic intensity contours (after Evans, 1967) and the locations of exploration adits (after Brech and Lumb, 1974).

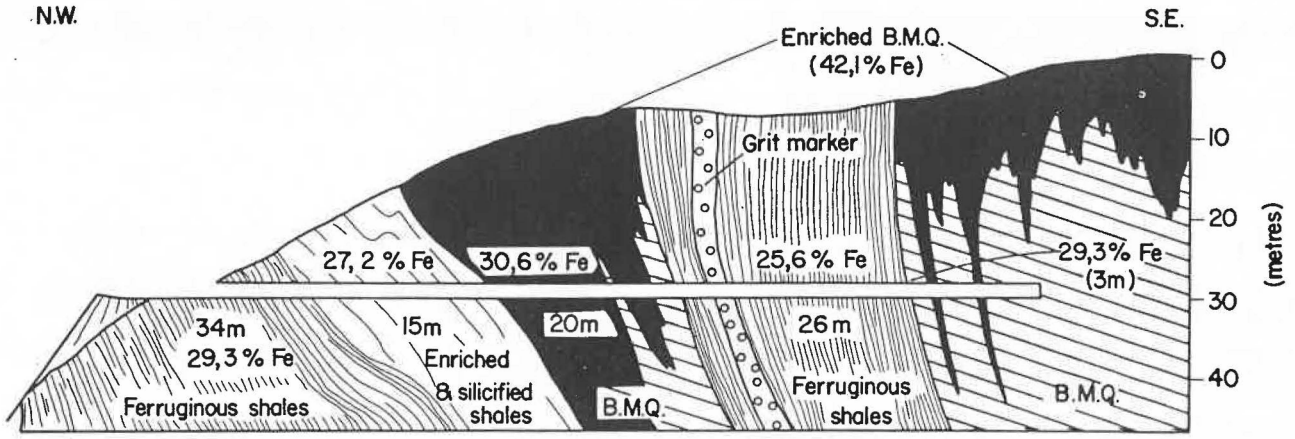

Figure 59

Cross-section through No. 1 adit Nottingham Peak (redrawn from Brech and Lumb, 1974), showing the effects of near surface supergene enrichment of Banded Magnetite Quartzite (BMQ). The structurally lowermost unit of shale is 60 m thick and rests with décollement on talcose schists of the Onverwacht Group.

effect of magnetic formations that crop out above the plane of observation.

Geological description

Structure

Intense deformation and structural repetition have disrupted the stratigraphic sequences that include the Nottingham Peak deposit. South of the Nkomozane River, the Fig Tree and Moodies Groups form part of an allochthonous or para-autochthonous sequence that includes shales, conglomerates and iron-formations. This tectonic unit was emplaced toward the northwest over thin (<1 km) mostly silicified volcanic lithologies of the Onverwacht Group. Slivers of talcose schists occur along the basal décollement surface.

North of the Nkomozane River, the same clastic sequences are deformed by a synformal fold. Lithological units close to the Peak are inclined at high angles toward the northwest, and the succession is thus repeated in outcrop. Detailed structural mapping is required to determine whether one or more than one major stratigraphic horizon of iron-formation is present within these sequences.

Small-scale fold structures are conspicuous in the Nottingham Peak iron-formation. Folds tend to occur in distinct horizons, usually well-laminated iron-rich and silica-poor horizons. Some zones of this type are chaotically deformed and typically have layers of jasper along the upper stratigraphic surface. Extensive fracturing and quartz-magnetite veining (1–50 mm-wide) is also common, and has not been observed in less deformed iron-formation elsewhere.

Lithology

When the effects of major tectonic duplication are removed, the maximum structural thickness of clastic sequences is no more than 350–450 m. The gross stratigraphy consists of basal silicified shales 60–100 m thick, overlain in turn by iron-formations and ferruginous shales (see Fig. 59), coarse sandstones and conglomerates and finally ferruginous shales and sandstones with chert and jasper layers.

All iron-formation at Nottingham Peak consists of Banded Magnetite Quartzite (BMQ). Near surface alteration to a lithology that contains mixed oxides (hematite-magnetite) is ubiquitous. Small pockets of enriched hematite formed by supergene leaching do occur, but are not extensive.

A regular 10 mm-wide banding (range 2–25 mm) separates iron oxide and silica layers in the iron-formation. Narrow interbeds (±100 mm) consisting of laminated graphitic shales that contain volcaniclastic detritus are common along the upper replacement surface of both eastern and western ore bodies, and also within the ferruginous chert sequence east of Nottingham Peak.

Thick ferruginous shales (25 m) with nodular chert textures are intercalated with BMQ in the western iron-formation (Fig. 59). Narrow horizons of conglomerate (grit marker in Fig. 59) that contain 5–20 mm clasts of white quartzite, green shales, black chert and banded ferruginous chert occur within the shale sequence. Conglomerates of this type are veined with hematite and again demonstrate that at least some iron oxide replacement occurred after the sedimentary reworking of early silicified sequences.

The lateral transition from iron-formation to shales and cherts is well displayed at the Nottingham Peak deposit. The southern termination of both the central and eastern units of iron-formation (Fig. 58) is a replacement surface where banded cherts and silicified and ferruginous shales pass into low-grade iron-formation. Thick ferruginous cherts immediately south of the reservoir exhibit an irregular, high-angle contact with the adjacent shale-sandstone sequence.

Mineralogy

Nottingham Peak iron-formation consists of quartz, magnetite and siderite, with secondary hematite and goethite. Iron oxides are fine-grained (20–200 μm) and occur as interlocking subhedral grains with hematite pseudomorphous after magnetite. Siderite is oxidised to goethite which itself occurs in both silica and mixed oxide layers; magnetite and hematite tend to be absent from silica layers. Microcrystalline ± 5 μm quartz grains (maximum size 60 μm) form most of the gangue, together with minor chlorite and sericite.

Quantitative mineralogical variations were documented by Brech and Lumb (1974) from samples collected at 10 m intervals in No. 2 adit (Fig. 60). Their data (Fig. 60) show that martitisation decreases with depth, and that prior to surface enrichment the iron-formation was a magnetite-siderite lithology. Oxidation and leaching are accompanied by an increase in grain size from 20 μm in unaltered lithologies, to 150–200 μm on outcrop.

Grade and tonnage estimates

Unleached iron-formation is accessible in two adits that were developed by SIODC during 1972. Adit No. 1 is located in the western body south of the reservoir (Fig. 58), where work consisted of 10 m portal establish-

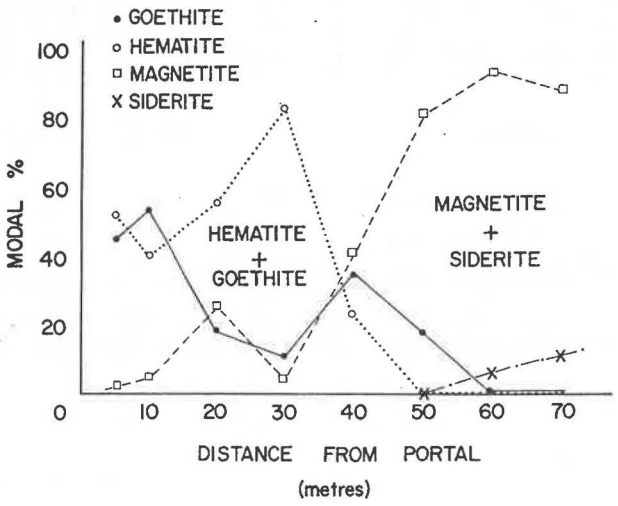

Figure 60
Mineralogy of low-grade iron-formation in No. 2 adit, Nottingham Peak. Modal oxide and carbonate percentages represent the proportion of total iron-bearing phases in each sample, and are redrawn from Brech and Lumb (1974). The change from a highly oxidised near surface assemblage hematite + goethite to less oxidised phases magnetite + siderite at depth is accompanied by a decrease in grain size from 150 μm near the portal to 20 μm, 60 m along the adit. Traces of pyrite occur in samples 60–70 m from the portal; gangue (60–72 modal per cent in individual samples) is mostly silica.

ment followed by 103 m development. A section drawn through the adit (Fig. 59) shows that irregular, surface enrichment decreases rapidly, and 25 m below surface the ore grade is 20–30 per cent lower than in outcrop.

It is noted here that Adit No. 1 samples a low-grade section of the western body, and surface indications suggest the grade to increase toward the north. In addition, adit development was stopped before intersecting much of the higher grade iron-formation seen in outcrop farther east. Future exploration could include extension of the adit and/or underground drilling across the strike.

Adit No. 2 is located below the Peak near the southern extension of the eastern body of iron-formation (Fig. 58). Total length of the adit is 100 m, and the average grade of iron-formation sampled is 34,3 per cent Fe. Brech and Lumb (1974) reported that laboratory tests on three samples from this adit showed that a head grade of 37 per cent Fe could readily be upgraded to 62–64,5 per cent Fe with an iron recovery of 77–83 per cent Fe. One large representative sample from Adit No. 2 was fed into the pilot plant at Ngwenya Mine and gave qualitatively similar results.

Borehole BH 361 (Fig. 58) drilled by the Geological Survey Department intersected 73,5 m iron-formation (32–125,5 m downhole), the cores of which returned assays of 34,6 per cent Fe (UNDP, 1970). Metallurgical tests carried out on these cores in Prague during 1970 showed that hematite accounted for 7–10 per cent of the iron oxides present.

In situ tonnage estimates (not mineable ore) given in Table 40 indicate 69,0, 75,9 and 32,7 .10^6 tons of low-grade iron-formation (±34 per cent Fe) are available to 100 m down-dip in the western, central and eastern bodies respectively. Considerably more exploratory work and bulk sampling are required to evaluate such a massive deposit.

MIDWAY

The Midway deposit is a lenticular shaped body of iron-formation that crops out on the main gravel road between Bulembu and Piggs Peak (Fig. 39). Because the iron-formation is overlain stratigraphically with quartzites and conglomerates of the Moodies Group it is described here with Fig Tree Group iron deposits. Both Fig Tree and Moodies Group sequences at Midway form the most northerly exposures of these stratigraphic units above the Maanhaar thrust (see Figs. 2 & 7).

Geophysical data

A positive anomalous field 3 000–5 000 gamma above background, of the type one would expect from induced magnetisation was recorded on two flight lines during the aeromagnetic survey of Swaziland. The 1 : 50 000 geophysical map series (UNDP, 1970) shows an anomaly trending northeast–southwest of just over 2 km in length. Magnetic fluctuations at Midway are 3–4 000 gamma lower than peak anomalies recorded at Nottingham Peak and Mhlatane.

A ground magnetic survey conducted by Evans (1967) defined a 2,4 km-long linear anomaly trending 045° with a peak amplitude of between 4 000 and 30 000 gamma (Fig. 61). The northeastern section of the anomaly has a high susceptibility but is very narrow, and is consistent with a steeply inclined tabular body only 21 m thick (Evans, 1967). Although closely parallel with the northeastern edge of the Moodies Group outcrop, this section of the anomaly cannot be directly correlated with iron-formation or other magnetic horizons exposed on surface.

The southwestern section of the anomaly is considerably wider (>100 m) but has a much lower magnetic susceptibility. There is good correlation here between the area of high magnetic intensity and the outcrop of iron-formation (Fig. 61). Finally, Evans (1967) reported that the main magnetic body at Midway was traversed on two lines with an EM gun and that the unit is not a good electro-magnetic conductor.

Geological description

A combination of complex thrust-belt deformation and thickly forrested terrain serve to obscure the nature of the Midway iron-formation. The lithological sequence and its interpretation are given in Fig. 62; other interpretations are possible.

The iron-formation forms part of a 120 m-thick ferruginous and silicified sequence of shales and tuffs. Thick

TABLE 40
Tonnage estimates of low-grade iron-formation at Nottingham Peak and Midway deposits.

	NOTTINGHAM PEAK					MIDWAY
	1	2	3	4	Total	5
in situ tonnage (10^6 tons)	45,9	23,1	75,9	32,7	177,6	34,3
[1]grade (% Fe)	32,6	34,6	35,0	34,3	34,2	

[1]assumes no surface enrichment.

Notes: 1. western body, eastern fold limb, 1 850 m strike, aggregate thickness 80 m (30 + 50 m), SG = 3,1; 2. western body, western fold limb, 1 000 m strike, 70 m thick, SG = 3,3; 3. central body mineable portion, 2 300 m strike includes 750 m northern extension not shown in Fig. 58, 100 m thick, SG = 3,3; 4. eastern body, 1 100 m strike, thickness 90 m, SG = 3,3; 5. 1 600 m strike, average thickness 65 m, SG = 3,3.

quartz-albite-chlorite (±biotite) schists occur structurally below part of the iron-formation but it is not known whether this sequence formed part of the original depositional basement. The mafic schists are interpreted from petrographic evidence and analogy with similar lithologies elsewhere as a deformed and metamorphosed volcanic sequence of broadly tholeiitic composition. The uppermost 50 m of mafic sequence is poorly exposed but includes a single horizon of banded chert (Fig. 61).

A thick talc-carbonate sequence is faulted against the western edge of the iron-formation. Thin quartz-chromiferous sericite schists occur along the surface between talcose schists and both iron-formation and a thin tectonic slice of ferruginous and silicified shales farther south (Fig. 61).

Laminated blue and red hematite ores (>50 per cent Fe) are present 50 m below the base of the Moodies Group sequence in a zone inclined steeply toward the southeast (75°–85°). The ore is strongly magnetic, and exhibits a patchy development of limonite and botryoidal goethite. In polished section, magnetite is strongly martitised and often totally replaced by either martite or hematite. Oxide grains are typically 20–50 μm sub- or anhedral magnetite-hematite intergrowths. Silica-rich layers afe often in the form of jasper, and consist in large part of 50–100 μm quartz grains.

Ferruginous shales that contain numerous 0,2 m-wide veins of coarsely crystalline silica form the immediate footwall of the iron-formation. Shales and tuffs replaced in part with iron oxides, and cut by narrow hematite and quartz-magnetite veins overlie the ferruginous horizon. The upper stratigraphic surface is gradational in nature and interpreted as a replacement front.

Pale green Moodies Group quartzites that exhibit a sugary texture, and relatively undeformed chert conglomerates rest with sheared stratigraphic contact on the iron-formation. Similar sugary-textured quartzites that contain sericite are associated elsewhere with the effects of intense alteration by fluids. The degree of deformation increases away from the basal Moodies Group contact, and highly deformed conglomerates with ellipsoidal clasts recording ±80 per cent strain occur close to the major thrust fault along the upper surface of the unit (Figs. 61 and 62). The entire Moodies Group sequence contains a closely-spaced vertical slatey cleavage.

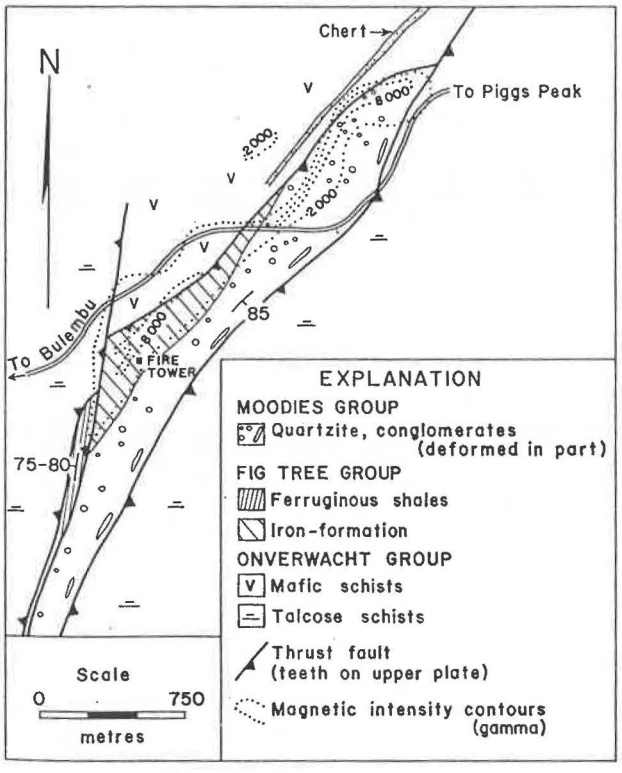

Figure 61
Geological plan of the Midway iron-formation with magnetic data (ground survey) from Evans (1967).

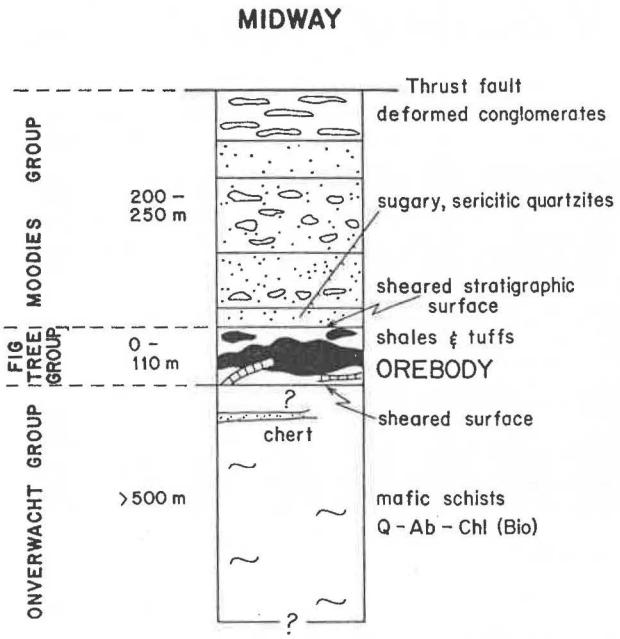

Figure 62
Interpretative lithological sequence of the Midway iron deposit.

Grade and tonnage estimates

An *in situ* tonnage of 34,3 .10^6 tons iron-formation to 100 m down-dip is indicated for the Midway deposit (Table 40). Very few quantitative geochemical data are available, and the grade estimated here (41,6 per cent Fe) is based on the average iron content of massive red ore, laminated blue ore and "incipient" low-grade iron-formation at surface (see Table 43).

Brech and Lumb (1974) reported that the Midway head grade of 34–35 per cent Fe responded well to reverse flotation in the laboratory with excellent upgrading to 64–65 per cent Fe, but rather poor recovery (65–72 per cent).

LOMATI IRON DEPOSIT*

A small body of low-grade ferruginous conglomerates is located between the Lomati and Mgudugudu Rivers in northern Hhohho (see Fig. 39). The iron-rich unit crops out on the southeastern slopes of a mountain known locally as Thabazimbi (orthophotomap series G 17) and is associated with a small (±500 gamma) aeromagnetic anomaly.

The Lomati iron-formation forms part of a 400 m-thick tectonic slice in a geologically complex area of overlapping thrust faults. At the base of the stack, talc-carbonate schists, amphibolites and serpentinites with spinifex-like textures are inclined at low angles (30°) toward the southeast and mark the trace of a thrust. Above the ultramafic sequence in the upper plate, laminated shales 60 m-thick are followed in turn by thin silicic greywackes that contain fining-upwards graded units. The greywackes are overlain by chert pebble conglomerates which near the confluence

* Footnote: The Lomati West deposit described by Clarke (1971) forms part of a lenticular ferruginous chert horizon within the Onverwacht Group. Although almost 5,5 km in strike length and a useful marker horizon within the Mgudugudu thrust sheet, this body is not considered to be of economic interest.

of the two rivers (Lomati and Mgudugudu) contain no visible iron oxides, but become progressively replaced with hematite along strike toward the southwest. The entire sequence is structurally overridden by the Mgudugudu thrust sheet.

Rounded chert pebbles several centimetres in diameter set in a hematitic matrix form the bulk of the deposit. Clasts are often brecciated, corroded and extensively fractured and veined with iron oxides. No detailed mineralogical data on opaque phases are available.

The 1,25 km-long outcrop attains a maximum width of 250 m which gradually tapers toward the Lomati River in the east; the total area underlain by iron-rich conglomerates is estimated to be ±20 hectares. Although a considerable *in situ* tonnage is represented (>20 .10^6 tons) the surface grade of the Lomati deposit is very low (17,2 per cent Fe, Table 43), and the occurrence is not considered to be a mining proposition.

OTHER IRON OCCURRENCES

The stratigraphic status of two occurrences of iron-formation is uncertain:

Lufafa iron-formation

Irregular horizons of hematite iron-formation less than 1 km in strike length crop out on the slopes of Lufafa Mountain (Fig. 33). Though structurally above thick Fig Tree Group sequences, the iron-formation together with associated cherts and talcose schists are located near a major tectonic break and are considered to be allochthonous. The iron-formation contains individual gold values as high as 10 g/t, and is described in more detail elsewhere (*see* Gold deposits).

Havelock West ironstone pipe

An unusual occurrence of goethitic and hematitic breccias is located above the Havelock West chrysotile prospect within a highly silicified Onverwacht Group sequence (Fig. 63). Though the silicified sequence consists in large part of banded cherts, reworked lapilli-tuffs and other volcaniclastic detritus can still be recognised. A discordant, pipe-shaped body formed of massive ironstone breccias and overlain with a 350 m-long jaspilite horizon cuts the sequence. The ironstone pipe narrows rapidly at depth (toward the asbestos prospect) and 60 m below the jaspilite horizon is only 2 m in diameter (Fig. 63).

Most ferruginous breccias contain angular fragments of silica that resemble wall-rocks that surround the pipe. In addition, vertical screens of iron oxide veins are present in banded cherts close to the edge of the pipe. Both relationships indicate that the iron was introduced after silicification and lithification of the Onverwacht Group country rocks.

Mineralogy of the breccias consists principally of goethite and hematite with conspicuous limonite developed at depth. The jaspilite horizon contains a mm-scale regular or podiform layering of white silica, jasper and magnetite. Intraformational breccias, and sedimentary structures that include possible slump folds occur within the jaspilite.

The ironstone breccias are geochemically distinctive and contain precious metals rich in silver (Au/Ag <0,6) as well as high contents of Ba, As, Cr, Co & Ni. Metal contents appear to increase in the direction of the chrysotile prospect (Table 44).

SUMMARY OF IRON RESERVES IN SWAZILAND

Available tonnage estimates of potential ore at thirteen iron deposits in northwest Swaziland are summarised in Table 41. Total reserves of 700 .10^6 tons iron-formation with an average content of 41,8 per cent Fe are indicated, of which 32 .10^6 tons are available on dumps at the Ngwenya deposit.

Apart from Ngwenya where 58,6 .10^6 tons of low-grade iron-formation (BHQ) and 23,4 .10^6 tons high-grade hematite (56–66 per cent Fe) below existing pit levels can be considered potential ore, deposits with the greatest economic value are the massive hematite occurrence at Nottingham Peak and the Mhlatane iron-formation. Because iron is stored largely in magnetite at Mhlatane, processes of upgrading may be relatively inexpensive compared with most Ngwenya-type hematite deposits. Bulk sam-

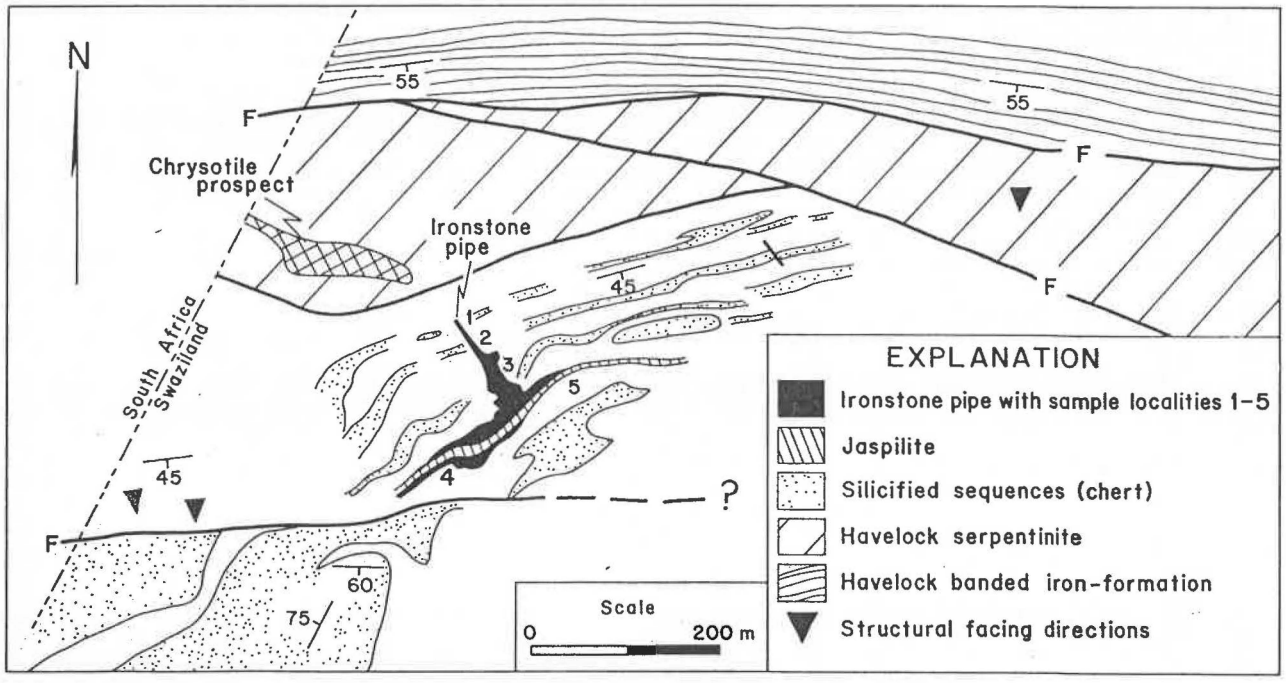

Figure 63
Geological plan of the Havelock West ironstone pipe. Geochemical analyses of samples taken from locations 1–5 are given in Table 44.

TABLE 41
Summary of available tonnages and grades of iron deposits in Swaziland[1]

	Onverwacht Group				Fig Tree and Moodies Groups										Pongola Supergroup				
	1	2	3	4	5	6	7	8	9	10	11	12	13	sub-total	14	15	16	sub-total	Grand total
tonnage (10^6 tons)	14,9	52,1	6,6	58,6	23,4	115,8	1,5	17,5	73,4	139,8	42,1	177,6	34,3	703,1	139,2	57,8	49,2	246,2	949,3
grade (% Fe)	36,8	39,1	45,8	43,2	60,0	42,9	37,0	34,1	34,4	37,4	40,8	34,2	41,6	41,8	32,3	35,8	35,0	33,7	39,7

[1]excludes all deposits where Fe <30 %, and small occurrences for which available data are sparse.

Notes: 1. Havelock magnetite iron-formation, south of Nkomozane River; 2. Mhlatane magnetite iron-formation; 3. Devils Reef high-Mn iron-formation in vicinity of disused gold workings; 4. Ngwenya Mine, total available hematite iron-formation (only 4,1 .10^6 tons 50,6 % Fe included in total, remainder included in 5 & 6); 5. potential ore (56–66 % Fe) *in situ* below economic pit levels, Ngwenya Mine; 6. BHQ *in situ* and on dumps, Ngwenya Mine; 7. Rashale siderite deposit; 8. Ngwenya North Extension (BHQ); 9. Ngwenya Jaspilite deposit (BMQ); 10. Makonjwa iron deposit and Intaba Section; 11. Iron Hill and Western Extension (BHQ); 12. Nottingham Peak deposit; 13. Midway hematite iron-formation; 14–16 magnetite iron-formation in Pongola Supergroup recalculated from Clarke (1971): 14. Maloma; 15. Gege; 16. Mkhondo Valley.

pling below the zone of surface enrichment is required to evaluate the Mhlatane deposit more carefully.

Low-grade iron deposits also occur in southern Swaziland, and tonnage estimates and grades of the three largest deposits are included in Table 41. Data given in Clarke (1971) indicate that deposits in the south of the country consist in large part of very low-grade magnetite iron-formation within the Pongola Supergroup. A systematic study of comparative grades and tonnages is not yet available.

GEOCHEMISTRY OF THE IRON DEPOSITS

Major and trace element analyses of iron deposits in the Onverwacht Group, the Fig Tree and Moodies Groups, and the Havelock ironstone pipe are given in Tables 42–44 respectively.

Major element abundances of the pillowed mafic sequence below the Havelock iron-formation (samples 1–4, Table 42) are consistent with a tholeiitic composition. Extreme hydration and carbonation (±8 per cent CO_2 by weight), high values of Na_2O and K_2O, and above average abundances of precious metals, As and Sb are also characteristic. Pillow centres contain very low total iron and MgO contents. Extensive hydrothermal alteration of the volcanic sequence is suggested below.

Analyses representative of the Havelock iron-formation (samples 5–8, Table 42) exhibit a gradual decrease in CO_2 and FeO/Fe_2O_3 consistent with the progressive metamorphic change from carbonate to oxide iron. Recalculated on a carbonate-free basis, major element abundances of both carbonate and magnetite iron-formation are similar, though total iron content increases toward the stratigraphic top of the unit.

In common with analyses of Archean iron-formation of sedimentary origin (James, 1966), the present samples contain low Al_2O_3 (0,1–0,4 per cent), low P_2O_5 and with the exception of sample 3, low alkali contents. Havelock samples contain unusually high contents of CaO and MgO

TABLE 42 (a)
Chemical compositions of iron-formations and adjacent units in the Onverwacht Group:
I. Major elements (weight per cent)

	Havelock										Mhlatane		Elangeni	
	1	2	3	4	5	6	7	8	9	10	11	12	13	14
SiO_2	46,90	49,03	60,80	45,20	56,10	45,50	56,10	53,70	46,10	44,45	30,70	28,70	41,60	50,30
TiO_2	1,45	0,35	0,37	1,68	<0,05	<0,05	<0,05	<0,05	<0,05	0,12	0,22	0,08	0,06	0,38
Al_2O_3	12,80	12,90	18,60	11,70	<0,10	0,20	0,40	0,10	2,10	4,65	3,90	<0,10	0,10	12,90
Fe_2O_3	3,74	0,48	0,78	2,32	0,99	<0,10	11,30	12,30	3,82	2,11	59,30	65,45	12,25	1,60
FeO	8,96	2,55	1,44	12,31	9,78	20,80	9,69	22,05	19,99	4,88	1,44	2,38	30,28	6,77
MnO	0,14	0,12	<0,05	0,19	0,57	0,87	0,46	0,62	0,53	0,13	0,24	0,36	1,00	0,27
MgO	4,90	3,47	1,50	5,60	4,05	5,40	3,60	3,10	16,70	33,10	<0,10	<0,10	4,15	8,80
CaO	5,79	13,98	1,86	8,21	8,42	5,13	5,02	5,13	8,80	0,49	<0,05	<0,05	4,46	11,00
Na_2O	2,70	2,31	0,30	1,50	<0,10	<0,10	0,10	<0,10	<0,10	0,10	<0,10	<0,10	0,10	1,60
K_2O	0,77	2,01	8,88	0,40	<0,05	<0,05	2,35	<0,05	<0,05	<0,05	0,32	<0,05	<0,05	<0,05
P_2O_5	<0,05	0,22	<0,05	<0,05	<0,05	<0,05	<0,05	<0,05	<0,05	<0,05	<0,05	<0,05	<0,05	<0,05
SO_3	0,35	n.d.	0,05	0,20	1,00	0,22	0,00	0,00	0,00	0,01	0,00	0,03	0,70	0,03
CO_2	3,69	8,28	0,09	5,00	18,45	21,70	9,70	<0,10	0,34	0,10	0,12	1,80	2,78	0,09
H_2O^+	3,63	3,49	1,91	4,35	2,76	n.d.	n.d.	n.d.	n.d.	8,86	2,23	1,86	2,12	1,64
Loss	5,98	n.d.	4,58	8,40	15,80	19,80	9,76	0,07	2,97	8,92	3,59	1,73	0,23	1,86

n.d. = not determined.

Notes: 1–10 Havelock Mine. 1–4 spilites (depositional basement to the Havelock iron-formation); 1. vertical shaft cross-cut 465 level, 170 m below iron-formation; 2. pillow centre, 6W 390 level, 38 m below iron-formation (analysts: Geological Survey, Pretoria); 3. massive spilite, 6W 390 level, 13 m below iron-formation; 4. centre mafic inclusion, 355 level 6W; 5–8 Havelock iron-formation. 5. unmetamorphosed carbonate member (zone 1), 29 m below serpentinite; 6. slightly metamorphosed silicate-carbonate member (metamorphic zone 2), 14–15,5 m below serpentinite; 7–8. moderately metamorphosed oxide member (metamorphic zone 3), 6 m and 1,5–2 m below serpentinite respectively; 9. basal amphibolite, immediately below Havelock serpentinite; 10. basal talc zone, Havelock serpentinite body; 5–10 6W 390 level (for locations see Fig. 40); 11. orange-weathered magnetite iron-formation, Mhlatane deposit, 350 m north of Mhlatane River; 12. Mhlatane magnetite iron-formation, Mhlatane River; 13. Elangeni magnetite-pyrrhotite zone, borehole EL2, 167,5–175 m down-hole; 14. Elangeni mafic schist unit, borehole EL2, 45 m down-hole.

TABLE 42(b)
Chemical compositions of iron-formations and adjacent units in the Onverwacht Group:
II. Trace elements (ppm)

	Havelock									Mhlatane		Elangeni	
	1	3	4	5	6	7	8	9	10	11	12	13	14
Au	0,43	0,09	<0,05	<0,05	0,07	0,10	0,07	0,08	<0,05	<0,05	<0,05	<0,05	<0,05
Ag	<0,10	<0,10	<0,10	<0,10	0,10	0,30	0,10	<0,10	<0,10	<0,10	<0,10	<0,10	<0,10
Pt	<0,10	0,10	<0,10	<0,10	<0,10	0,10	0,10	0,30	<0,10	<0,10	<0,10	0,20	<0,10
B	560	225	675	122	43	22	37	28	128	120	345	224	187
Ba	203	67	25	20	34	52	31	27	20	413	115	33	20
As	2 444	<30	<30	31	<30	<30	<30	<30	<30	<30	<30	35	128
Sb	7	3	1	4	1	1	1	<1	3	1	1	2	3
Cr	146	645	86	100	<340	<340	<340	1 026	2 476	207	33	60	453
Co	70	100	90	45	40	40	60	50	80	50	80	50	60
Ni	180	290	180	215	82	168	114	442	1 435	160	120	200	250
Cu	200	109	232	22	12	6	5	3	19	28	20	36	82
Pb	80	70	70	80	43	40	40	37	70	80	100	80	70
Zn	112	56	146	27	168	60	93	102	45	73	69	186	56
[1]Hg	1 070	810	290	1 140	294	176	227	239	645	5 340	1 710	985	1 180
Sn	<20	35	20	<20	<20	<20	<20	<20	<20	<20	<20	<20	<20
W	<20	<20	<20	<20	<20	<20	<20	<20	<20	<20	<20	<20	<20
Y	25	<10	18	<10	<10	<10	<10	<10	<10	18	<10	<10	<10
Zr	125	39	109	19	13	16	16	14	23	40	19	21	40

[1]reported as ppb; see notes in Table 42(a).

(stored in carbonate) and small values of combined precious metals (0,1–0,4 g/t).

The narrow amphibolite at the base of the Havelock body (sample 9, Table 42) has major and trace element abundances intermediate in character between iron-formation and serpentinised dunite.

For reasons given below, major element abundances of Fig Tree and Moodies Group hematite iron-formation are not very helpful in the geochemical evaluation of these deposits. Analyses of essentially unleached iron-formation are only available from the Rashale siderite deposit (sample 2, Table 43), and are consistent with a lithology that contains ±80 per cent siderite. The relatively high contents of CaO (3,21 per cent but as much as 12,24 per cent in BH 275) and MgO (5,64 per cent) indicate that, at least in part, the ferroan carbonate may be ankeritic in composition.

The basal, laminated facies of the Makonjwa iron-formation (sample 3, Table 43) exhibits exceptional patterns of element distribution. On surface, this unit has a relatively high Al_2O_3 content and significantly high values of precious metals (0,8 g/t). A comparable geochemistry is

TABLE 43 (a)
Chemical compositions of iron-formations in the Fig Tree and Moodies Groups:
I. Major elements (weight per cent)

	Ngwenya North	Rashale Siderite	North Makonjwa		Intaba Section	Iron Hill	Nottingham Peak		Midway			Lomati
	1	2	3	4	5	6	7	8	9	10	11	12
SiO_2	50,40	2,92	5,60	47,80	40,60	44,70	44,00	59,80	47,90	6,60	3,30	72,60
TiO_2	<0,05	0,10	0,44	0,13	<0,05	0,06	0,20	0,13	<0,05	0,19	0,33	0,18
Al_2O_3	0,90	4,20	4,77	0,40	0,20	0,10	1,50	2,20	0,40	2,00	2,60	0,50
Fe*	30,10	38,00	57,80	34,41	39,11	38,01	34,63	25,46	32,73	54,81	61,10	17,15
Fe_2O_3	43,00	n.d.	77,14	45,64	53,10	54,01	47,74	34,32	46,14	78,30	86,05	23,46
FeO	<0,05	n.d.	4,94	3,20	2,52	0,26	1,58	1,87	0,56	<0,10	1,12	0,94
MnO	1,13	0,16	0,12	0,49	0,18	0,06	0,31	0,13	0,27	0,29	0,25	<0,05
MgO	<0,10	5,64	0,43	<0,10	0,10	<0,10	<0,10	<0,10	<0,10	<0,10	<0,10	<0,10
CaO	<0,05	3,21	<0,05	<0,05	<0,05	<0,05	<0,05	<0,05	<0,05	<0,05	<0,05	<0,05
Na_2O	<0,10	0,27	<0,10	<0,10	<0,10	<0,10	<0,10	<0,10	<0,10	<0,10	<0,10	<0,10
K_2O	<0,05	n.d.	0,36	<0,05	0,14	<0,05	<0,05	0,09	0,11	0,33	<0,05	<0,05
P_2O_5	<0,05	0,04	<0,05	<0,05	<0,05	<0,05	<0,05	<0,05	<0,05	<0,05	<0,05	<0,05
SO_3	0,02	0,13	0,02	0,03	0,01	0,00	0,03	0,04	0,01	0,01	0,02	0,10
CO_{2+}	0,12	33,38	1,79	0,26	2,27	0,38	0,53	0,10	0,32	0,18	0,81	0,55
H_2O^+	n.d.	n.d.	3,96	0,82	1,80	0,22	2,76	0,91	3,72	9,19	4,11	1,19
Loss	4,66	n.d.	3,11	1,39	3,44	0,62	3,61	2,17	4,02	10,30	4,57	2,04

Fe* = (0,7 Fe_2O_3 + 0,77 FeO); n.d. = not determined.

Notes: 1. deformed basal iron-formation (BHQ), Ngwenya North Extension, southern (ore reserve) block; 2. 3 m representative cores from BH 72, Rashale siderite deposit, analysis 278, Bulletin 6; 3. basal laminated facies, Makonjwa iron-formation (mean 3 analyses); 4. upper jaspilite facies, Makonjwa iron-formation; 5. Banded Hematite Jaspilite, Intaba Section; 6. Iron Hill, Mehliss Grade II/III (northeast of dyke); 7. Nottingham Peak laminated BMQ, 40 m from portal, adit no. 1; 8. Nottingham Peak, limonitic laminated BMQ, 95 m from portal, adit no. 1; 9. Midway iron-formation, uppermost low-grade ferruginous tuffs with replacement features (mean 2 analyses); 10. Midway iron-formation, high-grade laminated ore with limonite; 11. Midway iron-formation, high-grade red ore; 9–11 Peak Timbers fire tower section; 12. Lomati iron-formation, coarse ferruginous conglomerate.

TABLE 43 (b)
Chemical compositions of iron-formations in the Fig Tree and Moodies Groups:
II. Trace elements (ppm)

	Ngwenya North	North Makonjwa		Intaba Section	Iron Hill	Nottingham Peak		Midway			Lomati
	1	3	4	5	6	7	8	9	10	11	12
Au	<0,05	0,53	<0,05	<0,05	<0,05	<0,05	<0,05	<0,05	<0,05	<0,05	<0,05
Ag	0,10	0,20	<0,10	<0,10	<0,10	0,10	<0,10	<0,10	0,10	0,10	<0,10
Pt	0,10	0,13	<0,10	<0,10	<0,10	<0,10	<0,10	0,10	<0,10	<0,10	0,10
B	43	467	115	150	218	125	105	130	545	115	100
Ba	29	467	87	95	44	638	73	719	1 146	489	25
As	<30	64	<30	<30	55	<30	<30	48	1 125	396	259
Sb	1	1	<1	2	3	<1	3	2	3	1	5
Cr	<340	1 222	153	<20	<20	249	109	82	118	288	171
Co	70	97	60	50	55	50	30	40	80	80	30
Ni	79	627	150	100	140	130	120	175	310	290	110
Cu	12	26	45	22	17	24	13	17	38	25	19
Pb	46	103	80	100	90	70	50	95	120	80	50
Zn	43	36	10	43	11	66	36	36	71	51	43
[1]Hg	209	1 240	300	340	1 235	1 220	130	870	1 220	320	490
Sn	<20	<20	<20	<20	<20	<20	<20	<20	27	<20	<20
W	<20	<20	22	24	<20	<20	<20	<20	22	<20	26
Y	<10	<10	<10	<10	<10	<10	<10	<10	<10	10	<10
Zr	22	48	14	10	20	32	23	19	25	34	25

[1]reported as ppb; see notes in Table 43(a).

TABLE 44(a)
Chemical compositions of the Havelock West ironstone pipe
I. Major elements (weight per cent)[1]

	1	2	3	4	5
SiO_2	1,40	3,65	6,40	19,40	80,20
TiO_2	0,07	0,10	0,09	0,07	0,07
Al_2O_3	0,90	0,55	0,40	1,80	0,10
Fe_2O_3	84,90	20,90	77,06	67,40	16,54
FeO	<0,10	<0,10	0,58	0,14	0,86
MnO	1,12	57,45	0,20	0,40	0,13
MgO	<0,10	0,10	<0,10	0,20	<0,10
CaO	<0,05	<0,05	0,15	<0,05	<0,05
Na_2O	<0,10	<0,10	0,10	<0,10	<0,10
K_2O	<0,05	<0,05	<0,05	<0,05	<0,05
P_2O_5	0,14	<0,05	0,37	<0,05	<0,05
SO_3	0,01	0,01	0,20	0,05	0,01
CO_2	0,32	0,62	1,41	1,38	0,79
H_2O^+	10,20	3,79	9,83	8,86	0,79
Loss	12,20	13,45	12,00	9,76	1,72

[1]for sample location see Fig. 63.
Notes: 1. 2 m-diameter, massive goethite with limonite, 75 m structurally below jaspilite horizon; 2. manganiferous breccia with fragments of silica wall-rock, 60 m below jaspilite (mean 2 analyses); 3. 3–4 m diameter pipe, red coloured ore, 35 m below jaspilite; 4. uppermost ferruginous breccias with goethite, minor sulphides and angular quartz fragments; 5. magnetic jaspilite horizon.

TABLE 44 (b)
Chemical compositions of the Havelock West ironstone pipe
II. Trace elements (ppm)

	1	2	3	4	5
Au	<0,05	<0,05	0,06	0,05	<0,05
Ag	0,30	0,45	0,10	<0,10	<0,10
Pt	<0,10	<0,10	0,10	<0,10	<0,10
B	110	38	110	265	30
Ba	200	3 765	66	108	43
As	175	40	303	42	30
Sb	2	1	1	<1	<1
Cr	536	20	40	64	65
Co	230	345	70	80	40
Ni	2 800	865	240	430	90
Cu	126	81	39	121	20
Pb	100	85	90	80	30
Zn	139	96	103	168	14
[1]Hg	410	1 095	900	1 350	350
Sn	<20	<20	<20	<20	<20
W	<20	<20	<20	<20	<20
Y	<10	14	<10	18	<10
Zr	20	14	25	28	23

[1]reported as ppb; see notes in Table 44(a).

recorded from massive goethitic breccias that form the Havelock ironstone pipe (Table 44) and suggests that the two deposits are in some way related.

ORIGIN OF THE IRON DEPOSITS

Onverwacht Group

Several geochemical arguments put forward by Goodwin (1964) to explain the origin of the Helen iron-formation in western Ontario are also applicable to the Havelock iron-deposit. Like Havelock, the Helen iron-formation consists of a basal carbonate member that lies structurally above a highly altered volcanic sequence. Both volcanic sequences have gained CO_2, Na_2O and K_2O, while a number of major elements, particularly Fe, Mn, Mg, Ti and possibly Si and Al appear to have been lost (if an original tholeiitic composition is assumed for the Havelock sequence).

Following Goodwin, it can be inferred that while the mafic volcanic sequence was flat-lying, the upward migration of fluids produced extensive chemical transport which resulted in the deposition of carbonate iron-formation. Though the source of the fluids is uncertain, the spilitic metamorphism of the underlying mafic sequence is most easily explained in terms of hydrothermal circulation associated with submarine tholeiitic volcanism. It seems probable that ferroan carbonate and silica formed by inorganic precipitation from hydrothermal solutions

which leached material from the underlying igneous sequence. The absence of silicified volcaniclastic detritus indicates that processes of replacement were relatively unimportant (compare with deposits in the Fig Tree and Moodies Groups).

Because the Mhlatane, Elangeni and Black Diamond Creek iron deposits are also closely associated with mafic volcanic sequences, similar exhalative processes may also have operated during their formation. The Devils Reef iron deposit contains features that indicate formation by replacement of volcaniclastic detritus and suggests that the unit should more properly be considered as a deposit of the Ngwenya-type. Good exposures of adjacent sequences at Devils Reef are not available.

Fig Tree and Moodies Groups

From detailed descriptions of Fig Tree and Moodies Group iron deposits the following general observations can be made:

1. Wherever sampled below the present level of sub-tropical weathering, iron in Fig Tree and Moodies Group deposits is stored for the most part in carbonate. At Ngwenya, massive hematite ores pass into banded siderite iron-formation 130–150 m below outcrop (see Fig. 49a). Siderite is present in the sub-surface at Rashale (Fig. 53), and the proportion of ferroan carbonate in iron-formation exposed by exploration adits driven at Nottingham Peak (Fig. 60), increases progressively in unweathered material.

2. Most important hematite deposits occur on relatively flat-lying ridges ±1 200 m in elevation, in areas with good sub-surface drainage. Strong relief and steep slopes (which promote the circulation of ground water) are associated with all high-grade deposits. Near surface removal of silica (supergene enrichment) is inferred from the measured decrease in iron content with depth.

3. Field relations and textural evidence show processes of replacement to have been important. Gradational contacts between iron-formation, ferruginous cherts, shales and conglomerates, and lateral transitions from iron-formation and chert to unreplaced clastic sedimentary sequences are ubiquitous, as was first pointed out by Mehliss (1946). Core zones of small folds and areas adjacent to dykes are often relatively rich in iron.

4. All Ngwenya-type deposits south of Havelock belong to a single province floored by talc-carbonate schists. Tholeiitic volcanic sequences have either been removed by erosion from this area, or were never deposited. Analyses of talcose lithologies contain relatively small values of iron and silica.

5. Anomalously high values of precious metals in laminated iron-formation, and a small pipe-shaped body of argentiferous ironstone occur at Havelock West and near Diepgezet mountain. In addition, the Devils Reef and Midway iron deposits contain unusually large abundances of precious metals. All occurrences of this type are located along the northern and northwestern extension of the iron-formation province and suggest that the source of precious metals lay in that direction.

A full interpretation of these data is not given here (see Table 45). In terms of the economic concentration of iron, it appears that downward-moving solutions directed toward dip-slopes have oxidised ferrous carbonate to hematite. This process must have been controlled in part by recent rates of uplift. Partial leaching to depths exceeding 200 m have been described in hematite iron-formation exposed to similar sub-tropical weathering in Brazil (Dorr, 1964).

TABLE 45
Some characteristic features of iron-formations in the Swaziland Supergroup

	ONVERWACHT GROUP	FIG TREE AND MOODIES GROUPS
Dimensions	small, lenticular-shaped bodies ±5 km strike length (2,75–7 km) maximum thickness 40–45 m	extensive formations >30 km strike length and 10 km width (±35 000 ha and 5 .10^{10} tons iron) before deformation. maximum thickness 100–120 m
Base	mafic (tholeiitic) pillowed volcanics subjected to a 'spilitic' metamorphism	thick talc-carbonate schists *or*, silicified sedimentary sequences *or* both
Hangingwall	thin volcaniclastic units; frequently the locus of major horizontal translations	clastic sedimentary sequences with jaspilite horizons
Primary mineralogy	ankerite/ferrodolomite — silica (±siderite-pyrite-graphite)	siderite — silica (±ankerite/ferrodolomite-pyrite)
Metamorphic mineralogy	magnetite-minnesotaite-ferroactinolite-silica	magnetite-silica
Oxidised mineralogy	hematite-goethite-silica (±limonite) *or*, magnetite-hematite-orange weathered silicates	hematite-goethite-silica (±limonite-magnetite)
Iron content	20 % Fe (unmetamorphosed carbonate facies). 35–40 % Fe (metamorphosed oxide-silicate facies)	±38 % Fe (carbonate facies) 30–45 % Fe (B.H.Q.) with supergene enrichment to 66 % Fe
Geochemistry	MnO ± 0,6 %; Al_2O_3 ± 0,7 %; Σ(MgO>+CaO+Alk) = >6 %; total precious metals of 100 ppb typical	MnO ± 0,3 %; Al_2O_3 ± 1,4 %; (MgO+CaO+Alk) = <1 %, (in weathered material only) total precious metals usually <50 ppb, though exceptionally high values occur near feeders
Reserves to 100 m down-dip	±75 .10^6 tons (39,2 % Fe)	±630 .10^6 tons (42,1 % Fe)
Origin	inorganic precipitation of ferroan carbonates and silica on spilitised and pillowed tholeiitic extrusives	replacement and exhalative processes

MANGANESE

All manganese occurrences in northwest Swaziland are described in full in sections dealing with gold, iron and cobalt deposits, and are summarised as follows:

Devils Reef — pockets of manganiferous and ferruginous wad are present at Devils Reef and are associated with fault zones in iron-formation (Fig. 34). Manganese is contained in oxides and hydroxides that often include high values of gold and barium. Systematic sampling of wad in disused mine workings indicates average values of 5–8 per cent Mn (Jones, 1961; Table 32), and values of ±13 per cent Mn are recorded from surface exposures alone (samples 2 and 3, Table 27). Approximately 1,5 $.10^6$ tons wad are present *in situ* in the vicinity of old mine workings.

Ngwenya hematite deposit — ores from the central mining block of the Ngwenya iron deposit (Saddle block, Fig. 48) are richer in manganese, often by several factors, than ores elsewhere in the dormant mine. An average value of ±3,5 per cent Mn (Fig. 51) and isolated values as high as 20 per cent Mn are recorded in goethitic red ores from Saddle block. In large part, manganese is stored in psilomelane, and is thought to form by the weathering of manganiferous carbonates.

Iron Hill — small tonnages of manganiferous ores (27–37 per cent Mn) are present at the Iron Hill hematite deposit and along the southern margin of the Western Extension of Iron Hill (Fig. 57). Both manganite and psilomelane occur in banded manganese-formation.

Intaba Beacon — a deposit of botryoidal manganite and psilomelane is located in the area 600 m southeast of Intaba Beacon (Fig. 55). Approximately 7 $.10^3$ tons visible potential ore (±44 per cent Mn) is exposed in outcrop.

Havelock West ironstone pipe — massive manganiferous breccias occur at the structural base of a pipe-shaped body of ironstone close to the Havelock West chrysotile prospect (Fig. 63). Grab samples contain ±45 per cent Mn and anomalously high values of precious metals. The manganiferous pipe may have formed in a hydrothermal vent from fluids released during deformation of the Havelock serpentinite body.

Cobalt prospect — small pockets of manganese oxides (±20 per cent Mn) occur in deformed, silicified and sericitised Onverwacht Group sequences in the central part of the greenstone belt (Fig. 55). This occurrence is the only manganese deposit in northwest Swaziland that is associated with high values of base metals of the type known to form on the present-day sea floor.

MOLYBDENUM

Over thirty years ago, Davies (1951) wrote a report describing the occurrence of potential ore-grade molybdenum (±0,12 per cent Mo) near the old bridge site on the Komati River (see Fig. 2). In the report, the author suggested that molybdenum sulphides may be disseminated in a zone at least 50 m wide and 400 m along the strike.

The Komati River exposes an atypical section across the eastern edge of the Barberton greenstone belt: instead of a granitoid margin, the Swaziland Supergroup is there separated from the AG3 batholith by a gneissic unit. Both gneisses and adjacent sequences in the Schist Belt are inclined west at high angles and share a tectonic contact.

The gneissic foliation is defined by an alternation of quartzo-feldspathic layers with layers rich in biotite. The unit has a structural thickness of 350 m measured across the foliation. A 50 m-wide zone of migmatites with augen textures is present between gneisses and AG3 granite.

Large rafts of banded gneiss ±20 m in size are present in the granite up to 1,75 km east of the greenstone belt margin in the Komati valley. The orientation of gneissic foliation is remarkably consistent across the entire section, even though each gneiss block is enclosed by granite (see also Hunter, 1974). Small isoclinal folds deform the gneissic layering and record a structural event not present in the granite.

The presence of Molybdenum sulphides was confirmed in two localities on either side of the Komati River (Fig. 2). In both cases, mineralisation occurs in the basal gneiss unit, immediately adjacent to the zone of migmatites.

Molybdenite is present as very coarse flakes associated with pegmatites, and as joint coatings in pegmatitic gneisses. There is no fine-grained or stockwork-type molybdenite typical of sub-volcanic and rhyolitic environments.

Grade and extent of mineralisation were determined by 120 line metres of channel samples cut from trenches dug over a strike length of 350 m. Samples submitted for assay returned values in the 0,00X–0,000X per cent Mo range, and included 60 per cent below detection limit (3 ppm). Sparse mineralisation of this type does not justify further exploration.

NICKEL

WATERFALL NICKEL DEPOSIT

A high tonnage but extremely low-grade occurrence of nickel sulphides is present in the area immediately west of the Waterfall gold deposit (Fig. 36). Nickel occurs in the form of finely disseminated gersdorffite (NiAsS) within carbonate-rich talcose schists.

A description of the deposit was first given by Davies (1953) who reported the presence of nickel sulphides in drill cores recovered from the scheelite prospect (Fig. 36). Silvery-white-coloured gersdorffite is not present in a visible form and was only detected in cores of talcose schist after crushing and panning.

Panned concentrates were studied by X-ray diffraction (Davies, 1953) and the resulting data indicate the presence of two nickel-bearing phases within the cobaltite-gersdorffite group: a minor phase with a composition close to cobaltite, and a ubiquitous phase that approaches pure gersdorffite. Spectrographic analysis reveals the presence of As, Ni, Co, Fe and Cu, and confirms the XRD identifications.

Traces of chalcopyrite, pyrrhotite, cobaltite, platinum and sphalerite were also recovered from panned concentrates of crushed cores. Dolomite, ankerite and siderite are recorded in association with mineralised portions of the schist.

Thirteen boreholes involving intersections that totalled 923 m were drilled around the old scheelite mine. An average nickel content of 0,11 per cent in cores (maximum 0,42 per cent) was reported by Davies (1953). The proportion of sulphide: silicate nickel is given by the same author as 5:1 at depth and 1:1 in the oxide zone. Mineralised talcose schists were not bottomed in the deepest intersection, 135 m below surface.

Davies (1953) suggested that the mineralised zone strikes north-south and is inclined west at ±50°. The deposit has a strikelength of at least 300 m proved by drilling. Prospection in short adits and trenches indicates that the mineralisation persists in the area west of the old scheelite mine to a point below the ruby tin workings, and there contains 0,17 per cent nickel. Based on a strike length of 900 m, a width of 600 m and a depth of 120 m, Davies estimated that 125 $.10^6$ tons of talcose schist with 0,11 per cent nickel are present *in situ*.

The origin of the deposit is not known. Nickel sulphides are known to form by recrystallisation of phases liberated from the lattice silicate of talcose schists. Such a process might have occurred in the Waterfall area during a hydrothermal event. Ultramafic sequences with broadly comparable total nickel contents are widespread in the greenstone belt, though even when most of the nickel is in the form of sulphide, concentrations of this type are too low to be of economic interest.

ENTABENE NICKEL PROSPECTS

A nickel sulphate gossan associated with a stockwork of quartz veins is located close to the Mngwaisa cobalt prospect (Fig. 55), and was first described by Bushell (1972). The stockwork occurs in chert with chromiferous sericite and closely resembles that associated with manganiferous and cobalt-bearing sequences farther south. The nickeliferous gossan crops out in the nose of the same recumbent structure that contains the cobalt prospect within the upright fold limb.

Geochemical analyses of the gossan are sparse. Bushell (1972) reported initial values of 1 200 ppm nickel, 190 ppm antimony and 300 ppm cobalt. According to this author, the presence of both moronosite (nickel sulphate) and annabergite (nickel arsenate) were identified by X-ray diffraction scans.

Two shallow exploration boreholes were drilled at the prospect (Bushell, 1972). The first caved in chromiferous sericite schist with pyrite and unidentified schistose material 36,5 m down-hole. The second hole was drilled vertically from the top of the oxidised stockwork and was abandoned at 26,5 m depth, still in gossan.

Further work to define more carefully the extent and grade of the mineralisation is required. Both the nickel occurrence and the cobalt prospect farther south may represent base metal deposits of a syngenetic-type, and mineralogical and other studies are considered worthwhile.

A nickel prospect on the bank of the Entabene River was also described by Bushell (1972; prospect 2, Fig. 55). The prospect consists of a green-coloured gossan developed along a tectonic surface between talcose schists and various siliceous and ferruginous sequences. Test pits were sunk to a depth of 8,5 m over the gossan, and were stopped in "sulphide facies iron-formation" (*op. cit.*). The presence of unoxidised pyrite with values of 400 ppm each of nickel, copper and cobalt was recorded.

ORNAMENTAL STONE

Though they cannot strictly be termed mineral resources, two lithologies that have a potential ornamental use are described here for the sake of completion. Both lithologies occur in remote terrane south of Havelock Mine; their locations were first given by Bushell (1972).

Green chert

Translucent chrome green-coloured silica occurs along the faulted margins of the Mngwaisa serpentinite body (Fig. 64). Silica with chromiferous sericite is widely distributed along fault zones that cut Onverwacht Group ultramafic sequences, though it is unusual to find green-coloured chert without mesoscopic inclusions. Apart from small amounts of pyrite, the Mngwaisa lithology is almost pure silica (hardness = 7).

Ornamental-grade material occurs principally along the western margin of the serpentinite body (Fig. 64). Both chert unit and the associated tectonic surface are inclined ENE at ±65°. Though precise geochemical data from the main body of green chert are not available, semi-quantitative anlayses indicate above average abundances of barium.

The green chert has an average width of ±2 m and is exposed on a cliff face which Clarke (1977) estimated to be 30 m high and at least 100 m long. A high proportion of the 15 000 tons available is low-quality material in

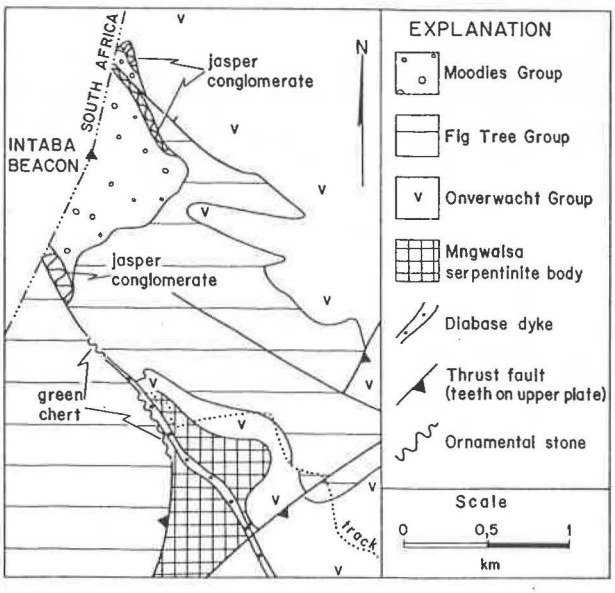

Figure 64
Locations and geological plan of the green chert and jasper conglomerate ornamental stones (based on 1:25 000 geological map series, with additions).

which the intensity of green coloration varies considerably. Nonetheless, several hundred tons of green chert could be easily extracted with the use of wedges and bars.

Ornamental stone of the green chert-type could be used as a jade or chrysoprase substitute. It is noted that the main body of dark green-coloured silica is near a motorable track completed during 1973.

Jasper conglomerate

A distinctive conglomerate that contains rounded clasts of red jasper and green-coloured silica occurs at the base of Moodies Group quartzites near the hill known as Intaba (Fig. 64). The jasper conglomerate consists essentially of silica clasts set in a silica cement, and resembles a "puddingstone". Clasts of volcanic material (silicified in part) are also present.

As Fig. 64 shows, the jasper conglomerate crops out in an area where the underlying Fig Tree Group sequences are extremely attenuated or absent. According to Reimer (pers.comm., 1980), a similar jasper conglomerate is frequently associated with barite desposits and redeposited sequences elsewhere in the Barberton area.

The distribution of jasper conglomerate is restricted to two or three main areas (Fig. 64). A northern zone 600 m long, ±20 m wide inclined southwest at 70°, and a southern zone 160 m long, ±50 m wide inclined at 80° towards the northeast both contain isolated lenses and pods of jasper conglomerate. Accurate tonnage estimates are not available, but like the green chert, several hundred tons are exposed in outcrop.

TALC

Planimeter studies of 1:25 000 geological maps published by the Geological Survey Department show that more than 18 per cent of the greenstone belt outcrop in northwest Swaziland is occupied by talcose schists (±11 500 ha). South of the Komati River alone, a third of the Swaziland Supergroup consists of lithological units mapped as talcose or talc-bearing Onverwacht Group sequences.

No high purity talc, of the type used in the manufacturing and chemical industries is known to occur within this extensive area of ultramafic schists. However, a number of soft, pale-coloured talcose bodies are present in areas where the effects of intense hydrothermal activity have been inferred from other evidence. Massive talc with carbonate impurities is common within the eastern limb of the Forbes Reef synform and at Motjane Reefs. A chemical analysis of Motjane soapstone of the type used in local carvings is given as sample 10, Table 27.

TIN AND TUNGSTEN

Lode tin and tungsten deposits are known to occur near the southern extension of the greenstone belt, within the eastern limb of the Forbes Reef synform (Fig. 36). Though large tonnages are not available, these occurrences demonstrate the extent to which pegmatites associated with the AG3 batholith have invaded the talcose sequences of the Onverwacht Group.

Cassiterite-bearing pegmatites aligned parallel with talcose foliation surfaces occur in two localities in the Forbes Reef area (Fig. 36). The southernmost pegmatite crops out along a strike length of 36,5 m and has average width of 0,76 m (Pretorius, 1961). A reddish-coloured micaceous zone which passes gradationally into unaltered talcose schists is present along both margins of the pegmatite. Cassiterite occurs as sparse anhedra within a totally kaolinised pegmatitic matrix. The grade of the deposit is not known.

A broadly linear zone of reddish-coloured micaceous alteration is also present 30 m above the hanging wall surface of the same pegmatite. This alteration zone can be traced parallel with the regional structural trend for 1,37 km by a discontinuous capping of tourmaline gossan (Mehliss *in* Pretorius, 1961). Large euhedral crystals of cassiterite (±75 mm) occur in pockets along the length of the zone though their distribution is not known with any certainty. The largest tourmaline gossan is ±20 m long and assayed 0,08 per cent tin (Pretorius, 1961). Margarite has been identified in tourmaline-rich float in the area.

A small deposit of scheelite occurs in the same area, approximately 600 m NNW of the old Forbes Reef hotel (Fig. 36). Scheelite is associated with a 7,6 m-wide lens of amphibolite within talcose schists (Pretorius, 1961). The amphibolite consists of near-monomineralic actinolitic hornblende, and is rimmed by a ±1 m-wide layer of biotite schist. Scheelite occurs principally in the biotite schist layer, and to a lesser extent in association with quartz veins in the surrounding talcose sequence.

Pretorius (1961) reported that calcite is always associated with scheelite, and that the proportion of calcite appears to be directly related to the amount of scheelite present. Albite, black quartz and minor amounts of pyrite, pyrrhotite and chalcopyrite are also associated with the tungsten mineralisation.

Four boreholes with intersections that totalled 150 m in length were drilled at the prospect though only minor quantities of scheelite were observed in the cores recovered (Davies, 1953). As estimate of ±500 tons of scheelite-bearing biotite schist is given by Pretorius (1961) of which only a small proportion consists of potential ore that assays 1,75 per cent WO_3.

The association of scheelite with lode gold at the Waterfall and Wyldsdale deposits has been noted elsewhere. Extremely high values of tungsten (244 ppm) are also associated with visible mercury mineralisation at the Cinnabar Prospect (sample 5, Table 27).

Finally, it is noted that alluvial tin has been worked along the Malolotja River in the area between Forbes Main Reef and Malolotja Falls. Cassiterite occurs with alluvial gold and minor scheelite, and all three were recovered together. The potential for present-day alluvial operations in this area is not known.

Cassiterite-bearing gravels and lower-grade alluvial deposits have also been worked near the southern tip of the greenstone belt. This ground forms the northwest extension of the so-called "Tin-Belt" in Swaziland, but the area is thought to be less payable than tinfields elsewhere in the country.

The age and origin of the Tin Belt are not known. Tin mineralisation is usually considered to be related in some way to pegmatites associated with the AG3 granitoid batholith. If this association is correct, the Swaziland deposits may form part of the oldest tin belt known from any orogenic belt. (A. Leube, pers. comm., 1981).

URANIUM

Radioactive anomalies have been described from two localities within the upper clastic sequences of the Swaziland Supergroup. Both uranium prospects occur near the southernmost known extension of the Moodies Group outcrop.

At Rashale (Fig. 52), anomalous levels of radioactivity are associated principally with ferruginous and sericitic quartzites and conglomerates. A prominent but discontinuous radioactive "shale" horizon as much as 3,6 m thick occurs within this sequence (Davies, 1956). Both uranium and thorium are present within the horizon and occur adsorbed onto fine-grained iron hydroxide minerals, principally goethite. In addition to goethite, both talc and sericite are present in the "shale" on surface, and chlorite (possibly pale green sericite) is described occurring at depth (borehole logs BH 72 and 275, Fig. 53). A distinctive feature of the radioactive horizon is a heavy mineral assemblage that includes chromite, zircon and rutile. (Ann. Rept., 1955).

X-ray powder photography conducted by the Atomic Energy Department, London (reported in Clarke, 1971) showed that the main radioactive source is thorite ($ThSiO_4$). *In situ* gamma spectrometric determinations given by Michie (1979; see Table 46) are also consistent with a thorite source. These measurements show that radioactivity is due to both U and Th, with the most active area containing over 700 ppm Th and nearly 250 ppm U, with very low K (samples 4 and 5, Table 46). Th/U ratios generally exceed 1. Equivalent data for Onverwacht Group talcose schist, Moodies Group quartzites, and intercalated (weakly radioactive) ferruginous conglomerates (Fig. 52; see Rashale iron deposit) are given in Table 46.

The positions of three boreholes (BH 72–74), sited to intersect the radioactive horizon at depth are shown in Fig. 53. No significant radioactive anomalies were detected in any of the borehole intersections (Davies, 1956). However, it appears that the intersection in BH 72 was very close (less than 10 m) to a major fault between the Onverwacht and Moodies Groups, and may not have been wholly representative of the down-dip extension. From surface data alone, Michie (1979) concluded that because the radioactive mineralisation is enriched in Th, and is sporadic in distribution, it does not have economic potential.

Moodies Group quartzites and conglomerates are also radioactive in the area west of Forbes Reef dam (Ann. Rept., 1955; sample 6 Table 46). As at Rashale, reddish-brown thorite occurs as part of a varied heavy mineral assemblage that here includes zircon, tourmaline, garnet and spinel. The radioactive horizon is a 0,3 m-thick conglomerate unit with bulk content of 240–270 ppm Th and 50–80 ppm U (Michie, 1979).

The occurrence of small amounts of thorite within coarse clastic sequences points strongly to a detrital source for this mineral. Similarities with the main radioactive horizon at Rashale led Michie (1979) to propose that the sequence at Forbes Reef may represent a distal placer equivalent of Rashale with a sediment transport direction toward the northeast (uncorrected for the effects of deformation). Detailed sedimentological studies are required to substantiate the suggestion.

Moderate radioactive anomalies are associated with pegmatites in AG3 granite near the eastern margin of the Swaziland Supergroup outcrop (Michie, 1979; sample 7 Table 46). Although the radioactive phase(s) within the pegmatites has not been identified, small tonnages of placer columbite (±100 tons) are known to occur in the Forbes Reef area (Davies, 1952; 1953). The uranium content of the pegmatite in sample 7 is less than twice the average value of uranium in AG5 granite (sample 10), and is unlikely to be of economic interest.

TABLE 46
Gamma-ray spectrometric determinations[1]

	1	2	3	4	5	6	7	8	9	10
Th (ppm)	4	6	11	148	710	260	26	18	24	69
U (ppm)	1	2	15	150	246	63	28	6	7	16
K (%)	0	0,23	0,29	1,56	0,16	2,14	3,91	2,90	3,18	3,66
Th/U	3,6	2,3	0,7	1,1	2,9	4,3	0,9	3,2	4,0	4,5

[1]compiled from Michie (1979).

Notes: 1. talcose schists, Onverwacht Group, Rashale area; 2. Moodies Group quartzites and conglomerates, Rashale, mean 3 determinations; 3. Moodies Group ferruginous conglomerate, Rashale; 4. Rashale average, mean 6 determinations; 5. Rashale most active spot, mean 2 determinations; 6. Moodies Group conglomerate, Forbes Reef dam (850 m N 32° E Waterfall Mine), mean 3 determinations; 7. Pegmatite in AG3 granite, Forbes Reef dam, mean 2 determinations; 8. AG3 granite, Forbes Reef area, mean 3 determinations; 9. AG3 granite, Mbabane area, mean 19 determinations; 10. AG5 granite, Mbabane area, mean 19 determinations.

REFERENCES

Ainsworth, J. Contribution from iron ore development by Swaziland Iron Ore Development Corporation to the economy of Swaziland. *Trans. Inst. Min. Metall.* (in press).

Anhaeusser, C.R., (1973). The evolution of the early Precambrian crust of southern Africa. *Trans. R. Soc. Lond.*, Ser. A, **273**, 359–388.

– – – – (1976a). The geology of the Sheba hills area of the Barberton Mountain Land, South Africa, with particular reference to the Eureka syncline. *Trans. geol. Soc. S. Afr.*, **79**, 253–280.

– – – – (1976b). The nature of chrysotile asbestos occurrences in southern Africa: A review. *Econ. Geol.*, **71**, 96–116.

– – – – (1976c). The nature and distribution of Archean gold mineralisation in southern Africa. *Miner. Sci. Engng.*, **8**, 46–84.

Attridge, R.L., Brown, H.T. and Traviss, R.S., 1972. Pre-feasibility study on the benefication of Ngwenya Bonded Haematite Quartzite (BHQ). *Unpubl., rept., Swaziland Iron Ore Development Company Limited.*

Bacon, L.O., (1970). A regional interpretation of the aeromagnetic survey. Bull. No. 7, *Swaziland geol. Surv. Mines Dept.*, 17–35.

Bailey, E.H., Clark, A.L. and Smith, R.M., (1975). Mercury. *U.S. Geol. Surv., Prof. Pap.*, **820**, 401–414.

Barnes, I., La Marche, V.C. and Himmelberg, G., (1967). Geochemical evidence of present-day serpentinisation. *Science N.Y.*, **156**, 830–832.

– – – – and O'Neil, J.R., (1969). The relationship between fluids in some fresh Alpine-type ultramafics and possible modern serpentinisation, western United States. *Bull. geol. Soc. Am.*, **80**, 1947–1960.

Bertine, K.K., and Keene, J.B., (1975). Submarine barite-opal rocks of hydrothermal origin. *Science*, N.Y., **188**, 150–152.

Boyle, R.W., (1979). The geochemistry of gold and its deposits *Bull. geol. Surv. Can.*, **280**, 584 pp.

Brech, G.E., (1972). Report on the Ngwenya banded ironstone deposits. *Unpubl. rept., Swaziland Iron Ore Development Company Limited.*

– – – – and Lumb, M.D., (1974). Piggs Peak iron ore deposits. *Unpubl. rept., Anglo American Corporation of South Africa Limited,* 7 pp.

Burley, A.J., and Andrew, E.M., (1969). Induced polarisation surveys in North West Swaziland. *Geophys. rept., No. GP/O/42,* Overseas Div., Inst. geol. Sci., 21 pp.

– – – –, Evans, R.B., Gillingham, J.M. and Masson Smith, D., (1970). Gravity anomalies in Swaziland. Bull. No. 7, *Swaziland geol. Surv. Mines Dept.*, 4–16.

Burnham, C.W., (1967). Hydrothermal fluids at the magmatic stage. *In* Barnes, H.L. Ed., *Geochemistry of hydrothermal ore deposits.* Holt, Rinehart and Winston, 34–76.

Bursill, C., Luyt, J.F.M. and Urie, J.G., (1964). The Bomvu ridge iron ore deposit, *In* Haughton, S.H. Ed., *The geology of some ore deposits in southern Africa.* Vol. II. Geol. Soc. S. Afr., 405–413.

Bushell, D.W., (1972). Exploration in Mineral Concession No. 41, Swaziland. *Unpubl. repts., Lonhro Swaziland Limited.* [*sic* Lonrho]

Carter, N.G., (1966). Interim report on Pigg's Peak gold mine (Swaziland). *Unpubl. rept., Falconbridge of Africa Ltd.,* 13 pp.

Clarke, M.C.G., (1971a). Notes and recommendations on the Motshane Reef area (U.N. location No. 56). *Unpubl. rept., Swaziland geol. Surv. Mines Dept.*, M.C.G.C./5/71.

– – – – (1971b). Notes and recommendations on the She Mine area. (U.N. location No. 53). *Unpubl. rept., Swaziland geol. Surv. Mines Dept.*, M.C.G.C./4/71.

– – – – (1971c). A review of Swaziland ironstones. *Unpubl. rept., Swaziland geol. Surv. Mines Dept.*, M.C.G.C./8/71.

– – – – (1973). Report on work at the Londosi Barytes Mine during January 1973. *Unpubl. rept., Swaziland geol. Surv. Mines Dept.*, M.C.G.C./4/73.

– – – – (1975). Interim report on investigations at Peak Mine, Part I: Geological and analytical data. *Unpubl. rept., Swaziland geol. Surv. Mines Dept.*, M.C.G.C./1/75.

– – – – (1976). Survey of ore reserves at the Londosi Barytes Mine as in various reports. *Unpubl. rept., Swaziland geol. Surv. Mines Dept.*, M.C.G.C./1/76.

– – – – (1977). Report on the green chert outcrops south of Havelock. *Unpubl. rept., Swaziland geol. Surv. Mines Dept.*, M.C.G.C./4/77.

– – – – (1978). Gold investigations in 1976 and 1977. *Unpubl. rept., Swaziland geol. Surv. Mines Dept.*, M.C.G.C./6/78.

– – – –, and de Vletter, D.R., (1975). A summary of past work and identification of possible future studies concerning iron ore in Swaziland. *Unpubl. rept., Swaziland geol. Surv. Mines Dept.*, Stencil No. 267.

Coleman, R.G., (1967). Low-temperature reaction zones and Alpine ultramafic rocks of California, Oregon and Washington. *Bull. U.S. geol. Surv.*, **1247**, 49 pp.

– – – – (1971). Petrologic and geophysical nature of serpentinites. *Bull. geol. Soc. Am.*, **82**, 897–918.

– – – – (1977). *Ophiolites.* Springer-Verlag, Berlin. 229 pp.

– – – –, and Keith, T.E., (1971). A chemical study of serpentinisation — Burro Mountain, Calfornia. *J. Petrology,* **12**, 311–328.

Condie, K.C. Macke, J.E. and Reimer, T.O., (1970). Petrology and geochemistry of early Precambrian graywackes from the Fig Tree Group, South Africa. *Bull. geol. Soc. Am.*, **81**, 2759–2776.

Darracott, B.W., (1975). The interpretation of the gravity-anomaly over the Barberton Mountain Land, South Africa. *Trans. Geol. Soc. S. Afr.*, **78**, 123–128.

Dart, R.A. and Beaumont, P., (1967). Amazing antiquity of mining in Southern Africa. *Nature, Lond.*, **216**, 407–408.

Davies, D.N., (1951a). Report on the molybdenum prospect at the Komati River pont, Crown mineral area No. 7, Mbabane District, Swaziland. *Unpubl. rept. Swaziland geol. Surv. Mines Dept.*, Stencil No. 52.

– – – – (1951b). Summary of the drilling results on the barytes deposits in the Londosi valley, Crown mineral area No. 7, Mbabane District, Swaziland. *Unpubl. rept., Swaziland geol. Surv. Mines Dept.*, Stencil No. 159.

– – – – (1952). The prospecting of columbite placer deposits on Crown mineral area No. 7 and Mineral Concession No. 25, Mbabane District, Swaziland. *Unpubl. rept., Swaziland geol. Surv. Mines Dept.*, Stencil No. 193.

– – – – (1953a). Columbite prospecting on Crown mineral area No. 7, Forbes Reef area, Mbabane District Swaziland. *Unpubl. rept., Swaziland geol. Surv. Mines Dept.*, Stencil No. 214.

– – – – (1953b). Report on the nickel-tungsten-gold deposits at Forbes Reef Crown Mineral Reserve and Crown Mineral Area No. 7, Mbabane District, Swaziland. *Unpubl. rept., Swaziland geol. Surv. Mines Dept.*, Stencil No. 240.

– – – – (1956). Brief note on the preliminary diamond drilling on the radio-active shale prospect, Crown mineral area No. 7, Forbes Reef, Mbabane District, Swaziland. *Unpubl. rept., Swaziland geol. Surv. Mines Dept.*, Stencil No. 342.

– – – – and Urie, J.G., (1957). The Bomvu ridge haematite deposits, Crown mineral area No. 7, Mbabane District, Swaziland. *Swaziland geol. Surv. Mines Dept.*, Special rept. No. 3, 24 pp.

Davies, D.N. and Hunter, D.R., (1964). The gold deposits of the Barberton Mountain Land in Swaziland, *In* Haughton, S.H., Ed., *The geology of some ore deposits in Southern Africa.* Vol II. Geol. Soc. S. Afr., 59–76.

De Villiers, J.E., (1957). The mineralogy of the Barberton gold deposits. Bull. No. 24, *Geol. Surv. S. Afr.*, 60 pp.

De Wit, M.J. Gliding and overthrust nappe tectonics in the Barberton greenstone belt. *J. Struct. Geol.*, (in press).

Dick, H.J.B. and Sinton, J.M. (1979). Compositional layering in Alpine peridotites: Evidence for pressure solution creep in the mantle. *J. Geol.*, **87**, 403–416.

Dlamini, A.S., (1972). Annual report for 1971. *Unpubl. rept., Swaziland geol. Surv. Mines Dept.*, G.S.D. 101.

Dorr, J.V.N., (1964). Supergene iron ores of Minas Gerais, Brazil. *Econ. Geol.*, **59**, 1203–1240.

Durney, D.W. and Ramsay, J.G., (1973). Incremental strains measured by syntectonic crystal growths. *In* De Jong, K.A. and Scholter, R., Eds., *Gravity and Tectonics,* New York, J. Wiley and Sons., 67–96.

Eriksson, K.A., (1977). Tidal deposits from the Archean Moodies Group, Barberton Mountain Land, South Africa. *Sed. Geol.*, **18**, 257–281.

Evans, R.B., (1967). Ground geophysical surveys in Swaziland, September 1966–January 1967. *Geophys. Rept. No. 37.*, Overseas Div., Inst. geol. Sci., 36 pp.

Floran, R.J. and Papike, J.J., (1978). Mineralogy and petrology of the Gunflint iron-formation, Minnesota-Ontario: Correlation of compositional and assemblage variations at low to

moderate grade. *J. Petrology.*, **19**, 215–288.
Forgeron, D., (1979). Regional stream sediment geochemical reconnaissance of Swaziland. Bull. No 8, *Swaziland geol. Surv. Mines Dept.*, 120 pp.
Gay, N.C., (1968). The composition of gold from the Barberton Mountain Land. *Trans. geol. Soc. S. Afr.*, **71**, 274–290.
Goodwin, A.M., (1964). Geochemical studies at the Helen Iron Range. *Econ. Geol.*, **59**, 684–718.
Graham, C.M. and England, P.C., (1976). Thermal regimes and regional metamorphism in the vicinity of overthrust faults: An example of shear heating and inverted metamorphic zonation from Southern California. *Earth Planet.Sci.Lett.*, **31**, 142–152.
Groeneveld, D. *(compiler)*, (1975). The economic mineral deposits in the Archean complex of the Barberton area. Closed file rept., *S.Afr. Dept. Mines.*, 353 pp.
Hales, H.L. and Gough, D.I., (1962). Gravity anomalies and crustal structure in South Africa. *Geophys. J.*, **2**, 324–336.
Hall, A.L., (1918). The geology of the Barberton gold mining district. Memoir No. 9. *Geol. Surv. S.Afr.*, 324 pp.
Hamilton, P.J., Eversen, N.M., O'Nions, R.K., Smith, H.S. and Erlank, A.J., (1979). Sm-Nd dating of Onverwacht Group volcanics, Southern Africa. *Nature*, **279**, 298–300.
Hamilton, W. and Myers, B., (1967). The nature of batholiths. *US. geol. Surv. Prof. Pap.*, **554-C**, C1–C30.
Heinrichs, T.K. and Reimer, T.O., (1977). A sedimentary barite deposit from the Archean Fig Tree Group of the Barberton Mountain Land (South Africa). *Econ. Geol.*, **72**, 1426–1441.
Hess, H.H., (1964). The oceanic crust, the upper mantle and the Mayagüez serpentinised peridotite. *In* Burk, C.A. Ed., A study of serpentinite (the AMSOC core hole near Mayagüez, Puerto Rico). *Natl. Acad. Sci., Natl. Res. Council Publ.*, **1185**, 175 pp.
Honnorez, J. and Kirst, P., (1975). Petrology of rodingites from the equatorial mid-Atlantic fracture zones and their geotectonic significance. *Contr. Miner. Petrol.*, **49**, 233–257.
Hostetler, P.B., Coleman, R.G. and Evans, B.W., (1966). Brucite in Alpine serpentinites. *Am. Miner.*, **51**, 75–98.
Hunter, D.R., (1951). A chrysotile asbestos occurrence on Crown mineral area No. 14, Mbabane District, Swaziland. *Unpubl. rept., Swaziland geol. Surv. Mines Dept.*, Stencil No. 170.
– – – – (1959a). An occurrence of chrysotile asbestos, Mineral Concession No. 25, Mbabane District. *Unpubl. rept., Swaziland geol. Surv. Mines Dept.*, Stencil No. 402.
– – – – (1959b) The gold occurrences in the vicinity of Wyldsdale Ridge and Lomati gold mine, Mineral Concession No. 51, Piggs Peak District, Swaziland. *Unpubl. rept., Swaziland geol. Surv. Mines Dept.*, Stencil No. 414.
– – – – (1960a). The barytes deposit, Crown mineral area No. 7, Mbabane District. *Unpubl. rept., Swaziland geol. Surv. Mines Dept.*, Stencils Nos. 426 and 505.
– – – – (1960b). The Emlembe gold mine, Mineral Concession No. 41, Piggs Peak District, Swaziland. *Unpubl. rept., Swaziland geol. Surv. Mines Dept.*, Stencil No. 415.
– – – – (1961). The Nottingham Hill gold mine, Mineral Concession No. 41. *Unpubl. rept., Swaziland geol. Surv. Mines Dept.*, Stencil No. 429.
– – – – *(compiler)*, (1962). Mineral resources of Swaziland. Bull. No. 2, *Swaziland geol. Surv. Mines Dept.*, 111 pp.
– – – – (1963). Report on the drilling at Droxford Farm barytes occurrence, Mineral Concession No. 25, Mbabane District. *Unpubl. rept., Swaziland geol. Surv. Mines Dept.*, Stencil No. 504.
– – – – (1966). Report on drilling programme, Swaziland Barytes Limited, Oshoek, Hhohho District. *Unpubl. rept., Swaziland geol. Surv. Mines Dept.*, Stencil No. 438.
– – – – (1969). An investigation of the dormant Forbes Reef gold mine, Hhohho District. *Unpubl. rept., Swaziland geol. Surv. Mines Dept.*, Stencil No. 489.
– – – – (1974). Crustal development in the Kaapvaal Craton, 1. The Archean. *Precambrian Res.*, **1**, 259–294.
– – – – and Jones, D.H., (1963). The geology of the gold mines and prospects at Horo, Pigg's Peak District, Bull. No. 3 *Swaziland geol. Surv. Mines Dept.*, 45–53.
– – – – and – – – – (1968). Geological map series (1:25 000). Sheet 1, Hhohho. *Swaziland geol. Surv. Mines Dept.*
– – – – and – – – – (1969). Geological map series (1:25 000). Sheet 2, Pigg's Peak. *Swaziland geol. Surv. Mines Dept.*
Issacs, K.N. and Hartman, R.R., *Canadian Aero Service Ltd.*, (1966). Interpretation of geophysical survey of Swaziland for the United Nations, *United Nations Development Programme*, New York.
James, H.L., (1966). Chemistry of the iron-rich sedimentary rocks, *In* Data of geochemistry. *U.S. geol. Surv., Prof. Pap.*, **440-W**, W1–W61.
Jones, D.H., (1962). Report on the Devil's Reef gold mine area, lapsed Mineral Concession No. 32B, Pigg's Peak District. *Unpubl. rept., Swaziland geol. Surv. Mines Dept.*, Stencil No. 442.
– – – – (1963). Report on the geology of the Kobolondo area with reference to the Kobolondo and Black Diamond Creek gold mines (Mineral Concession No. 32A, and Crown mineral area No. 1) Pigg's Peak District. *Unpubl. rept. Swaziland geol. Surv. Mines Dept.*, Stencil No. 463.
– – – – (1969). Geology and gold mineralisation of the Hhohho area, northwestern Swaziland. *Unpubl. M.Sc. thesis*, Univ. Witwatersrand 165 pp.
Kerrich, R., (1980). Archean gold bearing chemical sediments and veins: A synthesis of stable isotope and geochemical reactions, *In* Roberts, R.G., Ed., *Archean hosted gold deposits.* Symposium, March 1980, Ontario, Univ. Waterloo, 137–211.
– – – – and Fryer, B.J., (1981). The separation of rare elements from abundant base metals in Archean lode gold deposits: Implication for low water/rock source regions. *Econ. Geol.*, **76**, 160–166.
Knopf, A., (1929). The Mother Lode system of California. *U.S. geol. Surv. Prof. Pap.*, **157**, 88 pp.
Lane, R.W., (1974). Final report to the Swaziland Geological Survey and Mines Department on the Forbes Reef area. *Unpubl. rept., Eland Exploration Limited*, 10 pp.
Laubscher, D.H., (1964). The occurrence and origin of chrysotile asbestos and associated rocks, Shabani, Southern Rhodesia. *In* Haughton, S.H. Ed., *The geology of some ore deposits in southern Africa. Vol. II.* Geological Society of South Africa, 593–624.
– – – – (1968). The origin and occurrence of chrysotile asbestos in the Shabani and Mashaba areas, Rhodesia. *Trans. geol. Soc. S. Afr.*, **71**, 195–204.
Laurent, R., (1975). Petrology of the Alpine-type serpentinites of Asbestos and Thetford Mines, Quebec. *Schweiz. miner. petrogr. Mitt.*, **55**, 431–455.
Lee, J.E., (1964). Final report on the She Mine area (Swaziland). *Unpubl. rept., Falconbridge of Africa Limited*, 8 pp.
Linsell, C.P., (1974). Feasibility report on Swaziand barytes. Closed file rept., submitted to Swaziland geol. Surv. Mines Dept., J.B. Mudd and Partners.
Lowe, D.R. and Knauth, L.P., (1977). Sedimentology of the Onverwacht Group (3,4 billion years), Transvaal, South Africa, and its bearing on the characteristics and evolution of the early earth. *J. Geol.*, **85**, 699–723.
Masson Smith, D.J. and Evans, R.B., (1966). Gravity survey of Swaziland, 1965. Field work and reduction of observations. *Geophys. Rept., No. 33*, Overseas Div., Inst. geol. Sci., 8 pp.
Mehliss, A.T.M., (1945). Report on the barytes deposit on Crown Mineral area No. 7, Mbabane District. *Unpubl. rept., Swaziland geol. Surv. Mines Dept.*, Stencil No. 16.
– – – – (1946). The haematite deposits, Mineral Concession No. 41, north-western Swaziland. *Special Rept. No. 1, Swaziland geol. Surv. Mines Dept.*
Michie, U. McL., (1979). An evaluation of the uranium potential of Swaziland. *Unpubl. rept.*, M.M.A.G.U., Inst. geol. Sci.
Miyashiro, A., Shido, F. and Ewing, M., (1969). Composition and origin of serpentinites from the mid-Atlantic ridge near 24° and 30° north latitude. *Contr. Miner. Petrol.*, **23**, 117–127.
Mumpton, F.A. and Thompson, C.S., (1975). Mineralogy and origin of the Coalinga asbestos deposit. *Clays and Clay Minerals*, **23**, 131–143.
Nur, A., (1972). Dilatancy, pore fluids, and premonitory variations of ts/tp travel times. *Seismol. Soc. Am Bull.*, **62**, 1217–1222.
Page, N.J., (1967). Serpentinisation at Burro Mountain, California. *Contr. Miner. Petrol.*, **14**, 321–342.
Pretorius, D.A., (1948). Estimated potential ore reserves of the Londosi River barytes deposit. *Unpubl. rept., Swaziland geol. Surv. Mines Dept.*, Stencil No. 66.
– – – – (1961). The geology of a portion of the country between the Komati and Usushwana Rivers. *Swaziland geol. Surv. Mines Dept.*, Bull. No. 1, 56–83.
Raleigh, C.B. and Paterson, M.S., (1965). Experimental defor-

mation of serpentinite and its tectonic implications. *J. Geophys. Res.*, **70**, 3965–3985.

Randell, R.N., (1978). Final report on S.E.P.L. No. 1/77, Elangeni, Swaziland. *Unpubl. rept., Eland Exploration Limited.*

– – – – (1979). Final report on S.E.P.L. No. 1/78, Pigg's Peak, Swaziland. Closed file, *Eland Exploration Limited.*

Reimer, T.O., (1967). Die Geologie der Stolzburg Synkinale, Barberton Bergland (Transvaal — Suidafrika). *Diplom. Arbeit, Goethe-Univ.*, Frankfurt, Germany.

– – – – (1980). Archean sedimentary baryte deposits of the Swaziland Supergroup (Barberton Mountain Land, South Africa). *Precambr. Res.*, **12**, 393–410.

Riordan, P.H., (1955). The genesis of asbestos in ultrabasic rocks. *Econ. Geol.*, **50**, 67–81.

Ross, C.S. and Smith R.L., (1961). Ash-flow tuffs: Their origin, geologic relations and identification. *U.S. geol. Surv., Prof. Pap.*, 366, 81 pp.

Scholz, C.H., Sykes, L.R. and Aggarwal, Y.P., (1973). Earthquake prediction: A physical basis. *Science, N.Y.*, **181**, 803–810.

Sims, D.H.R., (1981). A historical review of the Swaziland gold mining industry. Bull. No. 9, *Swaziland geol. Surv. Mines Dept.*, 86 pp.

Tchalenko, J.S. and Ambraseys, N.N., (1970). Structural analysis of the Dasht-e Bayaz (Iran) earthquake fractures. *Geol. Soc. Am. Bull.*, **81**, 41–60.

Thayer, T.P., (1963). Flow layering in alpine peridotite — gabbro complexes. *Min. Soc. Am. Sp. Paper 1*, 55–61.

Turekian, K.K. and Wedepohl, K.H., (1961). Distribution of the elements in some major units of the earth's crust. *Geol. Soc. Am. Bull.*, **72**, 175–192.

Turner, F.J., (1968). *Metamorphic petrology*. New York, McGraw-Hill.

United Nations Development Programme, (1970). Mineral Survey, Swaziland. *U.N.D.P., New York*, 204 pp.

Urie, J.G., (1958). The geology of the Bomvu Ridge iron deposits, North-western Swaziland. *Unpubl. M.Sc. thesis.* Univ. Witwatersrand, 107 pp.

– – – – (1960). Report on the Cinnabar Prospect, Mineral Concession No. 41, Piggs Peak District, Swaziland. *Unpubl. rept., Swaziland geol. Surv. Mines Dept.*, Stencil No. 419.

– – – – (1961). Asbestos. Report on a prospecting programme undertaken on Mineral Concession No. 41, Piggs Peak District, Swaziland. *Unpubl. rept., Swaziland geol. Surv. Mines Dept.*, Stencil No. 428, 27 pp.

– – – – (1967). A reconaissance structural investigation in the Forbes Reef area, Swaziland. *Unpubl. rept., Swaziland geol. Surv. Mines Dept.*

– – – – (1970). Geological map series (1:25 000). Sheet 3, Forbes Reef. *Swaziland geol. Surv. Mines Dept.*

– – – – (1971). Geological map series. (1:25 000). Sheet 4, Motshane *Swaziland geol. Surv. Mines Dept.*

Van Biljoen, W.J., (1959). The nature and origin of the chrysotile asbestos deposits of Swaziland and the Eastern Transvaal. *Unpubl. PhD. thesis*, Univ. Witwatersrand.

Viljoen, M.J. and Viljoen, R.P., (1969a). Evidence for the existence of a mobile extrusive peridotitic magma from the Komati Formation of the Onverwacht Group. *Trans. geol. Soc. S.Afr., Spec. Publ. No. 2*, 87–112.

Viljoen, R.P. and Viljoen, M.J., (1969b). The geological and geochemical significance of the upper formations of the Onverwacht Group. *Trans. geol. Soc. S.Afr., Spec. Publ., No. 2*, 113–151.

– – – – and – – – –, (1969c). The relationship between mafic and ultramafic magma derived from the upper mantle and the ore deposits of the Barberton region. *Trans. geol. Soc. S.Afr., Spec. Publ. No. 2*, 221–244.

– – – –, Saager, R. and Viljoen, M.J., (1969). Metallogenesis and ore control in the Steynsdorp goldfield, Barberton Mountain Land, South Africa. *Econ. Geol.*, **64**, 778–797.

Visser, D.J.L. *(compiler)*, (1956). The geology of the Barberton area. *Geol. Surv. S.Afr.*, Spec. Publ.., **15**, 253 pp.

Williams, D.A.C. and Furnell, R.G., (1979). Reassessment of part of the Barberton type area. *Precambr. Res.*, **9**, 325–347.

Wiseman, E., (1975). Interim report on investigations at Peak Mine, Part II: Economic and financial data. *Unpubl. rept., Swaziland geol. Surv. Mines Dept.*, 10 pp.

Woodcock, N.H. and Robertson, A.H.F., (1977). Origins of some ophiolite — related metamorphic rocks of the 'Tethyan' belt. *Geology*, **5**, 373–376.